Identification and validation of Sirtuin 3 as a new common target of non-steroidal anti-inflammatory drugs (NSAIDs) to induce gastric mucosal injury and gastric adenocarcinoma cell death

Thesis submitted to Jadavpur University for the degree of
Doctor of Philosophy (Science)

By

Subhashis Debsharma

CSIR-Indian Institute of Chemical Biology
Kolkata-700032, India

&

Jadavpur University
Kolkata-700032, India

2023

संदर्भ सं. / Ref. No. _____

दिनांक / Date : 14/08/2023

CERTIFICATE FROM THE SUPERVISOR

This is to certify that the thesis entitled "**Identification and validation of Sirtuin 3 as a new common target of non-steroidal anti-inflammatory drugs (NSAIDs) to induce gastric mucosal injury and gastric adenocarcinoma cell death**" submitted by **Sri Subhashis Debsharma** who got his name registered on **08/03/2018** for the award of **Ph. D. (Science)** degree of Jadavpur University, is absolutely based upon his own work under the supervision of **Prof. (Dr.) Uday Bandyopadhyay** and that neither this thesis nor any part of it has been submitted for either any degree / diploma or any other academic award anywhere before.

(Uday Bandyopadhyay) 14/08/23
Signature of the Supervisor
& date with official seal

उदय बंदोपाध्याय / Uday Bandyopadhyay
निदेशक / Director
बसु विज्ञान मंदिर
BOSE INSTITUTE
कोलकाता / Kolkata

Declaration

I, **Subhashis Debsharma**, hereby declare that the research work in this thesis is my own, which has been carried out at CSIR-Indian Institute of Chemical Biology, Kolkata under the supervision of **Prof. (Dr.) Uday Bandyopadhyay**, former Senior Principal Scientist, CSIR-Indian Institute of Chemical Biology, Kolkata and present Director of Bose Institute, Kolkata. The whole work in this thesis is absolutely original and has not been submitted to any other Institution or University for any degree whatsoever.

Subhashis Debsharma

Date: 14/08/2023

DEDICATED TO
MY BELOVED FAMILY

Acknowledgment

The path to attaining the Doctor of Philosophy (Ph.D.) degree was far from linear, characterized by moments of exhilarating discoveries, daunting challenges, and unwavering perseverance. As I stand at the threshold of this milestone, I am compelled to acknowledge the profound impact this journey has had on shaping my intellect, character, and aspirations. Completing this piece of work would not have been possible without the profound support and encouragement of numerous people.

*In the beginning, I would like to express my deepest gratitude to my esteemed Ph.D. supervisor, **Prof. (Dr.) Uday Bandyopadhyay** for his invaluable guidance, unwavering support, and profound expertise throughout my doctoral journey. His exceptional mentorship and tireless commitment to my academic and personal growth have been instrumental in shaping me into the researcher I am today. I am truly fortunate to have had the privilege of working under his tutelage, benefiting from his wisdom, spirituality and witnessing his genuine passion for our field of study. His constant encouragement and constructive feedback have inspired me to push my boundaries and strive for excellence. This remarkable experience under his supervision has not only enriched my academic pursuits but also instilled in me a lifelong commitment to the pursuit of knowledge. I owe an immeasurable debt of gratitude to my supervisor for his remarkable mentorship and firm belief in my potential. His exceptional guidance has been the cornerstone of my academic success, and I will forever cherish the invaluable lessons I have learned under his guidance.*

*I would like to extend my heartfelt gratitude to **Prof. Arun Bandyopadhyay, Director, Indian Institute of Chemical Biology, Kolkata** for providing me with all the instrumental and laboratory facilities.*

*Next, I would like to acknowledge the financial support provided by the **Department of Biotechnology (DBT), Government of India.** Their investment in my research has enabled me to carry out this study and pursue my scholarly aspirations.*

*I am extremely thankful to **Dr. Subrata Adak**, **Dr. Partha Chakraborti**, **Dr. Nahid Ali, and Dr. Sib Sankar Roy** for providing me with the opportunity to use their laboratory instrument facilities. I am highly grateful to **Dr. Nakul Chandra Maiti** for in silico data analysis. I am thankful to **Dr. Aditya Konar,** the animal house in charge, and **Mr. Pasupati Midya**, the animal house technician for providing us with the rats as per my animal experiment requirement.*

*I am deeply grateful to **Dr. Indu Bhusan Deb,** Principal Scientist, CSIR-IICB, Kolkata for his exceptional dedication, support, and commitment to taking care of our lab in the absence of my guide. His invaluable contribution has been instrumental in maintaining the continuity of our research work and ensuring the smooth functioning of the laboratory.*

*I am honored to acknowledge **Dr. Zhumur Ghosh,** Associate Professor, Biological Sciences, Bose Institute, Kolkata for her invaluable expertise, guidance, and contributions to the transcriptomics data analysis in my research project.*

*I extend my deepest indebtedness and heartfelt gratitude to my dear senior, **Dr. Somnath Mazumder**, whose exceptional qualities and firm support have played a pivotal role in shaping my Ph.D. journey. His presence has been an incredible blessing, and I am truly fortunate to have him as both a senior and a caring figure. His extraordinary sense of punctuality and time management, and dedication to his work and research, which has been a guiding light for me throughout my research. His encouragement to work in a time-bound manner has been instrumental in keeping me focused and ensuring progress in my academic pursuits. His immense knowledge and expertise in the subject served as a constant source of inspiration. Beyond his role as a senior, Somnath da has taken on the responsibility of caring*

about me like a brother. Besides research, he has looked after our snacks and ensured we dined out frequently, creating a warm and enjoyable environment during our research journey. His genuine concern and encouragement have motivated me during challenging times and instilled in me a sense of confidence and assurance. I am deeply honored to have him as my senior as a part of my journey, and I will forever cherish his invaluable contributions to my research goal.

*Additionally, I owe a debt of gratitude to **Dr. Samik Bindu** for his key role in project design and implementation. His strategic guidance, constructive feedback, and meticulous attention to detail have been indispensable in shaping the experimental approach.*

*I would like to take a moment to express my gratitude to the most super cool senior, **Dr. Rudranil De**, whose infectious humor and exceptional guidance have made this Ph.D. journey an unforgettable and enjoyable experience. In addition to being the master of one-liners, Rudranil da provided me the hands-on demonstrations and troubleshooting assistance for cell culture. His creative approach to problem-solving inspired me to explore unconventional avenues, leading to exciting discoveries.*

*I extend my heartfelt gratitude to **Dr. Asim Azhar Siddiqi** and **Chinmoy Banerjee**, two of my favourite seniors whose humble, polite, and ever-supportive approach has profoundly influenced my academic pursuit during this Ph.D. journey. They never hesitated to offer a helping hand, patiently answering my questions and providing guidance with the utmost kindness and respect. I would like to thank my senior **Dr. Subha Jyoti Saha** for his constant support and encouragement whenever I required it.*

*I am immensely grateful for the untiring support, camaraderie, and joyful moments shared with my dear junior, **Saikat Pramanik** throughout my Ph.D. journey. His presence has brought immense joy, laughter, and inspiration to this challenging academic pursuit. Saikat possesses an exceptional musical sense. His sharp wit, presence of mind, and sense of humor have added a delightful spark to our shared experiences. Beyond their musical and humorous talents, Saikat is a remarkable cook who has infused our shared living space with delicious aromas and hearty meals. Our time together, hanging around, sharing experiences, and exchanging ideas, has been an invaluable part of my Ph.D. journey. Our bond goes beyond the walls of academia, and I am fortunate to have shared this significant chapter of my life with someone as caring and genuine as Saikat.*

*I would like to extend my deepest appreciation and gratitude to my esteemed Ph.D. colleague, **Dr. Shiladitya Nag** and **Debanjan Saha** for their exceptional support, camaraderie, and collaboration throughout our doctoral journey. The vibrant academic discussions, exchange of ideas, and mutual motivation over the cup of tea have helped push the boundaries of my research. Their presence has made this journey more enjoyable, memorable, and fulfilling. I am fortunate to have had such an exceptional colleague by my side, and I will forever cherish the memories and lessons learned from our shared experiences.*

*I would like to acknowledge our lab attendant **Surjendu da**, for his indispensable support and assistance that ensured the smooth functioning of our lab. I am deeply grateful for his invaluable contributions.*

*I would like to express my sincere appreciation to **Troyee Das** for her unpaid contributions to transcriptomics data analysis. Her in-depth knowledge of bioinformatics tools and her meticulous approach to handling complex datasets have been invaluable in unraveling the intricate patterns within the transcriptomic data. I would also like to express my deep gratitude to **Dr. Uttam Pal** for his expertise in in-silico data analysis. His proficiency in computational methods and his keen insights into data interpretation have been crucial in uncovering essential information from the virtual experiments conducted in this research.*

*In the pursuit of my Ph.D., I have been fortunate to receive untiring support and invaluable contributions from two exceptional individuals, **Dr. Saroj Biswas** and **Dr. Milon Banik**, who are my brothers in spirit in the true sense. Their encouragement, thought-provoking ideas, and selfless assistance have been crucial factors in shaping the success of this thesis. I am deeply grateful for the constant motivation and encouragement they provided throughout this journey. I will never forget our late-night philosophical discussions and brainstorming sessions over a cup of coffee.*

*In the pursuit of my research journey at this esteemed institution, I have been blessed to have a friend and confidante like **Dr. Sonali Das** by my side. Her continuous support and assistance have been invaluable during the whole journey, and I am deeply grateful for her presence throughout this enriching experience. Her willingness to share her knowledge, resources, and expertise has been a guiding light during challenging times. Whether it was brainstorming ideas, troubleshooting technical issues, or providing insightful feedback, Sonali's contributions have been contributory to the progress of my research.*

*The successful completion of this Ph.D. thesis would not have been possible without the support and valuable contributions of several individuals from outside our lab. I would like to acknowledge **Sumit, Puja, Yuthika, Ayan Da, Swati di, Anirban da, Parash, Sampurna, Eshani, Dipsikha, Sromona, Sukanya, Priti, Pratiti, Animesh da, Dipesh, Dipankar, Samrat, Sunny da, Sujay, Kaushik da, Shatadeepa** I am deeply grateful for their involvement throughout this academic journey.*

*I would like to acknowledge **Dr. Sarmistha Saha** and **Debapria Ghatak** for their constant support and motivation during my entire Ph.D. journey.*

*I would like to extend my deepest appreciation and acknowledge the invaluable guidance provided by my MSc teacher, **Dr. Soma Chaki**. She played a pivotal role in shaping my academic pursuits and nurturing my passion for research. I am truly grateful for the time, effort, and guidance she has invested in me and I consider myself fortunate to have had the opportunity to learn from her. Their mentorship has not only enriched my Ph.D. journey but will continue to inspire me.*

*I would like to acknowledge **Amit Anand and Sonali** for their constant motivation and support since my college days. Our countless conversations and shared experiences have enriched my research and expanded my horizons. Their friendship has been a cherished gift, and I am grateful for their unwavering support. I am thankful to **Sumit Anand and Namatra Anand** as well for their constant support and motivation.*

*I would like to express my heartfelt gratitude and acknowledge the unwavering support and friendship of my childhood companion, **Subhajit, Amit, Suman, Satyajit, Tarak, Amar, Saptarshi, Shantu,** and **Ananta.** I am truly grateful for their friendship, which extends far beyond our shared memories of childhood. Their unwavering support has been a source of inspiration and has shaped my academic journey in ways I cannot adequately express.*

*I would like to express my deepest gratitude and gratefulness to my beloved parents, **Lakshman Debsharma** and **Parama Debsharma**. whose unwavering love, support, and sacrifices have been the foundation of my academic journey and the completion of this Ph.D. thesis. Throughout my life, they have been my constant source of inspiration, encouragement, and strength. Their constant reassurance, understanding, and firm belief in my abilities have been the pillars of my success. I am profoundly grateful for their sacrifices, which have allowed me to focus on my studies and pursue my passion. This accomplishment would not have been possible without them by my side. Next, my special appreciation goes to my sister, **Rishika Debsharma**. Her presence in my life has been a source of inspiration, joy, and comfort, and I am truly fortunate to have a sister like her and I will forever cherish the bond we*

PREFACE

Nonsteroidal anti-inflammatory drugs (NSAIDs) are immensely applicable in therapeutic intervention of pain and inflammation. Globally, millions of people consume NSAIDs daily to manage inflammatory disorders including pyrexia, rheumatic disorders, fever, osteoarthritis and musculoskeletal disorders, thereby rendering these drugs almost unavoidable. Notably, despite the advent of disease-modifying anti-rheumatic drugs (DMARDs) for controlling the progression of arthritis, clinicians still rely on NSAIDs for rapid pain alleviation thereby justifying the inclusion of these drugs in the World Health Organization's analgesic ladder. In addition, drug-repurposing studies have lately identified the efficacy of NSAIDs in anti-cancer chemotherapy owing to their myriad effects including apoptosis induction, cell cycle arrest, chemo/radio-sensitization of resistant tumors and cancer stem cells. Incidentally, long-term NSAID users have revealed a relatively lower risk of developing GI tract, breast, prostate and lung cancers. However, despite this vast clinical utility spectrum, NSAIDs are defamed due to their inevitable toxic effects on multiple organs with the gastrointestinal (GI) tract being most severely affected. Contextually, escalating incidences of upper and lower gut complications in chronic NSAID users are forcing clinicians to prescribe supplementary acid-suppressing drugs to tame the GI-eroding effects owing to the notion that acid further aggravates NSAID injuries.

Initially, the cyclooxygenase (COX)-inhibitory activity of NSAIDs was thought to be solely responsible for their toxic attributes and anti-cancer effects. However, it is noteworthy that celecoxib, a selective COX2 inhibitor was found to arrest cell growth of certain COX2-deficient human prostate cancer cell lines, thereby further complicating the situation. In fact, COX-independent anticancer effect of NSAIDs is further confirmed by the fact that anti-proliferative concentrations of NSAIDs were much higher than COX-inhibitory concentrations. Moreover, deletion of COX1 in mice did not induce spontaneous ulcers while rectal administration of certain NSAIDs failed to induce gastric ulcers (although successfully reduced prostaglandin production), thereby clearly pointing towards an underlying cyclooxygenase-independent mode of NSAIDs in eliciting gastrotoxicity.

In light of the multi-dimensional facts about the effect and complex nature of NSAIDs, the present thesis aims at an in-depth exploration of the mode of action of NSAIDs while trying to identify precise sub-cellular targets responsible for the gastrotoxic and anticancer attributes of these drugs. The thesis is mainly divided into two segments; the review of literature, divided into two chapters and subsequently the experimental work divided into next two chapters. The review chapters mainly deal with discussing the current perspectives on the pathogenesis of NSAID-induced gastric injury. Focus has been laid on discussing the gradual shift in the concept of the mode of action of NSAIDs from the age-old notion of exclusive cyclooxygenase-based pathways to the modern concepts of cyclooxygenase-independent and mitochondria-dependent pathways responsible for inducing cell death. The role of mitochondrial redox dyshomeostasis, aberrant protein quality control and associated bioenergetic crisis as crucial determinants of NSAID-induced cell death have been extensively addressed. Because the specific sub-mitochondrial targets of NSAIDs are yet elusive, the putative role of NAD-dependent mitochondrial deacetylase sirtuin-3 in controlling gastrointestinal pathologies has been discussed in great detail for the first time to identify and ascribe its potential role as a hitherto unreported prospective therapeutic target.

The experimental chapters majorly emphasize exploring the mechanistic basis of NSAID toxicity in two experimental models; a non-malignant acute rodent gastropathy model and an *in vitro* gastric cancer model. To rule out any COX1/COX2 bias, indomethacin has been used in the study as a representative NSAID due to its negligible cyclooxygenase selectivity as well as its rampant usage in experimental studies and clinical trials on cancer.

Chapter 1 specifically deals with exploring the putative gastroprotective role of SIRT3 in NSAIDs-induced gastric mucosal injury. Next-generation sequencing-based transcriptomics has been used as the initial point to get an insight into the differential gene expression profiles in the indomethacin-treated rat gastric mucosa compared to control. Transcriptome mining was followed by a wide array of

functional validation experiments to identify a prospective candidature of SIRT3 as an important target of indomethacin. SIRT3 activity analysis was next performed to check whether indomethacin exerts any direct inhibitory effect on the deacetylase action *per se*. A direct functional impact of indomethacin on SIRT3-regulated downstream cellular events was checked by assessing cellular redox status, mitochondrial acetylation profile, mtDNA integrity and mitochondrial respiratory chain functioning through gene and protein expression studies as well as flowcytometric and microscopic experiments. Mitochondrial dynamics was also checked to follow the impact of indomethacin on mitochondrial structure which may be controlled through SIRT3 regulation. Finally, the functional validation relied on specific stimulation of endogenous SIRT3 by a phytopolyphenol, honokiol, in a dose-dependent manner. The putative effect of honokiol against indomethacin-induced mitochondrial dysfunctions and inflammatory gastric mucosal injury was checked by ulcer scoring and mitochondrial functional assays. It was also checked whether honokiol affected basal gastric acid production and whether it holds the merit for qualifying as a putative gastroprotective agent against NSAIDs.

Chapter 2 specifically focuses on exploring whether SIRT3 is at all targeted by NSAIDs to induce gastric cancer cell death. Here again, the study initiated with high-depth transcriptome sequencing of control and indomethacin-treated human gastric adenocarcinoma (AGS) cells followed by multi-level functional validation of the observed sequencing data. A meta-analysis of TCGA datasets was also undertaken followed by human protein atlas (HPA) data mining to check the relevance of SIRT3 expression in regards to gastric cancer prognosis and overall survival. In-depth interaction studies by molecular dynamic simulation were next performed to check/predict any putative direct binding of indomethacin with SIRT3 as well as identify the nature of the interaction. The plausible effect of indomethacin on upstream regulators of SIRT3 like PGC1α and ERRα was also checked to elucidate the putative mode of regulation of the SIRT3 signaling axis. The validation arm of the study involved silencing of endogenous expression of SIRT3 as well as its upstream transcriptional regulators (PGC1α and ERRα) in the AGS cells followed by treatment with indomethacin and subsequently evaluating vital parameters including mitochondrial proteome acetylation status, mtDNA damage, ETC complex gene expression, analysis of mitochondrial dynamics and mitophagy. Cell cycle progression and apoptosis were also monitored as terminal events of indomethacin-induced gastric cancer cell pathology which may be controlled by targeting SIRT3. Finally, the effect of other popular NSAIDs like diclofenac, aspirin and ibuprofen was also checked as well as the effect of indomethacin on other cancers like cervical, hepatocellular and colorectal carcinoma cell lines were checked to inquire whether SIRT3 is also targeted by these NSAIDs and whether SIRT3-targeting by indomethacin is a common/unanimous effect underlying the anti-neoplastic effect of this drug.

Because NSAIDs exhibit overwhelming therapeutic action against inflammation and prophylactic as well as therapeutic actions against cancer, identification of their precise sub-cellular/sub-mitochondrial target/s can certainly aid in their rational utilization while strategically bypassing the side effects for optimal benefit in both malignant as well as non-malignant inflammatory pathologies.

Abbreviations

- AIM2: Absent in melanoma 2
- AMPK: AMP-activated protein kinase
- APE1: Human apurinic/apyrimidinic endonuclease 1
- ARRIVE: Animal Research: Reporting of In Vivo Experiments
- ATP: Adenosine triphosphate
- ADP: Adenosine diphosphate
- Bak: Bcl-2 homologous antagonist/killer
- Bax: Bcl-2-associated X protein
- Bcl-2: B-cell lymphoma 2
- Bcl-xL: B-cell lymphoma-extra large
- BRAF: v-raf murine sarcoma viral oncogene homolog B1
- BSA: Bovine serum albumin
- CAT: Catalase
- CagA: Cytotoxin-associated gene A
- COX: Cyclooxygenase
- CXCR: C-X-C chemokine receptor
- DAMP: Damage-associated molecular patterns
- DAPI: 4',6-diamidino-2-phenylindole
- DIABLO: Direct IAP binding protein with low pI
- DMSO: Dimethyl sulfoxide
- DNA: Deoxyribonucleic acid
- DRP1: 4',6-diamidino-2-phenylindole
- ED_{50}: Effective dose 50
- EDTA: Ethylenediamine tetraacetic acid
- EGFR: Epidermal growth factor receptor
- ERRα: Estrogen-related receptor alpha
- ETC: Electron transport chain
- FACS: Fluorescence activated cell sorter
- FDA: United States Food and Drug Administration
- FDR: False discovery rate
- Fe-S: Iron-Sulphur
- FOXO3a: Forkhead box O3
- GC: Gastric cancer
- GEO: Gene expression omnibus
- GI: Gastrointestinal
- GLP-1: Glucagon-like peptide-1
- GPx: Glutathione peroxidise
- GR: Glucocorticoid receptor
- GSH: Glutathione (reduced)
- H_2O_2: Hydrogen peroxide
- HCl: Hydrochloric acid
- HIF: Hypoxia inducible factor
- HKL: Honokiol
- HMGB1: High mobility group box 1
- HO˙: Hydroxyl radical
- HO-1: Heme oxygenase-1
- HP: *Helicobacter pylori*
- HPA: Human protein atlas
- ICAM-1: Intercellular adhesion molecule-1
- IC_{50}: Inhibitory Concentration 50
- IDH2: Isocitrate dehydrogenase 2
- IFN-γ: Interferon gamma
- IL: Interleukin
- IMM: Inner mitochondrial membrane
- IND: Indomethacin
- iNOS: Inducible nitric oxide synthase
- IRI: Ischemia reperfusion injury
- IκBα: Inhibitory kappa B alpha
- JC-1: 5,5',6,6'-tetra-chloro-1,1',3,3'-tetraethylbenzimidazol carbocyanine iodide
- kDa: Kilodalton
- KM: Kaplan-Meier
- LIG3: Ligase III, DNA, ATP-dependent
- MAPK: Mitogen-activated protein kinase
- MCODE: Molecular complex detection
- Mdivi-1: Mitochondrial division 1

- MFF: Mitochondrial fission factor
- MFN: Mitofusin
- MIF: Macrophage migration inhibitory factor
- miRNAs: MicroRNAs
- MLKL: Mixed lineage kinase domain-like pseudokinase
- MitoQ: Mitoquinone
- MMI: 2-Mercapto-1-methylimidazole
- MMP: Metalloproteinase
- MOS: Mitochondrial oxidative stress
- MPP: Mitochondrial processing peptidase
- MTCO1: Mitochondrially encoded cytochrome c oxidase 1
- MTT: 3-(4,5-dimethylthiazol-2-yl)-2,5-diphenyl tetrazolium bromide
- MTA: Mitochondrially targeted antioxidants
- MTHFD2: Methylenetetrahydro folate dehydrogenase 2
- MTOR: Mammalian target of rapamycin
- MUTYH: MutY DNA glycosylase
- NAD: Nicotinamide adenine dinucleotide
- NAFLD: Non-alcoholic Fatty Liver Disease
- NAO: Nonyl acridine orange
- NADPH: Nicotinamide adenine dinucleotide phosphate
- NDUFB8: NADH:ubiquinone oxidoreductase subunit B8
- NEIL1: Endonuclease VIII-like 1
- NF-κB: Nuclear factor κB
- NLRC: NLR Family CARD Domain Containing
- NLRP3: nucleotide-binding domain, leucine-rich-containing family, pyrin domain-containing-3
- NO: Nitric oxide
- Nrf2: NF-E2 related factor 2
- NSAIDs: Non-steroidal anti-inflammatory drugs

- $O_2^{\cdot-}$: Superoxide anion radical
- OMM: Outer mitochondrial membrane
- OPA: Optic atrophy
- OD: Optical density
- OXPHOS: Oxidative phosphorylation
- Ox-mtDNA: Oxidized mitochondrial DNA
- PARP: Poly (ADP-ribose) polymerases
- PBS: Phosphate buffered saline
- PD: Parkinson's disease
- PG: Prostaglandin
- PGC-1α: Peroxisome proliferator-activated receptor γ coactivator-1α
- PGE: Prostaglandin E
- PI3K: Phosphatidylinositol 3-kinase
- PINK1: PTEN-induced putative kinase 1
- PGK-1: Phosphoglycerate kinase 1
- PKA: Protein kinase A
- PKC: Protein kinase C
- PMSF: phenylmethylsulfonyl fluoride
- PPIs: Proton pump inhibitors
- PTM: Posttranslational modification
- RMSF: Root mean square fluctuation
- RMSD: Root mean square deviation
- ROS: Reactive oxygen species
- RT-PCR: Reverse transcriptase polymerase chain reaction
- SENP1: Sentrin-specific protease 1
- Smac: Second mitochondria-derived activator of caspase
- SOD: Superoxide dismutase
- TCA: Trichloroacetic acid
- TCGA: The Cancer Genome Atlas Program
- TNF-α: Tumor necrosis factor alpha
- TOM: Translocase of the outer membrane
- TRPC4: Transient Receptor Potential Canonical 4

- UQCRC2: Ubiquinol-cytochrome c reductase core protein II
- VacA: Vacuolating toxin A
- VCAM-1: Vascular cell adhesion molecule-1
- VDAC: Voltage dependent anion channel
- VEGF: Vascular endothelial growth factor
- $\Delta\Psi m$: Mitochondrial trans-membrane potential
- %: Percentage
- °C: Degree celcius
- µg: Microgram

CONTENTS

REVIEW OF LITERATURE

A. GASTRIC INJURY: THE MECHANISTIC BASIS OF COX-DEPENDENT VERSUS COX-INDEPENDENT MODES OF MUCOSAL PATHOGENESIS

> **B. SIRTUIN 3: THE MITOCHONDRIAL METABOLIC GUARDIAN REGULATING GASTROINTESTINAL HEALTH AND MUCOSAL PATHOLOGY**

EXPERIMENTAL

CHAPTER 1: SIRTUIN 3 PROTECTS THE GASTRIC MUCOSA FROM NSAIDs-INDUCED MITOCHONDRIAL PATHOLOGY AND PRO-INFLAMMATORY DAMAGE

CHAPTER 2: NSAID, BY TARGETING SIRT3, ARRESTS GASTRIC CANCER CELL GROWTH THROUGH INDUCING MITOCHONDRIAL PROTEOME HYPERACETYLATION AND DISRUPTING FISSION-FUSION HOMEOSTASIS

Gastric injury: the mechanistic basis of COX-dependent *versus* COX-independent modes of mucosal pathogenesis

1. INTRODUCTION

The term gastric ulcer refers to the erosion (> 3-5 mm rupture) or lesion in the gastric lining resulting in mucosal break reaching the submucosa that interferes with the integrity of the gastrointestinal mucosal layer within the esophagus, stomach and proximal part of the small intestine, called duodenum. Over the past two centuries, gastric ulcer becomes one of the most common health issues affecting about 4 million people annually in the whole world with high morbidity and mortality. Around 10 to 20% of the patients face complications. There are numerous different causes of peptic ulcer development. However, widespread use of nonsteroidal anti-inflammatory drugs (NSAIDs), *Helicobacter pylori* infections, the use of histamine 2 receptor antagonists, selective serotonin reuptake inhibitors, and elevated physiological stress have all been implicated as risk factors for the development of gastric ulcers and altered landscape of gastric mucosal injuries in recent years (1). Children and people in their middle years have higher *H. pylori* prevalence rates whereas, elderly people are more likely to develop NSAID-induced ulcers due to their higher analgesic use. It is not fully understood how NSAIDs cause and may contribute to gastrointestinal complications. At the turn of the 20th century, stress and smoking were thought to be the main causes of ulcers. The substantial connection between ulcers and *H. pylori* was discovered later in 1994. The primary contributing factor to gastrointestinal harm, aside from *H. pylori*, is the widespread use of NSAIDs. Consuming excessive amounts of fatty and spicy food, as well as stress, are additional risk factors for illness (2, 3). Epidemiological studies have shown a dramatic decline in the incidence, hospital admission rates, and death associated with stomach ulcers in the past 20–30 years. However, the usage of NSAIDs has substantially grown in recent decades, particularly aspirin and other drugs, and these drugs frequently cause major problems in people with gastric mucosal bleeding/injuries. About 10% of peptic ulcer disease cases are caused by drugs like aspirin and other NSAIDs (1). Despites of these side effects NSAIDs are unavoidable and these drugs are the most often recommended medication (5-10% of all prescribed medicines) because, despite their anti-inflammatory effects, they are constantly utilized in analgesic and antipyretic treatment (4). The systemic effects of nonsteroidal anti-inflammatory treatments, which primarily include preventing prostaglandin production by inhibiting the cyclooxygenase (COX) enzymes COX-1 and COX-2, result in gastrointestinal damage through a combination of topical and systemic actions. However, more research on the NSAID's mode of action revealed complex chemical mechanisms and there is unquestionable proof that alternative prostaglandin-independent pathways play a significant role in the etiology of ulcers and that COX inhibition is not the only mechanism of NSAID-induced gastrointestinal damage (5). In this context, the primary COX-independent activity of NSAID causing damage to the gastric mucosa is mitochondrial oxidative stress (MOS) and intrinsic apoptosis.

2. GASTRIC MUCOSAL INJURY AND ULCEROGENESIS: CAUSATIVE FACTORS AND PATTERN OF MUCOSAL DAMAGE

Daily stress and strain, NSAID use, *H. pylori* infection, and alcohol use, are a few of the commonly recognized gastroduodenal ulcer-causing agents (6-8). Another known contributor to gastroduodenal mucosal damage and sluggish recovery is cigarette smoking (9, 10). Below is a description of several common causes of stomach mucosal damage. Both the causative and protective factors of gastric ulcers have been depicted in Figure 1
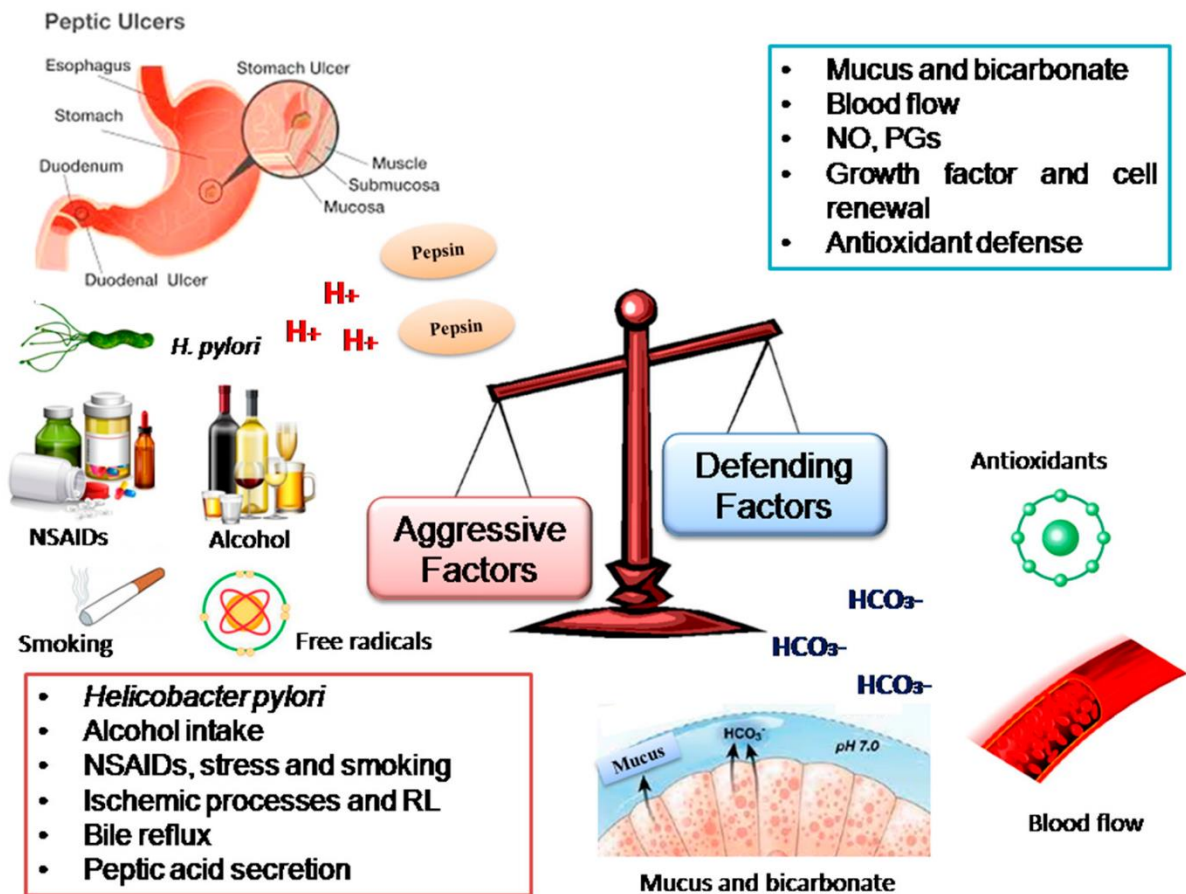
Fig. 1. This illustration portrays the key causative factors and protective factors of gastric mucosal ulcers. The ulcerogenic process begins when there is an imbalance between hostile and protective factors. Although there are various contributors, two factors, *Helicobacter pylori* infection (which mainly causes duodenal ulcers) and the use of non-steroidal anti-inflammatory drugs (which mainly cause gastric ulcers), are particularly important in disrupting the protective mucosal layer and exposing the gastric epithelium to acid. Additionally, several other factors such as smoking, alcohol, and certain medications can further enhance the ulcerogenic process. This process ultimately leads to erosion. Over time, the serosal lining is breached, and if the breach results in a perforation, the stomach contents, including acidic fluid, will enter the abdominal cavity. This occurrence leads to intense pain, localized peritonitis that can spread throughout the abdomen, and eventually trigger a systemic inflammatory response syndrome, sepsis, and the risk of multi-organ failure and death.This figure has been adapted from Serafim *et. al.* (135)

2.1. Helicobacter pylori

One of the main causes of gastric ulcer disease is *Helicobacter pylori*. Around 15% of *H. pylori*-infected people develops gastric mucosal ulcer (11). To generate an alkaline environment that is favorable for its survival, it secretes urease. It can adhere to the stomach epithelium because it expresses the blood group antigen adhesin (BabA) and the outer inflammatory protein adhesin (OipA) (12). Additionally, the bacteria express virulence proteins such CagA and PicB, which inflame the stomach mucosa (12). It is unknown how the vacuolating cytotoxin that the VacA gene encodes results in peptic ulcers. Such stomach mucosal inflammation may be caused by either hypochlorhydria or hyperchlorhydria (increased stomach acid output) (reduced stomach acid secretion). Additionally, *H. pylori* secrete substances that block hydrogen potassium ATPase, activate *calcitonin* gene-related peptide sensory neurons, boost somatostatin secretion to prevent parietal cells from producing acid, and block gastrin

secretion (13). Gastric ulcer is induced by this decrease in acid production. On the other hand, in 10% to 15% of instances of *H. pylori* infection, increased acid production at the pyloric antrum is linked to duodenal ulcers. In this instance, somatostatin synthesis is inhibited and gastrin production is elevated, which causes the enterochromaffin cells to secrete more histamine, boosting acid production.

2.2. Non-steroidal anti-inflammatory drugs (NSAIDs)

Long-term usage of NSAIDs such as indomethacin, ibuprofen, aspirin, and diclofenac increases the development of gastric ulcers (14). NSAIDs induce gastric mucosal injury by inhibiting COX-1 and COX-2, which catalyze the producton of prostaglandin endoperoxide (PGG$_2$) and prostanoids from arachidonic acid (15). Prostaglandin plays a protective role against the development of gastric ulcers by inhibiting gastric acid secretion, enhancing the release of more mucus and bicarbonate from epithelial cells and reducing the release of proinflammatory cytokines (16). It has been demonstrated that the ability of NSAIDs to decrease stomach prostaglandin production and their preference for COX-1 over COX-2 are strongly correlated with their capacity to produce ulcers (16). The key factor defining an NSAID's potential to produce bleeding issues may be the inhibition of platelet COX-1, which also results in reduced thromboxane production and increased bleeding tendency. Apart from the cox-dependent pathway, the cox-independent pathway for NSAIDs for the development of gastric mucosal injury is also relevant which indicates that the mechanism by which NSAIDs induce stomach damage may be far more complicated than first believed. NSAIDs cause gastric mucosal injury through a mechanism other than one mediated by prostaglandins (17). According to multiple published studies, it has been demonstrated that oxidative stress, specifically mitochondrial oxidative stress (MOS), is a key factor in several models of gastric mucosal damage. According to multiple published studies, it has been demonstrated that oxidative stress, specifically mitochondrial oxidative stress (MOS), disbalance in mitochondrial dynamics are the key factors in several models of gastric mucosal damage (17-19).

2.3. Stress

Physical homeostasis is altered by persistent mental illnesses like anxiety and depression, which have a substantial negative impact on human health. One such symptom that has been observed in individuals who are under stress all around the world is stress-related mucosal disease (SRMD) (20). One of the key stress-associated phenomena in critically sick patients in the intensive care unit (ICU) is moderate to acute mucosal bleeding, and the death rate is alarmingly high (40–50%) (21). The lining of the human gut, known as the enteric nervous system (ENS), contains 500 million nerves and houses the stomach's partially autonomous neurological system. Numerous neurotransmitters are either stored there or produced there. The enteric nervous system (ENS), sometimes known as the "second brain," develops from the same tissue as the central nervous system (CNS). Lifelong interactions between the CNS and ENS cause functional gastrointestinal diseases, mucosal bleeding, inflammation, discomfort, and other bowel symptoms to occur more quickly through the ENS than any other organ. On the other side, several psychophysical illnesses have been linked to poor gut health (22).

2.4. Alcohol

Alcoholism can affect stomach function in several ways, both acutely and chronically (23). Alcohol, for instance, even in very moderate doses, can modify stomach acid output, cause acute gastric mucosal damage. Studies on animals have revealed that high doses of alcohol administration either by mouth or via intravenous route can influence gastric acid output (24). Alcohol may stimulate the stomach mucosa topically (a direct interaction) or it may work via a more general mechanism that affects hormone release and the control of neuronal processes that produce acid. Alcohol misuse is a significant contributor to bleeding (i.e., hemorrhagic) stomach lesions that can obliterate portions of the mucosa. Heavy drinking even once might result in bleeding lesions and mucosal irritation. However, persistent

alcohol consumption disrupts the microcirculation and causes increasing structural mucosal damage. It has been observed that NSAIDs like aspirin and ibuprofen may exacerbate alcohol-induced acute gastric lesions. (23, 25).

2.5. Smoking

Smoking increases the risk of developing gastro-intestinal injury (26). Each puff of cigarette smoke includes between 10^{14} and 10^{16} free radicals which causes damage to the gastrointestinal tract. Apart from that aldehydes, quinones, benzo(a)pyrene, epoxides, and peroxides are among the active substances, and they can trigger the creation of reactive oxygen species and if they are not stabilized, oxidative stress develops, leading to tissue damage. There is evidence that long-term cigarette smoking (those who have smoked for more than two years) may cause an increase in gastric acid output and a decrease in the pH of the stomach. (25, 26).

3. ENDOGENOUS GASTROPROTECTIVE FACTORS AND THEIR REGULATION

The basic physiopathology of gastric ulcer is caused by an imbalance of cytoprotective factors, such as the function of the prostaglandins (PG), mucus-bicarbonate barrier, surface active phospholipids, cell renewal and migration, mucosal blood flow, nonenzymatic and enzymatic antioxidants, and some growth factors, with some endogenous aggressive factors (hydrochloric acid, pepsin, refluxed bile, leukotriene (16). The gastroprotective factors have been described schematically (Fig. 1) The key gastroprotective factors have been described below.

3.1. Mucus Gel

Mucin granules produce mucus gel by their apical extrusion from surface epithelial cells, and it is composed primarily of water (95%) and mucin (5%), which is a by-product of the MUC2 (MUC5AC), MUC5B (MUC5B), and MUC6 (MUC6) mucin genes (27). The gel composition and thickness of the adhering mucus layer determine how effective the mucus is (28, 29). This gel layer is a stable, undisturbed layer that has buffers embedded within it to assist acid surface neutralization and further inhibit the possible diffusion of luminal pepsin molecules (30). Additionally, as fatty acids are structurally connected to the molecules of gastric mucin, the hydrophobicity of these molecules increases, decreasing the back diffusion of H^+ ions.

3.2. Phospholipids

Up to 25% of the dry weight of gastric mucus is made up of lipids, which include neutral lipids, glycolipids, and phospholipids (31). The luminal surface of the mucus is covered with a layer of surfactant phospholipids, which has a strong hydrophobic effect and hinders hydrogen ion transport (28). The phospholipids, glycolipids, and neutral lipids that makeup mucus have the greatest impact on the ability to slow down hydrogen ion transport (32). The protective quality of gastric mucin is determined by phospholipids, which considerably increase the mucus layer's viscosity and permeability (33). Aspirin and bile salts, which are ulcerogenic chemicals, damage the phospholipid layer and mucus gel, leading to mucosal injury (28). Additionally, the mucin-lipid network is proteolyzed and lipolyzed by *H. pylori*, compromising the body's defenses and providing a strong causal link to gastritis, duodenitis, gastric ulcer, and duodenal ulcer (34, 35).

3.3. Trefoil Factor Family (TFF) Peptides

Trefoil factor family peptides (TFF1, TFF2, and TFF3) are important regulators in gastrointestinal tract defense, maintenance, and repair (36). As a result, they have the potential to be therapeutic in the treatment and prevention of many gastrointestinal complications linked to mucosal injury. They are

especially well-known for their roles in the gastrointestinal system, where they control gut homeostasis (37, 38). TFF peptides have a role in the intracellular assembly and packing of mucins and are found in mucin secretory vesicles (39). Through their support of mucosal epithelial restoration and reepithelialization, they contribute significantly to epithelial defenses (39). The mucosal layer's viscosity is increased by TFF2, and the gel network is stabilized (40, 41). TFF1/2 plays its cytoprotective role and reduces the damage in NSAID-induced stomach injury model (42). Only at the maximum dose can monomeric TFF1 greatly lessen the damage, doing so by around 30%, while its homodimeric counterpart does much more significantly lessen the injury by about 70% (43). As a result, they have the potential to treat conditions including gastric ulcers, inflammatory bowel disease (IBD) and gastritis induced by nonsteroidal anti-inflammatory drugs (NSAIDs) (38)

3.4. Prostaglandins (PG)

Endogenous PGs have a role in the control of several gastrointestinal processes that support gastric protection (28). According to studies, PGE_2 enhanced mucus and $HCO3^-$ secretion through Prostaglandin E2 receptor 4 (EP_4) receptors and reduced acid secretion or motility through Prostaglandin E2 receptor 3 (EP_3) or Prostaglandin E2 receptor 1 (EP_1) receptors, respectively (44). PGE_2's ability to limit acid secretion was mediated by EP_3 receptors in two different ways: directly by preventing acid secretion at parietal cells and indirectly by preventing histamine release at enterochromaffin-like (ECL) cells (16). Prostanoids with an affinity for EP_1 receptors reduced gastric motility and shielded the stomach from damage caused by indomethacin, a common NSAID (45). The EP_4 antagonist ONO-AE3-208 was able to mimic the healing-impairment effect of indomethacin, but the EP4 agonist ONOAE1-329 was able to counteract this effect. The etiology of NSAID-induced stomach injury involves neutrophils as well (45). PGE_2 impairs chemotaxis and other neutrophil activities (45). Butaprost and 11-deoxy PGE_1 also had an inhibitory impact on neutrophil migration, but not 17-phenyl PGE_2, sulprostone, or ONONT-012, indicating that EP_2/EP_4 receptors were involved in the anti-neutrophil activity of PGE_2 (46). It's also likely that indomethacin intensified gastric mucosal injury by inhibiting the synthesis of PGI_2 and encouraging leukocyte adhesion to the vascular endothelium (2). It is also known that PGE_2 blocks neutrophil migration by activating EP_4 receptors (47). The repeated injection of indomethacin, following the ulceration in both rats and mice, delayed the healing of the stomach ulcer. The injection of rofecoxib, a COX-2 selective inhibitor, was able to recreate this effect but not SC-560, a COX-1 specific inhibitor (48, 49) indicating that COX-2/PGE2 may be involved in the process of ulcer healing. In fact, COX-2 knockout mice had delayed healing of stomach ulcers (49, 50). Indomethacin, rofecoxib, but not SC-560, reduced the reaction in which the mucosal PGE2 concentration rose following ulcer development. When 11-deoxy PGE_1, an EP_3/EP_4 agonist, was also administered, the delayed healing caused by indomethacin was dramatically sped up. Additionally, the injection of specific EP_4 antagonists on a regular basis, such as ONO-AE3-208 and CJ42794, delayed the healing of stomach ulcers in rats and mice (49).

3.5. Bicarbonate and non-bicarbonate buffers barrier

Bicarbonate is mostly released and maintained inside the mucus gel layer to neutralize the acid and pepsin. It produces the mucus-buffer barrier, which acts as the first line of mucosal defense, and extremely hydrophobic phospholipids to generate a pH gradient from the stomach's and duodenum's very acidic luminal surface to their neutral epithelial surface (30). Bicarbonate production is also stimulated by corticotrophin-releasing factor (CRF), luminal acid, uroguanylin, melatonin, and orexin-A (51). The surface epithelial cells import secreted bicarbonate, which dramatically increases mucosal and surface alkalinity (51). Although bicarbonate buffers have a greater ability to neutralize hydrogen ions and/or gastric acid than other buffers, the gastric and duodenal secretions' non-bicarbonate buffers,

which are primarily made of inorganic phosphates and various proteins/glycoproteins, also play a crucial supporting role (52).

3.6. Mucosal blood flow

Blood flow is crucial for both the preservation of healthy gastric mucosa and the repair of damaged mucosa. By feeding the mucosa with oxygen and HCO_3^- and eliminating H^+ and harmful substances that diffuse into the mucosa from the lumen, blood flow aids in protection (53). High blood flow defends against harmful chemicals, whereas low blood flow puts the mucosa at risk for damage. Increased blood flow that follows superficial mucosal injury promotes healing and stops superficial lesions from becoming deep ones. The hyperemic reaction enhances the supply of $HCO3^-$ to the mucosa and strengthens the mucosa's resistance to back-diffusing H^+ and potent medications like ethanol (adaptive protection) (54).

4. CYCLOOXYGENASE SYSTEM AND COX-DEPENDENT MECHANISM OF ULCER DEVELOPMENT

To maintain the integrity of the stomach mucosal defense, COX-1 and COX-2, which catalyze the production of prostaglandin endoperoxide (PGG_2) and prostanoids from arachidonic acid, must continuously produce prostaglandin E2 (PGE_2) and prostacyclin (PGI_2) (55). Most tissues, such as the stomach, kidney, and platelets, express COX-1, which is involved in the production of prostaglandins in response to physiological stimuli. However, inflammation-related factors trigger COX-2, which then produces prostaglandins that control both the inflammatory response and pain perception. Potent vasodilators PGE_2 and PGI_2 regulate practically every aspect of stomach mucosal defense and repair. Different signaling routes are used by EP receptors; for example, when PGE_2 attaches to and signals through EP_1 or EP_2 EP_4 receptors, respectively, it raises intracellular Ca^{2+} or cyclic adenosine monophosphate (cAMP) and when it signals through EP3 receptors, it reduces cAMP (44). Laboratory animal experiments have demonstrated that COX-1-dependent PGE_2 depletion reduces stomach mucosal blood flow whereas COX-2 suppression increases leucocyte adhesion (56). COX-1 or COX-2 knockout mice treated with selective COX-1 or selective COX-2 inhibitors do not have spontaneous gastrointestinal injury despite little prostaglandin production. However, when both isoenzymes are stopped at the same time or when an NSAID is administered, they have severe stomach lesions (57, 58). On the other hand, selective inhibition of either COX-1 or COX-2 is ulcerogenic in compromised stomach mucosa (such as after acid challenge, inhibition of nitric oxide generation, or ablation of afferent neurons) (59). Researchers have found a strong correlation between NSAIDs' capacity to inhibit stomach prostaglandin formation and their capacity to induce ulcers. (But not always), and preference for COX-1 over COX-2. An NSAID's potential to produce bleeding issues may be primarily determined by the inhibition of platelet COX-1, which also causes reduced thromboxane synthesis and increased bleeding tendency. COX-2 expression is low in healthy stomachs, in contrast to COX-1, which is prevalent in the stomach's mucosa. However, COX-2 is quickly elevated following damage or the presence of ulcers or when COX-1 is blocked (60). When COX-2-produced prostaglandins are insufficient, COX-1-derived prostaglandins take on more significance even though Prostaglandins generated from COX-2 are the main mediators in the recovery of gastric ulcers. (by encouraging epithelial cell proliferation and angiogenesis mediated by growth factors) (61). In contrast to rats, where only COX-2 is upregulated, COX-1 and COX-2 are both overexpressed in the edges of gastric ulcers in humans (62, 63). Schmassmann et al. used knockout mice to show that combined inhibition of COX-1 and COX-2 worsened ulcer healing compared to selective COX-2 inhibition, but suppression of COX-1 had no impact on ulcer healing (61). Starodub et al. found that COX-1 knockout mice with superficial gastric injury had delayed healing and restoration, indicating that COX-1-produced PGE_2 may be a

possible mediator of gastric protection against the early events that cause gastric damage progression (64). It has been demonstrated that selective and nonselective COX inhibitors both slow the healing of ulcers in humans. In line with the outcomes of animal investigations, Dikman et al. demonstrated that in comparison to aspirin or celecoxib, naproxen significantly prolonged the time it took for human volunteers' iatrogenic ulcers to heal. (5).

5. COX-INDEPENDENT MODE OF GASTRIC MUCOSAL INJURY

Previously it was thought that NSAIDs function their actions by inhibiting COX-1 and COX-2 activity. Both isoforms are key enzymes for the biosynthesis of prostaglandin. COX-1 is constitutively expressed in gastric mucosa synthesizing the prostaglandin which is mainly responsible for maintaining gastric mucosal integrity. COX-2 on the other hand, is inducible and synthesizes prostaglandin at the site of inflammation. Some NSAIDs, such as indomethacin and ibuprofen, block both COX isoforms, that damage the gastric mucosa. On the other hand, celecoxib, rofecoxib and other COX-2-specific inhibitor were supposed to be not pernicious for the gastric mucosa. But several contradictory reports are available. Even COX-1 knockout mice have been demonstrated to have gastric mucosal damage when given NSAIDs, which is not possible unless NSAIDs are involved in some other mechanism of gastric mucosal damage apart from COX inhibition. Thus, the search for a novel pathway of NSAID-mediated damage was investigated. Mitochondrial pathology as a consequence of NSAID- treatment and the subsequent oxidative stress and apoptosis are considered to be the major perpetrators of NSAID-induced gastropathy. Electron paramagnetic resonance studies of NSAIDs on sub-mitochondrial particles revealed that indomethacin bound to an area near Complex I and ubiquinone to generate radical species. Thus, a prostaglandin-independent pathway is evident in NSAID-induced gastropathy. The major aspects of the COX-independent mode of gastric mucosal injury have been highlighted below.

5.1. *Mitochondria as the gatekeeper of gastric mucosal barrier and luminal function*
Maintaining healthy mitochondria is crucial for cellular physiology. By controlling crucial activities including energy generation, maintaining intracellular calcium levels, and most significantly, regulation of cell death, mitochondria, the primary intracellular signaling center, control cellular lifespan and bioenergetic state (65, 66). Due to the high energy demand for preserving the stomach function and cellular turnover, to replace the continuously shedding gastric mucosal surface, mitochondrial wellbeing is essential for sustaining gastric mucosal integrity. Therefore, mitopathology might be a key factor contributing to the development and/or recurrence of gastric mucosal damage. Numerous internal and external cues can start the mitochondrial route of apoptosis, which eventually causes cellular death (67). When the mitochondrial electron transport chain (ETC) fails, an intracellular redox imbalance results, which strongly correlates with the beginning of mitochondrial apoptosis. Through the release of cytochrome c and stimulation of Ca^{2+} signalling, indomethacin in vitro promotes apoptosis in gastric mucosal cell line (68, 69). Studies indicate that NSAIDs considerably contribute to the apoptotic death of gastric mucosal cells by activating the mitochondrial death pathway (17). Different mechanisms of cell death are activated by the production of reactive oxygen species (ROS) (72), which is followed by the release of proteins from the mitochondria (73). Additionally, mitochondrial protein release is linked to increased ROS generation by this organelle (74). In addition to being a significant generator of ROS in aerobic cells, mitochondria are also a susceptible target for ROS's harmful effects. Increased mitochondrial ROS production can result in oxidative damage to cellular macromolecules such as nucleic acids, lipids, and proteins as well as a reduction in cellular antioxidants, all of which can induce cellular injury (75, 76). Numerous components of the mitochondrial death pathway have been implicated in the beginning of gastric mucosal cell death during NSAID-induced gastropathy (17, 77). The outcome was the production of MOS, which is linked to inflammation, and mitochondrial

malfunction. Through specific chemical pathways, reactive oxidants produced from mitochondria serve as signal-transducing molecules that amplify the up-regulation of certain inflammatory cytokine subsets (78, 79). Inflammatory diseases are frequently induced by the production of free radicals and tissue damage caused by reactive oxidants (80, 81). One characteristic event in the beginning of inflammation is the recruitment of leukocytes to the particular tissue location. Mazumder et al. have demonstrated that one of the most important processes behind NSAID-induced gastric cell death is abnormal mitochondrial fission. This is mostly because of the unfavourable activation of DRP1, which plays a role in both initiating fission and promoting apoptosis. Targeting abnormal mitochondrial dynamics and contextually modulating hyper fission can undoubtedly aid in enhancing the therapeutic utility of NSAIDs. Furthermore, they have demonstrated that NSAIDs induce mitochondrial hyper fission to induce apoptosis in both gastric cancer and normal gastric mucosal cells (17).

5.2. *Redox perturbation and induction of mitochondrial damage toward bioenergetic crisis*

Since mitochondrial redox dyshomeostasis is the primary sub-cellular source and sink of many oxygen and nitrogen-mediated free radicals, it spreads from afflicted cells to the entire tissue. By negatively signaling nearby healthy mitochondria in gastrointestinal diseases, oxidative stress causes downstream cytopathology (2, 82, 83). Despite their therapeutic use, NSAIDs are cytotoxic agents, as was already mentioned. NSAIDs can induce the cytopathological condition known as mitochondrial oxidative stress (MOS), which is characterized by significant mitochondrial damage carried on by the activation of harmful redox-active chain responses, severe bioenergetic crisis, and ultimately cell death. The role of mitochondrial oxidative stress in NSAID-induced gastric mucosal damage has been depicted schematically (Fig. 2). The primary target of NSAIDs is the mitochondrial electron transport chain (ETC) complex-I. Notably, among the NSAIDs, diclofenac is the most effective at suppressing ETC complex I activity, which results in electron leakage from the respiratory chain (84). The reactive oxygen species (ROS) progenitor superoxide, $O_2^{\cdot-}$, is produced when molecular oxygen undergoes a partial reduction due to the leaky e^- (85). The mitochondrial super oxide dismutase, SOD2, instantly converts intra-mitochondrial $O_2^{\cdot-}$, which is membrane impermeable, to H_2O_2 as a defense mechanism against oxidative stress. Due to its membrane permeability, H_2O_2 exits the mitochondria (before being neutralized), oxidizing cellular macromolecules including DNA, protein, lipids, and carbohydrates and making them inactive. In the mitochondria, $O_2^{\cdot-}$ destroys several Fe-S cluster proteins, such as aconitase and cytochrome c, causing the release of $Fe2^+$, which then interacts with H_2O_2 via the Fenton reaction to form the most harmful ROS, the hydroxyl radical ($\cdot OH$) (86). All of these events disrupt the cellular redox equilibrium, which activates the intrinsic apoptotic pathway. Additionally, increased ROS causes mitochondria to depolarize and adversely shifts the balance of mitochondrial structural dynamics toward hyper-fission (17). NSAIDs further increase mitochondrial clearance that is ubiquitination-dependent.
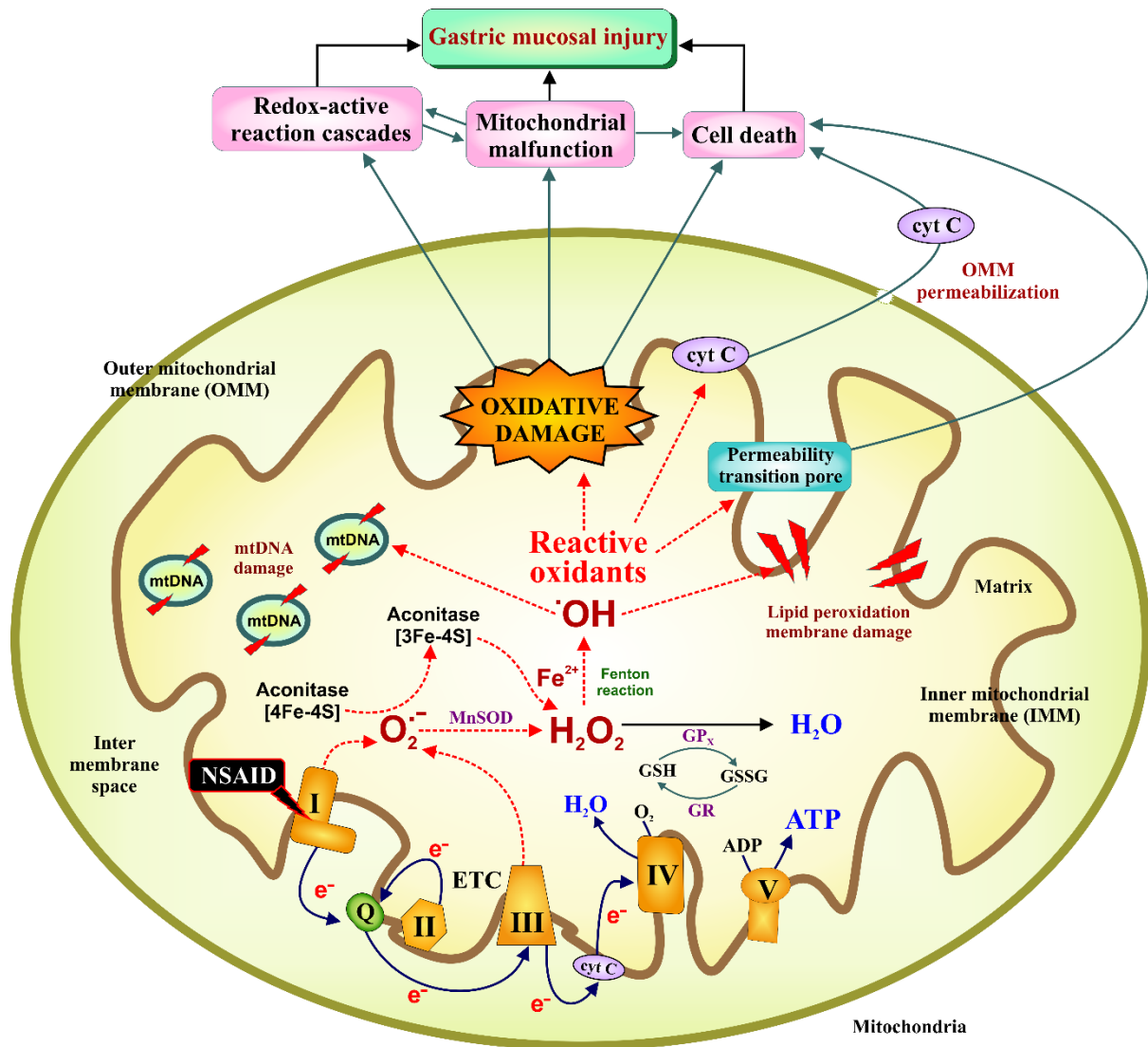
Fig. 2. **Summary of NSAID-induced generation of reactive oxygen species in mitochondria resulting in cellular damage.** NSAIDs initiate the leakage of electrons from complex I in the electron transport chain, leading to incomplete reduction of molecular oxygen and the production of superoxide ($O2^{.-}$). Superoxide serves as the precursor for most reactive oxygen species (ROS) and is rapidly converted to hydrogen peroxide (H_2O_2) by the enzyme superoxide dismutase (SOD_2). In the presence of transitional metals like iron (Fe^{2+}), H_2O_2 can be converted into hydroxyl radicals ($HO^{.}$). Glutathione peroxidase (GPx) can scavenge H_2O_2 in the presence of glutathione (GSH), which is then regenerated from its oxidized form (GSSG) by glutathione reductase (GR) with the help of NADPH. The accumulation of ROS leads to a decrease in mitochondrial membrane potential ($\Delta\Psi m$). Reactive radicals react with biomolecules such as membrane lipids, proteins, and mitochondrial DNA, resulting in the production of lipid peroxides, protein carbonyls, and DNA damage. The release of cytochrome C from damaged mitochondria into the cytosol occurs through the permeabilization of the outer mitochondrial membrane (OMM) and activates the apoptotic pathway. These interconnected events contribute to a wide range of cellular pathologies. The dotted arrows indicate harmful reactions involving free radicals. This figure is adapted from Bindu *et. al.* (2).

In this way, MOS causes tissue inflammation, which acts as a positive feedback loop when there are ongoing insults that harm the organs.
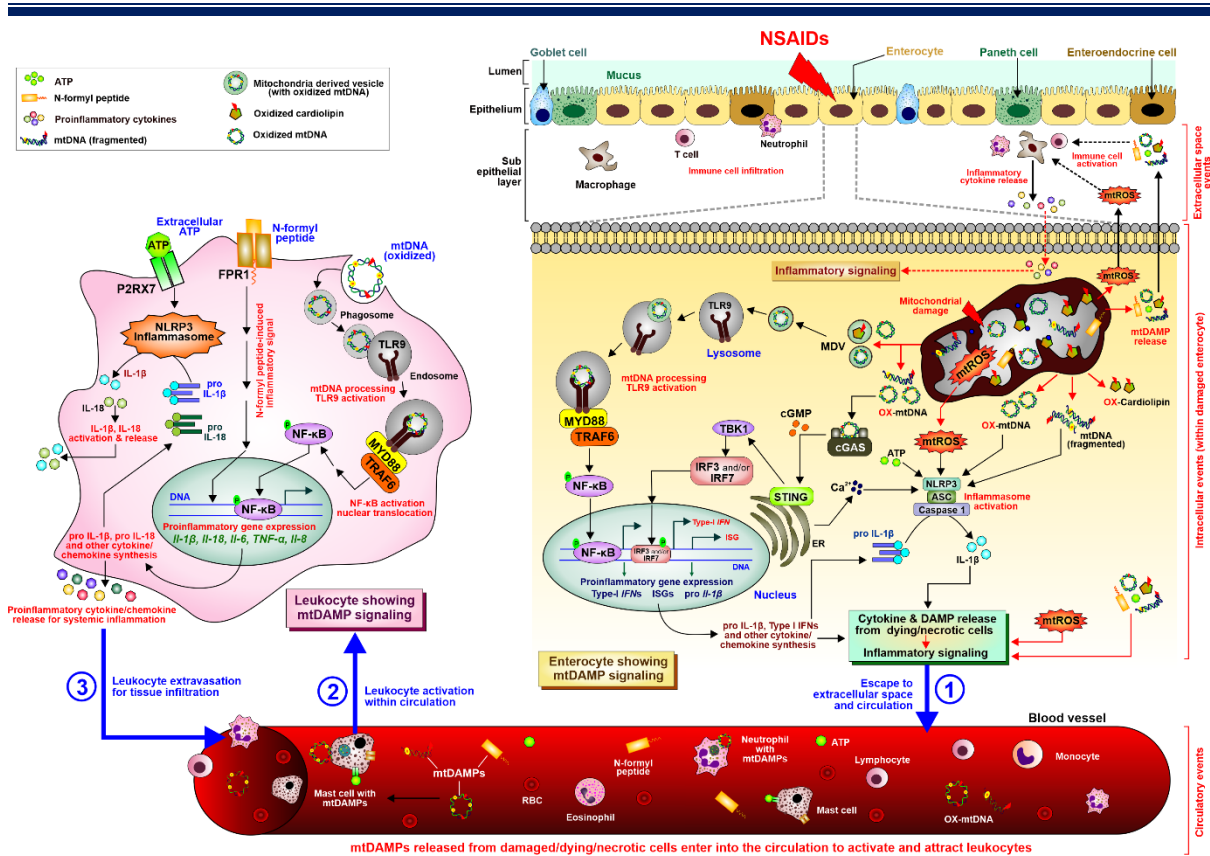
Fig. 3. Gastrointestinal pathogenesis involves a signaling process called Mitochondrial DAMPs-associated signaling. Various harmful factors from both internal and external sources can cause damage to mitochondria, resulting in the release of mitochondrial DAMPs (mtDAMPs). These mtDAMPs primarily activate three pathways that lead to inflammation. In the enterocytes, oxidized mitochondrial DNA (OX-mtDNA) is released into the cytosol, enclosed within structures called mitochondria-derived vesicles (MDVs). These MDVs are then taken up by lysosomes, where Toll-like receptor 9 (TLR9) is activated. This activation subsequently triggers downstream signaling through MYD88-TRAF6, ultimately leading to the activation of NF-κB, a key regulator of inflammation. The second pathway involves the activation of cytosolic cGAS-STING signaling by freely available OX-mtDNA. This activation stimulates interferon regulatory factors (IRFs), which in turn enhance the production of type-1 interferon and consequently promote inflammation. The third pathway involves the activation of NLRP3 inflammasome by OX-mtDNA, which occurs in the presence of mitochondrial reactive oxygen species (mtROS) and ATP. This activation leads to the production and release of active IL-1β from dying or necrotic mucosal cells, triggering inflammation. Additionally, mtDAMPs released from the damaged mucosal cells enter the bloodstream and bind to receptors on the surface of leukocytes. This binding activates pro-inflammatory cytokines and chemokines, facilitating the extravasation of leukocytes into the damaged gastrointestinal mucosa. The inflammatory signaling within leukocytes involves multiple pathways, including OX-mtDNA-mediated activation of TLR9, ATP-mediated activation of NLRP3 inflammasome, and mitochondria-derived N-formyl peptide-mediated expression of inflammatory genes. Activated leukocytes produce more pro-inflammatory cytokines and chemotactic factors, further promoting the recruitment of inflammatory cells in the inflamed gut. The damaging stimuli to enterocytes primarily involve factors derived from harmful bacteria (pathobionts) that cause damage to the intestinal barrier function. Mitochondrial dysfunction and a decline in cellular energy production exacerbate gut inflammation. The escape of DAMPs and inflammatory cytokines into the extracellular space and circulation from enterocytes represents deleterious events indicated as "1" in the figure. Similarly, deleterious events in leukocytes leading to leukocyte activation and release of inflammatory cytokines are indicated as "2". Extravasation of leukocytes for tissue infiltration is indicated as "3". Inset indicates various DAMPs involved here. These events occur concurrently. The figure is adapted from Mazumder and Bindu *et. al.* (3).

5.3. *Canonical inflammation and inflammasome activation in damaged mucosa: role of mtDAMPs*

It is important to focus on the involvement of macromolecular signals obtained from damaged mitochondria that underlie the activation of the inflammatory cascade that causes gastric tissue injury. DAMPs are endogenous molecular fingerprints that, in the absence of any pathogenic stimulus, cause sterile inflammation and frequently trigger autoimmune reactions. S100A calgranulins, heat shock proteins, HMGB1, interleukins (IL-1, IL-33), calprotectin, Tenascin-C, lactoferrin, hyaluronan, Galectin, and ATP are just a few of the DAMPs that have been implicated in the pathophysiology of gastric system. Gastric mucosal injury has been linked to a variety of mitochondria-derived factors, often known as mtDAMPs, including mtDNA and other mitochondrial components such as mitochondria-derived formyl peptides and oxidized cardiolipin (87). These DAMPs cause inflammatory reactions because their respective pattern recognition receptors (PRRs) identify them. Surprisingly, DAMPs can potentially be used as disease progression biomarkers. The pathophysiology of peptic ulcer is tightly entwined with bioenergetic crisis (caused by mitochondrial ETC malfunction) and cell death. Dying cells (mostly necrotic epithelial cells) communicate with the local phagocytic cells by sending them "eat me" signals to activate them and help clean the area of the cellular debris. After activation, phagocytic cells (mostly neutrophils and macrophages) secrete proinflammatory cytokines, which further encourage inflammatory cells from capillaries to invade the area of injury. Additionally, in a context-dependent way, the expression of pro-inflammatory genes originating from NF-κB enhances the progression of acute to chronic inflammation (88). In this cycle, dying cells also emit DAMPs, sometimes known as "alarmins." During necrotic and other types of cellular injuries, cell-free oxidized mtDNA is a typical example of mtDAMP, which is first released in the cytosol of the injured cell upon mitochondrial damage and then transported to the extracellular milieu either through mitochondrial-derived vesicles (MDVs) or through mitochondrial permeability transition pores (MPT). These mtDNA ultimately enter the circulation. In gastric mucosal injury, the gastric epithelial cells mainly undergo cellular injury thereby releasing mtDNA. The role of mtDAMPs-related molecular signaling in NSAID-induced gastric mucosal injury has been shown schematically (Fig. 3). The initial catalyst for cyto-damage may or may not come from mitochondria. However, once mitochondrial damage starts, a pathological chain of events develops that intensifies the damage in a never-ending loop. The sections that follow focus on certain mtDAMPs and precisely detail how they contribute to tissue inflammation. The most well-known effect of multifactorial redox disturbance is mtDNA oxidation. The resulting MOS oxidizes mtDNA to a degree beyond the ability of the mitochondrial base excision repair DNA glycosylase, 8-OH-dG DNA glycosylase (OGG1) to repair it. In fact, significant 8-OHdG levels were observed in the mucosal samples of UC patients (89). OGG1 serves as the primary mitochondrial base excision repair enzyme, hence its expression or activity being lost or inhibited is directly linked to an increase in 8-OHdG levels. OGG1 depletion and 8-OH-dG accumulation in mtDNA during the onset of GI pathology have a complex molecular foundation that is still unknown. Similar to this, there is currently no direct evidence of mtDNA oxidation or of OGG1's potential cytoprotective involvement in the etiology of gastric mucosal disease. In our recent study, indomethacin was observed to trigger the inflammasome pathway by activating NLRP3-Caspase1- IL-1β axsis pathway in rodent gastric mucosa (77). The activation of inflammasomes is caused by cytosolic mtDNA. The affected/dying cells eventually release oxidized mtDNA (OX-mtDNA) into the cytoplasm, which is followed by extracellular release. OX-mtDNA-containing MDVs can merge with lysosomes in the cytosol, where mtDNA can activate PRRs such as toll-like receptor 9 (TLR9) and cause nuclear translocation of NF-κB for the activation of inflammatory genes (Fig. 3). Additionally, mtDNA found in the cytosol can directly connect to and activate the NLRP3 inflammasome, which in turn causes the production of pro-inflammatory IL-1 and IL-18 (90). It is important to note at this point that the inflammasome is a multiprotein complex of the innate immune system that is essential for the release of the pro-inflammatory cytokines IL-1 and IL-18 and the caspase 1-dependent proteolytic

processing of these two essential cytokines. AIM2, NLRP1, NLRP3, and NLRC4 are among the inflammasomes that particularly function in various physiological and pathological contexts (91). Due to the important function of NLRP3 as a sensor for microbial signals and endogenous DAMPs (including those generated from mitochondria), NLRP3 inflammasome activation is strongly linked to IBD in terms of GI pathophysiology (92). OX-mtDNA (the ultimate ligand), ATP, ionic flux ($Ca2^+$, Na^+, and K^+), lysosomal damage, and even mtROS are among the several endogenous activators of NLRP3 (91). These activators cause the development of the inflammasome complex, where NLRP3 interacts with the bipartite adaptor apoptosis-associated speck-like protein (ASC), which in turn recruits pro-caspase 1 to the inflammasome complex for the processing of IL-1 and IL-18 (93). While IL-1β is linked to the transcription of several pro-inflammatory genes required for immune cell infiltration, IL-18 is crucial for the generation of interferon-gamma (IFN- γ), which in turn regulates the intensity of inflammation as seen in colitis (94). In leukocytes and injured gut cells, circulating mtDNA acts as an inflammasome activator. In addition to activating the intracellular inflammasome (inside the damaged enterocytes), mtDNA released into the bloodstream also activates TLR9 in dendritic cells and neutrophils, resulting in the generation of proinflammatory cytokines and a corresponding systemic inflammatory response (95). Neutrophils, macrophages, and NK cells, among others, are tissue-resident/infiltrated and circulating leukocytes that recognize mtDNA and take it up; this leads to the activation of TLR9 on those leukocytes. Mitogen-activated protein kinase (MAPK) and NF-κB dependent pro-inflammatory pathways are both activated by TLR9 signalling, which results in systemic inflammation.Additionally, mtDNA promotes the cyclic GMP-AMP synthase (cGAS)-stimulator of interferon genes (STING) pathway, which in turn stimulates the IRF3 and IRF7 interferon regulatory factors. This enhanced type-1 interferon response causes systemic inflammation (96). These pathways may occur in injured enterocytes (with cytosolic mtDAMP accumulation) as well as stimulated leukocytes in the blood or injured tissue, releasing pro-inflammatory cytokines/chemokines (like IL-1β, IL-6, IFNs, TNF-α, etc.) to further potentiate inflammation as well as cyto-damaging factors causing tissue injury. The two obvious commonalities across the several pathways that mtDAMPs appear to activate are activation of NF-κB signaling and increase of IL-1β (3). Most notably, mtDAMP signaling results in the production of pro-inflammatory cytokines, which in turn activate MOS and cause a vicious positive feed-forward loop that is visible in gastrointestinal diseases.

5.4. *Mitochondrial structural damage and aberrant mitophagy*

The compromised structural dynamics of mitochondria and the inability of the quality control system (mitophagy) to get rid of the damaged-fragmented mitochondria that have accumulated as a result of oxidative stress point to yet another important feature of mitochondrial participation in gastric mucosal pathophysiology (97). The opposing actions of fusion and fission, which occur in mitochondria, fine-tune the organellar state at any given time. Mitochondria live in a state of dynamic structural equilibrium. Mitochondria may fuse in response to a cell's bioenergetic needs (98, 99). Even under low levels of stress, nearby mitochondrial particles combine to produce enough ATP to get through the crisis, reducing the severity of the local functional change. As a coping mechanism for the crisis, damaged mitochondria merge with nearby healthy mitochondria (98). Acute stress, on the other hand, causes the mitochondrial reticular network to collapse. To remove injured organelles from the cell, a wave of depolarization travels over the filament and destroys the mitochondrial network. Here, the detrimental effects of abnormal mitophagy and aberrant mitochondrial dynamics in endangering the integrity of gastric mucosal tissue following multifactorial toxic exposures have been emphasized. Loss of mitochondrial structural dynamic equilibrium has been demonstrated to promote mucosal inflammation and tissue damage in gastric mucosal injury (22, 100). In response to NSAID treatment and acute mental stress, recently it has been observed that stomach mucosal cells undergo oxidative stress-induced mitochondrial hyper-fission (17, 22). The role of mitochondrial dynamics in NSAID-
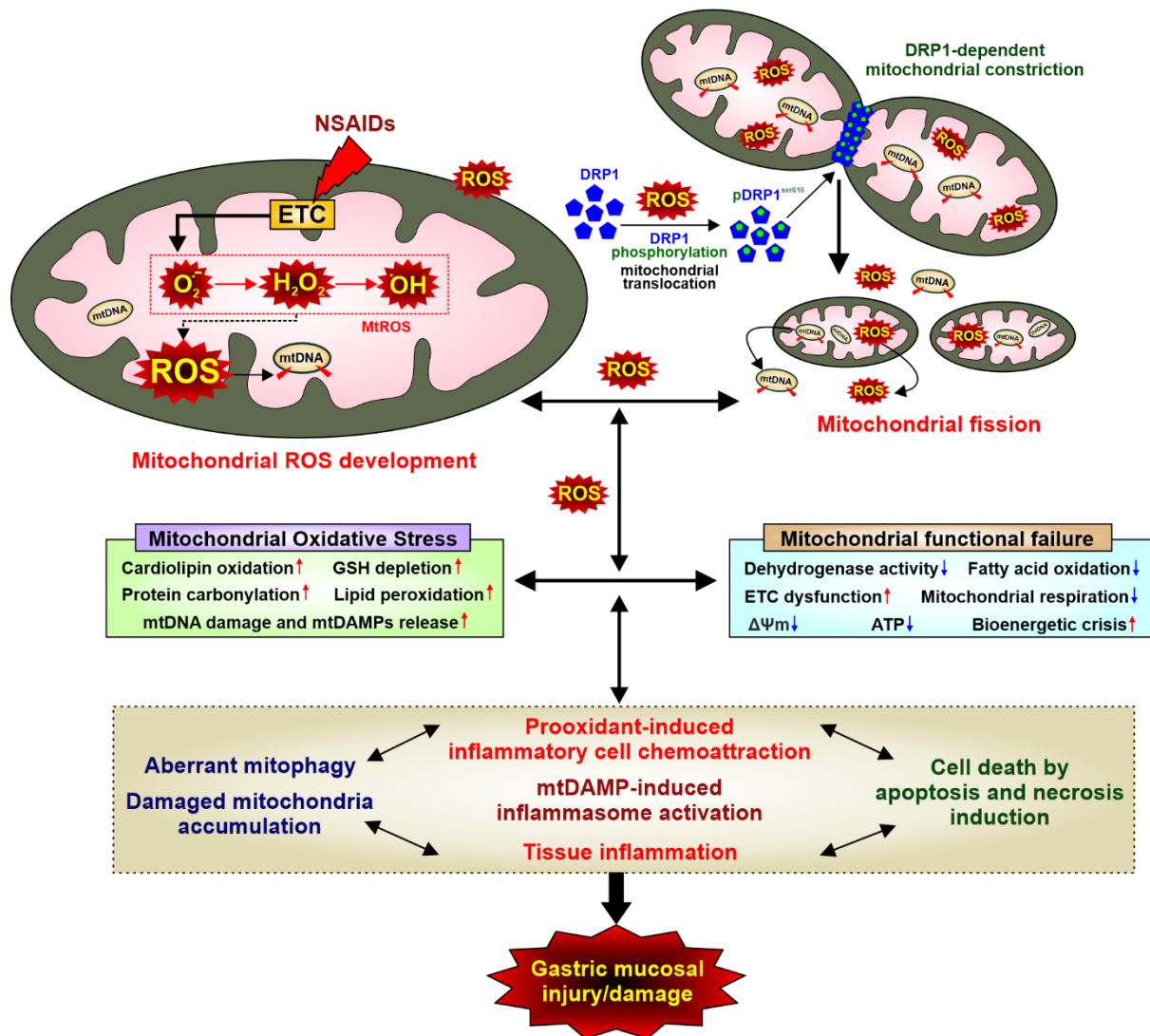
Fig. 4. **The connection between mitochondrial oxidative stress (MOS), abnormal mitochondrial dynamics, mitophagy, and cell death in gastric mucosal injury.** MOS occurs as a result of damage to the mitochondrial electron transport chain (ETC), leading to an imbalance in redox reactions within mitochondria. This oxidative stress disrupts the normal process of mitochondrial fission and fusion, causing fragmentation of mitochondria. This fragmentation exacerbates MOS and induces a state of mitochondrial metabolic and bioenergetic crisis, ultimately resulting in apoptosis, a form of programmed cell death. The generation of MOS and the consequent mitochondrial damage also triggers the release of mitochondrial DAMPs, which are molecules that activate immune responses and promote inflammation. This inflammation further contributes to the pathogenesis of gastrointestinal conditions. Moreover, the quality control mechanism responsible for removing dysfunctional mitochondria, known as mitophagy, becomes dysregulated in this context. Aberrant mitophagy leads to the accumulation of dysfunctional mitochondria within cells, amplifying the overall mitochondrial damage. This accumulation of damaged mitochondria eventually triggers cell death and consequently, causes gastrointestinal injury. The figure is adapted from Mazumder and Bindu *et. al.* (3).

induced gastric mucosal injury has been shown schematically (Fig. 4). In this instance, NSAID-mediated ETC malfunction and subsequent O_2^- buildup that causes MOS may be the primary cyto-damaging trigger. However, the cellular pathology is orchestrated in a harmful feed-forward loop by MOS-mediated raised mitochondrial fragmentation, mitochondrial depolarization, and failure of the quality control system to remove the damaged mitochondria in front of tenacious cyto-damaging stimuli. These have been found in gastric mucosal injury (77, 82, 97). In addition to MOS, it has been

observed that H. pylori infection causes gastric epithelial cell death as a result of increased mitochondrial fission, which is caused by the pathogenic bacteria's vacuolating cytotoxin A (VacA), which activates the mitochondrial fission machinery (101). During oxidative stress, it has also been observed that mitochondrial fusion mediators, such as outer membrane fusogenic GTPases (mitofusin 1 and 2) and inner membrane proteins (OPA1), are decreased in the rat stomach mucosa. Uncontrolled fusion is harmful and is linked to many diseases, even though excess fission is the predominant manifestation of oxidative mitochondrial damage. In the course of GI illness development, increased fusion and its pathological connection are still obscure. Since fusion occurs before fission (when the degree of damage is low and the mitochondria are attempting to resist the insult), mechanistic studies on the function of abnormal mitochondrial dynamics in GI pathologies should be precisely and carefully designed to track the early, subtle transient events. To rationally target the complex molecular players for mitochondria-based next-generation gastroprotective drug developing, the intricate molecular players should be thoroughly deconstructed.

6. GASTRIC MUCOSAL CELL DEATH DURING GASTROPATHY: INVOLVEMENT OF APOPTOSIS, NECROSIS, FERROPTOSIS

6.1. Apoptosis

Recent research has focused on the regulation of cell death as a second important mitochondrial function in addition to energy metabolism (102). Reactive oxygen species (ROS), which are mostly produced in Complex I and III of the respiratory chain in the mitochondria, are primarily derived from the mitochondrial respiratory chain. More significantly, the mitochondrial respiratory chain serves as a crucial target for ROS's harmful effects. The release of pro-apoptotic factor, cytochrome c, which can trigger the activation of caspases and cause apoptosis., is significantly influenced by ROS from mitochondria. The primary target of NSAIDs is intracellular organelle mitochondria. To dissipate the mitochondrial transmembrane potential (MTP), NSAIDs inhibit or uncouple oxidative phosphorylation. This causes the release of ROS like superoxide ($O_2^{\bullet-}$) and hydrogen peroxide (H_2O_2), the activation of caspase 9 and caspase 3, and cellular lipid peroxidation, all of which lead to cellular apoptosis (103-105). Increased permeability and resultant mucosal injury were caused by the uncoupling of mitochondria, which also caused a drop in intracellular ATP content, Ca^{2+} leakage from mitochondria, cellular osmotic imbalance, and a loss of control over intracellular junctions (106). Some NSAIDs, such as salicylic acid or diclofenac, can cause the mitochondrial permeability transition (MPT), which decouples mitochondrial respiration from ATP synthesis (107). Indomethacin causes mitochondrial pathology, a degradation of the structure and function of the mitochondria, which results in mitochondrial oxidative stress and the production of intramitochondrial reactive oxidants. In addition to gastric mucosal cells, NSAIDs also cause apoptosis in other gastrointestinal cells (108). The mucosal cells underwent apoptosis after receiving modest dosages of indomethacin over an extended period (109). However, in vivo, results indicate that the pathogenesis of NSAID-induced gastropathy may be significantly more affected by the activation of apoptosis (77, 86). It has been discovered that NSAIDs, such as aspirin, celecoxib, sodium diclofenac, and indomethacin, cause the stomach mucosal cells to undergo apoptosis (17, 86, 110, 111). The NSAID-induced mucosal apoptosis is thought to be mediated by reactive oxidants, specifically TNF- and NO produced by nitric oxide synthase-2 (iNOS) (69, 112). NOS-2 is thought to take part in the cascade of apoptotic signals that are amplified (112). The majority of NSAIDs work by blocking the COX enzymes that are involved in the generation of prostaglandins. However, when prostaglandin is given exogenously, it is unable to stop the NSAID-induced apoptotic DNA fragmentation. Furthermore, there is frequently a sizable difference between an NSAID's ability to inhibit COX-1 and/or COX-2 and its ability to suppress the proliferation of tumour cells both in vitro and in vivo. This reveals a distinct mechanism implicated in gastric mucosal apoptosis other than the

suppression of prostaglandin production (113, 114). However, the addition of caspase inhibitors significantly lowers the amount of DNA fragmentation and apoptosis caused by NSAIDs, indicating that caspases are involved in NSAID-mediated mucosal apoptosis (69, 113). Recent research demonstrates that the mechanism of indomethacin-induced mucosal cell apoptosis is driven by the release of cytochrome c from mitochondria and subsequent activation of caspase-3-like protease (69). Indomethacin causes the release of cytochrome c from the mitochondria to the cytosol, albeit the exact process is still unclear. The activation of caspases during the induction of apoptosis may depend on the release of cytochrome c (69). Stomachs that are exposed to NSAIDs regularly get tolerant to their gastro toxicity. Aspirin strongly promotes apoptosis in the surface epithelial and glandular compartments of the rat stomach after a single exposure. On the other hand, animals receiving chronic or recurrent aspirin administration have considerably less severe levels of apoptosis in their stomachs. The stomach adapts to the harm caused by aspirin when it is administered repeatedly, and resistance to apoptosis is thought to be the mechanism underpinning this adaptation (115).

6.2. Necrosis

According to the parameters of the therapy, In primary culture, NSAIDs cause the necrosis of guinea pig stomach mucosal cells. Short-term high concentrations of NSAIDs and long-term low concentrations of NSAIDs cause necrosis in the cells (109).

6.3. Ferroptosis

A unique kind of regulated cell death (RCD) called ferroptosis is frequently associated with lipid peroxidation and iron build-up. Ferroptosis differs from apoptosis, autophagy, and necroptosis in that it has particular pathological traits and biological processes. Ferroptosis has garnered interest on a global scale ever since it was initially presented in 2012. Ferroptosis has a role in the course of many diseases and may one day serve as a brand-new therapeutic target. Significant progress has been made in understanding the relationship between ferroptosis and gastrointestinal diseases, such as NSAID-mediated gastric mucosal injury, intestinal ischemia/reperfusion injury, gastric cancer (GC), inflammatory bowel disease (IBD), and colorectal cancer (CRC) (116). Recently, compelling evidence has shown that ferroptosis also plays a significant role in the manipulation of gut health. Numerous studies have demonstrated a connection between the oxidative stress induced by NSAIDs and the ferroptosis they cause and damage to the stomach mucosa. A controlled type of cell death known as ferroptosis is characterized by the loss of the lipid repair enzyme glutathione peroxidase 4 (GPX4) and the disorderly build-up of lipid peroxides, which are primarily driven by lipid hydroperoxides (117). First, the deposited lipid peroxides prevent COX-1 and PGE2 from protecting the gastric mucosa by inhibiting their expression. They also encourage the Fenton reaction, which further compromises the integrity of the gastric mucosa by promoting the production of free radicals and lipid peroxides. Second, the accumulating peroxides decrease glutathione (GSH) and GPX4 antioxidants and suppress the expression of antioxidant genes, speeding ferroptosis and causing mucosal injury (118). To treat the damage to the stomach mucosa, it is crucial to remove lipid peroxide accumulation and to prevent oxidative stress and ferroptosis (119).

7. MITOCHONDRIA AS THE SUB-CELLULAR TARGET FOR NEXT-GENERATION GASTROPROTECTIVE DRUG DISCOVERY

Acid-neutralizing formulations, proton pump inhibitors, and histamine 2 receptor antagonists are the mainstays of established gastroprotective methods. The idea that acid aggravates injuries serves as the main foundation for this method. It is also indisputable that acid, in addition to promoting medicine absorption and mineral metabolism, safeguards the GI tract against opportunistic pathobiont

colonization. Uncontrolled acid suppression produces serious long-term negative effects, such as parietal cell hyperplasia and stomach cancer brought on by hypergastrinemia (120). Other significant negative effects include colitis, hypomagnesemia, pneumonia, vitamin B12 deficiency, increased risk of gut dysbiosis, fractures, acute interstitial nephritis, subacute cutaneous lupus erythematosus, dementia, and pernicious anemia (120). There is therefore a need for an alternate gastroprotective technique because the acid-suppressive form of gastroprotection appears to be dangerous. Protecting mitochondria is undoubtedly a safer course of action because mitochondrial dysfunctions play a critical role in the regulation of GI diseases. Therapeutic approaches that target mitochondria precisely, however, fall well short of the ideal. Due to the precise tuning of the gut-brain axis by mitochondrial health and integrity, protecting gut mitochondria would also be a viable technique for stress management. The gastroprotective effects of many antioxidants including curcumin, gallic acid, melatonin, phenyl-alpha-tert-butyl nitrone (PBN), and neem against NSAID-induced gastropathy have already been demonstrated (6, 19, 121). In addition, morin and apple peel polyphenols have been found to have cytoprotective effects (122, 123). These compounds' mitochondriotropic properties help to reduce excessive mtROS levels. Resveratrol, curcumin, quercetin, and epigallocatechin-3-gallate are the phyto-polyphenols that have been most thoroughly studied because of their multi-organ protective effects shown in a variety of disorders (124). Additionally, caffeic acid (a derivative of hydroxycinnamic acid) and gallic acid (a derivative of hydroxybenzoic acid) are recognized for their metal-chelating and chain-breaking antioxidant properties (124). Studies showed their effectiveness against MOS-related inflammatory tissue damage while not being specifically targeted at mitochondria. However, difficulties with phyto-compound bioavailability as well as a lack of knowledge about the particular molecular targets and the active pharmacophore strongly encourage additional mechanistic investigations.

7.1. Mitochondria targeting compounds: efficacy and safety considerations

It is important to note that synthetic mitochondrially-targeted antioxidants (MTAs) and mitoprotective drugs had promising outcomes in several preclinical models, despite the valid concerns surrounding target specificity, bioavailability, and precise information of pharmacophore (125). Even clinical studies for several substances have been conducted for various ailments (126). In general, mitochondrial protection by synthetic compounds relies on two approaches: a) nonspecific approaches (using synthetic ROS scavengers that include various analogs of SOD-CAT mimetic like salen Mn complexes) and b) specific mitochondrial targeting by mitochondriotropic compounds. In the latter case, targeted delivery of antioxidants to mitochondria mostly relies on five strategies, including (1) conjugation to lipophilic cations (such as triphenylphosphonium, tetraphenylphosphonium, hemi-gramicidin S-moieties, rhodamine 123, certain anthracyclins, and flupiritine), (2) peptide-based targeting (which uses SS and XJB peptides), (3) delivery of liposomal packaging (using colloidal dequalinium vesicles), (4) mitochondria-specific bioactivation reactions. (5) Targeting utilizing Mn porphyrins and MnSOD mimics (127, 128). These methods are used in varying degrees (while taking into account the many subtleties of mtROS-producing processes) to produce a variety of mitoprotective drugs for preclinical testing in various disease models (128-130). Natural antioxidants like vitamin E, curcumin, ginkgo biloba, and melatonin may be helpful in the gastric mucosal context, along with TPP-based mitochondrially-targeted antioxidants like MitoQ, Mito-VitE, mito-lipoic acid, and mito-PBN, as well as small peptides like SS tetrapeptides like SS31, SS02, SS19, and SS20 against NSAID-induced gastric mucosal injury. AntiOxBENs, which are hydroxybenzoic acid-based, and antiOxCINs, which are hydroxycinnamic acid-based, are two unique classes of mitochondriotropic antioxidants that were recently designed by conjugating the TPP+ moiety to gallic acid and caffeic acid, respectively. In several pre-clinical conditions, these substances have demonstrated potential anti-oxidant properties; nonetheless, their purported gastroprotective impact is still ambiguous (124). MTAs are extremely

helpful in reducing oxidative mitochondrial damage. While certain targeted mitochondriotropic compounds, such as MitoQ and SkQ1, have already advanced to clinical trials with clear indications of reducing oxidative stress, other compounds, such as Mito-Quercetin, Mito-Curcumin, Mito-Resveratrol, and Mito-Honokiol, have been found to rise oxidative stress and induce mitopathology in the in vitro pre-clinical settings (124). These conflicting results strongly call for a thorough and careful examination of the potential effects of each newly synthesized mito-targeted compound because there seems to be a high chance that an antioxidant will lose its property or behave toxically upon specific enrichment in the mitochondria. Merely coupling a lipophilic cationic moiety like TPP does not guarantee the generation of an effective mitochondriotropic antioxidant with high safety profiles. Furthermore, an excessive buildup (adsorption) of lipophilic cations on the inner mitochondrial membrane's matrix side adversely affects the integrity of the membrane, which causes OXPHOS to become decoupled (129). The alkyl chain linker's length mostly determines the adverse effects; the greater the length, the better the hydrophobicity coupled with the increased likelihood of toxicities. Therefore, the discovery of next-generation mito-protective chemicals, such as mitoTEMPO, with comparatively higher safety profiles has been motivated by the search for shorter alkyl chain linker-bearing MTAs. In this context, we have earlier demonstrated that mitoTEMPO significantly reduced NSAID and stress-induced gastropathy in rats by selectively scavenging intra-mitochondrial O_2, preventing the ensuing gastric mucosal bioenergetic crisis and inflammatory tissue damage (2). Small compounds like Mdivi-1, P110, and dynasore that reduce mitochondrial hyperfission have been reported to protect a variety of disease models in addition to mito-targeted antioxidants (131). The most well-known small molecule fission inhibitor, Mdivi-1, is said to work by preventing DRP1 self-assembly and therefore inhibiting GTPase activity. Despite being extensively studied in several in vitro and in vivo disease models with known positive benefits, Mdivi-1 has also come under criticism for non-specific activities such as unintended mitochondrial elongation, reversible ETC complex-I inhibition, and elevated mtROS in some circumstances (132). The supposed harmful properties of Mdivi-1 are logically outweighed by positive effects, such as the suppression of cytochrome c release and the elimination of succinate-mediated ROS build-up (due to reverse electron transfer from ETC complex-I). More in-depth information regarding the beneficial effects and potential safety issues related to Mdivi-1 can be found in other sources (133). In this regard, the gastroprotective activity of Mdivi-1 has been reported in rats given acute NSAID treatment or mental stress, which was mediated by preventing metabolic and bioenergetic dysfunctions linked to mitochondrial hyperfission (17, 125). Even though several MTAs and small molecules that affect mitochondrial dynamics, particularly fission inhibitors, have demonstrated promising results, it is indisputable that each of these molecules also carries its own set of risks and side effects, including off-target effects in the mitochondria of healthy tissues, excessive accumulation on mitochondrial membranes, which can result in unwanted effects like ETC suppression and uncoupling, and excess ROS depletion (beyond pathologic levels). Another major issue is the uncontrolled suppression of mitochondrial fission, which can disturb the natural balance of fission-fusion and cause pathological hyperpolarization of the hyperfused mitochondria. In reality, it should be cautiously assessed for a specific condition if mitochondrial fission is genuinely a target for cytoprotection or cytodestruction (while taking into consideration the systemic consequences of dynamics regulation) (134). To achieve target-specific delivery, regulated loading, and optimum action, these logical restrictions fundamentally call for creativity of synthetic approaches. Extensive controls, such as accurate loading controls and scaffolds, should be included in experimental designs. To prevent intercalation in the membranes, alkyl side chains linking antioxidants with lipophilic cations that target mitochondria must be as short as feasible (which otherwise leads to ETC blockage and unwanted proton leakage). Pre-clinical research and clinical trials should carefully address long-term toxicity profiles on non-target organs, elimination half-life, possible adverse effects of metabolic intermediates, and most critically, potential hepatic and renal toxicities.

8. CONCLUSION

Here, the changing concept of NSAID-mediated gastric mucosal injury, starting from the COX-dependent pathway to the COX-independent pathway has been discussed. NSAID-mediated gastric mucosal injury is a multifactorial complication and is not fully understood yet. Finding appropriate targets/signaling pathways that lead to NSAID-mediated gastric mucosal damage is extremely difficult due to the complexity and variety of pathways that mediate the biological effects of NSAIDs. Here in this review, it has been explored several alternative cox-independent hypotheses/pathways of induction of gastric mucosal damage caused by NSAIDs suggest the alternative targets of NSAIDs worthy of pharmacologic exploitation. Further elucidation of COX-independent NSAID targets has the potential to contribute to the future repurposing of therapeutic strategies of NSAIDs by minimizing its side effect.

9. REFERENCES

1. Xie, X., Ren, K., Zhou, Z., Dang, C., and Zhang, H. (2022) The global, regional and national burden of peptic ulcer disease from 1990 to 2019: a population-based study. *BMC Gastroenterol* **22**, 58
2. Bindu, S., Mazumder, S., and Bandyopadhyay, U. (2020) Non-steroidal anti-inflammatory drugs (NSAIDs) and organ damage: A current perspective. *Biochem Pharmacol* **180**, 114147
3. Mazumder, S., Bindu, S., De, R., Debsharma, S., Pramanik, S., and Bandyopadhyay, U. (2022) Emerging role of mitochondrial DAMPs, aberrant mitochondrial dynamics and anomalous mitophagy in gut mucosal pathogenesis. *Life Sci* **305**, 120753
4. Wongrakpanich, S., Wongrakpanich, A., Melhado, K., and Rangaswami, J. (2018) A Comprehensive Review of Non-Steroidal Anti-Inflammatory Drug Use in The Elderly. *Aging Dis* **9**, 143-150
5. Musumba, C., Pritchard, D. M., and Pirmohamed, M. (2009) Review article: cellular and molecular mechanisms of NSAID-induced peptic ulcers. *Aliment Pharmacol Ther* **30**, 517-531
6. Bandyopadhyay, U., Biswas, K., Chatterjee, R., Bandyopadhyay, D., Chattopadhyay, I., Ganguly, C. K., Chakraborty, T., Bhattacharya, K., and Banerjee, R. K. (2002) Gastroprotective effect of Neem (Azadirachta indica) bark extract: possible involvement of H(+)-K(+)-ATPase inhibition and scavenging of hydroxyl radical. *Life Sci* **71**, 2845-2865
7. Biswas, K., Bandyopadhyay, U., Chattopadhyay, I., Varadaraj, A., Ali, E., and Banerjee, R. K. (2003) A novel antioxidant and antiapoptotic role of omeprazole to block gastric ulcer through scavenging of hydroxyl radical. *J Biol Chem* **278**, 10993-11001
8. Bhattacharjee, M., Bhattacharjee, S., Gupta, A., and Banerjee, R. K. (2002) Critical role of an endogenous gastric peroxidase in controlling oxidative damage in H. pylori-mediated and nonmediated gastric ulcer. *Free Radic Biol Med* **32**, 731-743
9. Maity, P., Biswas, K., Roy, S., Banerjee, R. K., and Bandyopadhyay, U. (2003) Smoking and the pathogenesis of gastroduodenal ulcer--recent mechanistic update. *Mol Cell Biochem* **253**, 329-338
10. Wang, H., Ma, L., Li, Y., and Cho, C. H. (2000) Exposure to cigarette smoke increases apoptosis in the rat gastric mucosa through a reactive oxygen species-mediated and p53-independent pathway. *Free Radic Biol Med* **28**, 1125-1131
11. Walsh, J. H., and Peterson, W. L. (1995) The treatment of Helicobacter pylori infection in the management of peptic ulcer disease. *N Engl J Med* **333**, 984-991
12. Alzahrani, S., Lina, T. T., Gonzalez, J., Pinchuk, I. V., Beswick, E. J., and Reyes, V. E. (2014) Effect of Helicobacter pylori on gastric epithelial cells. *World J Gastroenterol* **20**, 12767-12780
13. Yao, X., and Smolka, A. J. (2019) Gastric Parietal Cell Physiology and Helicobacter pylori-Induced Disease. *Gastroenterology* **156**, 2158-2173
14. Tai, F. W. D., and McAlindon, M. E. (2021) Non-steroidal anti-inflammatory drugs and the gastrointestinal tract. *Clin Med (Lond)* **21**, 131-134

15. Hawkey, C. J. (2001) COX-1 and COX-2 inhibitors. *Best Pract Res Clin Gastroenterol* **15**, 801-820

16. Wallace, J. L. (2008) Prostaglandins, NSAIDs, and gastric mucosal protection: why doesn't the stomach digest itself? *Physiol Rev* **88**, 1547-1565

17. Mazumder, S., De, R., Debsharma, S., Bindu, S., Maity, P., Sarkar, S., Saha, S. J., Siddiqui, A. A., Banerjee, C., Nag, S., Saha, D., Pramanik, S., Mitra, K., and Bandyopadhyay, U. (2019) Indomethacin impairs mitochondrial dynamics by activating the PKCzeta-p38-DRP1 pathway and inducing apoptosis in gastric cancer and normal mucosal cells. *J Biol Chem* **294**, 8238-8258

18. Pal, C., Bindu, S., Dey, S., Alam, A., Goyal, M., Iqbal, M. S., Maity, P., Adhikari, S. S., and Bandyopadhyay, U. (2010) Gallic acid prevents nonsteroidal anti-inflammatory drug-induced gastropathy in rat by blocking oxidative stress and apoptosis. *Free Radic Biol Med* **49**, 258-267

19. Maity, P., Bindu, S., Dey, S., Goyal, M., Alam, A., Pal, C., Mitra, K., and Bandyopadhyay, U. (2009) Indomethacin, a non-steroidal anti-inflammatory drug, develops gastropathy by inducing reactive oxygen species-mediated mitochondrial pathology and associated apoptosis in gastric mucosa: a novel role of mitochondrial aconitase oxidation. *J Biol Chem* **284**, 3058-3068

20. Krag, M., Perner, A., Wetterslev, J., Wise, M. P., Borthwick, M., Bendel, S., McArthur, C., Cook, D., Nielsen, N., Pelosi, P., Keus, F., Guttormsen, A. B., Moller, A. D., Moller, M. H., and Collaborators, S.-I. (2015) Stress ulcer prophylaxis in the intensive care unit: an international survey of 97 units in 11 countries. *Acta Anaesthesiol Scand* **59**, 576-585

21. Bardou, M., Quenot, J. P., and Barkun, A. (2015) Stress-related mucosal disease in the critically ill patient. *Nat Rev Gastroenterol Hepatol* **12**, 98-107

22. De, R., Mazumder, S., Sarkar, S., Debsharma, S., Siddiqui, A. A., Saha, S. J., Banerjee, C., Nag, S., Saha, D., and Bandyopadhyay, U. (2017) Acute mental stress induces mitochondrial bioenergetic crisis and hyper-fission along with aberrant mitophagy in the gut mucosa in rodent model of stress-related mucosal disease. *Free Radic Biol Med* **113**, 424-438

23. Bode, C., and Bode, J. C. (1997) Alcohol's role in gastrointestinal tract disorders. *Alcohol Health Res World* **21**, 76-83

24. Chari, S., Teyssen, S., and Singer, M. V. (1993) Alcohol and gastric acid secretion in humans. *Gut* **34**, 843-847

25. Chow, J. Y., Ma, L. I., and Cho, C. H. (1998) Cigarette smoking: Effects on P selectin expression and subsequent inflammatory responses in ethanol-induced gastric mucosal damage. *J Gastroenterol Hepatol* **13**, S199-S203

26. Berkowitz, L., Schultz, B. M., Salazar, G. A., Pardo-Roa, C., Sebastian, V. P., Alvarez-Lobos, M. M., and Bueno, S. M. (2018) Impact of Cigarette Smoking on the Gastrointestinal Tract Inflammation: Opposing Effects in Crohn's Disease and Ulcerative Colitis. *Front Immunol* **9**, 74

27. Kim, C. H., Oh, Y., Han, K., Seo, H. W., Kim, D., Kang, I., Park, C., Jang, K. Y., Kim, S. H., and Chae, C. (2012) Expression of secreted mucins (MUC2, MUC5AC, MUC5B, and MUC6) and membrane-bound mucin (MUC4) in the lungs of pigs experimentally infected with Actinobacillus pleuropneumoniae. *Res Vet Sci* **92**, 486-491

28. Laine, L., Takeuchi, K., and Tarnawski, A. (2008) Gastric mucosal defense and cytoprotection: bench to bedside. *Gastroenterology* **135**, 41-60

29. Porchet, N., and Aubert, J. P. (2004) [MUC genes: mucin or not mucin? That is the question]. *Med Sci (Paris)* **20**, 569-574

30. Allen, A., and Flemstrom, G. (2005) Gastroduodenal mucus bicarbonate barrier: protection against acid and pepsin. *Am J Physiol Cell Physiol* **288**, C1-19

31. (1993) *The Stomach- Physiology, Pathophysiology and Treatment*

32. Slomiany, B. L., Piasek, A., Sarosiek, J., and Slomiany, A. (1985) The role of surface and intracellular mucus in gastric mucosal protection against hydrogen ion. Compositional differences. *Scand J Gastroenterol* **20**, 1191-1196

33. Gindzienski, A., Zwierz, K., and Sarosiek, J. (2003) The role of mucus and its components in protection and repair within the alimentary tract mucosa: Polish experience. *J Physiol Pharmacol* **54 Suppl 3**, 127-144

34. Sarosiek, J., Slomiany, A., and Slomiany, B. L. (1988) Evidence for weakening of gastric mucus integrity by Campylobacter pylori. *Scand J Gastroenterol* **23**, 585-590

35. Allen, A., Flemstrom, G., Garner, A., and Kivilaakso, E. (1993) Gastroduodenal mucosal protection. *Physiol Rev* **73**, 823-857

36. Said, H., and Kaunitz, J. D. (2016) Gastrointestinal defense mechanisms. *Curr Opin Gastroenterol* **32**, 461-466

37. Aihara, E., Engevik, K. A., and Montrose, M. H. (2017) Trefoil Factor Peptides and Gastrointestinal Function. *Annu Rev Physiol* **79**, 357-380

38. Braga Emidio, N., Brierley, S. M., Schroeder, C. I., and Muttenthaler, M. (2020) Structure, Function, and Therapeutic Potential of the Trefoil Factor Family in the Gastrointestinal Tract. *ACS Pharmacol Transl Sci* **3**, 583-597

39. Hoffmann, W. (2021) Trefoil Factor Family (TFF) Peptides and Their Links to Inflammation: A Re-evaluation and New Medical Perspectives. *Int J Mol Sci* **22**

40. Thim, L., Madsen, F., and Poulsen, S. S. (2002) Effect of trefoil factors on the viscoelastic properties of mucus gels. *Eur J Clin Invest* **32**, 519-527

41. Aziz, R. S., Siddiqua, A., Shahzad, M., Shabbir, A., and Naseem, N. (2019) Oxyresveratrol ameliorates ethanol-induced gastric ulcer via downregulation of IL-6, TNF-alpha, NF-kB, and COX-2 levels, and upregulation of TFF-2 levels. *Biomed Pharmacother* **110**, 554-560

42. Babyatsky, M. W., deBeaumont, M., Thim, L., and Podolsky, D. K. (1996) Oral trefoil peptides protect against ethanol- and indomethacin-induced gastric injury in rats. *Gastroenterology* **110**, 489-497

43. Marchbank, T., Westley, B. R., May, F. E., Calnan, D. P., and Playford, R. J. (1998) Dimerization of human pS2 (TFF1) plays a key role in its protective/healing effects. *J Pathol* **185**, 153-158

44. Dey, I., Lejeune, M., and Chadee, K. (2006) Prostaglandin E2 receptor distribution and function in the gastrointestinal tract. *Br J Pharmacol* **149**, 611-623

45. Takeuchi, K. (2012) Pathogenesis of NSAID-induced gastric damage: importance of cyclooxygenase inhibition and gastric hypermotility. *World J Gastroenterol* **18**, 2147-2160

46. Norel, X., Sugimoto, Y., Ozen, G., Abdelazeem, H., Amgoud, Y., Bouhadoun, A., Bassiouni, W., Goepp, M., Mani, S., Manikpurage, H. D., Senbel, A., Longrois, D., Heinemann, A., Yao, C., and Clapp, L. H. (2020) International Union of Basic and Clinical Pharmacology. CIX. Differences and Similarities between Human and Rodent Prostaglandin E(2) Receptors (EP1-4) and Prostacyclin Receptor (IP): Specific Roles in Pathophysiologic Conditions. *Pharmacol Rev* **72**, 910-968

47. Konya, V., Maric, J., Jandl, K., Luschnig, P., Aringer, I., Lanz, I., Platzer, W., Theiler, A., Barnthaler, T., Frei, R., Marsche, G., Marsh, L. M., Olschewski, A., Lippe, I. T., Heinemann, A., and Schuligoi, R. (2015) Activation of EP(4) receptors prevents endotoxin-induced neutrophil infiltration into the airways and enhances microvascular barrier function. *Br J Pharmacol* **172**, 4454-4468

48. Ukawa, H., Yamakuni, H., Kato, S., and Takeuchi, K. (1998) Effects of cyclooxygenase-2 selective and nitric oxide-releasing nonsteroidal antiinflammatory drugs on mucosal ulcerogenic and healing responses of the stomach. *Dig Dis Sci* **43**, 2003-2011

49. Hatazawa, R., Tanaka, A., Tanigami, M., Amagase, K., Kato, S., Ashida, Y., and Takeuchi, K. (2007) Cyclooxygenase-2/prostaglandin E2 accelerates the healing of gastric ulcers via EP4 receptors. *Am J Physiol Gastrointest Liver Physiol* **293**, G788-797

50. Mizuno, H., Sakamoto, C., Matsuda, K., Wada, K., Uchida, T., Noguchi, H., Akamatsu, T., and Kasuga, M. (1997) Induction of cyclooxygenase 2 in gastric mucosal lesions and its inhibition by the specific antagonist delays healing in mice. *Gastroenterology* **112**, 387-397

51. Yandrapu, H., and Sarosiek, J. (2015) Protective Factors of the Gastric and Duodenal Mucosa: An Overview. *Curr Gastroenterol Rep* **17**, 24

52. Richardson, C. T. (1985) Pathogenetic factors in peptic ulcer disease. *Am J Med* **79**, 1-7

53. Forssell, H. (1988) Gastric mucosal defence mechanisms: a brief review. *Scand J Gastroenterol Suppl* **155**, 23-28

54. Sorbye, H., and Svanes, K. (1994) The role of blood flow in gastric mucosal defence, damage and healing. *Dig Dis* **12**, 305-317

55. Zarghi, A., and Arfaei, S. (2011) Selective COX-2 Inhibitors: A Review of Their Structure-Activity Relationships. *Iran J Pharm Res* **10**, 655-683

56. Wallace, J. L., McKnight, W., Reuter, B. K., and Vergnolle, N. (2000) NSAID-induced gastric damage in rats: requirement for inhibition of both cyclooxygenase 1 and 2. *Gastroenterology* **119**, 706-714

57. Gretzer, B., Maricic, N., Respondek, M., Schuligoi, R., and Peskar, B. M. (2001) Effects of specific inhibition of cyclo-oxygenase-1 and cyclo-oxygenase-2 in the rat stomach with normal mucosa and after acid challenge. *Br J Pharmacol* **132**, 1565-1573

58. Tanaka, A., Araki, H., Komoike, Y., Hase, S., and Takeuchi, K. (2001) Inhibition of both COX-1 and COX-2 is required for development of gastric damage in response to nonsteroidal antiinflammatory drugs. *J Physiol Paris* **95**, 21-27

59. Ehrlich, K., Sicking, C., Respondek, M., and Peskar, B. M. (2004) Interaction of cyclooxygenase isoenzymes, nitric oxide, and afferent neurons in gastric mucosal defense in rats. *J Pharmacol Exp Ther* **308**, 277-283

60. Tanaka, A., Araki, H., Hase, S., Komoike, Y., and Takeuchi, K. (2002) Up-regulation of COX-2 by inhibition of COX-1 in the rat: a key to NSAID-induced gastric injury. *Aliment Pharmacol Ther* **16 Suppl 2**, 90-101

61. Schmassmann, A., Zoidl, G., Peskar, B. M., Waser, B., Schmassmann-Suhijar, D., Gebbers, J. O., and Reubi, J. C. (2006) Role of the different isoforms of cyclooxygenase and nitric oxide synthase during gastric ulcer healing in cyclooxygenase-1 and -2 knockout mice. *Am J Physiol Gastrointest Liver Physiol* **290**, G747-756

62. To, K. F., Chan, F. K., Cheng, A. S., Lee, T. L., Ng, Y. P., and Sung, J. J. (2001) Up-regulation of cyclooxygenase-1 and -2 in human gastric ulcer. *Aliment Pharmacol Ther* **15**, 25-34

63. Bhandari, P., Bateman, A. C., Mehta, R. L., and Patel, P. (2005) Mucosal expression of cyclooxygenase isoforms 1 and 2 is increased with worsening damage to the gastric mucosa. *Histopathology* **46**, 280-286

64. Starodub, O. T., Demitrack, E. S., Baumgartner, H. K., and Montrose, M. H. (2008) Disruption of the Cox-1 gene slows repair of microscopic lesions in the mouse gastric epithelium. *Am J Physiol Cell Physiol* **294**, C223-232

65. Javadov, S., Kozlov, A. V., and Camara, A. K. S. (2020) Mitochondria in Health and Diseases. *Cells* **9**

66. Galluzzi, L., Kepp, O., Trojel-Hansen, C., and Kroemer, G. (2012) Mitochondrial control of cellular life, stress, and death. *Circ Res* **111**, 1198-1207

67. Galluzzi, L., Vitale, I., Aaronson, S. A., Abrams, J. M., Adam, D., Agostinis, P., Alnemri, E. S., Altucci, L., Amelio, I., Andrews, D. W., Annicchiarico-Petruzzelli, M., Antonov, A. V., Arama, E., Baehrecke, E. H., Barlev, N. A., Bazan, N. G., Bernassola, F., Bertrand, M. J. M., Bianchi, K., Blagosklonny, M. V., Blomgren, K., Borner, C., Boya, P., Brenner, C., Campanella, M., Candi, E., Carmona-Gutierrez, D., Cecconi, F., Chan, F. K., Chandel, N. S., Cheng, E. H., Chipuk, J. E., Cidlowski, J. A., Ciechanover, A., Cohen, G. M., Conrad, M., Cubillos-Ruiz, J. R., Czabotar, P. E., D'Angiolella, V., Dawson, T. M., Dawson, V. L., De Laurenzi, V., De Maria, R., Debatin, K. M., DeBerardinis, R. J., Deshmukh, M., Di Daniele, N., Di Virgilio, F., Dixit, V. M., Dixon, S. J., Duckett, C. S., Dynlacht, B. D., El-Deiry, W. S., Elrod, J. W., Fimia, G. M., Fulda, S., Garcia-Saez, A. J., Garg, A. D., Garrido, C., Gavathiotis, E., Golstein, P., Gottlieb, E., Green, D. R., Greene, L. A., Gronemeyer, H., Gross, A., Hajnoczky, G., Hardwick, J. M., Harris, I. S., Hengartner, M. O., Hetz, C., Ichijo, H., Jaattela, M., Joseph, B., Jost, P. J., Juin, P. P., Kaiser, W. J., Karin, M., Kaufmann, T., Kepp, O., Kimchi, A., Kitsis, R. N., Klionsky, D. J., Knight, R. A., Kumar, S., Lee, S. W., Lemasters, J. J., Levine, B., Linkermann, A., Lipton, S. A., Lockshin, R. A., Lopez-Otin, C., Lowe, S. W., Luedde, T., Lugli, E., MacFarlane, M., Madeo, F., Malewicz, M., Malorni, W., Manic, G., Marine, J. C., Martin, S. J., Martinou, J. C., Medema, J. P., Mehlen, P., Meier, P., Melino, S., Miao, E. A., Molkentin, J. D., Moll, U. M., Munoz-Pinedo, C., Nagata, S., Nunez, G., Oberst, A., Oren, M., Overholtzer, M., Pagano, M., Panaretakis, T., Pasparakis, M., Penninger, J. M., Pereira, D. M., Pervaiz, S., Peter, M. E., Piacentini, M., Pinton, P., Prehn, J. H. M., Puthalakath, H., Rabinovich, G. A., Rehm, M., Rizzuto, R., Rodrigues, C. M. P., Rubinsztein, D. C., Rudel, T., Ryan, K. M., Sayan, E., Scorrano, L., Shao, F., Shi, Y., Silke, J., Simon, H. U., Sistigu, A., Stockwell, B. R., Strasser, A., Szabadkai, G., Tait, S. W. G., Tang, D., Tavernarakis, N., Thorburn, A., Tsujimoto, Y., Turk, B., Vanden Berghe, T., Vandenabeele, P., Vander Heiden, M. G., Villunger, A., Virgin, H. W., Vousden, K. H., Vucic, D., Wagner, E. F., Walczak, H.,

Wallach, D., Wang, Y., Wells, J. A., Wood, W., Yuan, J., Zakeri, Z., Zhivotovsky, B., Zitvogel, L., Melino, G., and Kroemer, G. (2018) Molecular mechanisms of cell death: recommendations of the Nomenclature Committee on Cell Death 2018. *Cell Death Differ* **25**, 486-541

68. Redlak, M. J., Power, J. J., and Miller, T. A. (2005) Role of mitochondria in aspirin-induced apoptosis in human gastric epithelial cells. *Am J Physiol Gastrointest Liver Physiol* **289**, G731-738

69. Fujii, Y., Matsura, T., Kai, M., Matsui, H., Kawasaki, H., and Yamada, K. (2000) Mitochondrial cytochrome c release and caspase-3-like protease activation during indomethacin-induced apoptosis in rat gastric mucosal cells. *Proc Soc Exp Biol Med* **224**, 102-108

70. Shamas-Din, A., Kale, J., Leber, B., and Andrews, D. W. (2013) Mechanisms of action of Bcl-2 family proteins. *Cold Spring Harb Perspect Biol* **5**, a008714

71. Tsujimoto, Y. (1998) Role of Bcl-2 family proteins in apoptosis: apoptosomes or mitochondria? *Genes Cells* **3**, 697-707

72. Garrido, C., Galluzzi, L., Brunet, M., Puig, P. E., Didelot, C., and Kroemer, G. (2006) Mechanisms of cytochrome c release from mitochondria. *Cell Death Differ* **13**, 1423-1433

73. Circu, M. L., and Aw, T. Y. (2010) Reactive oxygen species, cellular redox systems, and apoptosis. *Free Radic Biol Med* **48**, 749-762

74. Zorov, D. B., Juhaszova, M., and Sollott, S. J. (2014) Mitochondrial reactive oxygen species (ROS) and ROS-induced ROS release. *Physiol Rev* **94**, 909-950

75. Pizzino, G., Irrera, N., Cucinotta, M., Pallio, G., Mannino, F., Arcoraci, V., Squadrito, F., Altavilla, D., and Bitto, A. (2017) Oxidative Stress: Harms and Benefits for Human Health. *Oxid Med Cell Longev* **2017**, 8416763

76. Guo, C., Sun, L., Chen, X., and Zhang, D. (2013) Oxidative stress, mitochondrial damage and neurodegenerative diseases. *Neural Regen Res* **8**, 2003-2014

77. Debsharma, S., Pramanik, S., Bindu, S., Mazumder, S., Das, T., Saha, D., De, R., Nag, S., Banerjee, C., Siddiqui, A. A., Ghosh, Z., and Bandyopadhyay, U. (2023) Honokiol, an inducer of sirtuin-3, protects against non-steroidal anti-inflammatory drug-induced gastric mucosal mitochondrial pathology, apoptosis and inflammatory tissue injury. *Br J Pharmacol*

78. Naik, E., and Dixit, V. M. (2011) Mitochondrial reactive oxygen species drive proinflammatory cytokine production. *J Exp Med* **208**, 417-420

79. Forrester, S. J., Kikuchi, D. S., Hernandes, M. S., Xu, Q., and Griendling, K. K. (2018) Reactive Oxygen Species in Metabolic and Inflammatory Signaling. *Circ Res* **122**, 877-902

80. Pham-Huy, L. A., He, H., and Pham-Huy, C. (2008) Free radicals, antioxidants in disease and health. *Int J Biomed Sci* **4**, 89-96

81. Mittal, M., Siddiqui, M. R., Tran, K., Reddy, S. P., and Malik, A. B. (2014) Reactive oxygen species in inflammation and tissue injury. *Antioxid Redox Signal* **20**, 1126-1167

82. Novak, E. A., and Mollen, K. P. (2015) Mitochondrial dysfunction in inflammatory bowel disease. *Front Cell Dev Biol* **3**, 62

83. Wang, Z., Li, S., Cao, Y., Tian, X., Zeng, R., Liao, D. F., and Cao, D. (2016) Oxidative Stress and Carbonyl Lesions in Ulcerative Colitis and Associated Colorectal Cancer. *Oxid Med Cell Longev* **2016**, 9875298

84. Sandoval-Acuna, C., Lopez-Alarcon, C., Aliaga, M. E., and Speisky, H. (2012) Inhibition of mitochondrial complex I by various non-steroidal anti-inflammatory drugs and its protection by quercetin via a coenzyme Q-like action. *Chem Biol Interact* **199**, 18-28

85. Murphy, M. P. (2009) How mitochondria produce reactive oxygen species. *Biochem J* **417**, 1-13

86. Mazumder, S., De, R., Sarkar, S., Siddiqui, A. A., Saha, S. J., Banerjee, C., Iqbal, M. S., Nag, S., Debsharma, S., and Bandyopadhyay, U. (2016) Selective scavenging of intra-mitochondrial superoxide corrects diclofenac-induced mitochondrial dysfunction and gastric injury: A novel gastroprotective mechanism independent of gastric acid suppression. *Biochem Pharmacol* **121**, 33-51

87. Boyapati, R. K., Rossi, A. G., Satsangi, J., and Ho, G. T. (2016) Gut mucosal DAMPs in IBD: from mechanisms to therapeutic implications. *Mucosal Immunol* **9**, 567-582

88. Chen, L., Deng, H., Cui, H., Fang, J., Zuo, Z., Deng, J., Li, Y., Wang, X., and Zhao, L. (2018) Inflammatory responses and inflammation-associated diseases in organs. *Oncotarget* **9**, 7204-7218

89. D'Inca, R., Cardin, R., Benazzato, L., Angriman, I., Martines, D., and Sturniolo, G. C. (2004) Oxidative DNA damage in the mucosa of ulcerative colitis increases with disease duration and dysplasia. *Inflamm Bowel Dis* **10**, 23-27

90. Shimada, K., Crother, T. R., Karlin, J., Dagvadorj, J., Chiba, N., Chen, S., Ramanujan, V. K., Wolf, A. J., Vergnes, L., Ojcius, D. M., Rentsendorj, A., Vargas, M., Guerrero, C., Wang, Y., Fitzgerald, K. A., Underhill, D. M., Town, T., and Arditi, M. (2012) Oxidized mitochondrial DNA activates the NLRP3 inflammasome during apoptosis. *Immunity* **36**, 401-414

91. Yang, Y., Wang, H., Kouadir, M., Song, H., and Shi, F. (2019) Recent advances in the mechanisms of NLRP3 inflammasome activation and its inhibitors. *Cell Death Dis* **10**, 128

92. Tourkochristou, E., Aggeletopoulou, I., Konstantakis, C., and Triantos, C. (2019) Role of NLRP3 inflammasome in inflammatory bowel diseases. *World J Gastroenterol* **25**, 4796-4804

93. Kelley, N., Jeltema, D., Duan, Y., and He, Y. (2019) The NLRP3 Inflammasome: An Overview of Mechanisms of Activation and Regulation. *Int J Mol Sci* **20**

94. Zhen, Y., and Zhang, H. (2019) NLRP3 Inflammasome and Inflammatory Bowel Disease. *Front Immunol* **10**, 276

95. Riley, J. S., and Tait, S. W. (2020) Mitochondrial DNA in inflammation and immunity. *EMBO Rep* **21**, e49799

96. Boyapati, R. K., Dorward, D. A., Tamborska, A., Kalla, R., Ventham, N. T., Doherty, M. K., Whitfield, P. D., Gray, M., Loane, J., Rossi, A. G., Satsangi, J., and Ho, G. T. (2018) Mitochondrial DNA Is a Pro-Inflammatory Damage-Associated Molecular Pattern Released During Active IBD. *Inflamm Bowel Dis* **24**, 2113-2122

97. Mancini, N. L., Goudie, L., Xu, W., Sabouny, R., Rajeev, S., Wang, A., Esquerre, N., Al Rajabi, A., Jayme, T. S., van Tilburg Bernandes, E., Nasser, Y., Ferraz, J. G. P., Shutt, T., Shearer, J., and McKay, D. M. (2020) Perturbed Mitochondrial Dynamics Is a Novel Feature of Colitis That Can Be Targeted to Lessen Disease. *Cell Mol Gastroenterol Hepatol* **10**, 287-307

98. Scott, I., and Youle, R. J. (2010) Mitochondrial fission and fusion. *Essays Biochem* **47**, 85-98

99. Zemirli, N., Morel, E., and Molino, D. (2018) Mitochondrial Dynamics in Basal and Stressful Conditions. *Int J Mol Sci* **19**

100. Zhu, M., Huang, X., Shan, H., and Zhang, M. (2022) Mitophagy in Traumatic Brain Injury: A New Target for Therapeutic Intervention. *Oxid Med Cell Longev* **2022**, 4906434

101. Jain, P., Luo, Z. Q., and Blanke, S. R. (2011) Helicobacter pylori vacuolating cytotoxin A (VacA) engages the mitochondrial fission machinery to induce host cell death. *Proc Natl Acad Sci U S A* **108**, 16032-16037

102. Ott, M., Gogvadze, V., Orrenius, S., and Zhivotovsky, B. (2007) Mitochondria, oxidative stress and cell death. *Apoptosis* **12**, 913-922

103. Brzozowski, T., Konturek, P. C., Konturek, S. J., Drozdowicz, D., Kwiecien, S., Pajdo, R., Bielanski, W., and Hahn, E. G. (2000) Role of gastric acid secretion in progression of acute gastric erosions induced by ischemia-reperfusion into gastric ulcers. *Eur J Pharmacol* **398**, 147-158

104. Tsutsumi, S., Tomisato, W., Takano, T., Rokutan, K., Tsuchiya, T., and Mizushima, T. (2002) Gastric irritant-induced apoptosis in guinea pig gastric mucosal cells in primary culture. *Biochim Biophys Acta* **1589**, 168-180

105. Nagano, Y., Matsui, H., Muramatsu, M., Shimokawa, O., Shibahara, T., Yanaka, A., Nakahara, A., Matsuzaki, Y., Tanaka, N., and Nakamura, Y. (2005) Rebamipide significantly inhibits indomethacin-induced mitochondrial damage, lipid peroxidation, and apoptosis in gastric epithelial RGM-1 cells. *Dig Dis Sci* **50 Suppl 1**, S76-83

106. Somasundaram, S., Hayllar, H., Rafi, S., Wrigglesworth, J. M., Macpherson, A. J., and Bjarnason, I. (1995) The biochemical basis of non-steroidal anti-inflammatory drug-induced damage to the gastrointestinal tract: a review and a hypothesis. *Scand J Gastroenterol* **30**, 289-299

107. Masubuchi, Y., Nakayama, S., and Horie, T. (2002) Role of mitochondrial permeability transition in diclofenac-induced hepatocyte injury in rats. *Hepatology* **35**, 544-551

108. Szabo, I., and Tarnawski, A. S. (2000) Apoptosis in the gastric mucosa: molecular mechanisms, basic and clinical implications. *J Physiol Pharmacol* **51**, 3-15

109. Tomisato, W., Tsutsumi, S., Rokutan, K., Tsuchiya, T., and Mizushima, T. (2001) NSAIDs induce both necrosis and apoptosis in guinea pig gastric mucosal cells in primary culture. *Am J Physiol Gastrointest Liver Physiol* **281**, G1092-1100

110. Ishihara, T., Tanaka, K., Tashiro, S., Yoshida, K., and Mizushima, T. (2010) Protective effect of rebamipide against celecoxib-induced gastric mucosal cell apoptosis. *Biochem Pharmacol* **79**, 1622-1633

111. Power, J. J., Dennis, M. S., Redlak, M. J., and Miller, T. A. (2004) Aspirin-induced mucosal cell death in human gastric cells: evidence supporting an apoptotic mechanism. *Dig Dis Sci* **49**, 1518-1525

112. Piotrowski, J., Slomiany, A., and Slomiany, B. L. (1999) Activation of apoptotic caspase-3 and nitric oxide synthase-2 in gastric mucosal injury induced by indomethacin. *Scand J Gastroenterol* **34**, 129-134

113. Kusuhara, H., Matsuyuki, H., Matsuura, M., Imayoshi, T., Okumoto, T., and Matsui, H. (1998) Induction of apoptotic DNA fragmentation by nonsteroidal anti-inflammatory drugs in cultured rat gastric mucosal cells. *Eur J Pharmacol* **360**, 273-280

114. Gurpinar, E., Grizzle, W. E., and Piazza, G. A. (2013) COX-Independent Mechanisms of Cancer Chemoprevention by Anti-Inflammatory Drugs. *Front Oncol* **3**, 181

115. Alderman, B. M., Cook, G. A., Familari, M., Yeomans, N. D., and Giraud, A. S. (2000) Resistance to apoptosis is a mechanism of adaptation of rat stomach to aspirin. *Am J Physiol Gastrointest Liver Physiol* **278**, G839-846

116. Xu, C., Liu, Z., and Xiao, J. (2021) Ferroptosis: A Double-Edged Sword in Gastrointestinal Disease. *Int J Mol Sci* **22**

117. Yang, W. S., and Stockwell, B. R. (2016) Ferroptosis: Death by Lipid Peroxidation. *Trends Cell Biol* **26**, 165-176

118. Zhu, J., Xiong, Y., Zhang, Y., Wen, J., Cai, N., Cheng, K., Liang, H., and Zhang, W. (2020) The Molecular Mechanisms of Regulating Oxidative Stress-Induced Ferroptosis and Therapeutic Strategy in Tumors. *Oxid Med Cell Longev* **2020**, 8810785

119. Chen, J., Zhang, J., Chen, T., Bao, S., Li, J., Wei, H., Hu, X., Liang, Y., Liu, F., and Yan, S. (2022) Xiaojianzhong decoction attenuates gastric mucosal injury by activating the p62/Keap1/Nrf2 signaling pathway to inhibit ferroptosis. *Biomed Pharmacother* **155**, 113631

120. Logan, I. C., Sumukadas, D., and Witham, M. D. (2010) Gastric acid suppressants--too much of a good thing? *Age Ageing* **39**, 410-411

121. Chattopadhyay, I., Bandyopadhyay, U., Biswas, K., Maity, P., and Banerjee, R. K. (2006) Indomethacin inactivates gastric peroxidase to induce reactive-oxygen-mediated gastric mucosal injury and curcumin protects it by preventing peroxidase inactivation and scavenging reactive oxygen. *Free Radic Biol Med* **40**, 1397-1408

122. Carrasco-Pozo, C., Speisky, H., Brunser, O., Pastene, E., and Gotteland, M. (2011) Apple peel polyphenols protect against gastrointestinal mucosa alterations induced by indomethacin in rats. *J Agric Food Chem* **59**, 6459-6466

123. Sinha, K., Sadhukhan, P., Saha, S., Pal, P. B., and Sil, P. C. (2015) Morin protects gastric mucosa from nonsteroidal anti-inflammatory drug, indomethacin induced inflammatory damage and apoptosis by modulating NF-kappaB pathway. *Biochim Biophys Acta* **1850**, 769-783

124. Teixeira, J., Deus, C. M., Borges, F., and Oliveira, P. J. (2018) Mitochondria: Targeting mitochondrial reactive oxygen species with mitochondriotropic polyphenolic-based antioxidants. *Int J Biochem Cell Biol* **97**, 98-103

125. Bhatti, J. S., Bhatti, G. K., and Reddy, P. H. (2017) Mitochondrial dysfunction and oxidative stress in metabolic disorders - A step towards mitochondria based therapeutic strategies. *Biochim Biophys Acta Mol Basis Dis* **1863**, 1066-1077

126. Jiang, Q., Yin, J., Chen, J., Ma, X., Wu, M., Liu, G., Yao, K., Tan, B., and Yin, Y. (2020) Mitochondria-Targeted Antioxidants: A Step towards Disease Treatment. *Oxid Med Cell Longev* **2020**, 8837893

127. Apostolova, N., and Victor, V. M. (2015) Molecular strategies for targeting antioxidants to mitochondria: therapeutic implications. *Antioxid Redox Signal* **22**, 686-729

128. Kagan, V. E., Wipf, P., Stoyanovsky, D., Greenberger, J. S., Borisenko, G., Belikova, N. A., Yanamala, N., Samhan Arias, A. K., Tungekar, M. A., Jiang, J., Tyurina, Y. Y., Ji, J., Klein-Seetharaman, J., Pitt, B. R., Shvedova, A. A., and Bayir, H. (2009) Mitochondrial targeting of electron scavenging antioxidants: Regulation of selective oxidation vs random chain reactions. *Adv Drug Deliv Rev* **61**, 1375-1385

129. Jin, H., Kanthasamy, A., Ghosh, A., Anantharam, V., Kalyanaraman, B., and Kanthasamy, A. G. (2014) Mitochondria-targeted antioxidants for treatment of Parkinson's disease: preclinical and clinical outcomes. *Biochim Biophys Acta* **1842**, 1282-1294

130. Sheu, S. S., Nauduri, D., and Anders, M. W. (2006) Targeting antioxidants to mitochondria: a new therapeutic direction. *Biochim Biophys Acta* **1762**, 256-265

131. Dhingra, A., Jayas, R., Afshar, P., Guberman, M., Maddaford, G., Gerstein, J., Lieberman, B., Nepon, H., Margulets, V., Dhingra, R., and Kirshenbaum, L. A. (2017) Ellagic acid antagonizes Bnip3-mediated mitochondrial injury and necrotic cell death of cardiac myocytes. *Free Radic Biol Med* **112**, 411-422

132. Bordt, E. A., Clerc, P., Roelofs, B. A., Saladino, A. J., Tretter, L., Adam-Vizi, V., Cherok, E., Khalil, A., Yadava, N., Ge, S. X., Francis, T. C., Kennedy, N. W., Picton, L. K., Kumar, T., Uppuluri, S., Miller, A. M., Itoh, K., Karbowski, M., Sesaki, H., Hill, R. B., and Polster, B. M. (2017) The Putative Drp1 Inhibitor mdivi-1 Is a Reversible Mitochondrial Complex I Inhibitor that Modulates Reactive Oxygen Species. *Dev Cell* **40**, 583-594 e586

133. Smith, G., and Gallo, G. (2017) To mdivi-1 or not to mdivi-1: Is that the question? *Dev Neurobiol* **77**, 1260-1268

134. Rosdah, A. A., J, K. H., Delbridge, L. M., Dusting, G. J., and Lim, S. Y. (2016) Mitochondrial fission - a drug target for cytoprotection or cytodestruction? *Pharmacol Res Perspect* **4**, e00235

135. Serafim, C., Araruna, M. E., Junior, E. A., Diniz, M., Hiruma-Lima, C., and Batista, L. (2020) A Review of the Role of Flavonoids in Peptic Ulcer (2010-2020). *Molecules* **25**

Review Chapter **2**

Sirtuin 3: The mitochondrial metabolic guardian regulating gastrointestinal health and mucosal pathology

1. INTRODUCTION

Sirtuins (class 1-7) are a group of NAD-dependent class III histone deacetylase (HDACs) family ubiquitous in all mammals. Silent mating type information regulator (Sir2) was the first sirtuin that was identified in yeast and initially was shown that overexpression of this protein enhanced the life span in various organisms including *Caenorhabditis elegans* and *Drosophila melanogaster* (1). Later, the NAD-dependent deacetylation property of Sir2 in the position of lysine 9 and 14 of histone 3 (H3) and 16 of histone 4 (H4) was suggested as the key feature behind its longevity-promoting mechanism (2). So far 7 orthologs of Sir2 are discovered in mammals (3). Among all the sirtuins, Sirt1, Sirt6 and Sirt7 are predominantly nuclear, Sirt2 is found in the cytoplasm whereas Sir3, Sirt4 and Sirt5 are predominantly localized to mitochondria. The most extensively studied modification is lysine acetylation (4). Nearly 20 percent of mitochondrial proteins are acetylated, and almost all aspects of mitochondrial functions are affected by this alteration (5). Acetylation modification is therefore essential for mitochondrial fate. The most significant mitochondrial sirtuin, SIRT3, has been shown in a recent study to have direct interactions with at least 84 different mitochondrial proteins. All aspects of the biological activity of mitochondria are regulated by these proteins (2). In metabolically active organs such as the brain, liver, kidney, brown adipose tissue, and heart, the mitochondrial deacetylase SIRT3 is highly expressed (6). Numerous cellular functions, such as bioenergetics, redox balance, mitochondrial metabolism, mitochondrial DNA damage repair, gene expression, and autophagy including the tricarboxylic acid (TCA) cycle, the urea cycle, amino acid metabolism, and fatty acid oxidation, are regulated by SIRT3. The mitochondrial unfolded protein response (UPR) and apoptosis are both regulated by SIRT3 (7-11). By interacting with and favorably regulating the incision activity and turnover of the DNA repair enzyme 8-oxoguanine DNA glycosylase 1 (OGG1), SIRT3 controls mtDNA repair. This has been suggested to prevent cells exposed to radiation from developing apoptosis caused by genotoxicity (11). SIRT3 also controls mitochondrial dynamics, a mitochondrial mechanism essential to overall mitochondrial function, in addition to mtDNA repair (12) Many tissues, including the kidney, heart, brain, liver, and stomach tissue, which are rich in mitochondria, express the SIRT3 protein. In these tissues, the mitochondrial function is maintained by the acetylation changes that SIRT3 controls. These highly metabolic tissues are particularly susceptible to mitochondrial malfunction because of the critical role that mitochondria play in energy production, metabolism, apoptosis, and intracellular signaling (13). SIRT3 has been shown to control neurodegeneration, aging, liver, kidney, heart, and other metabolic diseases (13). Furthermore, it's noteworthy how SIRT3 plays a dual function in the growth of cancer (14). Increasing evidence has shown that SIRT3 is playing a crucial role in several types of GI pathologies including intestinal I/R injury, gastric cancer, and colorectal cancer. However, the underlying mechanisms remain unclear. It may be associated with maintaining mitochondrial homeostasis or other functions including antioxidative stress and associated inflammation, and protecting GI system against excitotoxicity. However, the gastroprotection functions of SIRT3 in GI pathology warrant further evaluation. SIRT3 may be an effective therapeutic target for non-malignant and malignant GI pathology. In this review the complex mechanisms of SIRT3 in GI pathology, the development of small molecule drugs that target SIRT3 and their potential uses, and the advantages and disadvantages of potential future drug discoveries that include SIRT3 as a potential druggable target has been summarised.

2. STRUCTURE OF SIRTUIN 3

Like other sirtuins, SIRT3 performs the deacetylation activity through a conserved catalytic core (aa126–399) and functions as a NAD+-dependent enzyme. A large Rossmann fold domain for NAD+
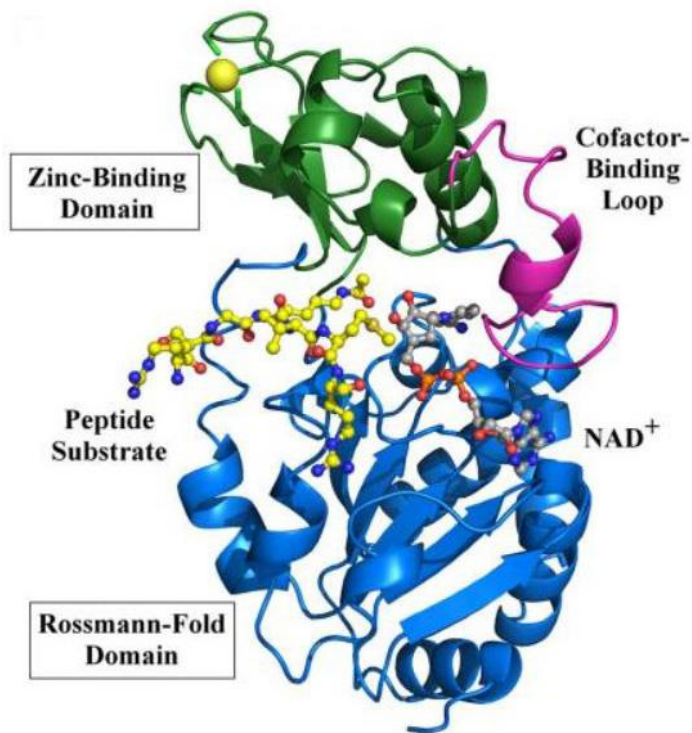
Fig. 1. The structure of SIRT3. AcetylCoA synthetase 2 peptide and a NAD+ analogue is coupled to the human SIRT3 protein in (A). A cartoon representation of SIRT3's structure (PDB entry 3glr) is displayed, with the Rossmann-fold domain and zinc-binding domain coloured in blue and green, respectively. The model was expanded to include a carba-NAD molecule based on a superposition with the structure of a Hst2/carba-NAD structure. The cofactor binding loop (magenta) is in a closed conformation and binds the carba-NAD molecule (grey) (1szc). AceCS2 (yellow), a peptide substrate with an acetylated lysine immediately pointing to the active site, is also present in the active site cleft.The figure is adapted from (172)

binding can be seen in the core area, and a smaller domain with a helical bundle and a zinc-binding motif is also present (Fig. 1). The smaller domain is created by two loops extending from the larger domain. The remaining binding sites for SIRT3 substrates make up the catalytic core. The NAD+-dependent SIRT3 deacetylation reaction mechanism formally entails four phases. To cause the active site to close and the NAD+ binding loop to stabilize, the acetylated substrate and the NAD+ co-substrate must first bind in a cleft between the Rossmann-fold and zinc-binding domains. The NAD+ nicotinamide moiety is then activated and buried in a favorable conformation in the neighboring highly conserved hydrophobic pocket. This conformation then positions NAD+'s -face toward the acyl substrate, exposing the C1 atom of the ribose ring to immediate nucleophilic attack from the acyl substrate's carbonyl oxygen. As a result, the acetyl group moves from the substrate to the NAD+ ADP-ribose moiety while the nicotinamide in NAD+ is also separated. The conserved His 224 then aids in the conversion of the C1'-O-alkylamidate

intermediate into the bicyclic intermediate by causing a nucleophilic attack of the 2'-OH group of the ribose onto the iminium carbon of the O-alkylamidate intermediate. An activated water molecule finally breaks apart the bicyclic intermediate to generate the deacetylated protein and 2'-O-acetyl-ADP-ribose. SIRT3 also eliminates crotonyl and myristoyl groups in addition to acetyl groups.

3. SUBCELLULAR LOCALIZATION OF SIRTUIN 3

The subcellular localization of SIRT3 is debatable. The subcellular localization of SIRT3 is schematically depicted in (Fig. 2). The mammalian SIRT3 presents inside the cell in two isoforms. The longer 44 kDa full-length isoform is located in the cytoplasm and nucleus (15). As it carries an N-terminal mitochondrial localization sequence (MLS), it is sliced off by matrix metalloprotease in the mitochondrial matrix and resulted in a shorter 28 kDa protein isoform which is believed to have the NAD+ dependent deacetylase property (15). A study in 3T3 fibroblast cells revealed that due to alternative splicing in the murine SIRT3 gene, there are 3 isoforms available for murine SIRT3 named M1, M2 and M3. Variant M1 and M2 possess MLS sequences that's why when they enter inside mitochondria, due to proteolytic cleavage, they become shorter isoform although in cytoplasm and nucleus, they are present.
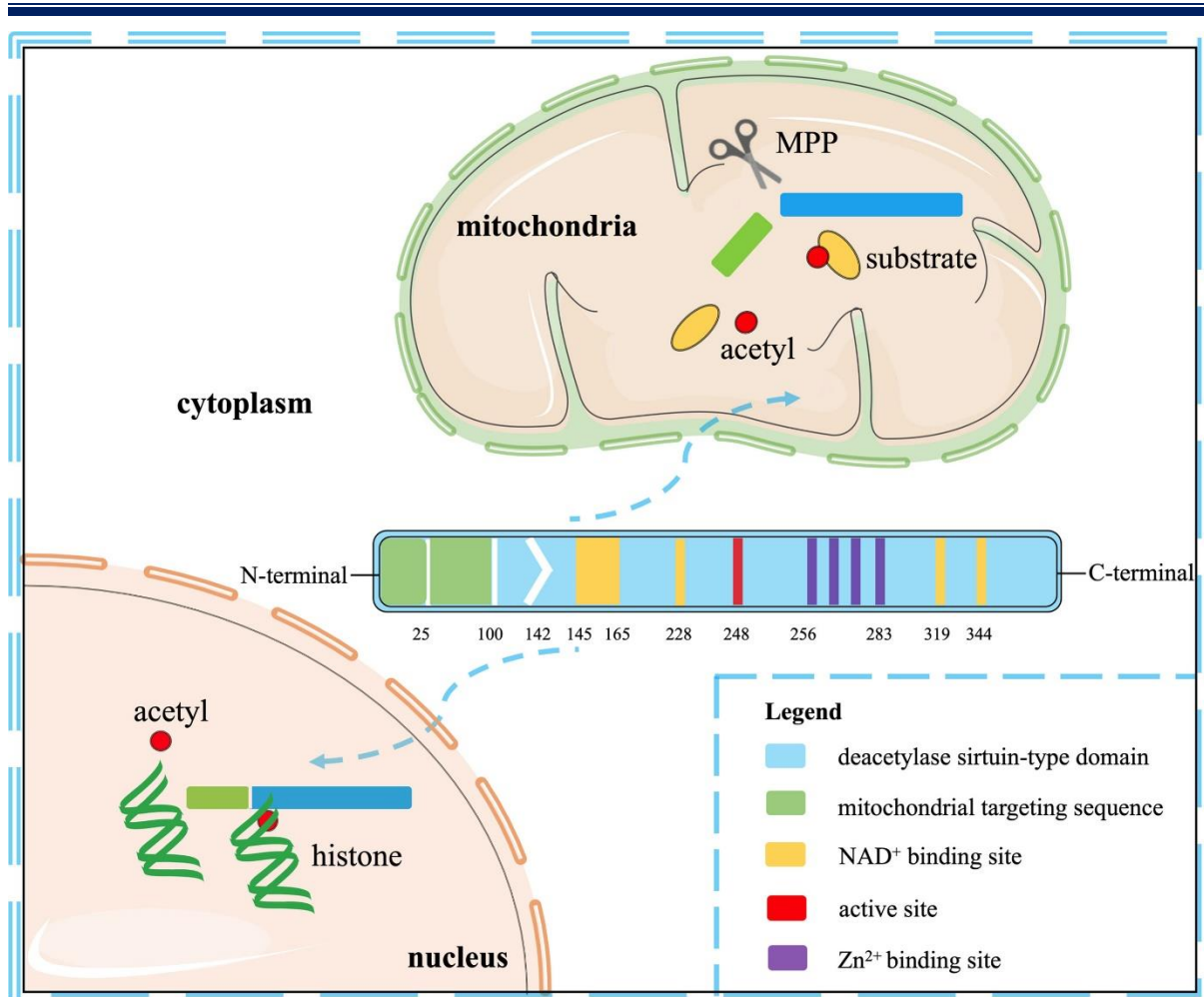
Fig. 2. The subcellular location and the structural makeup of SIRT3. SIRT3 has an active site, four Zn2+ sites, four NAD+ sites, and a mitochondrial targeting sequence in its conserved enzymatic core. Through the targeting sequence, SIRT3 is guided to the mitochondria, where it is cleaved by the mitochondrial MPP to create mature proteins. It is mostly found in mitochondria and functions as a deacetylase, but it also exhibits histone deacetylation activity in the nucleus. The figure is adapted from (173).

in full-length long isoform (16). In contrast to M1 and M2, M3 is a shorter isoform that carries an internal mitochondrial targeting sequence (MTS) and skips the proteolytic cleavage inside mitochondria. However, the M3 isoform predominantly localizes in the cytoplasm and nucleus (17). The subcellular distribution of the short and long isoforms of SIRT3 is arguable as previously the long isoform i.e., the inactive isoform of SIRT3 was thought to reside only in cytoplasm and nucleus whereas the short isoform I.e., the active isoform exists exclusively in mitochondria. Recent studies in cardiomyocyte cell line H9C2 showed that mitochondria possess both the short and long isoforms of SIRT3. Surprisingly, in the same cell line, it was observed that the abundance of the long isoform was higher in comparison to the short isoform. Thus, it has been concluded that subcellular distribution of SIRT3 isoform is specific to cell-type (18, 19).

4. FUNCTION OF SIRTUIN 3

Extensive proteomics study revealed that more than 2200 proteins are found acetylated in mammalian cells (20). With the recent advancement of proteomic research, reversible lysine acetylation has been established as one of the most important PTMs which directly regulates enzymatic activity, subcellular localization, dynamic regulation of protein-protein interaction and protein stability. It has been observed
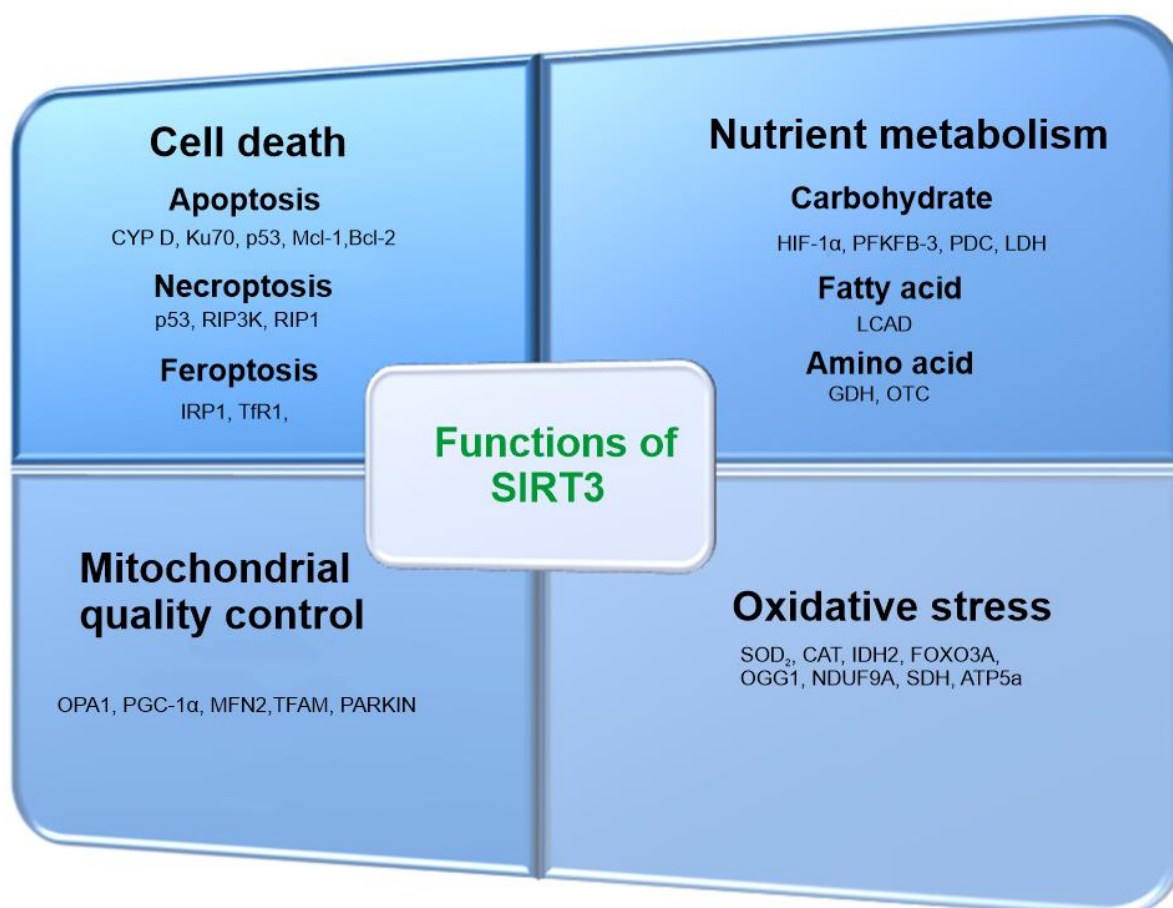
Fig. 3. **Sirtuin 3 (SIRT3) is involved in several processes, including nutrient metabolism, oxidative stress, mitochondrial quality control which are crucial for cellular functions.** Foxo3a: forkhead box O3; MnSOD: manganese superoxide dismutase; IDH2: isocitrate dehydrogenase; CH: carbohydrate; HKII: hexokinase II; AceCS2: acetyl-CoA synthase 2; PDC: pyruvate dehydrogenase complex; LCAD: long chain acyl-CoA dehydrogenase; GDH: glutamate dehydrogenase; OTC: ornithine transcarbamylase; LDH: lactate dehydrogenase; HIF: hypoxia-inducible factor. The figure is adapted from (98).

that almost 20% of mitochondrial proteins are acetylated (21). SIRT3, being the most important mitochondrial deacetylase, has a wide number of mitochondrial substrates and thus it controls various cellular processes such as metabolism, DNA repairs, redox balance, apoptosis in metabolically active organs including heart, liver, brain, kidney and adipose tissue that's why SIRT3 expressed at high levels in all those organs (22, 23). The most important functions of SIRT3 have been presented in (Fig. 3).

4.1. Metabolism

Numerous crucial enzymes in metabolic processes such as glycolysis, tricarboxylic acid (TCA) cycle, glycogen metabolism, gluconeogenesis, the urea cycle, and fatty acid oxidation, amino acid metabolism, are regulated by the acetylation-deacetylation process. Furthermore, key enzymes of the oxidative phosphorylation pathway were also found acetylated (20). Several studies revealed that acetylation of metabolic enzymes suppresses their enzymatic activity. SIRT3, being the most prominent mitochondrial deacetylase regulates many of those metabolic enzymes including Ac-CS2 (acetyl-CoA synthetase 2), LCAD (long-chain acetyl-CoA dehydrogenase), ALDH2 (aldehyde dehydrogenase 2), OTC (ornithine transcarboxylase) (24).

4.1.1. Glucose metabolism

The exact mechanism by which SIRT3 maintains glucose homeostasis is not clear yet. However not only the impaired hexokinase II (HKII) and glucose uptake but also the reduced insulin sensitivity and glucose tolerance was observed in SIRT3 $^{-/-}$ mice. Moreover, SIRT3 regulates glycolysis by targeting HIF-1α which controls the gene expression of glycolytic enzymes including *PGK-1* and *PFK1A* (25). Furthermore, SIRT3 influences glucose metabolism by upregulating the expression of fructose-2,6-bisphosphonate 3 (PFKFB3) /6-phosphofructo-2-kinase. Expression of SIRT3 is found downregulated in obesity. Research in obesity models revealed that in human and mice endothelial cells, SIRT3 can act as a positive controller of insulin sensitivity. SIRT3 regulates the TCA cycle in several ways including activating the Pyruvate dehydrogenase complex (PDC) directly. From several research, it has been observed that SIRT3 directly deacetylates several enzymes including isocitrate dehydrogenase, succinate dehydrogenase, malate dehydrogenase, aconitase, and citrate synthase.

4.1.2. Acetate metabolism

AceCS2 (acetyl-CoA synthetase II) was the first identified substrate of SIRT3 (26). Both the AceCS2 and SIRT3 are highly expressed in heart and skeletal muscle under ketogenic conditions. Under the ketogenic condition, the key role of acetate as an important energy source was validated in the study where it was shown that in AceCS2 $^{-/-}$ mice, due to the lack of AceCS2 enzymatic activity the oxidation of acetate is halted in peripheral tissue. During nutrient-deprived conditions, SIRT3 plays a very important role in the oxidation of acetate as an alternative energy source. Hence SIRT3$^{-/-}$ and AceCS2 $^{-/-}$ shares similar phenotype.

4.1.3. Fatty acid oxidation, ketogenesis

Several studies confirmed the role of SIRT3 in fatty acid oxidation especially during fasting and high-fat diet condition since SIRT3 expression is increased in the liver during fasting and high-fat diet. In SIRT3$^{-/-}$ mouse imbalance of fatty acid oxidation, higher accumulation of fatty-acid oxidation intermediate products, hepatic triacylglycerols was observed resulting in reduced ATP production and lack of tolerance to cold exposure. In the absence of SIRT3, the long-chain acyl-coenzyme A dehydrogenase (LCAD) was found in the hyperacetylated state with compromised enzymatic activity whereas, in wild-type mice, this enzyme was observed in deacetylate state.

4.1.4. SIRTUIN 3 and amino acid metabolism

SIRT3 deacetylates thus activate glutamate dehydrogenase (GDH), a key enzyme of amino acid metabolism, responsible for the production of α-ketoglutarate from Glutamine and Glutamate.

4.2. Role of SIRTUIN 3 in mitochondrial oxidative stress regulation

Excessive generation of mitochondrial oxidative stress (MOS) has been linked to inducing damage in macromolecules and structures inside and outside of mitochondria (27). Several pathophysiological conditions including aerogeneration, cardiovascular diseases metabolic disorders, aging, and cancer are associated with MOS (28). Numerous studies provided evidence that SIRT3 helps to maintain the steady flow of the ETC chain to minimize the production of ROS. From several studies, it is evident that SIRT3 directly influences ROS production by deacetylating several OXPHOS enzymes. Therefore, SIRT3's deacetylation control of these complexes directly changes the generation of mitochondrial ROS at these target locations, which also enhances mitochondrial bioenergetics. SIRT3 regulates the subunits of the TCA cycle enzymes pyruvate dehydrogenase (PDH) and aconitase, both of which are linked to increased production of mitochondrial ROS, in addition to its influence on ROS synthesis through control of the complexes of ETC. Under stress, these proteins can create a sizable quantity of O_2^- and H_2O_2, although the MRC is a large ROS generator in mitochondria under resting conditions (29, 30).

Involved in the production of ATP, PDH is a gatekeeper enzyme complex of the TCA cycle and OXPHOS (31). PDH activity has been regulated through the acetylation/deacetylation process. Ozden et al. showed that SIRT3 and PDH physically interact and that PDHA1 may be acetylated both in vitro and in vivo (32). By using both mass spectrometry and in vitro deacetylation experiments, they further showed that SIRT3 deacetylates PDHA1 lysine 321, which controls PDH activity (31). Another crucial enzyme in the TCA cycle is aconitase. The TCA cycle's conversion of citrate to isocitrate is catalyzed by mitochondrial aconitase. Since aconitase is sensitive to mitochondrial superoxide, this enzyme is predisposed to acting as a source of hydroxyl radicals through a Fenton-type mechanism, which in turn enhances the synthesis of hydroxyl radicals (33, 34). However, unlike most instances where the deacetylation caused by SIRT3 leads to the activation of its target proteins, the deacetylation of aconitase by this enzyme inhibits its activity (35). Numerous physical and pathological situations have been used to study the function of SIRT3 in the control of antioxidative stress. It has been well established that SIRT3 controls MnSOD activity by deacetylating lysine 68 (36, 37). When SIRT3 is genetically deleted, the liver tissues of SIRT3$^{-/-}$ mice produce more mitochondrial superoxide, which is correlated with less MnSOD activity (38). In SIRT3 $^{-/+}$ animals, the lack of SIRT3 results in decreased MnSOD activity and increased oxidative damage to mitochondrial proteins in the heart (39, 40). On the other hand, upregulating SIRT3 decreases mitochondrial oxidative stress by deacetylating MnSOD, improving its function. These data amply support the notion that SIRT3-dependent control of MnSOD plays a crucial role in pathological circumstances by demonstrating that MnSOD is a direct target of SIRT3. Another enzyme controlled by SIRT3 is isocitrate dehydrogenase (IDH). By providing NADPH to glutathione reductase, the isoform IDH2 is a mitochondrial enzyme that converts NADP+ to NADPH and aids in the regeneration of reduced glutathione (GSH). IDH2 is a key source of NADPH and, while not being an antioxidant enzyme, it plays a crucial role in the control of the NADPH-dependent glutathione reductase, an enzyme that detoxifies H_2O_2 (41). SIRT3 has been shown to control the deacetylation of IDH2 in a variety of studies (41-43). Additionally, the SIRT3-mediated deacetylation of IDH2 led to an increase in cellular GSH pool and NADPH levels, which had cytoprotective effects against H_2O_2-induced oxidative damage (41). These data support the idea that SIRT3 regulates the glutathione system indirectly by using IDH as a source of NADPH. Importantly, mtDNA is prone to oxidative damage due to the accumulation of 8-oxo-7,8-dihydroguanine (8-oxoG) adduct in mtDNA. SIRT3 has been found to activate one of the key mtDNA repairing enzymes, 8-oxoguanine-DNA glycosylase 1 (OGG1) (44). Moreover, SIRT3 targets and activates superoxide dismutase (SOD2) isocitrate dehydrogenase (IDH2), and catalase (CAT), responsible for lowering the oxidative burden inside the cell (2). In addition, SIRT3 mediated sequestration of forkhead box O3a (FOXO3A) in the nucleus leads to the transcriptional upregulation of antioxidant genes including SOD2 and catalase, during oxidative stress (45, 46).

4.3. *Regulation of mitochondrial quality control*

Cellular energy homeostasis relays on the number of healthy mitochondria present inside the cell. To maintain cellular energy homeostasis healthy mitochondria should be maintained and this is achieved by a complex process called mitochondrial quality control. The flawless/perfect coordination of mitochondrial biogenesis, fission/fusion (mitochondrial dynamics) and mitophagy i.e., the mitochondrial quality control regulates the sound health of mitochondria thus it ensures cellular energy homeostasis. When oxidative burden exceeded the threshold bearing level/ rescuing ability of the antioxidant defense system, mitochondrial damage started with aberrant mitochondrial fragmentation and was followed by clearance of damaged mitochondria by a process called mitophagy. To maintain the cellular energy flow, new mitochondria are formed by a complex physiological process called mitochondrial biogenesis. SIRT3 plays a pivotal role in the regulation of mitochondrial quality control (47). SIRT3 influences the mitochondrial dynamics by deacetylating and activating the mitochondrial

fusion protein, Optic atrophy 1 (OPA1) (48). In colorectal cancer cell line SW837, silencing of SIRT3 activates mitochondrial fragmentation by inducing the expression of fission regulators Drp1, Fis1 and MFF (49). In cultured human tubular cells, cisplatin-mediated suppression of SIRT3 enhanced the mitochondrial fragmentation via activation of Drp1whereas overexpression of SIRT3 maintained the balance of mitochondrial dynamics by upregulation of mitochondrial fusion trigger, OPA1 (50). Knockdown of SIRT3 in the H9c2 cell line reduced the gene and protein expression of mitochondrial fusion regulator, (Mfn2), and upregulated the gene and protein expression of Drp1 significantly whereas the overexpression of SIRT3 in the same cell line normalized the expression of OPA1 and Drp1 (51). SIRT3 deacetylates and activates Foxo3a which increases the expression of Parkin, a key mitophagy regulator and thus SIRT3 influences mitophagy. In cardiomyocytes, Loss of SIRT3 weakened Parkin-mediated mitophagy by strengthening the interaction of p53-Parkin, thereby preventing the mitochondrial translocation of Parkin (52). In several studies, the prominent role of SIRT3 in mitochondrial biogenesis has been explained. Knock down of SIRT3 impaired the expression of PGC-1α, and TFAM, the key regulator of mitochondrial biogenesis (53-55) Increasing lines of evidence from different cell systems support the notion that the positive feedback loop of SIRT3-AMPK axis acts on the upstream of several mitochondrial quality control regulators including PGC1 alpha, TFAM, OPA1, Parkin (56). Furthermore, SIRT3 deacetylates and activates FOXO3 to activate the essential genes requires for mitochondrial biogenesis (57).

4.4. SIRTUIN 3 and cell death

SIRT3 protects cells from several stress-induced cell death signals by maintaining mitochondrial structural and functional integrity (58), SIRT3 prevents apoptosis by lowering the mitochondrial oxidative burden and impeding the mitochondrial permeability transition pore formation (11, 59). Moreover, the loss of SIRT3 induces hypoxia and activates the mitochondrial pathway of apoptosis (60)SIRT3 prevents apoptosis by activating Ku70 which directly binds to bax and prevents it to translocate to mitochondria (61). In addition to that, SIRT3 prevents apoptosis by deacetylating cyclophilin D which repairs the mitochondrial permeability transition pore (mPTP) and maintained the structural integrity of mitochondria (62). Necroptosis is a type of controlled cell death that resembles necrosis morphologically and is reliant on receptor-interacting protein 3 (RIP3) and subsequent activation of mixed lineage kinase domain-like pseudokinase (MLKL) (63). SIRT3, a crucial regulator of mitochondrial antioxidants, can stop necroptosis (58). SIRT3 loss has been demonstrated to enhance the expression of RIP3K, RIP1, and caspase-3 in a mouse model of diabetic skin wound healing via increasing superoxide generation (64). SIRT3 accelerates tumor growth by blocking RIPK3-mediated necroptosis and the innate immune response in prostate cancer (65). In hypoxic cardiac fibroblasts, SIRT3 knockdown accelerated oxidative stress and necroptosis (66). The major characteristics of ferroptosis, an iron accumulation-mediated nonapoptotic cell death, are an increase in cellular ROS generation and a buildup of lipid peroxide caused by iron. SIRT3 controls the metabolism and transport of iron (67). Transferrin receptor 1 (TfR1) expression was established to be downregulated as a result of SIRT3's modulation of iron regulatory protein 1 (IRP1) function. Ferroptosis can be mediated by p53, which links this kind of cell death to apoptosis and necroptosis (68). SIRT3 can prevent p53-mediated ferroptosis, shielding human cancer cells from oxidative stress (69). Increased cellular ROS generation and the accumulation of iron-induced lipid peroxide are the two key characteristics of ferroptosis, a nonapoptotic cell death caused by iron accumulation (67). SIRT3 controls the metabolism and transport of iron. Transferrin receptor 1 (TfR1) expression was revealed to be downregulated by SIRT3 when iron regulatory protein 1 (IRP1) activity was shown to be modulated. Ferroptosis is related to apoptosis and necroptosis (68)and can be mediated by p53. SIRT3 can prevent p53-mediated ferroptosis, shielding human cancer cells from stress induced by an excess of ROS (69).

5. ROLE OF SIRTUIN 3 IN THE GASTROINTESTINAL SYSTEM

The gastrointestinal epithelium, which is located at the interface between an organism and its luminal environment, is susceptible to oxidative damage from luminal oxidants (70). Recent research has demonstrated a connection between reactive oxygen species (ROS), mitochondrial dysfunction, and gastrointestinal disorders. Oxidative stress is known to play a significant role in the development of inflammatory bowel disease (IBD) (71), with patients suffering from IBD exhibiting abnormal mitochondrial structure in their enterocytes. Additionally, the detrimental effects of nonsteroidal anti-inflammatory drugs (NSAIDs) on the gastrointestinal tract are associated with disruptions in mitochondrial structure and function (72). NSAIDs can trigger mitochondrial oxidative stress (MOS), a condition that causes extensive damage to mitochondria through harmful redox reactions, leading to a decline in cellular energy levels and eventual cell death (73, 74). SIRT3 has been demonstrated to have a protective effect against oxidative stress by modulating the activity of mitochondrial antioxidant enzymes, specifically superoxide dismutase 2 (SOD2) and glutathione peroxidase 1 (GPx1). SIRT3 achieves this by deacetylating these enzymes, which enhances their enzymatic activity, resulting in decreased oxidative stress and inflammation. Apart from its involvement in oxidative stress, SIRT3 also plays a role in regulating apoptosis, or programmed cell death, in the GI system. SIRT3 has been found to protect against apoptosis by modulating the expression of anti-apoptotic proteins like B-cell lymphoma 2 (Bcl-2) and B-cell lymphoma-extra-large (Bcl-xL). The deacetylation of these proteins by SIRT3 enhances their anti-apoptotic function, leading to increased cell survival. SIRT3 has been found to have a role in regulating metabolism in the gastrointestinal (GI) system. It does this by deacetylating enzymes involved in glucose and fatty acid metabolism, such as pyruvate dehydrogenase (PDH) and acetyl-CoA synthetase 2 (ACS2), which increases their activity. This leads to higher energy production and reduced inflammation. Additionally, SIRT3 has been associated with several GI disorders, including inflammatory bowel disease (IBD) and colorectal cancer. Studies have shown that SIRT3 expression is decreased in patients with IBD, and that deficiency of SIRT3 worsens colitis in mice. Furthermore, SIRT3 has been shown to have a tumor-suppressive role in colorectal cancer by regulating mitochondrial metabolism and apoptosis.

5.1. SIRTUIN 3 in Non-malignant diseases

The gastrointestinal (GI) system requires a significant amount of energy due to its reliance on energy-intensive processes such as digestion and absorption. Research has shown that although the portal-drained viscera (PDV) - which includes the stomach, intestines, pancreas, and spleen - account for less than 6% of body weight, they contribute to 20-35% of the body's total energy expenditure (75). To meet this high energy demand, the GI system is rich in mitochondria, and mitochondrial function plays a crucial role in maintaining energy balance in the intestines (76, 77). Mitochondrial superoxide radicals, which are harmful reactive oxygen species (ROS), are primarily produced at two specific points in the electron-transport chain: complex I and complex III. Complex III is known to be the main site of ROS production under normal metabolic conditions (78). The ROS attack at the mitochondrial respiratory chain complexes, including complexes I and III, can damage important macromolecules within the mitochondria, such as lipids, proteins, and DNA (79, 80). If mitochondrial DNA damage is not properly repaired, it can lead to dysfunction in complex I and/or III, resulting in increased production of superoxide. This increased flux of superoxide can contribute to metabolic oxidative stress, genomic instability, and cellular damage (81). According to the protein ATLAS database, the GI system has exceptionally high levels of SIRT3 expression. SIRT3 is strongly expressed in tissues including the heart, muscle, and brain that have high levels of metabolic activity and mitochondria.

Table 1: Role of SIRTUIN 3 GI pathology

SIRTUIN 3 in non-malignant GI pathology		
Animal Model/ Patient Sample/Cell Line	**Target/s, Signaling Pathways, Cellular Effects**	**Reference**
• Mice with an enterocyte-specific SIRT3 overexpression (iSIRT3) were fed with either refined low-fat control diet or high-fat diet (HFD) based.	• Increased glucose clearance was seen in response to an oral glucose load. • Induction of genes involved in ketogenesis, such as Hmgcs2, Cpt1a, and long-chain acyl CoA dehydrogenase (Lcad). • Comparing iSIRT3 animals to control mice on HFD, fatty acid oxidation was increased in the enterocytes but there were no differences in gene expression.	(83, 173, 174)
• C57BL/6 male mice were fed with a control diet, high-fat diet (HFD), or HFD + dihydromyricetin (DHM) diet for 12 weeks, • MNK3 cell line	• Increases the expression of IL-22 to preserve the integrity of the intestinal barrier. • Promotes the ERK-CREB signaling pathway, which in turn activates STAT3 in MNK3.	(84)
• High-fat diet (HFD)-induced intestinal injury model in zebrafish • ZF4 cell line	• Reduced propionylation of SOD2 at K132 led to an increase in SOD2 activity. • Decreased mitochondrial oxidative stress.	(85)
• Ecal ligation and puncture (CLP)- or endotoxemia-induced sepsis models in mice	• Affects the acetylation of SOD2 and its activity. • Decreases CAT expression, GSH level, and GSH/GSSG ratio. • Decrease in oxidative stress	(86)
• An H_2O_2-induced model of oxidative stress model in IEC-6 and a hemorrhagic shock model in rat	• Inhibits the acetylation and activity of SOD2. • Decreases oxidative stress	(87)
• Intestinal I/R model was established in mice. • Caco-2 cells	• Reduced the acetylation level of PRDX3 • Reduced lung neutrophilic infiltration • Inhibits the antioxidant activity of PRDX3 • Reduced acetylation of PRDX3 at K253 in Caco-2 cells	(88)
• Intestinal ischemia/reperfusion (I/R) injury model in rat	• Elevated levels of Atg5, Bcl-2, PINK1, and caspase-3 as well as reduced levels of p62, p53, Bax, and cleaved caspase-3.	(89)

SIRTUIN 3 in malignant GI pathology		
Animal Model/ Patient Sample/Cell Line	**Target/s, Signaling Pathways, Cellular Effects**	**Reference**
• Human gastric cancer cell lines MGC-803, HGC-27, SGC-7901 and AGS and immortalized human gastric epithelial cell line GES-1 • MGC-803 cells • Human gastric cancer cell lines MKN45 and AGS cells • Normal human rectal mucosa cell line (FHC) and human rectal cancer cell lines (SW837 and SW480 cells)	• Increased cell growth • Increased glucose uptake (1.9-fold in SGC-7901 and 1.4-fold in AGS and) and lactate secretion (1.3-fold in SGC-7901)1.2-fold in AGS and • Enhanced glycogen formation (1.5-fold in AGS and 1.3-fold in SGC-7901) • Upregulates ATP production. • Enhancing MnSOD activity and decreased ROS levels to 70% and 80% in AGS and SGC-7901 cells. • Decreased the acetylation level of LDHA and enhanced its activity. • increased • Increased the expression of HIF-1a • Decreased the expression of CXCR4 and CXCR7 • Reduced the transcription of metastatic related genes related to CRC such as EGFR and BRAF • Promotes CRC mitochondrial apoptosis • Activated mitochondrial fission	(98, 99, 101)
• Human colon cell lines SW480, SW620 • Human colon cancer cell line SW620	• Repressed Akt phosphorylation, followed by a decrease in PTEN expression • Decreased the acetylation of SOD2 (acetyl K68). • Suppresses apoptosis in colon cancer cells • Suppressed the mitochondrial oxidative stress. • Preserves the expression of PGC-1α • Decreased the mRNA expression of mitochondrial biogenesis genes including nrf1, tfam, mtssb, and sirt1 • Reduced the protein expression of PGC-1α and TFAM. • Decreased in the protein expression of OXPHOS subunits. • oxygen consumption rate (OCR) was decreased • Mitochondria seemed to cluster and aggregate in one particular region of the cell instead of occupying the whole cytoplasm as in control cells. • Reduces motility and clonogenicity of cancer cells	(49, 53, 104, 105)

SIRTUIN 3 in malignant GI pathology		
Animal Model/ Patient Sample/Cell Line	**Target/s, Signaling Pathways, Cellular Effects**	**Reference**
• HCT116, McCoy's5A, MEFs and 143B cell line	• Increases proliferation of gastric epithelial cells and HIF-1α activity through ROS generation • The expression of HIF-1α target genes, such as Vegf-a, Pdk1, and Ldha, were significantly elevated Increased the ROS level.	(111)
• Primary gastric carcinoma tissues • The human gastric cancer cell lines AGS, SGC-7901 and BGC-823 and the normal gastric epithelium cell line GES were used	• Inhibited the proliferation of gastric cancer cells • Over-expression of SIRT3 inhibits the expression of Notch-1 both in gene and protein levels. • The inhibitory effect of SIRT3 in gastric cell proliferation is mediated by Notch-1	(112)
• Human GC cell lines AGS, MKN-45, SGC-7901 and mouse xenograft model was used	• SIRT3 Inhibited GC Cell Proliferation and Invasion by Inhibiting Notch-1 Pathway	(113, 115)

Although SIRT3 is highly expressed in the GI system, its function in the GI system has not been well studied. However, research into its function in GI disease has accelerated recently (Table. 1). In the past several years, several studies have studied the role of SIRT3 in the preservation of the GI system. In their research, Ramachandran et al. discovered that when mice were fed a high-fat diet (HFD), SIRT3 overexpression prevented the animals from becoming insulin-resistant and developing glucose intolerance (IR). Additionally, postprandial systemic ketone body levels on the HFD were lower than on the CD in control animals, however, this difference was not significant in mice with enterocyte-specific SIRT3 overexpression. Small intestine enterocyte metabolic activity increased in response to an oral dose of oleic acid in animals that were continuously fed the HFD due to intestinal SIRT3 overexpression. Body weight, body composition, fat distribution, or small intestine shape were unaffected by SIRT3 overexpression. These results demonstrate that regardless of body weight, body composition, or fat distribution, an increase in enterocyte metabolic flux is adequate to improve whole-body glucose homeostasis in DIO (83). In Zhou et. al.'s investigation, the connection between HFD and SIRT3 expression dysregulation was further established. In their investigation, they demonstrated how the HFD diet reduced IL-22 expression to compromise the intestinal epithelial barrier's integrity and how dihydromyricetin (DHM) restored the damage by stimulating IL-22 synthesis in ILC3s. DHM encouraged the expression of IL-22 under this regulation by activating STAT3 through SIRT3 signaling (84). In their study, Ding et al. demonstrated that a high-fat diet and propionate caused oxidative damage to the gut of zebrafish. They identified a propionylation-based mechanism for intestine oxidative injury induced by propionate. At the lysine 132 location, superoxide dismutase 2 (SOD2) can be propionylated, which inhibits its function and causes oxidative damage in the gut. In addition, they discovered that in zebrafish fed a high fat plus propionate diet, lower intestine expression of SIRT3 was the cause of the greater propionylation of SOD2. Additionally, the high fat plus propionate diet-induced intestinal microbiota also contributed to intestinal oxidative stress in a SIRT3-unrelated way (85). Melatonin is a strong activator of SIRT3. According to a study, melatonin reduces the damage to the small intestine caused by sepsis by increasing SIRT3. Melatonin independently increases SIRT3 expression and activity in the mitochondria, which leads to SOD2 deacetylation and inhibits oxidative

stress while safeguarding mitochondrial function and triggering autophagy (86). Zeng et al. have proven SIRT3's protective function in the GI system against heat shock or oxidative damage. They have demonstrated that following heat shock or oxidative stress, both the expression and activity of SIRT3 were decreased in small intestinal tissue and IEC-6 cells, along with an elevated level of acetylated-SOD2 and damaged mitochondria. Treatment with polydatin or resveratrol increased SIRT3 activity significantly, modestly increased SIRT3 expression, and decreased acetylated-SOD2 levels, which improved mitochondrial function. The mitochondrial-protective effects of polydatin were partially reduced by the addition of 3-TYP (SIRT3 inhibitor). As a result, heat shock-induced mitochondrial dysfunction is caused via the SIRT3-SOD2 signaling pathway. A novel method of heat shock therapy, polydatin reduces mitochondrial dysfunction by activating the SIRT3-SOD2 pathway. (87). For intestinal ischemia/reperfusion (I/R) injury, PRDX3 is a critical protective factor, and SIRT3-mediated PRDX3 deacetylation on residue K253 can reduce intestinal I/R-induced mitochondrial oxidative damage and death in Caco-2 cells after intestinal H/R injury. Because of this, these findings offer a new therapeutic target for intestinal I/R damage and identify SIRT3/PRDX3 as a crucial signaling pathway in intestinal I/R injury (88). The findings demonstrated Dexmedetomidine's (Dex) protective role against mitochondrial dysfunction and apoptosis in enteric glial cells (EGCs) through the activation of the SIRT3-mediated PINK1/HDAC3/p53 pathway, which ultimately led to the amelioration of intestinal I/R injury, provide additional evidence in favour of the hypothesis that SIRT3 is necessary to maintain GI track function. (89).

5.2. SIRTUIN 3 in GI malignancy

Cancer cells need more cellular energy than healthy cells because they have an active metabolism. However, cancer cells primarily rely on aerobic glycolysis to synthesize ATP, a characteristic known as the Warburg effect (90). Since mitochondrial respiration is the primary generator of intracellular ROS, it is thought that such aerobic glycolysis will protect cancer cells from oxidative stress (90, 91). Naturally, OXPHOS is still their more suitable source of energy supply in some specific cancers or conditions (such as brain cancer and acute myeloid leukaemia), and the survival of these cancers is more dependent on the continuing activity of OXPHOS (92), (93). Varied malignancies have very different tumor microenvironments, and the urge to survive drives them to adopt the best metabolic pathway. In brief, SIRT3 regulates mitochondrial metabolism generally by promoting oxidative phosphorylation and inhibiting glycolysis (25, 94). It's interesting to note that a recent study discovered that SIRT3 transforms into an oncogene to support HFD-induced carcinogenesis in mice (95). As a result, SIRT3's function in cancer seems context-dependent (Table. 1) (96). Most often, it causes cancer in malignancies that are dependent on OXPHOS (92). Here, we have discussed SIRT3's dual functions in GI cancer: oncogene and tumor suppressor.

5.2.1. SIRTUIN 3 as an Oncogene
5.2.1.1. Gastric Cancer
Additionally, it has been shown that SIRT3 increases the activity of lactate dehydrogenase A (LDHA) via deacetylating it. The primary protein that controls glycolysis, which is essential for tumor development, is LDHA. Increased LDHA levels in GC patients are associated with improved treatment response and, regrettably, lower overall survival (97). When compared to healthy gastric epithelial cells, it has been found that a group of gastric cancer cells expressed SIRT3 at a higher level. Overexpression of SIRT3 promoted glucose uptake, ATP generation, cell proliferation, glycogen formation, SOD2 activity, and lactate production, which were inhibited by SIRT3 knockdown, demonstrating that SIRT3 plays a key role in reprogramming the bioenergetics in gastric tumor cells. SIRT3 expression levels were higher in the gastric tumor tissues compared to the adjacent healthy tissues. Additional research demonstrated that SIRT3 enhanced LDHA activity by interacting with and deacetylating lactate

dehydrogenase A (LDHA), a crucial enzyme in controlling anaerobic glycolysis. Consistently, a collection of genes linked to glycolysis were increased in the gastric tumor cells overexpressing SIRT3. Thus, SIRT3 may promote glycolysis and cell proliferation in SIRT3-expressing cancer cells (98). In contrast, another study found that SIRT3 expression boosted glucose absorption, lactate formation, manganese superoxide dismutase (MnSOD) activity, and ATP synthesis in GC cells. Knocking down the SIRT3 gene prevented these outcomes. These findings highlight SIRT3's involvement in procedures involving the reprogramming of GC cell bioenergy. Contrary to the diffuse kind of GC (99), patients with intestinal GC were observed to have higher SIRT3 expression. Recent studies have revealed a connection between GC etiology and genetic variants of mitochondrial sirtuins, notably SIRT3 (100). These genes are altered, which results in mitochondrial malfunction and encourages the development of cancer. If any single-nucleotide polymorphisms (SNPs) may be employed as predictive indicators of GC, more study is required. A potential therapeutic approach for treating gastric cancer could involve focusing on the mitochondrial protein SIRT3. However, it is still unclear how stemness is controlled in gastric cancer by inhibiting SIRT3. Tai et al. examined the efficacy of the resveratrol analog 4-BR, a SIRT3 inhibitor, to reduce stemness in human gastric cancer cells. Results showed that 4-BR reduced the stemness of gastric cancer cells via the SIRT3-c-Jun N-terminal kinase pathway and may be useful in the treatment of gastric cancer stem cells (101). Mammalian sterile 20-like kinase 1 (Mst1) plays a crucial role in regulating cell survival and cell death. The expression of Mst1 was found downregulated in AGS cells compared to GES-1 cells. Overexpression of Mst1 induces mitochondrial dysfunction by blocking the AMPK-SIRT3 pathway whereas activation of the AMPK-SIRT3 pathway negated the promoting effect of Mst1 overexpression on mitochondrial dysfunction (102). The kinase mammalian sterile 20-like 1(Mst1) is essential for controlling cell survival and apoptosis. When compared to GES-1 cells, Mst1 was downregulated in AGS cells. By inhibiting the AMPK-SIRT3 pathway, Mst1 overexpression causes mitochondrial dysfunction, whereas Mst1 overexpression has the opposite impact when the AMPK-SIRT3 pathway is activated (102).

5.2.1.2. Colon cancer

SIRT3 has been implicated in several papers as a colorectal cancer oncogene (CRC) (Table. 1). According to Wang *et al*. SIRT3 plays a crucial part in the CRC's migratory response and apoptosis. Mitochondrial fission, which is induced by SIRT3 downregulation, causes both mitochondrial malfunction and CRC apoptosis. By focusing on the SIRT3-Akt-PTEN-mitochondrial fission pathway, this may represent a novel approach for the treatment of CRC (49). Torrens-Mas et al. further demonstrated the oncogenic involvement of SIRT3 in CRC. In their research, they demonstrated that silencing SIRT3 in colon cancer cells impacts both the activity of antioxidant enzymes and its expression at the mRNA level, which may lower the cell's antioxidant capacity and hence increase cell death. (103). The low level of mitochondrial superoxide and apoptosis resistance in CRC cells is caused by SIRT3 activity, which was also made more active by mitochondrial NOS1. NOS1-induced apoptosis resistance could be restored by decreasing mitochondrial translocation of NOS1 (104). SIRT3 has also been shown to be a stand-alone prognostic factor in colon cancer. By controlling SOD2 and PGC-1α, SIRT3 promotes chemoresistance in colon cancer cells (105). Additionally, it was shown that the widely used anti-cancer medication Cisplatin inhibited SIRT3 expression and increased MTHFD2 acetylation, both of which led to a drop in NADPH levels and an increase in ROS levels. Further research revealed a substantial negative correlation between SIRT3 protein levels and acetylated K88 MTHFD2 in colorectal tumor tissues, suggesting that SIRT3 or MTHFD2 inhibitors may be a promising medication to use with cisplatin for the treatment of colorectal cancer (106). Additionally, it was shown that the absence of SIRT3 causes CRC cells to undergo PINK1/Parkin-mediated mitophagy, which results in cell death (107). According to recent research (108), tumor cells develop adaptive resistance to therapeutic radiation by improving SIRT3-mediated mitochondrial homeostasis through both gene

transcription and post-translational alterations of SIRT3 in the mitochondria. Studies on clinical CRC patients found a strong correlation between the SIRT3 expression level and the lymph node metastases (P = 0.001) and tumor stages (P = 0.001). Patients with high SIRT3 expressions had a 64.6 percent colon cancer-specific survival rate, while patients with low SIRT3 expressions had an 88.6 percent survival rate (log-rank P = 0.016). Patients with low SIRT3 expressions had an overall survival rate of 80.2%, whereas patients with high SIRT3 expressions had a survival rate of 55.9% (log-rank P = 0.002). Additionally, in vitro, research revealed that suppressing the SIRT3 gene reduced colon cell lines' ability to proliferate, invade, and migrate while increasing apoptosis (109). By deacetylating NEIL1, NEIL2, MUTYH, APE1, and LIG3 in CRC, SIRT3 affects cell survival 35440893. In research using the colon cancer cell line SW620, the knockdown of SIRT3 caused reduced mitochondrial biogenesis and mitochondrial malfunction, which eventually affected cell viability (53), further validating SIRT3's oncogenic involvement.

5.2.2.   *SIRTUIN 3 as a Tumour Suppressor*
5.2.2.1. *Gastric Cancer*

However, different research revealed that SIRT3 can act as a tumor suppressor in cases of gastric cancer, and several investigations have revealed a negative correlation between SIRT3 and the development of GC (Table. 1). According to the results of the multivariate analysis, SIRT3 could function as a standalone biomarker for predicting the prognosis of gastric cancer (110). Tumor invasion, differentiation, and stage are among the clinicopathological factors that have a negative correlation with SIRT3 expression. In contrast to overexpression of SIRT3, which destabilizes HIF-1a and reduces tumorigenesis in xenografts (25, 111), SIRT3 may regulate the formation of ROS and sustain the expression of HIF-1a and its transcriptional activity.

Furthermore, Notch-1 is down-regulated by SIRT3 to decrease cell proliferation in human gastric cancer, whereas Notch-1 overexpression reduces SIRT3's inhibitory effects on tumor cell proliferation (112). Results of clinical patient sample analysis revealed low SIRT3 expression in GC patient samples. The degree of SIRT3 expression was negatively linked with tumor infiltration, tumor differentiation, tumor stage, and 5-year survival in these patients (99). In a recent study, it was shown that the lncRNA fetal-lethal non-coding developmental regulatory RNA (FENDRR), which targets the miR-421 (113)gene, suppresses the Notch-1 pathway to prevent GC cancer cells from proliferating and invading. Additionally, the loss of SIRT3 occurred during the development of gastric cancer, reprogramming cancer cell metabolism, and favoring the Warburg effect, according to high-resolution mass spectrometry analysis data from 3914 different proteins extracted from patients with chronic gastritis, intestinal metaplasia, and gastric adenocarcinoma (114).

5.2.2.2. *Colon cancer*

Numerous studies back up SIRT3's ability to decrease tumor growth in CRC (Table. 1). It was shown that increasing the expression of SIRT3 decreased caused cell cycle arrest, decreased cell growth, and promoted apoptosis (115). By increasing the protein expression of SIRT3, ganoderic acid D (GAD), a highly oxygenated tetracyclic triterpenoid, prevents colon cancer cells from using glucose absorption, lactate synthesis, pyruvate, and acetyl-coenzyme formation as energy sources. Additionally, all of SIRT3's impacts on the energy reprogramming of colon cancer were dramatically reversed by stopping SIRT3 expression (116). In addition, SIRT3 inhibits colonic tumorigenesis via an interaction with the gut microbiome and thus it plays as a tumor suppressor in CRC (117). It was further observed that diet-derived ergothioneine induces necroptosis in colorectal cancer cells by triggering the SIRT3/MLKL pathway (118). Additionally, SIRT3 acts as a tumor suppressor in CRC by inhibiting colonic carcinogenesis through a relationship with the gut flora (117). The SIRT3/MLKL pathway was shown to be activated by dietary ergothioneine, which causes necroptosis in colorectal cancer cells (118).

6. ENDOGENOUS REGULATORS OF SIRTUIN 3

SIRT3, the protector of mitochondria, is controlled in a variety of ways (Table. 2). Numerous investigations have been done on this protein's post-translational modifications, transcriptional regulation, and endogenous regulators of its expression. Because SIRT3 is a sensor of mitochondrial energy, its activity is directly influenced by the amounts of the metabolic co-factor (NAD+) and its by-product, nicotinamide (4, 119). While nicotinamide inhibits this process by speeding the reverse reaction by attaching to the reaction product, NAD+, as a co-factor of SIRT3, supports the deacetylation process (119). As skeletal muscle is the primary location of energy expenditure during exercise, exercise can enhance SIRT3 expression and activity in a variety of tissues. Exercise may promote SIRT3 by several mechanisms, including increased NAD+ availability, AMPK activation, PGC-1α induction, and ROS generation. The precise mechanism by which exercise increases SIRT3 is not entirely known. These elements might work together to increase SIRT3 gene transcription and/or protein stability (23, 120, 121). The role of PGC-1α and ERRα alpha in SIRT3 regulation is important for various cellular processes, such as oxidative stress, mitochondrial biogenesis, and energy metabolism. PGC-1α α is a transcriptional coactivator that can activate the expression of SIRT3, a mitochondrial deacetylase, by interacting with ERRα, a nuclear receptor. ERRα binds to a specific element in the SIRT3 promoter and recruits PGC-1α to enhance its transcriptional activity (54), (82). SIRT1, another member of the sirtuin family protein regulates SIRT3 expression through AMPK-PGC1 pathway (122). SP1 (Specificity protein 1) is a transcription factor that binds to the promoter region of the SIRT3 gene and regulates its expression. Studies have shown that SP1 can positively regulate SIRT3 expression by binding to its promoter region and promoting its transcription. On the other hand, inhibition of SP1 can lead to a decrease in SIRT3 expression (59). Additionally, calorie restriction (CR) is a vital element that can undoubtedly promote SIRT3 production, which is a biological self-defense mechanism. The up-regulated SIRT3 activates mitochondrial Isocitrate Dehydrogenase 2 (IDH2) in response to CR by deacetylating it, raising the NADPH level to lower oxidative damage and strengthen the mitochondrial antioxidant defense system (119). SIRT3 activity is suppressed by the post-translational modification known as SUMOylation. To encourage mitochondrial metabolism, the SUMO-specific protease SENP1 can de-SUMOylate and activate SIRT3 (123). Carbonylation is a post-translational modification that can regulate protein function, stability, and localization1. Carbonylation of SIRT3 has been shown to reduce its activity, leading to increased mitochondrial protein carbonylation, oxidative stress, and cell death. A high-resolution mass spectrometry-based phosphoproteome investigation has shown six phosphorylated serine residues between locations 101 and 118. In the N-terminal extension, these phosphorylation sites are near the mitochondrial cleavage site. So, it's plausible that phosphorylation modifies SIRT3's enzymatic activity in mitochondria by controlling proteolytic cleavage, altering the contact between the N- and C-terminal extension, or controlling the interaction of the N-terminal area with the catalytic domain (124). Covalent modification can also control SIRT3. By occupying the zinc-binding residue (Cys 280) of SIRT3, 4-Hydroxynonenal (or 4-HNE) suppresses SIRT3 function (125). This residue is an endogenous by-product of lipid peroxidation. Transcriptional modification is yet another important mechanism controlling SIRT3. Recent research has revealed that the pleiotropic transcription factor NF-B may connect to the SIRT3 promoter and boost the gene's expression (126). The SIRT3 promoter activity is negatively regulated by SNAI1 and Zinc finger E-box-binding homeobox 1 (ZEB1), which prevents SIRT3 from being expressed (127, 128). MicroRNAs are single-stranded, non-coding tiny RNA molecules that can control SIRT3 activity by influencing mRNA stability and protein levels. MiRNAs are a family of non-coding RNA molecules that bind to complementary target mRNAs to prevent or slow down mRNA translation

Table 2. Endogenous regulators of SIRTUIN 3

Name	Classification	Regulatory Mechanism	Reference
NAD$^+$	Cofactor	Promotes the deacetylation activity of SIRT3	(119)
Nicotinamide	Deacetylation product	By rebinding the reaction product to the enzyme, nicotinamide inhibits SIRT3 and accelerates the reverse process.	(4, 24)
Calorie restriction	Physiological phenomenon	Enhances SIRT3 expression and activity	(119)
MPP	Peptidase	Proteolytic processing of FLSIRT3 to active SIRT3	(175)
SENP1	SUMO-specific protease	SENP1 can activate SIRT3 by its de-SUMOylation activity.	(123)
PGC-1α	Transcriptional coactivator	To control SIRT3 expression, PGC-1 binds to the SIRT3 promoter as its transcription factor.	(176, 177)
NF-κB	Transcription factor	The SIRT3 promoter is bound by NF-B to increase the expression of SIRT3.	(126)
miR-195	MicroRNA	Direct 3'-untranslated region targeting by miR-195 reduces SIRT3 expression	(178)
miR-421	MicroRNA	SIRT3's 3'UTR is targeted by miR-421, which lowers the amount of SIRT3 protein.	(179)
miR-31	MicroRNA	SIRT3 is a direct target of miR-31, which represses its expression.	(135)
miR-145	MicroRNA	SIRT3 is specifically targeted by miR-31, which lowers its expression.	(139)
miR-298	MicroRNA	Directly targeting SIRT3, miR-298 reduces the expression of SIRT3.	(137)
miR-210	MicroRNA	miR-210 aims and suppresses ISCU to alter the NAD$^+$/NADH ratio thus indirectly inhibiting SIRT3	(138)

(129). The 3'UTR of SIRT3 can be directly targeted by the miRNAs miR-195 (130), miR-214 (131), miR-421 (132), miR-494-3p (133), miR-708-5p (134), miR-31 (135), miR-145 (136), and miR-298 (137), which inhibits SIRT3's gene expression and protein levels. In addition, miR-210 targets and represses the ISCU protein, which modifies the NAD+/NADH ratio and indirectly affects SIRT3 (138). miRNAs and long non-coding RNA (LncRNAs) both have comparable functions. While LncRNA DYNLRB2-2 inhibits miR-298 to promote the transcription of SIRT3 (137), LncRNA TUG1 decreases the mRNA production of miR-145, which can further favorably regulate SIRT3 (139). Another important mechanism for controlling SIRT3 activity is the protein-protein network. Actin-associated protein profilin1 can interact with SIRT3 and increase the expression of SIRT3 (140). To prevent SIRT3 from being expressed, -catenin, a crucial downstream effector in the Wnt signaling pathway, can reduce SIRT3 promoter activity (141). As was already indicated, in response to cellular stressors, these endogenous regulators modify SIRT3's expression and actions, preserving homeostasis.

7. SIRTUIN 3 MODULATION AS A POTENTIAL THERAPEUTIC STRATEGY

The role of SIRT3 in aging, cancer, neurological disorders, and stress resistance has received a lot of attention. Through reversible protein lysine deacetylation, SIRT3 controls the TCA cycle, oxidative stress, hyperglycemia, fatty acid metabolism, and apoptosis, among other biosynthetic activities. A variety of SIRT3 activators and inhibitors have been created by academics and pharmaceutical firms as a result of SIRT3's involvement in a variety of illness disorders, making it a desirable pharmacological

target. Through a variety of ways, these substances can deacetylate SIRT3 or control its expression level. These substances were categorized into two main groups based on how they affected SIRT3: SIRT3 activators (technically "positive modulators") and inhibitors.

7.1. SIRTUIN 3 activation

Upregulating SIRT3 appears to be a successful method for the therapy of many diseases, and SIRT3 malfunction is strongly linked to the onset of many diseases (Table. 3) . SIRT3 can be stimulated by several positive modulators that increase SIRT3 expression. They have demonstrated potential therapeutic results in several diseases including heart hypertrophy, acute renal damage, and others. It should be noted that most activators of SIRT3 are derived from natural products. For instance, Honokiol, a natural lignan obtained from the bark of the Magnolia tree, is one of the most studied SIRT3 activators. Honokiol may improve SIRT3 expression and deacetylation activity, which is beneficial for renal disease (143), surgery/anesthesia-induced cognitive decline (144), heart disease (142), and Vitiligo (145). The role of honokiol in GI system was not explored yet. Notably, natural compounds are the source of the majority of SIRT3-positive regulators. As an illustration, the natural lignan Honokiol, which is produced from the bark of the Magnolia tree, is one of the most researched SIRT3 activators. Honokiol may boost SIRT3 expression and deacetylation activity, which is good news for patients with heart disease (142), renal diseases (143), surgery- or anesthesia-induced cognitive impairment (144), and Vitiligo (145). The role of honokiol as an activator of SIRT3 in the GI system hasn't yet been studied. Due to their topical irritancy, neutrophil activation, and decreased PGE synthesis, the most widely prescribed analgesics and traditional NSAIDs are harmful to the gastro intestinal tract. Honokiol's gastro-protective properties have previously been proven in earlier studies (146). However, the function of SIRT3 was not examined. The contractility of isolated ileum guinea pigs treated with acetylcholine or CaCl2 (147) and isolated gastric fundus strips of rats treated with acetylcholine and 5-hydroxytryptamine was considerably reduced by honokiol. To aid in the relaxing of intestinal smooth muscle, Honokiol targets TRPC4 channels and regulates external calcium influx (148). Honokiol-mediated activation of SIRT3 lowers MnSOD2 levels of acetylation, increases mitochondrial oxygen consumption, encourages mitochondrial fusion, and inhibits apoptosis (82, 143, 145). More intriguingly, tumor-xenograft animals that had SIRT3 activated by Honokiol can prevent doxorubicin- induced cardiotoxicity without compromising the anti-tumor activity of the drug (149). To stop the NF-B-TGF-1/Smad-regulated inflammation and fibrosis signaling in renal fibrosis mice model (143), honokiol increases SIRT3 activity. Surprisingly, Honokiol can prevent mice from developing cognitive impairment induced by anesthesia or surgery via SIRT3 activation mediating ROS removal and apoptosis suppression (144). It's interesting to note that honokiol may reduce vitiligo by inhibiting melanocyte death through activation of the SIRT3-OPA1 axis (145). According to this research, honokiol, whether taken orally or in combination with other treatments, may be beneficial in the management of many disorders. Another organic plant-derived SIRT3 activator is silybin. It is a hepatoprotective agent used in traditional Chinese medicine that is extracted from the seeds of blessed milkthistle (*Silybum marianum*). In a mouse model of cisplatin-induced acute kidney damage, it was found that silybin can enhance kidney mitochondrial function by activating SIRT3. To prevent the death of kidney cells, SIRT3 is upregulated, which reduces ROS and suppresses apoptosis (150). A well-known SIRT1 activator, resveratrol, can also boost SIRT3 expression to lessen acute kidney damage (151). Fascinatingly, Dihydromyricetin has a molecular structure that is comparable to Resveratrol, and it can cure osteoarthritis by increasing the expression of SIRT3 through SIRT3-mediated cytoprotection and inflammatory resistance (152). To protect cardiomyocytes from myocardial infarction, Polydatin,

Table 3: Activators of SIRTUIN 3

Molecule	Target/Pathway	Disease/Cell	Reference
Honokiol	Honokiol promotes the expression and activity of SIRT3	• Cardiac hypertrophy • Renal disease • Surgery/anaesthesia-induced cognitive decline • Vitiligo • Gastric ulcer	(142-144, 149)
Silybin	Silybin promotes SIRT3 expression	Acute Kidney Injury	(150)
Resveratrol	Resveratrol promotes SIRT3 expression	Acute Kidney Injury	(151)
Polydatin	Polydatin enhances SIRT3 activity	• Myocardial infarction • Sulfur mustard-induced hepatic injury	(153)
Dihydromyricetin	Dihydromyricetin promotes the expression and activity of SIRT3 via activation of PGC-1α	Osteoarthritis	(152)
Pyrroloquinoline quinone	Pyrroloquinoline quinone promotes the expression and activity of SIRT3	Liver metabolic diseases	(155)
Melatonin	Metformin enhances SIRT3 expression	Atherosclerosis	(159)

a polyphenolic substance derived from *Polygonum cuspidatum*, can initiate SIRT3-regulated mitochondrial autophagy (153). Additionally, this natural substance exerts its hepatoprotective properties via SIRT3 (154) in a mouse model of sulfur mustard-induced liver damage. Another natural substance called pyrroloquinoline quinone can treat liver metabolic disorders by boosting SIRT3 expression (155). Recent drug repurposing studies have shown that some "old drugs" can activate SIRT3 with a distinct action mechanism. By activating SIRT3, metformin can reduce atherosclerosis triggered by type 2 diabetes (156). Adjudin, through SIRT3 (157), stops gentamicin-induced hair cell loss.

Intriguingly, it has been shown that the hormone melatonin, which affects sleep by acting on the melatonin receptor, also activates SIRT3 and protects against, liver damage (158), heart disease (159) and atherosclerosis (160). Melatonin also promotes SIRT3 expression and activity to prevent cardiomyocyte apoptosis and keep mitochondrial metabolism stable in a rat model of myocardial ischemia/reperfusion (MI/R) damage (159). Melatonin also activates SIRT3 activity in cadmium-induced hepatotoxicity in vitro and in vivo models to suppress ROS generation and cadmium-triggered autophagic cell death (160). Additionally, melatonin promotes SIRT3-FOXO3a-Parkin-controlled mitophagy in a rat model of atherosclerosis to inhibit inflammation and the development of atherosclerotic disease (160).

Table 4: Inhibitors of SIRTUIN 3

Compound	Type	Disease/cell	Biological Activity	Reference
4'-Bromo-Resveratrol	Substrate competitive SIRT3 inhibitor	Melanoma	SIRT3 IC_{50}=143.0 ± 3.6 μM	(158, 180)
3-TYP	Nicotinamide competitive SIRT3 inhibitors	Tool medicine	SIRT3 IC_{50}=16 nM	(162)
YC8-02	Substrate competitive SIRT3 inhibitor	Lymphoma	SIRT3 IC_{50}=0.53 μM	(181)
JH-T4	Substrate competitive SIRT3 inhibitor	Lymphoma	SIRT3 IC_{50}=2.5 μM	(181)
(4- [(2-Hydroxy-6-phenylnaphthalen-1-yl) methyl]-5- (4-methylphenyl) -2,3-dihydro-1H-pyrazol-3-one)	Substrate competitive SIRT3 inhibitor	Cancer	SIRT3 IC_{50}=6 μM	(182)

7.2. *SIRTUIN 3 inhibition*

Development of SIRT3 inhibitors has been simpler than the discovery of SIRT3 activators (Table. 4). The SIRT3 deacetylation pathway logically points to a number of ways to stifle this chemical reaction. Structure-based design is an additional method for finding SIRT3 inhibitors now that the SIRT3 protein's crystal structure has been determined. The last but not least method for finding SIRT3 inhibitors is chemical library screening (4). Substrate competitive inhibitors are one of the most popular and efficient methods for designing inhibitors. A competitive inhibitor of the ACS2 peptide substrate found in 2013 was 4'-bromo-resveratrol (161). N-acyl-lysine analogs are crucial substrate-competitive SIRT3 inhibitors. One of the N-acyl-lysine analogs with exceptional proteolytic stability and cell permeability is peptide-based SIRT3 inhibitors. N-thioacetyl-lysine-containing peptides with SIRT3 inhibitory properties were created by Chen et al. The main disadvantage of nicotinamide as a SIRT inhibitor is that it has little selectivity for SIRTs. Nicotinamide analogs are unquestionably a crucial part of SIRT3 inhibitors, though. A nicotinamide analog in essence, 3-TYP is a commonly utilized medical tool with highly specific SIRT3 inhibition (SIRT3 IC_{50}=16 nM) (162). Using the published structure of SIRT3, docking and binding free energy calculations can be used to find new SIRT3 inhibitors. By doing this, Berin et al. found quite a few substances with effective SIRT3 inhibitory properties. Sadly, no biological activity has been found in them, therefore their applicability may need more research to support (163). Using chemical library screening, it is possible to find brand-new SIRT3 inhibitors. Recently, the DNA-encoded Dynamic Chemical Library was used to find the new SIRT3 inhibitor 77-39 (SIRT3 IC_{50} = 4.5 μM). Additionally, 77-39 shows good cellular SIRT3 inhibition efficacy and just little cytotoxicity (164). Another effective method to find new SIRT3 inhibitors is to filter libraries encoded with information. This method led to the discovery of the effective SIRT3 inhibitor 11c ((N2-(2-(1-(6-carbamoylthieno [3, 2-d] pyrimidin-4-yl) piperidin-4-yl)-N5-ethylthiophene-2, 5-dicarboxamide)) (SIRT3 IC_{50} = 4.0 nM) (165). Tenovin-6 is a biologically active

p53 activator that was subsequently shown to also have SIRT3 inhibitor (SIRT3 IC_{50} = 67 μM) and anti-tumor action. Although its ability to inhibit SIRT3 was previously unknown, (166) has now been shown to function as a non-competitive inhibitor. The mechanism of the synthetic SIRT3 inhibitor LC-0296, which has a good inhibitory effect (SIRT3 IC_{50} = 3.6 μM), is likewise unknown. LC-0296 could be a NAD^+ competitive inhibitor (167) based on its structural characteristics. Trimethylamine-N-oxide (TMAO), a choline metabolite, can increase vascular inflammation by activating ROS-NLRP3 when SIRT3 is inhibited (168). An anthelmintic medication having the capacity to target microtubules is albendazole. Recently, it was shown that albendazole causes SIRT3 to degrade, preventing leukaemia cells from surviving (169). In order to block SIRT3's function, it has been discovered that the anti-cancer medication 2-methoxyestradiol (2-ME) binds to both the usual and allosteric inhibitor binding sites (170).

8. CONCLUSIONS

It is well known that SIRT3, the primary deacetylase in mitochondria, regulates mitochondrial oxidative stress, energy balance, and all other aspects of mitochondrial metabolism. Cells' mitochondria perform a crucial function, and abnormalities with them can lead to several disorders. Many mitochondrial abnormalities have been linked to SIRT3 dysregulation. The secrets of SIRT3's innate biological roles and its potential therapeutic uses in treating human diseases have been gradually unraveled by an accumulation of recent research. From its basic function as the longevity gene to its potential as a prominent target in numerous disorders, SIRT3 has drawn a lot of attention. However, the role of SIRT3 in gastrointestinal system/ pathology mainly in non-malignant GI pathology is rarely discussed so far. Therefore, understanding the role of SIRT3 in GI pathology is essential to understand GI pathology in the context of mitochondrial dysfunction as well as for therapeutic purposes. Numerous studies have shown that the scavenging action of SIRT3 on ROS plays a key role in the improved function of SIRT3 in many diseases. A significant contributor to the onset of age-related illnesses, heart disease, cancer, and metabolic disorders is frequently an excessive build-up of ROS. By deacetylating its substrates, such as MnSOD2, IDH2, and PHD, SIRT3 activates them and subsequently expels extra ROS. In contrast, SIRT3 controls the metabolism of TCA, OXPHOS, fatty acids, and amino acids to preserve mitochondrial homeostasis in healthy or mildly damaged mitochondria, which affects cell fitness and survival. However, SIRT3 can deacetylate and activate FOXO3a to promote mitophagy, which eliminates and circulates mitochondria when the damage to the mitochondria is too great to be healed. SIRT3 has been shown to play the Janus function in cancer, which is interesting given its intrinsic complexity. This means that SIRT3 activators or inhibitors would be used as anti-tumor drugs in certain types of malignancies, respectively. For instance, it is indisputable that the use of SIRT3 inhibitors in some OXPHOS-dependent tumors appears to be extremely promising. However, because SIRT3 protects a number of human systems, inhibiting SIRT3 may potentially result in toxicities to several organs. On the other side, in some situations, the overzealous pursuit of SIRT3 activation may potentially result in unanticipated carcinogenesis. The search for novel small-molecule inhibitors or activators for the treatment of various forms of cancer, therefore, seems to be limited when taking either up-regulation or down-regulation of SIRT3 expression into consideration. Perhaps combining a SIRT3 activator/inhibitor with a different medication that targets a particular human organ would be a different potential therapeutic approach. There haven't been any effective findings of particular SIRT3 activators or powerful inhibitors that are now being used for prospective treatments. Nevertheless, it has been claimed that a number of small-molecule drugs have therapeutic potential. For instance, Honokiol, the most well-known SIRT3 activator, has some therapeutic benefits in heart disease, illnesses associated with inflammation, cancer, and metabolic disorders. However, not all of its beneficial effects are related to the activation of SIRT3. Therefore, it is still a puzzle how to create an efficient SIRT3 activator or

inhibitor for therapeutic applications. Scientific drug design methodology is crucial in this regard. At the moment, there aren't any efficient and reliable design techniques for SIRT3 activators. There is no foundation for structure-based drug design since the mechanism of the interaction between small molecule agonists and SIRT3 is still a mystery. Allosteric agonists are now one of the most effective approaches for creating SIRT3 agonists. Artificial intelligence has recently been used in the realm of medication design, ushering in a new age of ground-breaking drug development. But more work is still needed to clarify the molecular mechanism of SIRT3 allosteric activation. Together, SIRT3's transformation from a mitochondrial metabolic regulator to a viable therapeutic target would open new doors for the rapid development of novel drug candidates for the treatment of human ailments.

9. REFERENCES

1. Murugasamy, K., Munjal, A., and Sundaresan, N. R. (2022) Emerging Roles of SIRT3 in Cardiac Metabolism. *Front Cardiovasc Med* **9**, 850340
2. Singh, C. K., Chhabra, G., Ndiaye, M. A., Garcia-Peterson, L. M., Mack, N. J., and Ahmad, N. (2018) The Role of Sirtuins in Antioxidant and Redox Signaling. *Antioxid Redox Signal* **28**, 643-661
3. Frye, R. A. (2000) Phylogenetic classification of prokaryotic and eukaryotic Sir2-like proteins. *Biochem Biophys Res Commun* **273**, 793-798
4. Jiang, Y., Liu, J., Chen, D., Yan, L., and Zheng, W. (2017) Sirtuin Inhibition: Strategies, Inhibitors, and Therapeutic Potential. *Trends Pharmacol Sci* **38**, 459-472
5. Finley, L. W., and Haigis, M. C. (2012) Metabolic regulation by SIRT3: implications for tumorigenesis. *Trends Mol Med* **18**, 516-523
6. Lombard, D. B., Alt, F. W., Cheng, H. L., Bunkenborg, J., Streeper, R. S., Mostoslavsky, R., Kim, J., Yancopoulos, G., Valenzuela, D., Murphy, A., Yang, Y., Chen, Y., Hirschey, M. D., Bronson, R. T., Haigis, M., Guarente, L. P., Farese, R. V., Jr., Weissman, S., Verdin, E., and Schwer, B. (2007) Mammalian Sir2 homolog SIRT3 regulates global mitochondrial lysine acetylation. *Mol Cell Biol* **27**, 8807-8814
7. Sundaresan, N. R., Samant, S. A., Pillai, V. B., Rajamohan, S. B., and Gupta, M. P. (2008) SIRT3 is a stress-responsive deacetylase in cardiomyocytes that protects cells from stress-mediated cell death by deacetylation of Ku70. *Mol Cell Biol* **28**, 6384-6401
8. Ahn, B. H., Kim, H. S., Song, S., Lee, I. H., Liu, J., Vassilopoulos, A., Deng, C. X., and Finkel, T. (2008) A role for the mitochondrial deacetylase Sirt3 in regulating energy homeostasis. *Proc Natl Acad Sci U S A* **105**, 14447-14452
9. Sundaresan, N. R., Gupta, M., Kim, G., Rajamohan, S. B., Isbatan, A., and Gupta, M. P. (2009) Sirt3 blocks the cardiac hypertrophic response by augmenting Foxo3a-dependent antioxidant defense mechanisms in mice. *J Clin Invest* **119**, 2758-2771
10. Cimen, H., Han, M. J., Yang, Y., Tong, Q., Koc, H., and Koc, E. C. (2010) Regulation of succinate dehydrogenase activity by SIRT3 in mammalian mitochondria. *Biochemistry* **49**, 304-311
11. Cheng, Y., Ren, X., Gowda, A. S., Shan, Y., Zhang, L., Yuan, Y. S., Patel, R., Wu, H., Huber-Keener, K., Yang, J. W., Liu, D., Spratt, T. E., and Yang, J. M. (2013) Interaction of Sirt3 with OGG1 contributes to repair of mitochondrial DNA and protects from apoptotic cell death under oxidative stress. *Cell Death Dis* **4**, e731
12. Zhang, J., Xiang, H., Liu, J., Chen, Y., He, R. R., and Liu, B. (2020) Mitochondrial Sirtuin 3: New emerging biological function and therapeutic target. *Theranostics* **10**, 8315-8342
13. Verdin, E., Hirschey, M. D., Finley, L. W., and Haigis, M. C. (2010) Sirtuin regulation of mitochondria: energy production, apoptosis, and signaling. *Trends Biochem Sci* **35**, 669-675
14. Chen, Y., Fu, L. L., Wen, X., Wang, X. Y., Liu, J., Cheng, Y., and Huang, J. (2014) Sirtuin-3 (SIRT3), a therapeutic target with oncogenic and tumor-suppressive function in cancer. *Cell Death Dis* **5**, e1047
15. Hallows, W. C., Albaugh, B. N., and Denu, J. M. (2008) Where in the cell is SIRT3?--functional localization of an NAD+-dependent protein deacetylase. *Biochem J* **411**, e11-13

16. Cooper, H. M., Huang, J. Y., Verdin, E., and Spelbrink, J. N. (2009) A new splice variant of the mouse SIRT3 gene encodes the mitochondrial precursor protein. *PLoS One* **4**, e4986

17. Nakamura, Y., Ogura, M., Tanaka, D., and Inagaki, N. (2008) Localization of mouse mitochondrial SIRT proteins: shift of SIRT3 to nucleus by co-expression with SIRT5. *Biochem Biophys Res Commun* **366**, 174-179

18. He, X., Zeng, H., and Chen, J. X. (2019) Emerging role of SIRT3 in endothelial metabolism, angiogenesis, and cardiovascular disease. *J Cell Physiol* **234**, 2252-2265

19. Yang, Y., Hubbard, B. P., Sinclair, D. A., and Tong, Q. (2010) Characterization of murine SIRT3 transcript variants and corresponding protein products. *J Cell Biochem* **111**, 1051-1058

20. Guan, K. L., and Xiong, Y. (2011) Regulation of intermediary metabolism by protein acetylation. *Trends Biochem Sci* **36**, 108-116

21. Hebert, A. S., Dittenhafer-Reed, K. E., Yu, W., Bailey, D. J., Selen, E. S., Boersma, M. D., Carson, J. J., Tonelli, M., Balloon, A. J., Higbee, A. J., Westphall, M. S., Pagliarini, D. J., Prolla, T. A., Assadi-Porter, F., Roy, S., Denu, J. M., and Coon, J. J. (2013) Calorie restriction and SIRT3 trigger global reprogramming of the mitochondrial protein acetylome. *Mol Cell* **49**, 186-199

22. Ansari, A., Rahman, M. S., Saha, S. K., Saikot, F. K., Deep, A., and Kim, K. H. (2017) Function of the SIRT3 mitochondrial deacetylase in cellular physiology, cancer, and neurodegenerative disease. *Aging Cell* **16**, 4-16

23. Zhou, L., Pinho, R., Gu, Y., and Radak, Z. (2022) The Role of SIRT3 in Exercise and Aging. *Cells* **11**

24. Guan, X., Lin, P., Knoll, E., and Chakrabarti, R. (2014) Mechanism of inhibition of the human sirtuin enzyme SIRT3 by nicotinamide: computational and experimental studies. *PLoS One* **9**, e107729

25. Bell, E. L., Emerling, B. M., Ricoult, S. J., and Guarente, L. (2011) SirT3 suppresses hypoxia inducible factor 1alpha and tumor growth by inhibiting mitochondrial ROS production. *Oncogene* **30**, 2986-2996

26. Hirschey, M. D., Shimazu, T., Capra, J. A., Pollard, K. S., and Verdin, E. (2011) SIRT1 and SIRT3 deacetylate homologous substrates: AceCS1,2 and HMGCS1,2. *Aging (Albany NY)* **3**, 635-642

27. Kowalczyk, P., Sulejczak, D., Kleczkowska, P., Bukowska-Osko, I., Kucia, M., Popiel, M., Wietrak, E., Kramkowski, K., Wrzosek, K., and Kaczynska, K. (2021) Mitochondrial Oxidative Stress-A Causative Factor and Therapeutic Target in Many Diseases. *Int J Mol Sci* **22**

28. Gao, L., Laude, K., and Cai, H. (2008) Mitochondrial pathophysiology, reactive oxygen species, and cardiovascular diseases. *Vet Clin North Am Small Anim Pract* **38**, 137-155, vi

29. Starkov, A. A., Fiskum, G., Chinopoulos, C., Lorenzo, B. J., Browne, S. E., Patel, M. S., and Beal, M. F. (2004) Mitochondrial alpha-ketoglutarate dehydrogenase complex generates reactive oxygen species. *J Neurosci* **24**, 7779-7788

30. Angelova, P. R., and Abramov, A. Y. (2018) Role of mitochondrial ROS in the brain: from physiology to neurodegeneration. *FEBS Lett* **592**, 692-702

31. Zimmer, A. D., Walbrecq, G., Kozar, I., Behrmann, I., and Haan, C. (2016) Phosphorylation of the pyruvate dehydrogenase complex precedes HIF-1-mediated effects and pyruvate dehydrogenase kinase 1 upregulation during the first hours of hypoxic treatment in hepatocellular carcinoma cells. *Hypoxia (Auckl)* **4**, 135-145

32. Ozden, O., Park, S. H., Wagner, B. A., Song, H. Y., Zhu, Y., Vassilopoulos, A., Jung, B., Buettner, G. R., and Gius, D. (2014) SIRT3 deacetylates and increases pyruvate dehydrogenase activity in cancer cells. *Free Radic Biol Med* **76**, 163-172

33. Vasquez-Vivar, J., Kalyanaraman, B., and Kennedy, M. C. (2000) Mitochondrial aconitase is a source of hydroxyl radical. An electron spin resonance investigation. *J Biol Chem* **275**, 14064-14069

34. Spear, J. F., Prabu, S. K., Galati, D., Raza, H., Anandatheerthavarada, H. K., and Avadhani, N. G. (2007) beta1-Adrenoreceptor activation contributes to ischemia-reperfusion damage as well as playing a role in ischemic preconditioning. *Am J Physiol Heart Circ Physiol* **292**, H2459-2466

35. Fernandes, J., Weddle, A., Kinter, C. S., Humphries, K. M., Mather, T., Szweda, L. I., and Kinter, M. (2015) Lysine Acetylation Activates Mitochondrial Aconitase in the Heart. *Biochemistry* **54**, 4008-4018

36. Chen, Y., Zhang, J., Lin, Y., Lei, Q., Guan, K. L., Zhao, S., and Xiong, Y. (2011) Tumour suppressor SIRT3 deacetylates and activates manganese superoxide dismutase to scavenge ROS. *EMBO Rep* **12**, 534-541

37. He, C., Danes, J. M., Hart, P. C., Zhu, Y., Huang, Y., de Abreu, A. L., O'Brien, J., Mathison, A. J., Tang, B., Frasor, J. M., Wakefield, L. M., Ganini, D., Stauder, E., Zielonka, J., Gantner, B. N., Urrutia, R. A., Gius, D., and Bonini, M. G. (2019) SOD2 acetylation on lysine 68 promotes stem cell reprogramming in breast cancer. *Proc Natl Acad Sci U S A* **116**, 23534-23541

38. Tao, R., Coleman, M. C., Pennington, J. D., Ozden, O., Park, S. H., Jiang, H., Kim, H. S., Flynn, C. R., Hill, S., Hayes McDonald, W., Olivier, A. K., Spitz, D. R., and Gius, D. (2010) Sirt3-mediated deacetylation of evolutionarily conserved lysine 122 regulates MnSOD activity in response to stress. *Mol Cell* **40**, 893-904

39. Porter, G. A., Urciuoli, W. R., Brookes, P. S., and Nadtochiy, S. M. (2014) SIRT3 deficiency exacerbates ischemia-reperfusion injury: implication for aged hearts. *Am J Physiol Heart Circ Physiol* **306**, H1602-1609

40. Parodi-Rullan, R. M., Chapa-Dubocq, X., Rullan, P. J., Jang, S., and Javadov, S. (2017) High Sensitivity of SIRT3 Deficient Hearts to Ischemia-Reperfusion Is Associated with Mitochondrial Abnormalities. *Front Pharmacol* **8**, 275

41. Yu, W., Dittenhafer-Reed, K. E., and Denu, J. M. (2012) SIRT3 protein deacetylates isocitrate dehydrogenase 2 (IDH2) and regulates mitochondrial redox status. *J Biol Chem* **287**, 14078-14086

42. Smolkova, K., Spackova, J., Gotvaldova, K., Dvorak, A., Krenkova, A., Hubalek, M., Holendova, B., Vitek, L., and Jezek, P. (2020) SIRT3 and GCN5L regulation of NADP+- and NADPH-driven reactions of mitochondrial isocitrate dehydrogenase IDH2. *Sci Rep* **10**, 8677

43. Xu, Y., Liu, L., Nakamura, A., Someya, S., Miyakawa, T., and Tanokura, M. (2017) Studies on the regulatory mechanism of isocitrate dehydrogenase 2 using acetylation mimics. *Sci Rep* **7**, 9785

44. Pillai, V. B., Bindu, S., Sharp, W., Fang, Y. H., Kim, G., Gupta, M., Samant, S., and Gupta, M. P. (2016) Sirt3 protects mitochondrial DNA damage and blocks the development of doxorubicin-induced cardiomyopathy in mice. *Am J Physiol Heart Circ Physiol* **310**, H962-972

45. Rangarajan, P., Karthikeyan, A., Lu, J., Ling, E. A., and Dheen, S. T. (2015) Sirtuin 3 regulates Foxo3a-mediated antioxidant pathway in microglia. *Neuroscience* **311**, 398-414

46. Zhang, H., Dai, S., Yang, Y., Wei, J., Li, X., Luo, P., and Jiang, X. (2023) Role of Sirtuin 3 in Degenerative Diseases of the Central Nervous System. *Biomolecules* **13**

47. Meng, H., Yan, W. Y., Lei, Y. H., Wan, Z., Hou, Y. Y., Sun, L. K., and Zhou, J. P. (2019) SIRT3 Regulation of Mitochondrial Quality Control in Neurodegenerative Diseases. *Front Aging Neurosci* **11**, 313

48. Samant, S. A., Zhang, H. J., Hong, Z., Pillai, V. B., Sundaresan, N. R., Wolfgeher, D., Archer, S. L., Chan, D. C., and Gupta, M. P. (2014) SIRT3 deacetylates and activates OPA1 to regulate mitochondrial dynamics during stress. *Mol Cell Biol* **34**, 807-819

49. Wang, Y., Sun, X., Ji, K., Du, L., Xu, C., He, N., Wang, J., Liu, Y., and Liu, Q. (2018) Sirt3-mediated mitochondrial fission regulates the colorectal cancer stress response by modulating the Akt/PTEN signalling pathway. *Biomed Pharmacother* **105**, 1172-1182

50. Morigi, M., Perico, L., Rota, C., Longaretti, L., Conti, S., Rottoli, D., Novelli, R., Remuzzi, G., and Benigni, A. (2015) Sirtuin 3-dependent mitochondrial dynamic improvements protect against acute kidney injury. *J Clin Invest* **125**, 715-726

51. Bugga, P., Alam, M. J., Kumar, R., Pal, S., Chattopadyay, N., and Banerjee, S. K. (2022) Sirt3 ameliorates mitochondrial dysfunction and oxidative stress through regulating mitochondrial biogenesis and dynamics in cardiomyoblast. *Cell Signal* **94**, 110309

52. Li, Y., Ma, Y., Song, L., Yu, L., Zhang, L., Zhang, Y., Xing, Y., Yin, Y., and Ma, H. (2018) SIRT3 deficiency exacerbates p53/Parkin-mediated mitophagy inhibition and promotes mitochondrial dysfunction: Implication for aged hearts. *Int J Mol Med* **41**, 3517-3526

53. Torrens-Mas, M., Hernandez-Lopez, R., Pons, D. G., Roca, P., Oliver, J., and Sastre-Serra, J. (2019) Sirtuin 3 silencing impairs mitochondrial biogenesis and metabolism in colon cancer cells. *Am J Physiol Cell Physiol* **317**, C398-C404

54. Kong, X., Wang, R., Xue, Y., Liu, X., Zhang, H., Chen, Y., Fang, F., and Chang, Y. (2010) Sirtuin 3, a new target of PGC-1alpha, plays an important role in the suppression of ROS and mitochondrial biogenesis. *PLoS One* **5**, e11707

55. Torrens-Mas, M., Pons, D. G., Sastre-Serra, J., Oliver, J., and Roca, P. (2017) SIRT3 Silencing Sensitizes Breast Cancer Cells to Cytotoxic Treatments Through an Increment in ROS Production. *J Cell Biochem* **118**, 397-406

56. Chen, Y., Wu, Y. Y., Si, H. B., Lu, Y. R., and Shen, B. (2021) Mechanistic insights into AMPK-SIRT3 positive feedback loop-mediated chondrocyte mitochondrial quality control in osteoarthritis pathogenesis. *Pharmacol Res* **166**, 105497

57. Tseng, A. H., Shieh, S. S., and Wang, D. L. (2013) SIRT3 deacetylates FOXO3 to protect mitochondria against oxidative damage. *Free Radic Biol Med* **63**, 222-234

58. Yapryntseva, M. A., Maximchik, P. V., Zhivotovsky, B., and Gogvadze, V. (2022) Mitochondrial sirtuin 3 and various cell death modalities. *Front Cell Dev Biol* **10**, 947357

59. Pellegrini, L., Pucci, B., Villanova, L., Marino, M. L., Marfe, G., Sansone, L., Vernucci, E., Bellizzi, D., Reali, V., Fini, M., Russo, M. A., and Tafani, M. (2012) SIRT3 protects from hypoxia and staurosporine-mediated cell death by maintaining mitochondrial membrane potential and intracellular pH. *Cell Death Differ* **19**, 1815-1825

60. Qiao, A., Wang, K., Yuan, Y., Guan, Y., Ren, X., Li, L., Chen, X., Li, F., Chen, A. F., Zhou, J., Yang, J. M., and Cheng, Y. (2016) Sirt3-mediated mitophagy protects tumor cells against apoptosis under hypoxia. *Oncotarget* **7**, 43390-43400

61. Luo, K., Huang, W., and Tang, S. (2018) Sirt3 enhances glioma cell viability by stabilizing Ku70-BAX interaction. *Onco Targets Ther* **11**, 7559-7567

62. Yang, Y., Wang, W., Tian, Y., and Shi, J. (2022) Sirtuin 3 and mitochondrial permeability transition pore (mPTP): A systematic review. *Mitochondrion* **64**, 103-111

63. Galluzzi, L., Vitale, I., Aaronson, S. A., Abrams, J. M., Adam, D., Agostinis, P., Alnemri, E. S., Altucci, L., Amelio, I., Andrews, D. W., Annicchiarico-Petruzzelli, M., Antonov, A. V., Arama, E., Baehrecke, E. H., Barlev, N. A., Bazan, N. G., Bernassola, F., Bertrand, M. J. M., Bianchi, K., Blagosklonny, M. V., Blomgren, K., Borner, C., Boya, P., Brenner, C., Campanella, M., Candi, E., Carmona-Gutierrez, D., Cecconi, F., Chan, F. K., Chandel, N. S., Cheng, E. H., Chipuk, J. E., Cidlowski, J. A., Ciechanover, A., Cohen, G. M., Conrad, M., Cubillos-Ruiz, J. R., Czabotar, P. E., D'Angiolella, V., Dawson, T. M., Dawson, V. L., De Laurenzi, V., De Maria, R., Debatin, K. M., DeBerardinis, R. J., Deshmukh, M., Di Daniele, N., Di Virgilio, F., Dixit, V. M., Dixon, S. J., Duckett, C. S., Dynlacht, B. D., El-Deiry, W. S., Elrod, J. W., Fimia, G. M., Fulda, S., Garcia-Saez, A. J., Garg, A. D., Garrido, C., Gavathiotis, E., Golstein, P., Gottlieb, E., Green, D. R., Greene, L. A., Gronemeyer, H., Gross, A., Hajnoczky, G., Hardwick, J. M., Harris, I. S., Hengartner, M. O., Hetz, C., Ichijo, H., Jaattela, M., Joseph, B., Jost, P. J., Juin, P. P., Kaiser, W. J., Karin, M., Kaufmann, T., Kepp, O., Kimchi, A., Kitsis, R. N., Klionsky, D. J., Knight, R. A., Kumar, S., Lee, S. W., Lemasters, J. J., Levine, B., Linkermann, A., Lipton, S. A., Lockshin, R. A., Lopez-Otin, C., Lowe, S. W., Luedde, T., Lugli, E., MacFarlane, M., Madeo, F., Malewicz, M., Malorni, W., Manic, G., Marine, J. C., Martin, S. J., Martinou, J. C., Medema, J. P., Mehlen, P., Meier, P., Melino, S., Miao, E. A., Molkentin, J. D., Moll, U. M., Munoz-Pinedo, C., Nagata, S., Nunez, G., Oberst, A., Oren, M., Overholtzer, M., Pagano, M., Panaretakis, T., Pasparakis, M., Penninger, J. M., Pereira, D. M., Pervaiz, S., Peter, M. E., Piacentini, M., Pinton, P., Prehn, J. H. M., Puthalakath, H., Rabinovich, G. A., Rehm, M., Rizzuto, R., Rodrigues, C. M. P., Rubinsztein, D. C., Rudel, T., Ryan, K. M., Sayan, E., Scorrano, L., Shao, F., Shi, Y., Silke, J., Simon, H. U., Sistigu, A., Stockwell, B. R., Strasser, A., Szabadkai, G., Tait, S. W. G., Tang, D., Tavernarakis, N., Thorburn, A., Tsujimoto, Y., Turk, B., Vanden Berghe, T., Vandenabeele, P., Vander Heiden, M. G., Villunger, A., Virgin, H. W., Vousden, K. H., Vucic, D., Wagner, E. F., Walczak, H., Wallach, D., Wang, Y., Wells, J. A., Wood, W., Yuan, J., Zakeri, Z., Zhivotovsky, B., Zitvogel, L., Melino, G., and Kroemer, G. (2018) Molecular mechanisms of cell death: recommendations of the Nomenclature Committee on Cell Death 2018. *Cell Death Differ* **25**, 486-541

64. Du, Q., Zhu, B., Zhai, Q., and Yu, B. (2017) Sirt3 attenuates doxorubicin-induced cardiac hypertrophy and mitochondrial dysfunction via suppression of Bnip3. *Am J Transl Res* **9**, 3360-3373

65. Sun, F., Si, Y., Bao, H., Xu, Y., Pan, X., Zeng, L., and Jing, L. (2017) Regulation of Sirtuin 3-Mediated Deacetylation of Cyclophilin D Attenuated Cognitive Dysfunction Induced by Sepsis-Associated Encephalopathy in Mice. *Cell Mol Neurobiol* **37**, 1457-1464

66. Yang, S., Xu, M., Meng, G., and Lu, Y. (2020) SIRT3 deficiency delays diabetic skin wound healing via oxidative stress and necroptosis enhancement. *J Cell Mol Med* **24**, 4415-4427

67. Tinkov, A. A., Nguyen, T. T., Santamaria, A., Bowman, A. B., Buha Djordjevic, A., Paoliello, M. M. B., Skalny, A. V., and Aschner, M. (2021) Sirtuins as molecular targets, mediators, and protective agents in metal-induced toxicity. *Arch Toxicol* **95**, 2263-2278

68. Yamada, K., and Yoshida, K. (2019) Mechanical insights into the regulation of programmed cell death by p53 via mitochondria. *Biochim Biophys Acta Mol Cell Res* **1866**, 839-848

69. Jin, Y., Gu, W., and Chen, W. (2021) Sirt3 is critical for p53-mediated ferroptosis upon ROS-induced stress. *J Mol Cell Biol* **13**, 151-154

70. Hata, Y., and Nakajima, K. (1990) Disproportionally high concentrations of apolipoprotein E in the interstitial fluid of normal pulmonary artery in man. *Ann N Y Acad Sci* **598**, 49-57

71. Novak, E. A., and Mollen, K. P. (2015) Mitochondrial dysfunction in inflammatory bowel disease. *Front Cell Dev Biol* **3**, 62

72. Matsui, H., Shimokawa, O., Kaneko, T., Nagano, Y., Rai, K., and Hyodo, I. (2011) The pathophysiology of non-steroidal anti-inflammatory drug (NSAID)-induced mucosal injuries in stomach and small intestine. *J Clin Biochem Nutr* **48**, 107-111

73. Bindu, S., Pal, C., Dey, S., Goyal, M., Alam, A., Iqbal, M. S., Dutta, S., Sarkar, S., Kumar, R., Maity, P., and Bandyopadhyay, U. (2011) Translocation of heme oxygenase-1 to mitochondria is a novel cytoprotective mechanism against non-steroidal anti-inflammatory drug-induced mitochondrial oxidative stress, apoptosis, and gastric mucosal injury. *J Biol Chem* **286**, 39387-39402

74. Mazumder, S., De, R., Sarkar, S., Siddiqui, A. A., Saha, S. J., Banerjee, C., Iqbal, M. S., Nag, S., Debsharma, S., and Bandyopadhyay, U. (2016) Selective scavenging of intra-mitochondrial superoxide corrects diclofenac-induced mitochondrial dysfunction and gastric injury: A novel gastroprotective mechanism independent of gastric acid suppression. *Biochem Pharmacol* **121**, 33-51

75. Yang, H., Wang, X., Xiong, X., and Yin, Y. (2016) Energy metabolism in intestinal epithelial cells during maturation along the crypt-villus axis. *Sci Rep* **6**, 31917

76. Guerbette, T., Boudry, G., and Lan, A. (2022) Mitochondrial function in intestinal epithelium homeostasis and modulation in diet-induced obesity. *Mol Metab* **63**, 101546

77. Pan, J. S., He, S. Z., Xu, H. Z., Zhan, X. J., Yang, X. N., Xiao, H. M., Shi, H. X., and Ren, J. L. (2008) Oxidative stress disturbs energy metabolism of mitochondria in ethanol-induced gastric mucosa injury. *World J Gastroenterol* **14**, 5857-5867

78. Hollensworth, S. B., Shen, C., Sim, J. E., Spitz, D. R., Wilson, G. L., and LeDoux, S. P. (2000) Glial cell type-specific responses to menadione-induced oxidative stress. *Free Radic Biol Med* **28**, 1161-1174

79. Van Houten, B., Woshner, V., and Santos, J. H. (2006) Role of mitochondrial DNA in toxic responses to oxidative stress. *DNA Repair (Amst)* **5**, 145-152

80. Alexeyev, M. F. (2009) Is there more to aging than mitochondrial DNA and reactive oxygen species? *FEBS J* **276**, 5768-5787

81. Guo, C., Sun, L., Chen, X., and Zhang, D. (2013) Oxidative stress, mitochondrial damage and neurodegenerative diseases. *Neural Regen Res* **8**, 2003-2014

82. Debsharma, S., Pramanik, S., Bindu, S., Mazumder, S., Das, T., Saha, D., De, R., Nag, S., Banerjee, C., Siddiqui, A. A., Ghosh, Z., and Bandyopadhyay, U. (2023) Honokiol, an inducer of sirtuin-3, protects against non-steroidal anti-inflammatory drug-induced gastric mucosal mitochondrial pathology, apoptosis and inflammatory tissue injury. *Br J Pharmacol*

83. Ramachandran, D., Clara, R., Fedele, S., Hu, J., Lackzo, E., Huang, J. Y., Verdin, E., Langhans, W., and Mansouri, A. (2017) Intestinal SIRT3 overexpression in mice improves whole body glucose homeostasis independent of body weight. *Mol Metab* **6**, 1264-1273

84. Zhou, J., Yue, J., Yao, Y., Hou, P., Zhang, T., Zhang, Q., Yi, L., and Mi, M. (2023) Dihydromyricetin Protects Intestinal Barrier Integrity by Promoting IL-22 Expression in ILC3s through the AMPK/SIRT3/STAT3 Signaling Pathway. *Nutrients* **15**

85. Ding, Q., Zhang, Z., Li, Y., Liu, H., Hao, Q., Yang, Y., Ringo, E., Olsen, R. E., Clarke, J. L., Ran, C., and Zhou, Z. (2021) Propionate induces intestinal oxidative stress via Sod2 propionylation in zebrafish. *iScience* **24**, 102515

86. Xu, S., Li, L., Wu, J., An, S., Fang, H., Han, Y., Huang, Q., Chen, Z., and Zeng, Z. (2021) Melatonin Attenuates Sepsis-Induced Small-Intestine Injury by Upregulating SIRT3-Mediated Oxidative-Stress Inhibition, Mitochondrial Protection, and Autophagy Induction. *Front Immunol* **12**, 625627

87. Zeng, Z., Yang, Y., Dai, X., Xu, S., Li, T., Zhang, Q., Zhao, K. S., and Chen, Z. (2016) Polydatin ameliorates injury to the small intestine induced by hemorrhagic shock via SIRT3 activation-mediated mitochondrial protection. *Expert Opin Ther Targets* **20**, 645-652

88. Wang, Z., Sun, R., Wang, G., Chen, Z., Li, Y., Zhao, Y., Liu, D., Zhao, H., Zhang, F., Yao, J., and Tian, X. (2020) SIRT3-mediated deacetylation of PRDX3 alleviates mitochondrial oxidative damage and apoptosis induced by intestinal ischemia/reperfusion injury. *Redox Biol* **28**, 101343

89. Zhang, Q., Liu, X. M., Hu, Q., Liu, Z. R., Liu, Z. Y., Zhang, H. G., Huang, Y. L., Chen, Q. H., Wang, W. X., and Zhang, X. K. (2021) Dexmedetomidine inhibits mitochondria damage and apoptosis of enteric glial cells in experimental intestinal ischemia/reperfusion injury via SIRT3-dependent PINK1/HDAC3/p53 pathway. *J Transl Med* **19**, 463

90. Liberti, M. V., and Locasale, J. W. (2016) The Warburg Effect: How Does it Benefit Cancer Cells? *Trends Biochem Sci* **41**, 211-218

91. Liou, G. Y., and Storz, P. (2010) Reactive oxygen species in cancer. *Free Radic Res* **44**, 479-496

92. Baccelli, I., Gareau, Y., Lehnertz, B., Gingras, S., Spinella, J. F., Corneau, S., Mayotte, N., Girard, S., Frechette, M., Blouin-Chagnon, V., Leveille, K., Boivin, I., MacRae, T., Krosl, J., Thiollier, C., Lavallee, V. P., Kanshin, E., Bertomeu, T., Coulombe-Huntington, J., St-Denis, C., Bordeleau, M. E., Boucher, G., Roux, P. P., Lemieux, S., Tyers, M., Thibault, P., Hebert, J., Marinier, A., and Sauvageau, G. (2019) Mubritinib Targets the Electron Transport Chain Complex I and Reveals the Landscape of OXPHOS Dependency in Acute Myeloid Leukemia. *Cancer Cell* **36**, 84-99 e88

93. Pollyea, D. A., Stevens, B. M., Jones, C. L., Winters, A., Pei, S., Minhajuddin, M., D'Alessandro, A., Culp-Hill, R., Riemondy, K. A., Gillen, A. E., Hesselberth, J. R., Abbott, D., Schatz, D., Gutman, J. A., Purev, E., Smith, C., and Jordan, C. T. (2018) Venetoclax with azacitidine disrupts energy metabolism and targets leukemia stem cells in patients with acute myeloid leukemia. *Nat Med* **24**, 1859-1866

94. Finley, L. W., Carracedo, A., Lee, J., Souza, A., Egia, A., Zhang, J., Teruya-Feldstein, J., Moreira, P. I., Cardoso, S. M., Clish, C. B., Pandolfi, P. P., and Haigis, M. C. (2011) SIRT3 opposes reprogramming of cancer cell metabolism through HIF1alpha destabilization. *Cancer Cell* **19**, 416-428

95. Ahmed, M. A., O'Callaghan, C., Chang, E. D., Jiang, H., and Vassilopoulos, A. (2019) Context-Dependent Roles for SIRT2 and SIRT3 in Tumor Development Upon Calorie Restriction or High Fat Diet. *Front Oncol* **9**, 1462

96. Torrens-Mas, M., Oliver, J., Roca, P., and Sastre-Serra, J. (2017) SIRT3: Oncogene and Tumor Suppressor in Cancer. *Cancers (Basel)* **9**

97. Poniewierska-Baran, A., Warias, P., and Zgutka, K. (2022) Sirtuins (SIRTs) As a Novel Target in Gastric Cancer. *Int J Mol Sci* **23**

98. Cui, Y., Qin, L., Wu, J., Qu, X., Hou, C., Sun, W., Li, S., Vaughan, A. T., Li, J. J., and Liu, J. (2015) SIRT3 Enhances Glycolysis and Proliferation in SIRT3-Expressing Gastric Cancer Cells. *PLoS One* **10**, e0129834

99. Yang, B., Fu, X., Shao, L., Ding, Y., and Zeng, D. (2014) Aberrant expression of SIRT3 is conversely correlated with the progression and prognosis of human gastric cancer. *Biochem Biophys Res Commun* **443**, 156-160

100. Mahjabeen, I., Rizwan, M., Fareen, G., Waqar Ahmed, M., Farooq Khan, A., and Akhtar Kayani, M. (2022) Mitochondrial sirtuins genetic variations and gastric cancer risk: Evidence from retrospective observational study. *Gene* **807**, 145951

101. Tai, Y. S., Ma, Y. S., Chen, C. L., Tsai, H. Y., Tsai, C. C., Wu, M. C., Chen, C. Y., and Lin, M. W. (2021) Resveratrol Analog 4-Bromo-Resveratrol Inhibits Gastric Cancer Stemness through the SIRT3-c-Jun N-Terminal Kinase Signaling Pathway. *Curr Issues Mol Biol* **44**, 63-72

102. Yao, S., and Yan, W. (2018) Overexpression of Mst1 reduces gastric cancer cell viability by repressing the AMPK-Sirt3 pathway and activating mitochondrial fission. *Onco Targets Ther* **11**, 8465-8479

103. Torrens-Mas, M., Hernandez-Lopez, R., Oliver, J., Roca, P., and Sastre-Serra, J. (2018) Sirtuin 3 silencing improves oxaliplatin efficacy through acetylation of MnSOD in colon cancer. *J Cell Physiol* **233**, 6067-6076

104. Wang, Q., Ye, S., Chen, X., Xu, P., Li, K., Zeng, S., Huang, M., Gao, W., Chen, J., Zhang, Q., Zhong, Z., and Liu, Q. (2019) Mitochondrial NOS1 suppresses apoptosis in colon cancer cells through increasing SIRT3 activity. *Biochem Biophys Res Commun* **515**, 517-523

105. Paku, M., Haraguchi, N., Takeda, M., Fujino, S., Ogino, T., Takahashi, H., Miyoshi, N., Uemura, M., Mizushima, T., Yamamoto, H., Doki, Y., and Eguchi, H. (2021) SIRT3-Mediated SOD2 and PGC-1alpha Contribute to Chemoresistance in Colorectal Cancer Cells. *Ann Surg Oncol* **28**, 4720-4732

106. Wan, X., Wang, C., Huang, Z., Zhou, D., Xiang, S., Qi, Q., Chen, X., Arbely, E., Liu, C. Y., Du, P., and Yu, W. (2020) Cisplatin inhibits SIRT3-deacetylation MTHFD2 to disturb cellular redox balance in colorectal cancer cell. *Cell Death Dis* **11**, 649

107. D'Onofrio, N., Martino, E., Mele, L., Colloca, A., Maione, M., Cautela, D., Castaldo, D., and Balestrieri, M. L. (2021) Colorectal Cancer Apoptosis Induced by Dietary delta-Valerobetaine Involves PINK1/Parkin Dependent-Mitophagy and SIRT3. *Int J Mol Sci* **22**

108. Liu, R., Fan, M., Candas, D., Qin, L., Zhang, X., Eldridge, A., Zou, J. X., Zhang, T., Juma, S., Jin, C., Li, R. F., Perks, J., Sun, L. Q., Vaughan, A. T., Hai, C. X., Gius, D. R., and Li, J. J. (2015) CDK1-Mediated SIRT3 Activation Enhances Mitochondrial Function and Tumor Radioresistance. *Mol Cancer Ther* **14**, 2090-2102

109. Liu, C., Huang, Z., Jiang, H., and Shi, F. (2014) The sirtuin 3 expression profile is associated with pathological and clinical outcomes in colon cancer patients. *Biomed Res Int* **2014**, 871263

110. Huang, K. H., Hsu, C. C., Fang, W. L., Chi, C. W., Sung, M. T., Kao, H. L., Li, A. F., Yin, P. H., Yang, M. H., and Lee, H. C. (2014) SIRT3 expression as a biomarker for better prognosis in gastric cancer. *World J Surg* **38**, 910-917

111. Lee, D. Y., Jung, D. E., Yu, S. S., Lee, Y. S., Choi, B. K., and Lee, Y. C. (2017) Regulation of SIRT3 signal related metabolic reprogramming in gastric cancer by Helicobacter pylori oncoprotein CagA. *Oncotarget* **8**, 78365-78378

112. Wang, L., Wang, W. Y., and Cao, L. P. (2015) SIRT3 inhibits cell proliferation in human gastric cancer through down-regulation of Notch-1. *Int J Clin Exp Med* **8**, 5263-5271

113. Ma, J., Zhao, G., Du, J., Li, J., Lin, G., and Zhang, J. (2021) LncRNA FENDRR Inhibits Gastric Cancer Cell Proliferation and Invasion via the miR-421/SIRT3/Notch-1 Axis. *Cancer Manag Res* **13**, 9175-9187

114. Fernandez-Coto, D. L., Gil, J., Hernandez, A., Herrera-Goepfert, R., Castro-Romero, I., Hernandez-Marquez, E., Arenas-Linares, A. S., Calderon-Sosa, V. T., Sanchez-Aleman, M. A., Mendez-Tenorio, A., Encarnacion-Guevara, S., and Ayala, G. (2018) Quantitative proteomics reveals proteins involved in the progression from non-cancerous lesions to gastric cancer. *J Proteomics* **186**, 15-27

115. D'Onofrio, N., Martino, E., Balestrieri, A., Mele, L., Neglia, G., Balestrieri, M. L., and Campanile, G. (2021) SIRT3 and Metabolic Reprogramming Mediate the Antiproliferative Effects of Whey in Human Colon Cancer Cells. *Cancers (Basel)* **13**

116. Liu, Z., Li, L., and Xue, B. (2018) Effect of ganoderic acid D on colon cancer Warburg effect: Role of SIRT3/cyclophilin D. *Eur J Pharmacol* **824**, 72-77

117. Zhang, Y., Wang, X. L., Zhou, M., Kang, C., Lang, H. D., Chen, M. T., Hui, S. C., Wang, B., and Mi, M. T. (2018) Crosstalk between gut microbiota and Sirtuin-3 in colonic inflammation and tumorigenesis. *Exp Mol Med* **50**, 1-11

118. D'Onofrio, N., Martino, E., Balestrieri, A., Mele, L., Cautela, D., Castaldo, D., and Balestrieri, M. L. (2022) Diet-derived ergothioneine induces necroptosis in colorectal cancer cells by activating the SIRT3/MLKL pathway. *FEBS Lett* **596**, 1313-1329

119. Someya, S., Yu, W., Hallows, W. C., Xu, J., Vann, J. M., Leeuwenburgh, C., Tanokura, M., Denu, J. M., and Prolla, T. A. (2010) Sirt3 mediates reduction of oxidative damage and prevention of age-related hearing loss under caloric restriction. *Cell* **143**, 802-812

120. Vargas-Ortiz, K., Perez-Vazquez, V., and Macias-Cervantes, M. H. (2019) Exercise and Sirtuins: A Way to Mitochondrial Health in Skeletal Muscle. *Int J Mol Sci* **20**

121. Palacios, O. M., Carmona, J. J., Michan, S., Chen, K. Y., Manabe, Y., Ward, J. L., 3rd, Goodyear, L. J., and Tong, Q. (2009) Diet and exercise signals regulate SIRT3 and activate AMPK and PGC-1alpha in skeletal muscle. *Aging (Albany NY)* **1**, 771-783

122. Chen, T., Dai, S. H., Li, X., Luo, P., Zhu, J., Wang, Y. H., Fei, Z., and Jiang, X. F. (2018) Sirt1-Sirt3 axis regulates human blood-brain barrier permeability in response to ischemia. *Redox Biol* **14**, 229-236

123. Wang, T., Cao, Y., Zheng, Q., Tu, J., Zhou, W., He, J., Zhong, J., Chen, Y., Wang, J., Cai, R., Zuo, Y., Wei, B., Fan, Q., Yang, J., Wu, Y., Yi, J., Li, D., Liu, M., Wang, C., Zhou, A., Li, Y., Wu, X., Yang, W., Chin, Y. E., Chen, G., and Cheng, J. (2019) SENP1-Sirt3 Signaling Controls Mitochondrial Protein Acetylation and Metabolism. *Mol Cell* **75**, 823-834 e825

124. Flick, F., and Luscher, B. (2012) Regulation of sirtuin function by posttranslational modifications. *Front Pharmacol* **3**, 29

125. Fritz, K. S., Galligan, J. J., Smathers, R. L., Roede, J. R., Shearn, C. T., Reigan, P., and Petersen, D. R. (2011) 4-Hydroxynonenal inhibits SIRT3 via thiol-specific modification. *Chem Res Toxicol* **24**, 651-662

126. Neeli, P. K., Gollavilli, P. N., Mallappa, S., Hari, S. G., and Kotamraju, S. (2020) A novel metadherinDelta7 splice variant enhances triple negative breast cancer aggressiveness by modulating mitochondrial function via NFkB-SIRT3 axis. *Oncogene* **39**, 2088-2102

127. Zhang, J., Wang, G., Zhou, Y., Chen, Y., Ouyang, L., and Liu, B. (2018) Mechanisms of autophagy and relevant small-molecule compounds for targeted cancer therapy. *Cell Mol Life Sci* **75**, 1803-1826

128. Xu, W. Y., Hu, Q. S., Qin, Y., Zhang, B., Liu, W. S., Ni, Q. X., Xu, J., and Yu, X. J. (2018) Zinc finger E-box-binding homeobox 1 mediates aerobic glycolysis via suppression of sirtuin 3 in pancreatic cancer. *World J Gastroenterol* **24**, 4893-4905

129. Rupaimoole, R., and Slack, F. J. (2017) MicroRNA therapeutics: towards a new era for the management of cancer and other diseases. *Nat Rev Drug Discov* **16**, 203-222

130. Fan, X., Xiao, M., Zhang, Q., Li, N., and Bu, P. (2019) miR-195-Sirt3 Axis Regulates Angiotensin II-Induced Hippocampal Apoptosis and Learning Impairment in Mice. *Psychol Res Behav Manag* **12**, 1099-1108

131. Ding, Y. Q., Zhang, Y. H., Lu, J., Li, B., Yu, W. J., Yue, Z. B., Hu, Y. H., Wang, P. X., Li, J. Y., Cai, S. D., Ye, J. T., and Liu, P. Q. (2021) MicroRNA-214 contributes to Ang II-induced cardiac hypertrophy by targeting SIRT3 to provoke mitochondrial malfunction. *Acta Pharmacol Sin* **42**, 1422-1436

132. Zhou, B., Lei, J. H., Wang, Q., Qu, T. F., Cha, L. C., Zhan, H. X., Liu, S. L., Hu, X., Sun, C. D., Guo, W. D., Qiu, F. B., and Cao, J. Y. (2022) Cancer-associated fibroblast-secreted miR-421 promotes pancreatic cancer by regulating the SIRT3/H3K9Ac/HIF-1alpha axis. *Kaohsiung J Med Sci* **38**, 1080-1092

133. He, C., Aziguli, A., Zhen, J., Jiao, A., Liao, H., Du, C., Liu, W., Aihemaitijiang, K., and Xu, A. (2022) MiRNA-494 specifically inhibits SIRT3-mediated microglia activation in sepsis-associated encephalopathy. *Transl Cancer Res* **11**, 2299-2309

134. Huang, S., Guo, H., Cao, Y., and Xiong, J. (2019) MiR-708-5p inhibits the progression of pancreatic ductal adenocarcinoma by targeting Sirt3. *Pathol Res Pract* **215**, 794-800

135. Kao, Y. Y., Chou, C. H., Yeh, L. Y., Chen, Y. F., Chang, K. W., Liu, C. J., Fan Chiang, C. Y., and Lin, S. C. (2019) MicroRNA miR-31 targets SIRT3 to disrupt mitochondrial activity and increase oxidative stress in oral carcinoma. *Cancer Lett* **456**, 40-48

136. Wang, W., Chen, L., Shang, C., Jin, Z., Yao, F., Bai, L., Wang, R., Zhao, S., and Liu, E. (2020) miR-145 inhibits the proliferation and migration of vascular smooth muscle cells by regulating autophagy. *J Cell Mol Med* **24**, 6658-6669

137. Li, Y., Sun, T., Shen, S., Wang, L., and Yan, J. (2019) LncRNA DYNLRB2-2 inhibits THP-1 macrophage foam cell formation by enhancing autophagy. *Biol Chem* **400**, 1047-1057

138. Sun, W., Zhao, L., Song, X., Zhang, J., Xing, Y., Liu, N., Yan, Y., Li, Z., Lu, Y., Wu, J., Li, L., Xiao, Y., Tian, X., Li, T., Guan, Y., Wang, Y., and Liu, B. (2017) MicroRNA-210 Modulates the Cellular Energy Metabolism Shift During H2O2-Induced Oxidative Stress by Repressing ISCU in H9c2 Cardiomyocytes. *Cell Physiol Biochem* **43**, 383-394

139. Zeng, B., Ye, H., Chen, J., Cheng, D., Cai, C., Chen, G., Chen, X., Xin, H., Tang, C., and Zeng, J. (2017) LncRNA TUG1 sponges miR-145 to promote cancer progression and regulate glutamine metabolism via Sirt3/GDH axis. *Oncotarget* **8**, 113650-113661

140. Wei, Z., Song, J., Wang, G., Cui, X., Zheng, J., Tang, Y., Chen, X., Li, J., Cui, L., Liu, C. Y., and Yu, W. (2018) Deacetylation of serine hydroxymethyl-transferase 2 by SIRT3 promotes colorectal carcinogenesis. *Nat Commun* **9**, 4468

141. Jiang, W., He, T., Liu, S., Zheng, Y., Xiang, L., Pei, X., Wang, Z., and Yang, H. (2018) The PIK3CA E542K and E545K mutations promote glycolysis and proliferation via induction of the beta-catenin/SIRT3 signaling pathway in cervical cancer. *J Hematol Oncol* **11**, 139

142. Pillai, V. B., Samant, S., Sundaresan, N. R., Raghuraman, H., Kim, G., Bonner, M. Y., Arbiser, J. L., Walker, D. I., Jones, D. P., Gius, D., and Gupta, M. P. (2015) Honokiol blocks and reverses cardiac hypertrophy in mice by activating mitochondrial Sirt3. *Nat Commun* **6**, 6656

143. Quan, Y., Park, W., Jin, J., Kim, W., Park, S. K., and Kang, K. P. (2020) Sirtuin 3 Activation by Honokiol Decreases Unilateral Ureteral Obstruction-Induced Renal Inflammation and Fibrosis via Regulation of Mitochondrial Dynamics and the Renal NF-kappaBTGF-beta1/Smad Signaling Pathway. *Int J Mol Sci* **21**

144. Ye, J. S., Chen, L., Lu, Y. Y., Lei, S. Q., Peng, M., and Xia, Z. Y. (2019) SIRT3 activator honokiol ameliorates surgery/anesthesia-induced cognitive decline in mice through anti-oxidative stress and anti-inflammatory in hippocampus. *CNS Neurosci Ther* **25**, 355-366

145. Yi, X., Guo, W., Shi, Q., Yang, Y., Zhang, W., Chen, X., Kang, P., Chen, J., Cui, T., Ma, J., Wang, H., Guo, S., Chang, Y., Liu, L., Jian, Z., Wang, L., Xiao, Q., Li, S., Gao, T., and Li, C. (2019) SIRT3-Dependent Mitochondrial Dynamics Remodeling Contributes to Oxidative Stress-Induced Melanocyte Degeneration in Vitiligo. *Theranostics* **9**, 1614-1633

146. Chan, S. S., Zhao, M., Lao, L., Fong, H. H., and Che, C. T. (2008) Magnolol and honokiol account for the anti-spasmodic effect of Magnolia officinalis in isolated guinea pig ileum. *Planta Med* **74**, 381-384

147. Zhang, W. W., Li, Y., Wang, X. Q., Tian, F., Cao, H., Wang, M. W., and Sun, Q. S. (2005) Effects of magnolol and honokiol derived from traditional Chinese herbal remedies on gastrointestinal movement. *World J Gastroenterol* **11**, 4414-4418

148. Niu, L., Wang, J., Shen, F., Gao, J., Jiang, M., and Bai, G. (2022) Magnolol and honokiol target TRPC4 to regulate extracellular calcium influx and relax intestinal smooth muscle. *J Ethnopharmacol* **290**, 115105

149. Pillai, V. B., Kanwal, A., Fang, Y. H., Sharp, W. W., Samant, S., Arbiser, J., and Gupta, M. P. (2017) Honokiol, an activator of Sirtuin-3 (SIRT3) preserves mitochondria and protects the heart from doxorubicin-induced cardiomyopathy in mice. *Oncotarget* **8**, 34082-34098

150. Li, Y., Ye, Z., Lai, W., Rao, J., Huang, W., Zhang, X., Yao, Z., and Lou, T. (2017) Activation of Sirtuin 3 by Silybin Attenuates Mitochondrial Dysfunction in Cisplatin-induced Acute Kidney Injury. *Front Pharmacol* **8**, 178

151. Xu, S., Gao, Y., Zhang, Q., Wei, S., Chen, Z., Dai, X., Zeng, Z., and Zhao, K. S. (2016) SIRT1/3 Activation by Resveratrol Attenuates Acute Kidney Injury in a Septic Rat Model. *Oxid Med Cell Longev* **2016**, 7296092

152. Wang, J., Wang, K., Huang, C., Lin, D., Zhou, Y., Wu, Y., Tian, N., Fan, P., Pan, X., Xu, D., Hu, J., Zhou, Y., Wang, X., and Zhang, X. (2018) SIRT3 Activation by Dihydromyricetin Suppresses Chondrocytes Degeneration via Maintaining Mitochondrial Homeostasis. *Int J Biol Sci* **14**, 1873-1882

153. Zhang, M., Zhao, Z., Shen, M., Zhang, Y., Duan, J., Guo, Y., Zhang, D., Hu, J., Lin, J., Man, W., Hou, L., Wang, H., and Sun, D. (2017) Polydatin protects cardiomyocytes against myocardial infarction injury by activating Sirt3. *Biochim Biophys Acta Mol Basis Dis* **1863**, 1962-1972

154. Zhang, H., Chen, Y., Pei, Z., Gao, H., Shi, W., Sun, M., Xu, Q., Zhao, J., Meng, W., and Xiao, K. (2019) Protective effects of polydatin against sulfur mustard-induced hepatic injury. *Toxicol Appl Pharmacol* **367**, 1-11

155. Zhang, J., Meruvu, S., Bedi, Y. S., Chau, J., Arguelles, A., Rucker, R., and Choudhury, M. (2015) Pyrroloquinoline quinone increases the expression and activity of Sirt1 and -3 genes in HepG2 cells. *Nutr Res* **35**, 844-849

156. Diaz-Morales, N., Rovira-Llopis, S., Banuls, C., Lopez-Domenech, S., Escribano-Lopez, I., Veses, S., Jover, A., Rocha, M., Hernandez-Mijares, A., and Victor, V. M. (2017) Does Metformin Protect Diabetic Patients from Oxidative Stress and Leukocyte-Endothelium Interactions? *Antioxid Redox Signal* **27**, 1439-1445

157. Quan, Y., Xia, L., Shao, J., Yin, S., Cheng, C. Y., Xia, W., and Gao, W. Q. (2015) Adjudin protects rodent cochlear hair cells against gentamicin ototoxicity via the SIRT3-ROS pathway. *Sci Rep* **5**, 8181

158. Pi, H., Xu, S., Reiter, R. J., Guo, P., Zhang, L., Li, Y., Li, M., Cao, Z., Tian, L., Xie, J., Zhang, R., He, M., Lu, Y., Liu, C., Duan, W., Yu, Z., and Zhou, Z. (2015) SIRT3-SOD2-mROS-dependent autophagy in cadmium-induced hepatotoxicity and salvage by melatonin. *Autophagy* **11**, 1037-1051

159. Zhai, M., Li, B., Duan, W., Jing, L., Zhang, B., Zhang, M., Yu, L., Liu, Z., Yu, B., Ren, K., Gao, E., Yang, Y., Liang, H., Jin, Z., and Yu, S. (2017) Melatonin ameliorates myocardial ischemia reperfusion injury through SIRT3-dependent regulation of oxidative stress and apoptosis. *J Pineal Res* **63**

160. Ma, S., Chen, J., Feng, J., Zhang, R., Fan, M., Han, D., Li, X., Li, C., Ren, J., Wang, Y., and Cao, F. (2018) Melatonin Ameliorates the Progression of Atherosclerosis via Mitophagy Activation and NLRP3 Inflammasome Inhibition. *Oxid Med Cell Longev* **2018**, 9286458

161. Nguyen, G. T., Gertz, M., and Steegborn, C. (2013) Crystal structures of Sirt3 complexes with 4'-bromo-resveratrol reveal binding sites and inhibition mechanism. *Chem Biol* **20**, 1375-1385

162. Galli, U., Mesenzani, O., Coppo, C., Sorba, G., Canonico, P. L., Tron, G. C., and Genazzani, A. A. (2012) Identification of a sirtuin 3 inhibitor that displays selectivity over sirtuin 1 and 2. *Eur J Med Chem* **55**, 58-66

163. Karaman, B., and Sippl, W. (2015) Docking and binding free energy calculations of sirtuin inhibitors. *Eur J Med Chem* **93**, 584-598

164. Gertz, M., Fischer, F., Nguyen, G. T., Lakshminarasimhan, M., Schutkowski, M., Weyand, M., and Steegborn, C. (2013) Ex-527 inhibits Sirtuins by exploiting their unique NAD+-dependent deacetylation mechanism. *Proc Natl Acad Sci U S A* **110**, E2772-2781

165. Disch, J. S., Evindar, G., Chiu, C. H., Blum, C. A., Dai, H., Jin, L., Schuman, E., Lind, K. E., Belyanskaya, S. L., Deng, J., Coppo, F., Aquilani, L., Graybill, T. L., Cuozzo, J. W., Lavu, S., Mao, C., Vlasuk, G. P., and Perni, R. B. (2013) Discovery of thieno[3,2-d]pyrimidine-6-carboxamides as potent inhibitors of SIRT1, SIRT2, and SIRT3. *J Med Chem* **56**, 3666-3679

166. Lain, S., Hollick, J. J., Campbell, J., Staples, O. D., Higgins, M., Aoubala, M., McCarthy, A., Appleyard, V., Murray, K. E., Baker, L., Thompson, A., Mathers, J., Holland, S. J., Stark, M. J., Pass, G., Woods, J., Lane, D. P., and Westwood, N. J. (2008) Discovery, in vivo activity, and mechanism of action of a small-molecule p53 activator. *Cancer Cell* **13**, 454-463

167. Alhazzazi, T. Y., Kamarajan, P., Xu, Y., Ai, T., Chen, L., Verdin, E., and Kapila, Y. L. (2016) A Novel Sirtuin-3 Inhibitor, LC-0296, Inhibits Cell Survival and Proliferation, and Promotes Apoptosis of Head and Neck Cancer Cells. *Anticancer Res* **36**, 49-60

168. Chen, M. L., Zhu, X. H., Ran, L., Lang, H. D., Yi, L., and Mi, M. T. (2017) Trimethylamine-N-Oxide Induces Vascular Inflammation by Activating the NLRP3 Inflammasome Through the SIRT3-SOD2-mtROS Signaling Pathway. *J Am Heart Assoc* **6**

169. Wang, L. J., Lee, Y. C., Huang, C. H., Shi, Y. J., Chen, Y. J., Pei, S. N., Chou, Y. W., and Chang, L. S. (2019) Non-mitotic effect of albendazole triggers apoptosis of human leukemia cells via SIRT3/ROS/p38 MAPK/TTP axis-mediated TNF-alpha upregulation. *Biochem Pharmacol* **162**, 154-168

170. Gorska-Ponikowska, M., Kuban-Jankowska, A., Eisler, S. A., Perricone, U., Lo Bosco, G., Barone, G., and Nussberger, S. (2018) 2-Methoxyestradiol Affects Mitochondrial Biogenesis Pathway and Succinate Dehydrogenase Complex Flavoprotein Subunit A in Osteosarcoma Cancer Cells. *Cancer Genomics Proteomics* **15**, 73-89

171. Moniot, S., Weyand, M., and Steegborn, C. (2012) Structures, substrates, and regulators of Mammalian sirtuins - opportunities and challenges for drug development. *Front Pharmacol* **3**, 16

172. Zhao, Q., Zhou, J., Li, F., Guo, S., Zhang, L., Li, J., Qi, Q., and Shi, Y. (2022) The Role and Therapeutic Perspectives of Sirtuin 3 in Cancer Metabolism Reprogramming, Metastasis, and Chemoresistance. *Front Oncol* **12**, 910963

173. Ma, K., Lu, N., Zou, F., and Meng, F. Z. (2019) Sirtuins as novel targets in the pathogenesis of airway inflammation in bronchial asthma. *Eur J Pharmacol* **865**, 172670

174. Tang, L., Chen, Q., Meng, Z., Sun, L., Zhu, L., Liu, J., Hu, J., Ni, Z., and Wang, X. (2017) Suppression of Sirtuin-1 Increases IL-6 Expression by Activation of the Akt Pathway During Allergic Asthma. *Cell Physiol Biochem* **43**, 1950-1960

175. Schwer, B., North, B. J., Frye, R. A., Ott, M., and Verdin, E. (2002) The human silent information regulator (Sir)2 homologue hSIRT3 is a mitochondrial nicotinamide adenine dinucleotide-dependent deacetylase. *J Cell Biol* **158**, 647-657

176. Giralt, A., Hondares, E., Villena, J. A., Ribas, F., Diaz-Delfin, J., Giralt, M., Iglesias, R., and Villarroya, F. (2011) Peroxisome proliferator-activated receptor-gamma coactivator-1alpha controls transcription of the Sirt3 gene, an essential component of the thermogenic brown adipocyte phenotype. *J Biol Chem* **286**, 16958-16966

177. Nogueiras, R., Habegger, K. M., Chaudhary, N., Finan, B., Banks, A. S., Dietrich, M. O., Horvath, T. L., Sinclair, D. A., Pfluger, P. T., and Tschop, M. H. (2012) Sirtuin 1 and sirtuin 3: physiological modulators of metabolism. *Physiol Rev* **92**, 1479-1514

178. Zhang, X., Ji, R., Liao, X., Castillero, E., Kennel, P. J., Brunjes, D. L., Franz, M., Mobius-Winkler, S., Drosatos, K., George, I., Chen, E. I., Colombo, P. C., and Schulze, P. C. (2018) MicroRNA-195 Regulates Metabolism in Failing Myocardium Via Alterations in Sirtuin 3 Expression and Mitochondrial Protein Acetylation. *Circulation* **137**, 2052-2067

179. Cheng, Y., Mai, J., Hou, T., and Ping, J. (2016) MicroRNA-421 induces hepatic mitochondrial dysfunction in non-alcoholic fatty liver disease mice by inhibiting sirtuin 3. *Biochem Biophys Res Commun* **474**, 57-63

180. George, J., Nihal, M., Singh, C. K., and Ahmad, N. (2019) 4'-Bromo-resveratrol, a dual Sirtuin-1 and Sirtuin-3 inhibitor, inhibits melanoma cell growth through mitochondrial metabolic reprogramming. *Mol Carcinog* **58**, 1876-1885

181. Li, M., Chiang, Y. L., Lyssiotis, C. A., Teater, M. R., Hong, J. Y., Shen, H., Wang, L., Hu, J., Jing, H., Chen, Z., Jain, N., Duy, C., Mistry, S. J., Cerchietti, L., Cross, J. R., Cantley, L. C., Green, M. R., Lin, H., and Melnick, A. M. (2019) Non-oncogene Addiction to SIRT3 Plays a Critical Role in Lymphomagenesis. *Cancer Cell* **35**, 916-931 e919

182. Mahajan, S. S., Scian, M., Sripathy, S., Posakony, J., Lao, U., Loe, T. K., Leko, V., Thalhofer, A., Schuler, A. D., Bedalov, A., and Simon, J. A. (2014) Development of pyrazolone and isoxazol-5-one cambinol analogues as sirtuin inhibitors. *J Med Chem* **57**, 3283-3294

Sirtuin 3 protects the gastric mucosa from NSAIDs-induced mitochondrial pathology and pro-inflammatory damage

1. INTRODUCTION

Non-steroidal anti-inflammatory drugs (NSAIDs) are essential for the treatment of inflammatory diseases (1-2). In addition, drug-repurposing studies have established NSAIDs as effective anticancer agents. Consistent with this notion, it has been observed that GI tract, breast, prostate, and lung malignancies are considerably less common among long-term NSAID users than in non-users (3-5). Despite such a broad range of therapeutic benefits, using NSAIDs in long term seems unsafe due to their noxious effects on several organs, with the gastrointestinal (GI) tract being the most seriously affected (6-7). Hence, accurate knowledge about the subcellular target(s) of NSAIDs is critical to optimize their therapeutic use while rationally circumventing their harmful effects. NSAIDs are standard cyclooxygenase1/2 (COX-1/2) inhibitors (6,8). Nevertheless, COX-independent effects accounting for the toxicities incurred by NSAIDs are equally potent (9-12). The two main COX-independent modes of action of NSAID are mitochondrial oxidative stress (MOS) and intrinsic apoptosis (13). NSAIDs directly target the mitochondria to compromise cellular metabolism (6, 14-18). Therefore, it sounds rational that cytoprotective factors would retort promptly to NSAID treatment to fight stress. Clearly, protein deacetylation controls the activity of mitochondrial base excision repair enzyme 8-oxoguanine DNA glycosylase 1 (OGG1), antioxidants enzymes like superoxide dismutase (SOD2) as well as mitochondrial OXPHOS complex proteins and mitochondria-localized important proteins in metabolic processes (19-21). Contextually, Sirtuin-3 (SIRT3), an NAD^+-dependent class III histone deacetylase, serves as a gatekeeper of mitochondrial integrity against stress by stabilizing the mitochondrial structural dynamics and mitochondrial biogenesis primarily through regulating OPA1, and PGC-1α respectively (19,22). Evidently, the number of acetylated mitochondrial proteins is significantly higher in SIRT3 KO mice (20). Further, in several organ pathologies, the involvement of SIRT3 deficiency has been commonly documented (23-26). However, to date, very few reports are available regarding SIRT3's potential role in gastrointestinal complications or whether SIRT3 can be utilized as a potential gastroprotective strategy.

In the present study, a rat model of experimental acute gastric injury by NSAIDs has been used to check the involvement of SIRT3 therein. Indomethacin has been used as a typical NSAID and a forward strategy has been adopted for differential gene expression profiling and target mining by next-generation transcriptome sequencing of control and indomethacin-treated gastric mucosa. Lead/s obtained from the sequencing data has been subjected to functional validation through metabolic and biochemical assays of mitochondrial functionality as well as expression analyses for various targets involved in regulating mitochondrial dynamics, mitophagy, inflammation and cell death in specific regards to the SIRT3 signaling axis. The involvement of SIRT3 in NSAID gastropathy has been rigorously validated by using a commercially available phytopolyphenol SIRT3 inducer, honokiol (HKL). Dose-dependent studies followed by ulcer scoring and evaluation of gastric acid output have been performed to check any putative gastro-protective action of HKL as well as its impact on acid secretion. Both preventative as well as healing studies on gastric injury by NSAIDs have been performed to assess for putative prophylactic and therapeutic merits of HKL against NSAIDs.

2. MATERIALS AND METHODS

2.1. Reagents
Indomethacin, diclofenac, ibuprofen, aspirin, 3-(4,5-dimethylthiazol-2-yl)-2,5-diphenyltetrazolium bromide (MTT) assay kit, RNase ZAP, DMSO, were acquired from Sigma (St Louis, MO, USA). The TRIzol, RevertAid H Minus First Strand cDNA Synthesis kit, PureLink RNA Mini Kit, Nuclease-free water, PCR Master Mix, and PBS (HyClone) were purchased from Thermo. Alexa Fluor 647- and Alexa

Fluor 488-tagged antibodies Hoechst 33342 were obtained from Thermo. 5,5,'6,6'-tetrachloro1,1',3,3'-tetraethylbenzimidazol-carbocyanine iodide (JC-1) was obtained from Invitrogen. Mitochondria Isolation Kit was procured from BioChain. HT 8-oxo-dG ELISA Kit II was obtained from Trevigen. Honokiol (HKL), Luminata forte western blot HRP substrate, and for ECL-based chemiluminescence were obtained from Mark-Millipore. SIRT3 activity assay kit was obtained from Abcam.

2.2. NSAID-induced gastric mucosal damage model in vivo

All animal studies were carried out in strict accordance with the institutional animal ethics committee standards, registered with the Committee for Control and Supervision of Experiments on Animals (CPCSEA), India (Permit no. 147/1999/CPCSEA). The rats were handled during the experimental process with the utmost care to reduce their suffering and misery. For all *in vivo* tests, Sprague-Dawley rats (180–220 g) were employed and the animals received regular rat food and had unlimited access to water while being kept at a constant temperature of 24 2 °C with 12-hour light-dark cycles. Before the experiments, rats were fasted for 24 hours with free access to water. The administration of NSAIDs led to the development of stomach mucosal damage. As previously noted, distilled water with a little amount of alkali (Na_2CO_3) was used to dissolve indomethacin (48 mg kg^{-1} body weight) (27,28). Before use, the pH of the resulting solution was tested. Aspirin (400 mg kg^{-1} body weight) was provided in 1 % carboxymethylcellulose suspension as earlier indicated, while diclofenac (75 mg kg^{-1} body weight) and ibuprofen (400 mg kg^{-1} body weight) were obtained in sodium salts version and diluted in distilled water (29-32). A separate group of rats (n = 5) was additionally given vehicle treatment (1% carboxymethyl cellulose or alkaline water). There was no evidence of stomach mucosal damage. There was no evidence of stomach mucosal damage. After allowing the development of gastrointestinal damage for 4 hours, the rats were terminally euthanized, sacrificed, and gastric mucosal samples were collected for further research work. Intraperitoneal (i.p.) injection of HKL (40 mg kg^{-1}) was given to rats first then 30 minutes later indomethacin was given orally for the HKL-induced protection set (HKL+Indo). As previously mentioned, HKL was dissolved in peanut oil and administered intraperitoneally (24). The dose-response study that ranged from 5 mg kg^{-1} to 60 mg kg^{-1} body weight was performed to determine the ED_{50} of HKL. A different group of rats (n = 5) was likewise given the vehicle (peanut oil) before receiving indomethacin orally. The intensity of mucosal damage was equivalent to treatment with indomethacin in the vehicle-treated group, where no discernible protection was shown. To compare the efficiency of i.p. and i.g. HKL treatment, intragastric (i.g.) administration of HKL at various dosages (20, 40, 60, and 80 mg kg^{-1} body weight) was also carried out in a second set of rats. For i.g administration, HKL was prepared in a 0.5% solution of sodium carboxymethylcellulose salt as reported previously. (33). The development of stomach mucosal injury was allowed. The rats were sacrificed after 4 hours, then their stomach mucosa was examined for the scoring of injury index (II) and the efficiency of HKL administered intraperitoneally vs intragastrically was juxtaposed. An oral dose of indomethacin was administered to a separate group of rats (n = 5) after intra-gastric injection of a 0.5% carboxymethylcellulose solution. The vehicle-treated group showed no discernible protection. Indomethacin was administered to two sets of 20 rats each for the studying the healing of stomach mucosal injury. The mucosal damage was allowed to progress for 4 hours. One group of rats (n = 20) received HKL treatment once after 4 hours, and samples were obtained at various time points following terminal euthanasia and sacrifice. The injury index of 0 hr healing is equivalent to the 4 hrs of indomethacin treatment i.e the peak injury index. To study the comparison between HKL-induced healing and spontaneous healing, a parallel group of rats (n = 20) was administered the vehicle (instead of HKL) and kept in the same manner. Rats treated with a vehicle were likewise sacrificed for sample collection at the same intervals as rats treated with HKL. The number of rats was kept constant at n = 5 in each group. To prevent bias, II scoring was carried out by a person who was not aware of

the treatment scenario. II was calculated as a percentage of the stomach's damaged region, which was made up of bleeding lesions, visible blood clots. Mean II was calculated as the sum of the total scores for each group of rats divided by the quantity of each group of rats. Tissues for protein expression analysis were snap-frozen and kept in storage until further use, tissue samples for next-generation sequencing and PCR-based gene expression profiling were stored by keeping in RNALater. Using a commercially available mitochondria isolation kit, tissue samples were subjected to subcellular fractionation for the preparation of the mitochondria.

2.3. Histological study of gastric mucosa
First, stomach mucosal tissues were fixed in buffered formalin-fixed next paraffin-embedded and finally semi-thin (5 µm) slices were created. To double-stain with hematoxylin and eosin, the semi-thin slices were collected on a glass slide, deparaffinized, and passed through varying ethanol solutions. Under a microscope, the stained slices were inspected under microscope.

2.4. Next-generation sequencing
Utilizing Illumina's TruSeq Stranded Total RNA Library preparation kit, total RNA sequencing libraries are created. In a nutshell, total RNA was obtained from the gastric tissue using Thermo's PureLink RNA Mini Kit, as directed by the manufacturer. 45 mg of tissue was taken. The purity and concentration of the RNA samples were estimated in Nanodrop 2000 (Thermo) and Agilent 2100 Bioanalyzer. Following that, samples with RIN 7.0 were utilized for library preparation The kit's Ribo-Zero Human/Mouse/Rat depletion module was used to first deplete ribosomal RNA from an identical amount (200 ng) of RNA from each sample. This was followed by purification and divalent cation-based fragmentation. The resultant fragments underwent cDNA synthesis, A-tailing, and dual index adapter ligation after being purified. The products were then PCR enhanced and purified. The resultant RNA libraries underwent equimolar pooling, quantification, normalization, and check in Agilent 2200 TapeStation (Agilent Technologies). Finally, 100 bp paired-end massively parallel sequencing of the pooled libraries was performed on the Novaseq 6000 sequencer using a sequencing run flow cell (Illumina) (Illumina). The resulting Bcl files were converted to Fastq files, and FastQC v.0.11.7 was used to perform a quality check on the data (34). The Illumina Universal Adapter was then used to trim the adapter using Cutadapt v1.16 (35). To align the trimmed reads with the Rat Rno6 reference genome, Hisat2 2.1.0.(36) was utilized (for rat samples). Samtools v1.19 was used to sort the Bam files (37) Gene count was then carried out using FeatureCounts(38), then differential analysis was carried out using DESeq2 (39). Filtering was done on differentially expressed genes having an expression change of 1.5 or more-fold, a p value of 0.05, and an FDR of 0.05. IPA (Ingenuity Pathway Analysis) software was then used to undertake gene enrichment and pathway analysis. To include genes affecting mitochondrial metabolism and functions, data for rat stomach mucosal samples were additionally filtered using or 1.2-fold expression change, p value, and FDR cut off of 0.05. Rat transcriptome data are available in GEO under accession number GSE201565.

2.5. Isolation of mitochondria
Using the Mitochondria Isolation Kit (BioChain, Cat# KC010100), mitochondria were isolated from tissue samples by following the manufacturer's instructions. In theory, the mitochondrial separation method utilized here relies on two-step differential centrifugations. After homogenization and mechanical breakdown of the tissue (in a hypotonic lysis solution supplemented with protease inhibitors), precipitated debris, unfragmented cells, and large cellular organelles are removed by low-speed centrifugation. To isolate healthy and enzymatically active mitochondria, high-speed centrifugation of the supernatant from the first stage is next carried out. By repeatedly washing the final pellet, pure mitochondrial fraction may be extracted. In this work, 200 mg of stomach mucosal tissues

from each experimental group were treated to mitochondria isolation in equal proportion. There was a little homogeneity of the samples. The mitochondrial fraction was obtained by centrifuging the supernatant at 12,000 g for 15 min after removing the nuclei and cell debris at 600 g for 10 min. Lysing for the dehydrogenase activity assay or respiratory chain complex assay or immunoblotting were carried out using the roughly 99% pure mitochondrial pellets that were obtained after the mitochondrial pellets had been rinsed three times in mitochondria separation buffer (28).

2.6 Immunoblot analysis

To extract total protein for immunoblot analysis, stomach mucosal tissues were homogenized in the previously mentioned mammalian cell lysis solution (added with protease inhibitors) (28). As earlier stated, mitochondrial fractions were produced from tissue samples via subcellular fractionation. For studying mitochondrial protein acetylation, nicotinamide (50 mM) and trichostatin A (10 µM) were added to the mitochondrial isolation and lysis solutions. Using Lowry's technique for protein quantification, the same quantity of protein was added to each well of the 10% polyacrylamide-SDS gels, electrophoresed, and then analyzed using wet transfer-based immunoblotting on nitrocellulose membrane. 5% skim milk or 5% BSA solution was used as a blocking solution before being incubated with the primary antibodies overnight as per manufactured protocol. The blots were then incubated with an HRP-conjugated secondary antibody for two hours at room temperature after being rinsed in TBS solution with 0.1% Tween 20 added. Finally in Bio-Rad Chemidoc system immunoblot bands were developed. For total protein and mitochondrial protein, respectively, the loading controls were actin and TOM20. The detailed description of all antibodies used for immunoblotting studies in this chapter may be found in the annexure where the published paper of this study has been attached.

2.7. Analysis of mitochondrial transmembrane potential (ΔΨm)

Using 5,5,6,6'-tetrachloro-1,1',3,3' tetraethylbenzimidazoyl carbocyanine iodide (JC-1), ΔΨm was measured. In theory, JC-1 is a lipophilic cationic dye that enters mitochondria, accumulates there in a concentration-dependent way, and begins producing reversible complexes. Therefore, JC-1 enters mitochondria (negatively charged) and concentrates there to create red luminous J-aggregates in healthy cells and mitochondria with normal ΔΨm. On the other hand, in damaged cells/mitochondria, the JC-1 entrance is significantly decreased because the mitochondrial inner membrane becomes less negative due to the loss of mitochondrial transmembrane electrical potential. In this situation, JC-1 remains monomeric and green because it falls short of the threshold level required for the production of J aggregates. ΔΨm was measured in the isolated mitochondria from control and treated stomachs using an F-7000 Fluorescence Spectrophotometer (Hitachi High-Technologies Corporation). In 500 µL of ATP-supplemented JC-1 assay solution containing 300 nM of JC-1, mitochondria were incubated for 15 min in the dark. At 530 nm and 590 nm, respectively, JC1 monomers and aggregates were examined using a single excitation-dual emission technique. As previously noted, ΔΨm was represented as a fluorescence ratio of 590 nm/530 nm (28).

2.8. Measurement of ATP content

To check the bioenergetic status of the mucosal cells following indomethacin treatment, the amount of ATP in stomach mucosal tissue was determined. Since the majority of tissue ATP generation is attributable to healthy, functioning mitochondria, a decrease in ATP would be indicative of mitochondrial malfunction and the resulting bioenergetic deficit in the afflicted tissue. The manufacturer's recommendations were followed while measuring the stomach mucosal ATP level in control and treated rats using an ATP measurement kit (A22066; Invitrogen Corp., Carlsbad, CA, USA). Recombinant firefly luciferase and its substrate, D-luciferin, are both included in this kit, which uses bioluminescence as its basis for analysis. The assay's basic premise is that the luciferase enzyme

needs ATP to produce light, with an emission maximum of 560 nm at pH 7.8. The quantity of light emitted from the following reaction will increase in direct proportion to the amount of ATP contained in the tissue extract.

$$\text{Luciferin} + \text{ATP} + O_2 \xrightarrow{\text{Mg}^{2+} \text{ and luciferase}} \text{Oxyluciferin} + \text{AMP} + \text{Pyrophosphate} + CO_2 + \text{Light}$$

Briefly, 50 mg of tissue from each sample was lysed in a solution of 5% sulfosalicylic acid (for sample deproteinization) and processed by centrifugation at 12000g. The supernatants were utilized to quantify ATP in a luminometer (BioTek). As previously noted, the data were standardized by the protein concentrations of the individual samples (29,41).

2.9. RNA isolation and real-time RT-PCR (qRT-PCR)

Following the manufacturer's instructions, total RNA was isolated using TRIzol and quantified using a Maestrogen nano Spectrophotometer (Life Teb Gen co, Tehran-Iran). Utilizing Thermo's RevertAid H Minus first strand cDNA synthesis kit, obtained total RNA (2 μg) was reverse transcribed using an oligo-dT primer. This was followed by rDNAse treatment. After suitable dilution, the generated cDNAs were utilized for qPCR using primers from Integrated DNA Technologies Inc. The qPCR was conducted using a Roche LightCycler 96 qPCR equipment and SYBR green master mix under the following cycle conditions: initially denaturing at 95°C for 10 minutes; then denaturing at 72°C for 15 seconds for 40 cycles; then annealing for 30 seconds at the respective annealing temperatures; and finally subjected to an extension at 72°C for 25 sec. Relative gene expression was determined using the $2^{-\Delta\Delta Cq}$ calculation, and the results have been reported as fold change relative to control (28, 41-42). The internal control employed was *Gapdh*. The detailed description of all primers used for q-RT-PCR reaction in this chapter may be found in the annexure where the published paper of this study has been attached.

2.10. Determination of SIRT3 deacetylase activity

SIRT3 deacetylase activity was assessed in the presence or absence of indomethacin using the SIRT3 fluorometric activity assay kit (Abcam, ab156067). The experiment followed the manufacturer's instructions. In a nutshell, the activity of purified human recombinant SIRT3 was evaluated in the presence of increasing concentrations of indomethacin (100-500 μM) using kinetic measurements every two minutes for 45 minutes with excitation at 350 nm and emission at 450 nm.

2.11. Mitochondrial dehydrogenase assay

The mitochondrial dehydrogenase activity was examined to determine the mitochondrial metabolic integrity in tissue samples. For mitochondrial isolation, equivalent amounts of gastric tissue (200 mg) from several experimental sets were employed. The resulting fractions were then incubated in MTT solution (1 mg/mL in PBS) for 3.5 hours at 37°C/5% CO_2. After centrifuging the samples, the pellets were dissolved in equal parts of anhydrous DMSO. As previously noted, the purple solution's absorbance was determined spectrophotometrically at 570 nm (28,41). Every fraction's estimated mitochondrial protein was utilized to normalize the ODs corresponding to the relevant samples.

2.12. Mitochondrial DNA isolation and quantification of 8-oxo-dG by ELISA

The phenol-chloroform method was used to extract the DNA from the isolated mitochondrial pellets. The mitochondrial pellet was briefly dissolved in 100 μL of Proteinase K-added lysis buffer and kept at 50°C for 3 hours before being added to and thoroughly mixed with 200 μL of phenol-chloroform. To separate the phases, the contents were spinned at 10,000 rpm. After collecting the aqueous phase, 500 mL of ethanol and 200 mL of 7.5 M ammonium acetate were added. For two hours, the tubes were held

at -20°C. The samples were then centrifuged for 30 minutes at 10,000 g. The pellets were then cleaned with 500 μL of 70% ethanol before being dissolved in 30 μL of TE buffer. Finally, the spectrophotometric estimation of the mtDNA was made. Then, using a HT 8-oxo-dG ELISA Kit II from Trevigen as previously described, same quantity of mtDNA from each experimental set was extracted for 8-oxo-dG measurement by ELISA (43)

2.13. Confocal immunohistochemical analysis

Confocal fluorescence immunohistochemical analyses were used to track the accumulation of 8-Oxo-dG in the gastric mucosal tissue of "Con," "Indo," and "HKL+Indo" rats. Sections of tissues that had been formalin-fixed and paraffinized underwent deparaffinization, rehydration, and antigen retrieval by heating in sodium citrate buffer. The tissue slices were then blocked with 10% goat serum and 1% BSA in TBS for two hours. The antibody solution containing 8-oxo-dG (Anti-DNA/RNA Damage antibody) was incubated overnight with tissue slices. The slides were washed before being incubated with an anti-mouse secondary antibody that was labeled with Alexa fluor 647. The sides were washed once again. Nuclear staining was performed using DAPI. The washed slides were mounted in 30 % glycerol in PBS. Using the Leica Application Suite X (LAS X) program, confocal images were captured using the Leica TCS-SP8 confocal microscope (Leica Microsystems, Wetzlar, Germany). The confocal images provided are randomly selected segments of the stomach mucosal sections. CorelDraw X7 was used for image assembly, image cropping, and general brightness/contrast changes (28,41). The experimental setup described here is in full compliance with the BJP Guidelines (40). Confocal fluorescent immunohistochemical investigations were used to count the accumulation of 8-Oxo-dG content in the gastric mucosal tissue of "Con," "Indo," and "HKL+Indo" rats. Sections of tissues that had been formalin-fixed and paraffinized underwent deparaffinization, rehydration, and antigen retrieval by heating in sodium citrate buffer. The tissue slices were then blocked with 10% goat serum and 1% BSA in TBS for two hours. The main antibody solution containing 8-oxo-dG (Anti-DNA/RNA Damage antibody) was incubated overnight with tissue slices. Slides with Alexa fluor 647-tagged anti-mouse secondary antibodies were washed and incubated. Once more, the sides were cleaned. To stain the nuclei, DAPI was used. The cleaned slides were mounted in PBS solution containing 30% glycerol and examined under a microscope. The Leica TCS-SP8 confocal microscope was used to capture confocal images. The detailed description of all antibodies used for immunofluorescent studies in this chapter may be found in the annexure where the published paper of this study has been attached.

2.14. Detection of mitochondrial superoxide anion ($O_2^{·-}$)

As previously noted, MitoSox staining was carried out to identify mitochondrial $O_2^{·-}$ in isolated stomach mucosal cells (41). In a nutshell, gastric mucosal scrapings were washed in Hanks Balanced Salt Solution (HBSS) and incubated for 80 minutes under shaking conditions at 37°C/5% CO2 in a pre-aerated solution supplemented with 100 μg ml^{-1} penicillin 100 μg ml^{-1} streptomycin, 0.05% hyaluronidase and 0.1% collagenase. 50 μm cell strainers were used to aseptically filter the cell suspension. The filtered cells were resuspended in PBS after being washed three times in pre-warmed HBSS. Following that, the cells' vitality was evaluated (using Trypan blue exclusion method). After counting the viable cells, 10^6 cells from each group were treated with MitoSox Red (Thermo) for 30 minutes at 37°C. Following three rounds of washing, the cells were analyzed by flow cytometry in FACS, LSR Fortessa, and BD. Standard settings were used for the FACS DIVA data analysis. The studies were run three times with 104 cells in each set.

2.15. Mitochondrial electron transport chain complex I and III activity assay

As previously described, oxidation rate of NADH (measured as a change in $OD_{340\,nm}$) and cytochrome c reduction (measured as a change in $OD_{340\,nm}$) in mitochondrial ETC complex-I (NADH: ubiquinone

oxidoreductase) and complex-III (decylubiquinol cytochrome c oxidoreductase) was determined by spectrophotometrical analysis (44-45). Shortly before utilizing them for enzymatic tests, identical amounts of isolated mitochondria (15 μg of protein) were lysed in a hypotonic buffer. NADH and ubiquinone were utilized as substrates for the complex-I test. By calculating the rotenone-sensitive NADH-ubiquinone oxidoreductase activity of the mitochondrial extract from control and treatment samples, specific complex-I activity was calculated. Ubiquinol and oxidized cytochrome c were utilized as substrates for the complex-III test. By calculating the antimycin A-sensitive decylubiquinol cytochrome c oxidoreductase action, the specific complex-III activity was determined.

2.16. Measurement of gastric luminal pH

Rats were allowed unrestricted access to water while they were fasted for 24 hours. On the day of the experiment, rats were given injections of lansoprazole (20 mg kg^{-1} b.w, i.p.) or HKL (40 mg kg^{-1} b.w, i.p.) 30 minutes before receiving the previously indicated dose of 2-mercapto-1-methylimidazole, or MMI, which is 40 mg kg^{-1} b.w, i.p (29). Since MMI promotes acid production, this set was marked as "stimulated". Without administering MMI injection, lansoprazole or HKL was administered to the second group of hungry rats. This group was designated as "basal (unstimulated)". For 4 hours, treated rats were incubated. Then rats were then sacrificed. To stop the escape of the gastric secretion, the abdomen was opened and the oesophageal and pyloric ends of the stomach were bound with thread.

2.17. Statistical analyses

The data and statistical analysis adhere to the British Journal of Pharmacology's guidelines for experimental design and analysis, which call for trials to be set up to produce groups of equal size and to use blinded analysis and randomization (46). Rats were divided randomly for all animal experiments. The animal number was kept constant for each batch at 5 (n = 5), as previously reported and standardized (27-29). The in vitro tests were carried out three times. At least three times each experiment was run. The mean and standard deviation were used to represent the data from experiments. Unpaired t-tests with Welch correction were used to compare two experimental groups, and one-way ANOVAs followed by Bonferroni's Multiple-Comparison tests were used to compare more than two experimental groups. P values less than 0.05 ($P < 0.05$) were regarded as statistically significant for all data. The number of independent values is the group size specified above, and it was these independent values that were used in the statistical analysis. Microsoft Office Excel 2019 and GraphPad Prism 8 were used to statistically analyze the data.

3. RESULTS

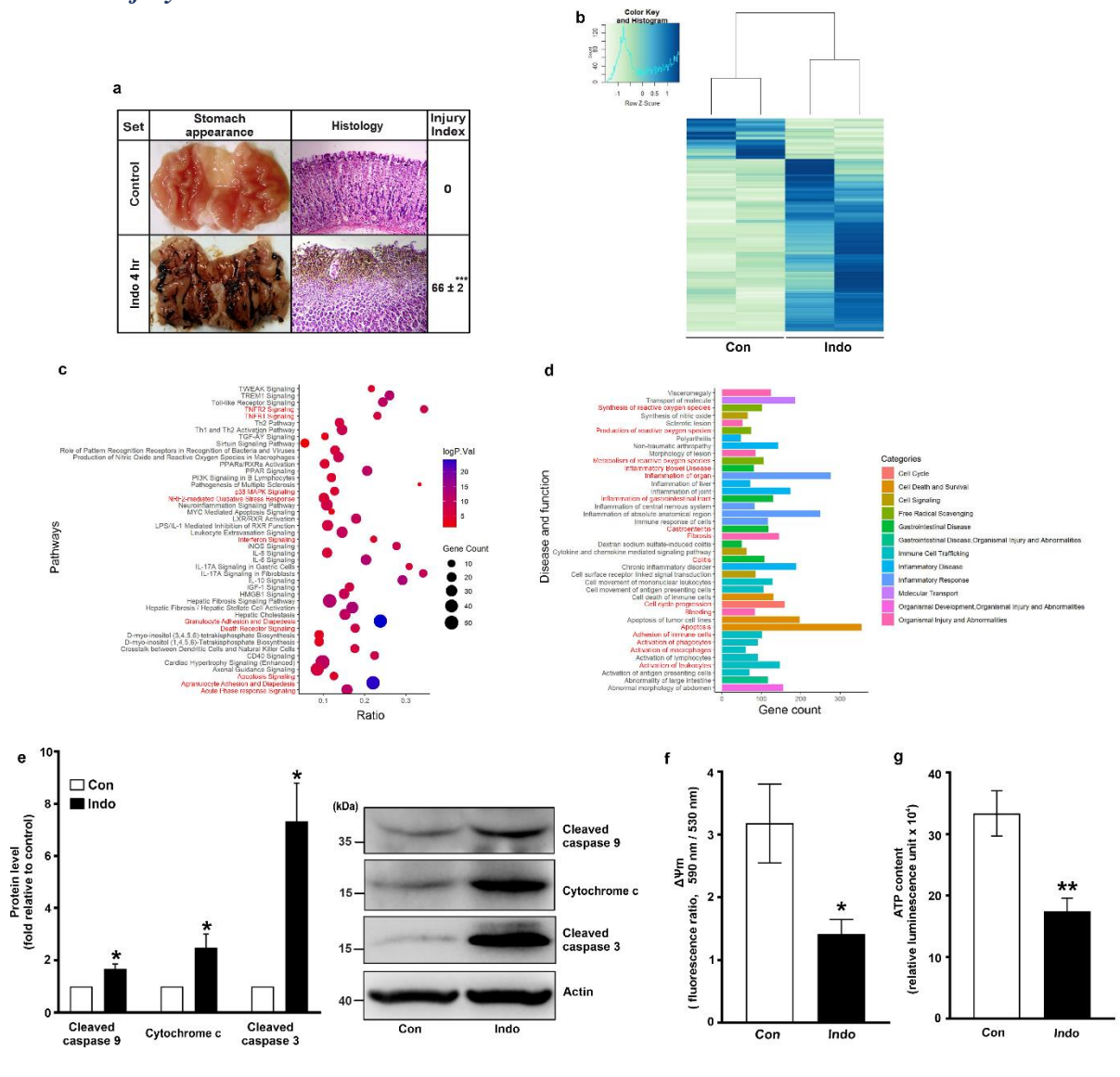## 3.1. Transcriptome data analysis revealed the connotation of SIRT3 in NSAID-induced gastric mucosal injury

Fig. 1. Effects of indomethacin on the gastric mucosa, including transcriptome alteration, intrinsic apoptosis, and mitochondrial dysfunction. (**a**) The panel displays the gastric mucosal morphology and histology stained with hematoxylin/eosin in control rats and rats treated with indomethacin. Representative images are provided for visual comparison. (**b**) A heatmap demonstrates the clustering of samples based on gene expression data of differentially expressed genes (DEGs) between the control group ('Con') and the indomethacin-treated group ('Indo'). The clustering was performed using the Euclidean distance metric. Genes with expression values analyzed above a fold change cutoff of 1.5 are represented by a color gradient scale, where white indicates significant downregulation and blue indicates significant upregulation. (**c**) A dot plot presents enriched canonical pathways, showing the proportion of genes involved in each signaling pathway. The color range indicates the statistical significance of enrichment, with Bonferroni corrected p values (-log transformed). The ratio indicates the number of genes within a pathway relative to the total number of genes mapped to that pathway. (**d**) A bar graph demonstrates the enrichment of disease and functional categories in

the set of genes affected by indomethacin treatment. **(e)** Immunoblots show the protein levels of cleaved caspase 9, cytochrome c, and cleaved caspase 3 in gastric mucosal tissues from both control and indomethacin-treated rats. Actin serves as the loading control. Representative blots are provided. **(f)** The panel presents the measurement of mitochondrial transmembrane potential ($\Delta\Psi$m) in gastric mucosal tissues from control and indomethacin-treated rats. **(g)** The bar graph displays the quantification of ATP content in gastric mucosal tissues from control and indomethacin-treated rats. The indomethacin treatment involved a dosage of 48 mg kg-1 body weight administered for 4 hours. The data presented in panels **(a),** and **(e-g)** represent the mean $\pm$ standard deviation. Statistical significance was determined using the unpaired Student's t-test with Welch correction, where *$P < 0.05$ and **$P < 0.01$ compared to the control group. The experiments were conducted independently thrice to meet statistical integrity of the data.

Since NSAIDs have the most adverse effects on the stomach, high-depth transcriptome sequencing was performed on the gastric mucosa of control and indomethacin-treated rats to thoroughly examine the changes in gene expression that occur during gastropathy. Indomethacin was selected as a prototype COX non-selective NSAID. Indomethacin-treated samples with high-grade mucosal damage and control samples' tissues were taken for transcriptome sequencing (Fig. 1a). When filtered using a log fold change (FC) cut-off of 1.5, a p value 0.05, and an FDR 0.05, a heat map showed the differentially expressed gene (DEG) set with 885 up-regulated and 211 down-regulated genes when compared to "control" (Fig. 1b) (GSE201565). The major pathways and "disease and function" involved in indomethacin-induced gastric cytotoxicity were identified by gene-enrichment analysis utilizing "ingenuity pathway analysis" (IPA) (Fig. 1c-d). 'TNFR signaling', 'interferon signaling', 'Apoptosis and death receptor signaling', 'p38 MAPK signaling', 'granulocyte and agranulocyte adhesion and diapedesis', 'acute phase signaling' and 'NRF2-mediated oxidative stress response' were prominently highlighted (Fig. 1c), whereas the pathways associated with 'synthesis, production and metabolism of reactive oxygen species', 'gastroenteritis', 'apoptosis', 'cell cycle progression', 'bleeding', 'inflammation of gastrointestinal tract', 'inflammatory bowel disease', 'colitis' 'fibrosis', and 'phagocyte and macrophage activation' were highlighted in major class of 'disease and function' (Fig. 1d). These indications logically directed towards exploring the status of caspase 9 and 3 as well as cytochrome c as final indicators of intrinsic apoptosis which are triggered by mitochondrial malfunction (Fig. 1e). The major rationale underlying this was the fact that mitochondria are connected to a wide range of pathways and activities which were found in the transcriptome data. Mitochondrial transmembrane potential and ATP concentration were also examined (Fig. 1f-g). Immunoblotting data indicated mitochondrial dysfunction, so I examined the transcriptome data more carefully to look for key genes controlling the electron transport chain (ETC) and mitochondrial metabolism (Fig. 2). When the analysis was done with an FC cut-off of 1.5, ETC complex genes did not show up in the transcriptome data, although indomethacin-treated tissues had obvious mitopathology and ATP depletion. To look for DEGs influencing mitochondrial processes, the normal FC cut-off (of 1.5) was logically reduced to 1.2. (Fig. 2a). It's noteworthy that "oxidative phosphorylation" and "mitochondrial failure" were highly emphasized as important routes (Fig. 2b). Proapoptotic indicators were increased, antioxidant and anti-apoptotic markers were downregulated, ETC complex-related gene expression was considerably compromised. 160 DEGs with organ inflammation, 272 DEGs were associated with gastrointestinal inflammation, 74 DEGs with epithelial tissue necrosis, 147 DEGs with leukocyte migration, and 49 DEGs with ROS generation, according to functional enrichment analysis. Intriguingly, the "sirtuin signaling pathway" was brought to light, with SIRT3 revealing itself to be a common gene linked to numerous disease categories and biological processes, including "gastrointestinal disease," "free radical scavenging," "inflammatory response," "cell death and survival," "cellular function and maintenance," "cell to cell signaling and interaction," "molecular transport," "protein synthesis," "tissue morphology," "organismal development," and "injuries (Fig. 2c). Next, the gene interaction network was constructed using the MCODE (47) plugin for Cytoscape (48)

and screened the hub gene or genes controlling mitochondrial metabolism and cellular integrity. SIRT3 emerged as a key hub gene in charge of several signaling mechanisms that govern mitochondrial metabolism and cellular integrity (Fig. 2d). Next, the functional connection of this protein in NSAID-induced gastric damage is investigated.
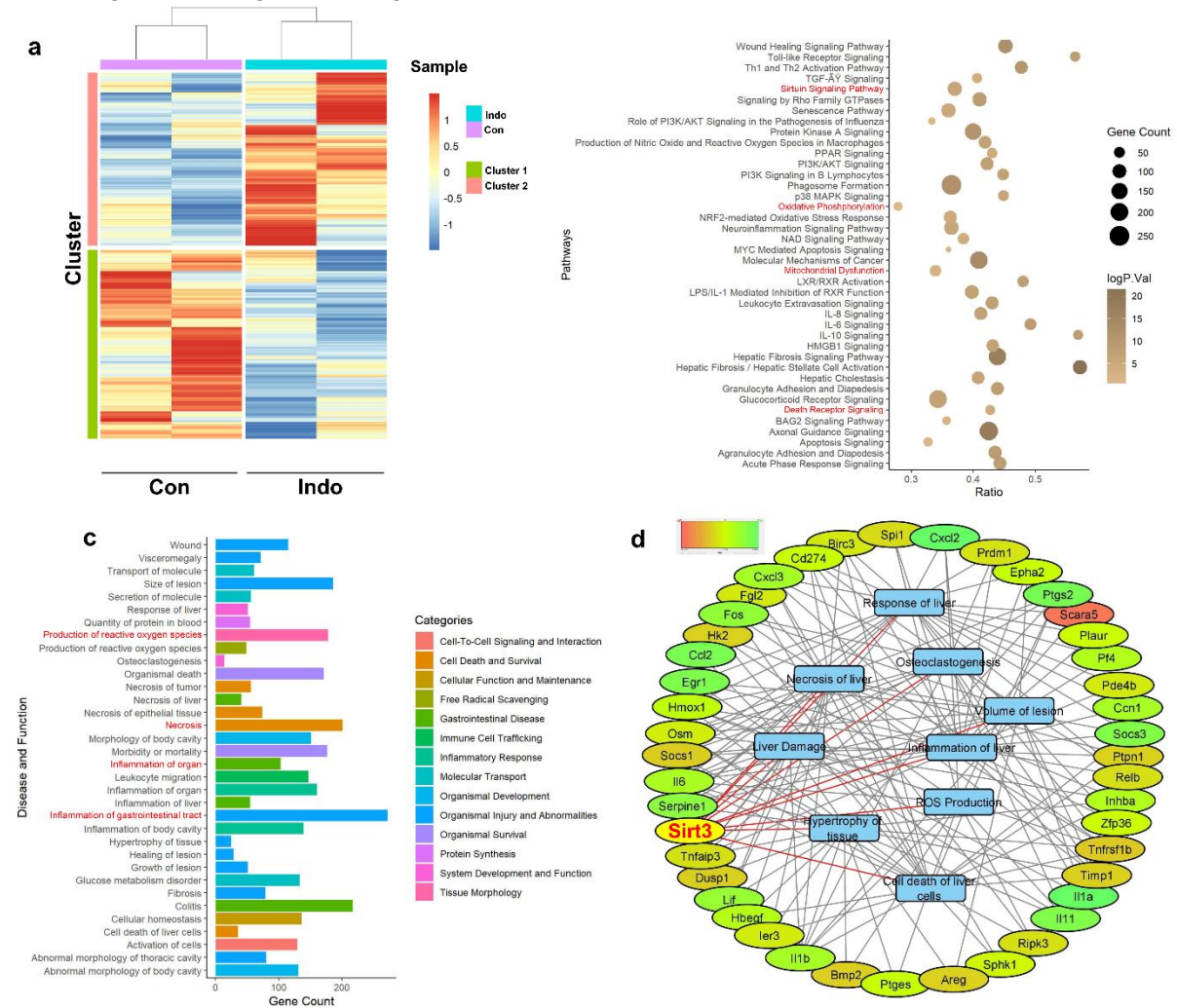

Fig. 2. Indomethacin modifies the genetic programs that control the functioning of mitochondria and sirtuin signaling. (a) The heatmap illustrates distinct clusters of samples labeled as 'Con' (control) and 'Indo' (indomethacin). The clustering of gene expression data for the differentially expressed genes (DEGs) was performed using the Euclidean distance metric. The expression levels of genes were analyzed using a fold change cutoff of 1.2. The color gradient scale ranges from blue (indicating significant downregulation) to red (indicating significant upregulation). (b) The dot plot visualizes the enriched canonical pathways. The size of the dots represents the proportion of genes involved in a specific signaling pathway, and the color range indicates the significance of the enrichment (Bonferroni corrected p-values, -log transformed). The ratio denotes the number of genes within a pathway fraction relative to the total number of genes associated with that pathway. (c) The bar graph displays the diseases and functions that are enriched in the set of genes affected by indomethacin. (d) The hub gene network is depicted, where gene names: oval shapes, associated functions: rectangular boxes. The color gradient scale of gene expression values ranges from red (highly downregulated) to green (highly upregulated). Grey lines indicate connections between genes and associated functions, while red lines indicate the association of SIRT3 (the hub gene) with its respective associated functions.

3.2. NSAID reduces SIRT3 expression thereby inducing gastric mucosal cell injury and preventing deacetylase activity of purified SIRT3

The mechanistic details of SIRT3's downregulation was examined. SIRT3 was significantly depleted when tissue damage was at its worst, according to immunoblotting and qRT-PCR analyses that confirmed the transcriptome results (Fig. 3a-b). OGG1 depletion in the damaged mucosa demonstrated the functional importance of SIRT3 (Fig. 3b). I looked at the kinetics of SIRT3 expression to comprehend the pattern of SIRT3 expression during damage induction and subsequent spontaneous healing. Following the induction of mucosal injury from 0 to 4 hours of indomethacin treatment, both SIRT3 and OGG1 followed a coordinated temporal depletion. By 72 hours, however, the lesions had healed on their own, as shown by tissue restitution (Fig. 3c-d). I measured SIRT3's deacetylase activity when it was incubated with increasing concentrations of indomethacin to check if there was any direct impact of the drug on SIRT3's deacetylase activity. Data showed that purified SIRT3's deacetylase activity was dose-dependently reduced by indomethacin (Fig. 3e). Additionally, it was found that indomethacin administration notably increased the acetylation of the mitochondrial proteome (Fig. 3f), associated with a considerable accumulation of 8-oxo-dG content in the mtDNA, suggesting oxidative mtDNA damage (Fig. 3g). Ogg1, Xrcc6, Pdha1, Aco1, Idh1, Sdhb, Mdh1, Ndufa9, Glud1, and Acadl all demonstrated strong down-regulation even in the transcriptome sequencing data. Additionally, a simultaneous decrease in the activity of the mitochondrial dehydrogenase was observed (Fig. 3h) and an increase in the ubiquitination of the mitochondrial proteome (Fig. 3i), suggesting that SIRT3 depletion caused mitochondrial dysfunction followed by an increase in the removal of damaged mitochondria. So far, how the depletion of SIRT3 contributes to cell death and mitopathology induced by indomethacin was shown. But how exactly do NSAIDs downregulate SIRT3? Since indomethacin reduced SIRT3 gene expression, it was investigated if it targeted any transcriptional regulators upstream. Surprisingly, considerable depletion of both PGCα and ERRα in the damaged mucosa was observed, revealing the mechanism behind SIRT3 transcriptional depletion (Fig. 3j).

3.3. SIRT3 activation by HKL averts NSAID-mediated transcriptome alteration and mitochondrial pathology to prevent mucosal cell death and decrease stomach mucosal injury

Next, it was analyzed whether SIRT3 activation may avert NSAID-induced mucosal damage and stomach cell death. Rats were given an i.p. injection of HKL, a specific pharmacological inducer of SIRT3 (24). The best dosage for gastroprotection against indomethacin was 40 mg kg-1, with an ED_{50} of 12.32 mg kg^{-1} body weight (Fig. 4a-b). After seeing the gastroprotective effects of HKL administered i.p., it was checked whether i.g. route of HKL administration would bear any putative gastroprotective effect against indomethacin. The non-invasive mode of administration is undoubtedly more favorable in terms of the simplicity of drug delivery; therefore, this may potentially represent any improved therapeutic relevance in the future. Dose response study clearly showed that honokiol at 80 mg/kg body weight provided a similar level of protection as honokiol at 40 mg/kg body weight when administered i.p. (Fig 4c). In the following studies, the i.g. route of administration was logically avoided in favor of the i.p. route to prevent unnecessarily administering an excess quantity of HKL into the system (rat body). The gastric transcriptome profiles of rats treated with indomethacin after receiving HKL pre-treatment (HKL+Indo) were then examined. Sequencing results showed that the gene expression pattern in "HKL+Indo" was considerably different from "Indo" while being mostly similar to "control" (Fig. 4d-g). 417 genes were upregulated and 815 genes were downregulated in HKL+Indo compared to 'Indo,' with 505 upregulated and 85 downregulated genes exhibiting restored expression in 'HKL+Indo,' suggesting a protective impact of HKL-induced SIRT3 activation (Fig. 4e). When compared to "HKL+Indo," 4215 elevated and 3176 downregulated genes in "Indo" had reversed expression (Fig. 4f-g). Significant DEGs mostly consisted of genes involved in apoptotic,
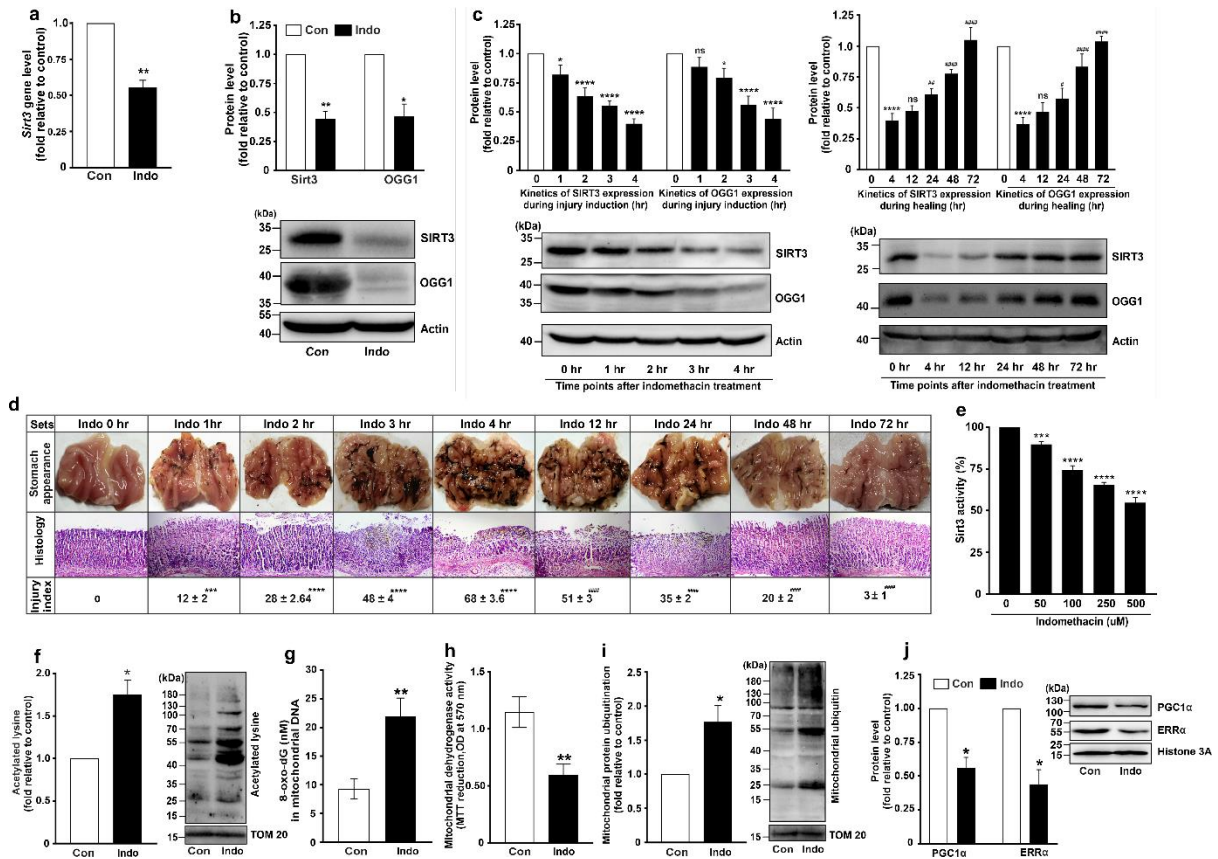
Fig. 3. Relationship between impaired SIRT3 expression and activity with the damage to gastric mucosal cells caused by indomethacin. (a) Quantitative PCR (qPCR) was conducted to analyze the expression of the SIRT3 gene in gastric mucosal tissues from two groups of rats: 'Con' (control) and 'Indo' (indomethacin-treated). The results are depicted as a bar graph showing the fold change in gene expression compared to the control group after normalizing by Gapdh. (b) Immunoblots of SIRT3 and OGG1 proteins in gastric mucosal tissues from the 'Con' and 'Indo' rats. Representative blots are shown below the bar graph. (c) Presents immunoblots of SIRT3 and OGG1 proteins in the 'Indo' rats at different time points. Actin is used as the loading control for both panels (b and c). (d) The gastric mucosal morphology and histology stained with haematoxylin-eosin from 'Indo' rats at the indicated time points. Representative images and micrographs are provided to visualize the tissue damage. (e) The deacetylase activity of purified SIRT3 is measured in the presence of increasing concentrations of indomethacin. (f) Shows an immunoblot of acetylated lysine in the mitochondrial fraction of gastric mucosal tissues from the 'Con' and 'Indo' rats. TOM20 is used as the loading control. (g) presents the measurement of mtDNA damage using 8-oxo-dG ELISA in gastric mucosal tissues from the 'Con' and 'Indo' rats. (h) The measurement of mitochondrial dehydrogenase activity through the MTT reduction assay in the mitochondrial fraction of gastric mucosal tissues from the 'Con' and 'Indo' rats. (i) Immunoblot of ubiquitination in the mitochondrial fraction of the 'Con' and 'Indo' rats. TOM20 is used as the loading control. (j) Immunoblot of PGC1α and ERRα proteins in the nuclear fraction of the 'Con' and 'Indo' rats. Histone 3A is used as the loading control. Representative blots are provided alongside the bar graph in panels (f, i, and j). The data in panels (c-d) are presented as the mean ± standard deviation. Statistical significance is indicated by asterisks and hashtags: *P < 0.05; **P < 0.01; ***P < 0.001; ****P < 0.0001 versus 'Indo 0hr,' and #P < 0.05; ##P < 0.01; ###P < 0.001; ####P < 0.0001 versus 'Indo 4hr,' calculated using one-way ANOVA followed by Bonferroni's post hoc test. The data in panel (e) are presented as the mean ± standard deviation. Statistical significance is indicated by asterisks: *P < 0.05; **P < 0.01; ***P < 0.001; ****P < 0.0001 versus 'Indo 0 µM,' calculated using one-way ANOVA followed by Bonferroni's post hoc test. The data in panels (a-b, f-j) were analyzed using an unpaired Student's t-test with Welch correction for comparing two groups. "ns" indicates non-significant. The number of independent experiments: 3
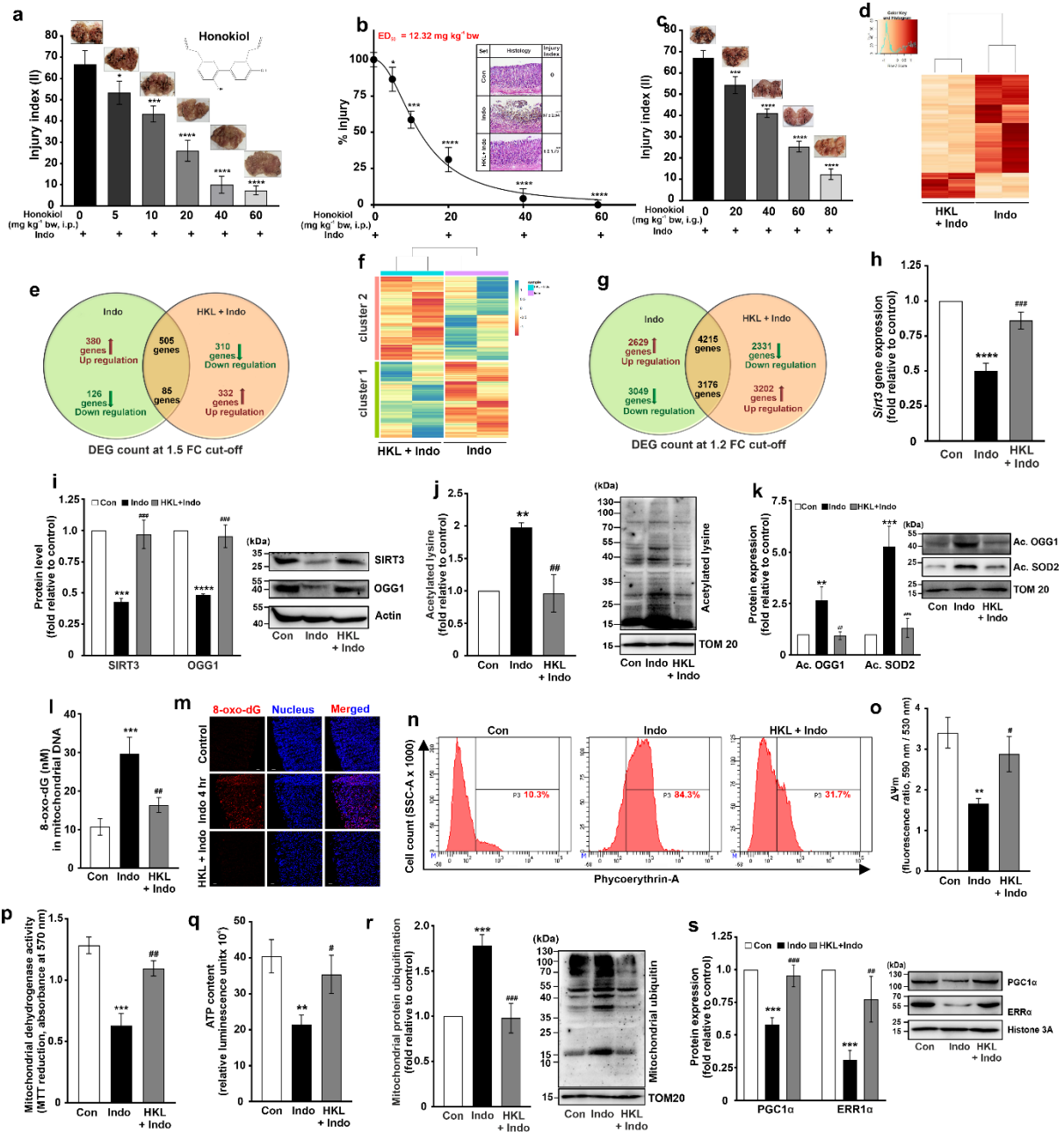
Fig. 4. Effect of SIRT3 stimulation on preventing gastric transcriptome alteration, mitochondrial dysfunction, and tissue injury induced by indomethacin. (a) A bar graph shows the dose response of HKL pre-treatment on indomethacin-induced gastric mucosal injury when administered via intra-peritoneal (i.p.) route. The inset image displays representative gastric mucosal morphology corresponding to different doses of HKL. The chemical structure of HKL is also presented. (b) A dose response curve of HKL is shown, indicating the effective dose (ED50). The histology of gastric mucosa stained with haematoxylin/eosin is presented for the control group ('Con'), indomethacin group ('Indo'), and HKL pre-treated group ('HKL+Indo'). Representative micrographs are provided. (c) Similar to (a), a bar graph illustrates the dose response of HKL pre-treatment on indomethacin-induced gastric mucosal injury, but this time when administered via intra-gastric (i.g.) route. The inset image displays representative gastric mucosal morphology for different doses of HKL. (d) A heatmap demonstrates separate clustering of gene expression data for the 'HKL+Indo' and 'Indo' groups. The clustering is based on the analysis of genes with fold change cut off of 1.5. The color gradient scale represents the degree of upregulation(brown) or downregulation (white) of gene expression. (e) A Venn diagram shows the count of differentially expressed genes (DEGs) in the 'Indo' group compared to the control group and in the 'HKL+Indo' group compared to the 'Indo' group,

69

considering a fold change cut off of 1.5. **(f)** A heatmap is presented for the 'HKL+Indo' and 'Indo' groups after analysis with a fold change cut off of 1.2. The color gradient scale represents the degree of upregulation (blue) or downregulation (red) of gene expression. **(g)** Another Venn diagram shows the count of DEGs in the 'Indo' group compared to the control group and in the 'HKL+Indo' group compared to the 'Indo' group. This time, the analysis considers a fold change cut off of 1.2, with a focus on genes controlling mitochondrial functions. The diagram includes brown upward arrows and green downward arrows to indicate upregulation and downregulation of gene expression, respectively. The intersection regions of the Venn diagrams indicate common genes that were upregulated or downregulated in the 'Indo' group compared to the control group, and their expression was found to be reverted in the 'HKL+Indo' group compared to the 'Indo' group. **(h)** The gene expression of SIRT3 in gastric mucosal tissues from the control group, 'Indo' group, and 'HKL+Indo' group is analyzed using qPCR. A bar graph represents the fold change in SIRT3 gene expression relative to the control group after normalization by Gapdh. **(i)** Immunoblots of SIRT3 and OGG1 in tissues from the control group, 'Indo' group, and 'HKL+Indo' group are presented. Actin is used as a loading control. **(j-k)** Immunoblots show the levels of acetylated lysine **(j)**, acetylated OGG1, and acetylated SOD2 **(k)** in the mitochondrial fraction of tissues from the control group, 'Indo' group, and 'HKL+Indo' group. TOM20 is used as loading control. **(l)** Measurement of mitochondrial DNA damage using 8-Oxo-dG ELISA. **(m)** Visualization of 8-Oxo-dG (green) and nucleus (blue) through confocal immunohistochemical staining in 'Con', 'Indo', and 'HKL+Indo'. **(n)** Analysis of mitochondrial superoxide accumulation using flow cytometry in 'Con', 'Indo', and 'HKL+Indo'. **(o)**. Assessment of mitochondrial transmembrane potential ($\Delta\Psi$m). **(p)** Evaluation of mitochondrial dehydrogenase activity. **(q)** Measurement of ATP content. **(r)** Immunoblot analysis of ubiquitination in the mitochondrial fraction of tissues from 'Con', 'Indo', and 'HKL+Indo'. TOM20 is used as a loading control. **(s)** Immunoblot analysis of PGC1α and ERRα in the nuclear fraction of tissues from 'Con', 'Indo', and 'HKL+Indo'. Histone 3A is used as a loading control. Representative blots are displayed alongside the corresponding bar graphs **(i-k, r-s)**. Data are presented as mean ± SD. Statistical significance: *$P < 0.05$; ***$P < 0.001$; ****$P < 0.0001$ compared to 'HKL 0 mg kg-1', calculated using one-way ANOVA followed by Bonferroni's post hoc test. The number of independent experiments conducted for **(a-c)** is 3. Data are presented as mean ± SD. Statistical significance: *$P < 0.05$; **$P < 0.01$; ***$P < 0.001$; ****$P < 0.0001$ compared to 'Con' and #$P < 0.05$; ##$P < 0.01$; ###$P < 0.001$; ####$P < 0.0001$ compared to 'Indo', calculated using one-way ANOVA followed by Bonferroni's post hoc test for **(b, h-l, o-s)**. The experiments were performed on 5 rats. The number of independent experiments conducted is 3.

inflammatory, and mitochondrial functions as well as those involved in stomach damage. Significantly high levels of Hmox1, Txnrd1, Sod1, Mmp13, Mmp3, Tnf1b, Ccl2, Cxcl2, Icam1, Vcam1, Hif1a, Cxcl3, Il6, Il1b, Il1a, Nfkb2, Nfkb1, Nlrp3, Fas, Bcl2, and Tlr9 were found, showing that HKL resisted inflammation and mitochondrial oxidative stress. It is noteworthy that expression of SIRT3 was observed with comparable expression in "HKL+Indo" and "control." Restoration of SIRT3 expression made the protective effect of HKL against indomethacin. (Fig. 4h-i). Additionally, evidence of the stimulatory effects of HKL on the expression of key SIRT3 targets is provided here. Next, the state of SIRT3 targets and the acetylation status of the mitochondrial proteome were investigated to understand the molecular underpinnings of HKL-dependent SIRT3 activation and protection of NSAID-induced gastropathy. It was observed that HKL pre-treatment prevented indomethacin-induced OGG1 depletion (Fig. 4i) and restored SIRT3 activity as shown by a reduction in the hyperacetylation of the mitochondrial proteome (Fig. 4j) and selective acetylation of OGG1 and SOD2 (Fig. 4k). Indomethacin-induced 8-oxo-dG accumulation in mtDNA was lessened, which further demonstrated the prevention of OGG1 deactivation, as shown by ELISA (Fig. 4l) and immunohistochemistry examination (Fig. 4m), which showed tissue levels of 8-oxo-dG in situ. Because the accumulation of 8-oxo-dG is a direct result of mtDNA oxidation, the MitoSox-based flow cytometry was used to measure the amount of superoxide ($O_2^{\bullet-}$), a progenitor reactive oxygen species (ROS) molecule, in the gastric mucosal cells that were isolated from rats that had received indomethacin treatment in the presence or absence of HKL. As shown in (Fig. 4n), HKL pre-treatment prevented the accumulation of intracellular $O_2^{\bullet-}$ caused by NSAIDs while also restoring $\Delta\Psi$m, maintaining mitochondrial dehydrogenase activity, and preventing
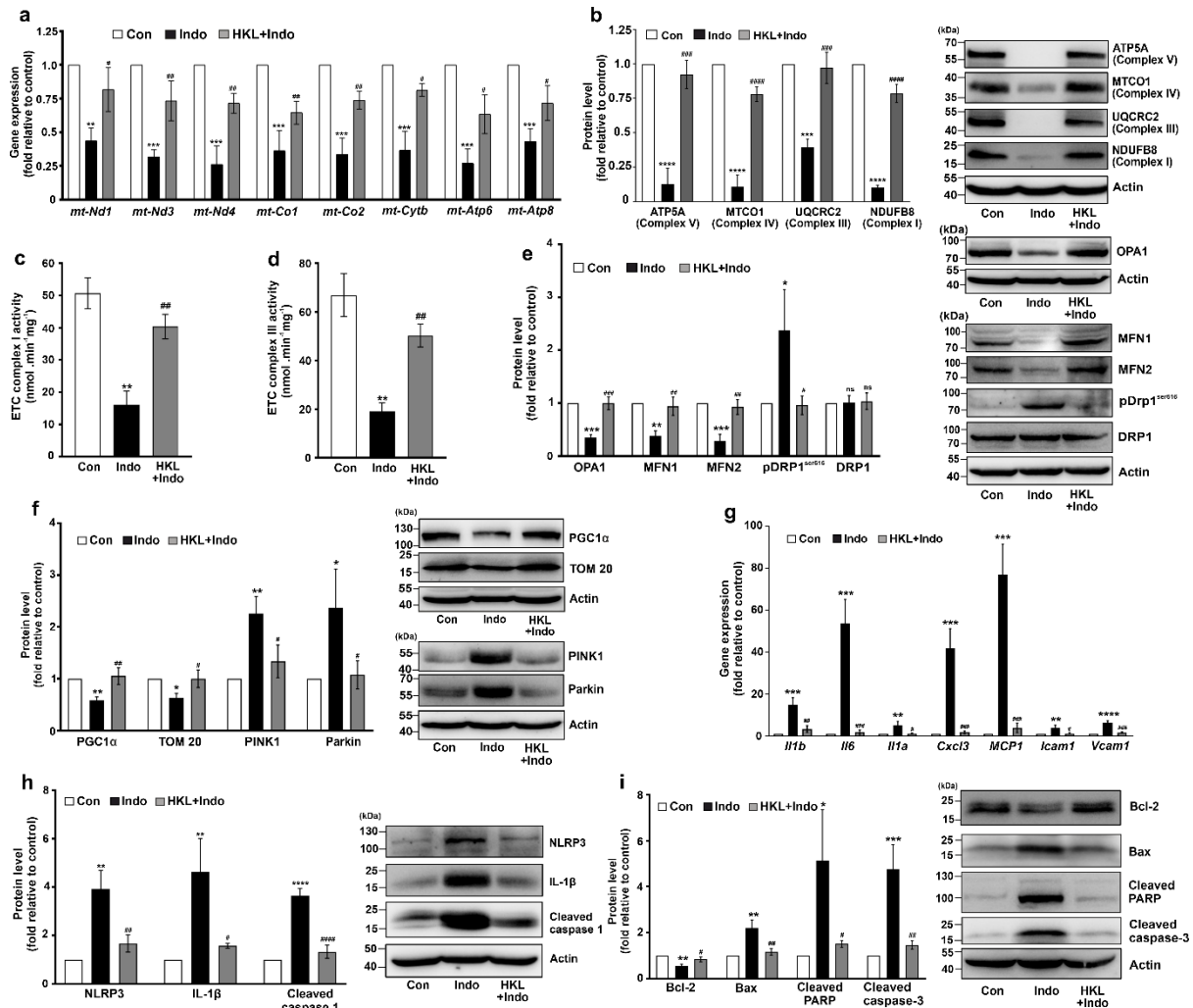
Fig. 5. The activation of SIRT3 prevents the negative effects of indomethacin on the expression of genes related to the electron transport chain (ETC) complex, abnormal mitochondrial dynamics, mucosal inflammation, and apoptosis. (a) Quantitative RT-PCR analysis of mt-Nd1, mt-Nd3, mt-Nd4, mt-Cytb, mt-Co1, mt-Co2, mt-Atp6, and mt-Atp8 gene expression in 'Con', 'Indo', and 'HKL+Indo' rats. Bar graphs show the fold change in gene expression compared to the control group (normalized to Gapdh). (b) Immunoblot analysis of ATP5A, MTCO1, UQCRC2, and NDUFB8 in tissues from 'Con', 'Indo', and 'HKL+Indo'. (c) Measurement of ETC complex I activity. (d) Measurement of ETC complex III activity in the mitochondrial fraction of tissues from 'Con', 'Indo', and 'HKL+Indo'. (e) Immunoblot analysis of MFN1, MFN2, OPA1, pDRP1ser616, and DRP1 in tissues from 'Con', 'Indo', and 'HKL+Indo'. (f) Immunoblot analysis of PGC1α, TOM20, PINK1, and Parkin in tissues from 'Con', 'Indo', and 'HKL+Indo'. (g) Quantitative RT-PCR analysis of Il1b, Il6, Il1a, Cxcl3, Mcp1, Icam1, and Vcam1 gene expression in 'Con', 'Indo', and 'HKL+Indo'. Bar graphs represent the fold change in gene expression compared to the control group (normalized to Gapdh). (h) Immunoblot analysis of NLRP3, IL-1β, and cleaved caspase 1 in tissues from 'Con', 'Indo', and 'HKL+Indo'. (i) Immunoblot analysis of Bcl-2, Bax, cleaved PARP, and cleaved caspase 3 in tissues from 'Con', 'Indo', and 'HKL+Indo'. Actin was used as the loading control, and representative blots are shown alongside the bar graphs (b, e, f, h, i). Data are presented as mean ± SD. Statistical significance: *$P < 0.05$; **$P < 0.01$; ***$P < 0.001$; ****$P < 0.0001$ compared to 'Con', and #$P < 0.05$; ##$P < 0.01$; ###$P < 0.001$; ####$P < 0.0001$ compared to 'Indo', calculated using one-way ANOVA followed by Bonferroni's post hoc test. The experiments were independently conducted thrice.

bioenergetic crisis (Fig. 4o-q). In fact, indomethacin-induced mitochondrial ubiquitination was dramatically inhibited by HKL-dependent SIRT3 activation (Fig. 4r). A feedback regulation was
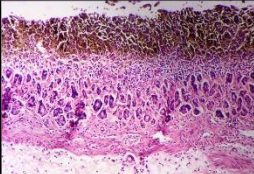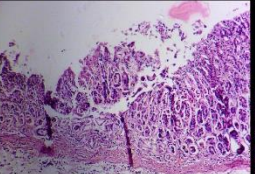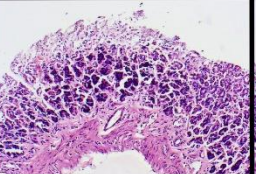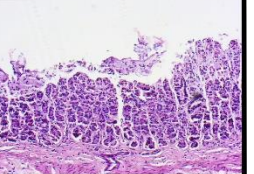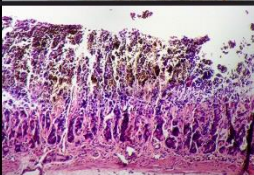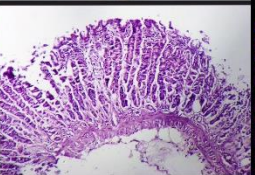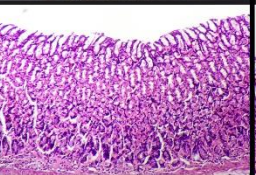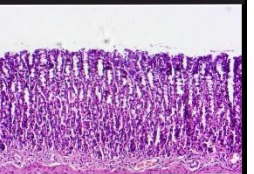
Experimental Conditions		0 hrs	8 hrs	12 hrs	20 hrs
Indo	Stomach appearance				
	Histology				
	Injury Index	67	52 ± 3**	41 ± 3.60****	32 ± 3.60****
HKL+ Indo	Stomach appearance				
	Histology				
	Injury Index	68	28 ± 2****	11 ± 1****	04 ± 1****

Fig. 6. HKL promotes the faster recovery of pre-existing gastric lesions caused by indomethacin. The upper panel shows the stomach morphology and histology of 'Indo' (indomethacin-treated group), while the lower panel shows the stomach morphology and histology of 'HKL+Indo'.

apparent when it was found that indomethacin-induced downregulation of PGC1α and ERRα was considerably resisted by endogenous SIRT3 activation by HKL (Fig. 4s).

Table 1. pH of gastric luminal secretion of different experimental groups of rats.

Experimental set	Stomach luminal pH
Control	2.73 ± 0.45
Control + HKL	2.48 ± 0.17^{Ns}
Control + Lansoprazole	7.09 ± 0.26****
MMI	1.63 ± 0.15*
MMI + HKL	1.83 ± 0.35*
MMI + Lansoprazole	6.61 ± 0.52****

*Stomach luminal pH in 'Control', 'Control + HKL', 'Control + Lansoprazole', '2-mercapto-1-methylimidazole, MMI', 'MMI + Honokiol' and 'MMI + Lansoprazole' treated rats (n=5). Data represent mean ± SD against "Control." One-way ANOVA with Bonferroni's post hoc test was used to determine the p value (***P < 0.001, ****P < 0.0001) There are three separate experiments. Ns: Non-significant.*
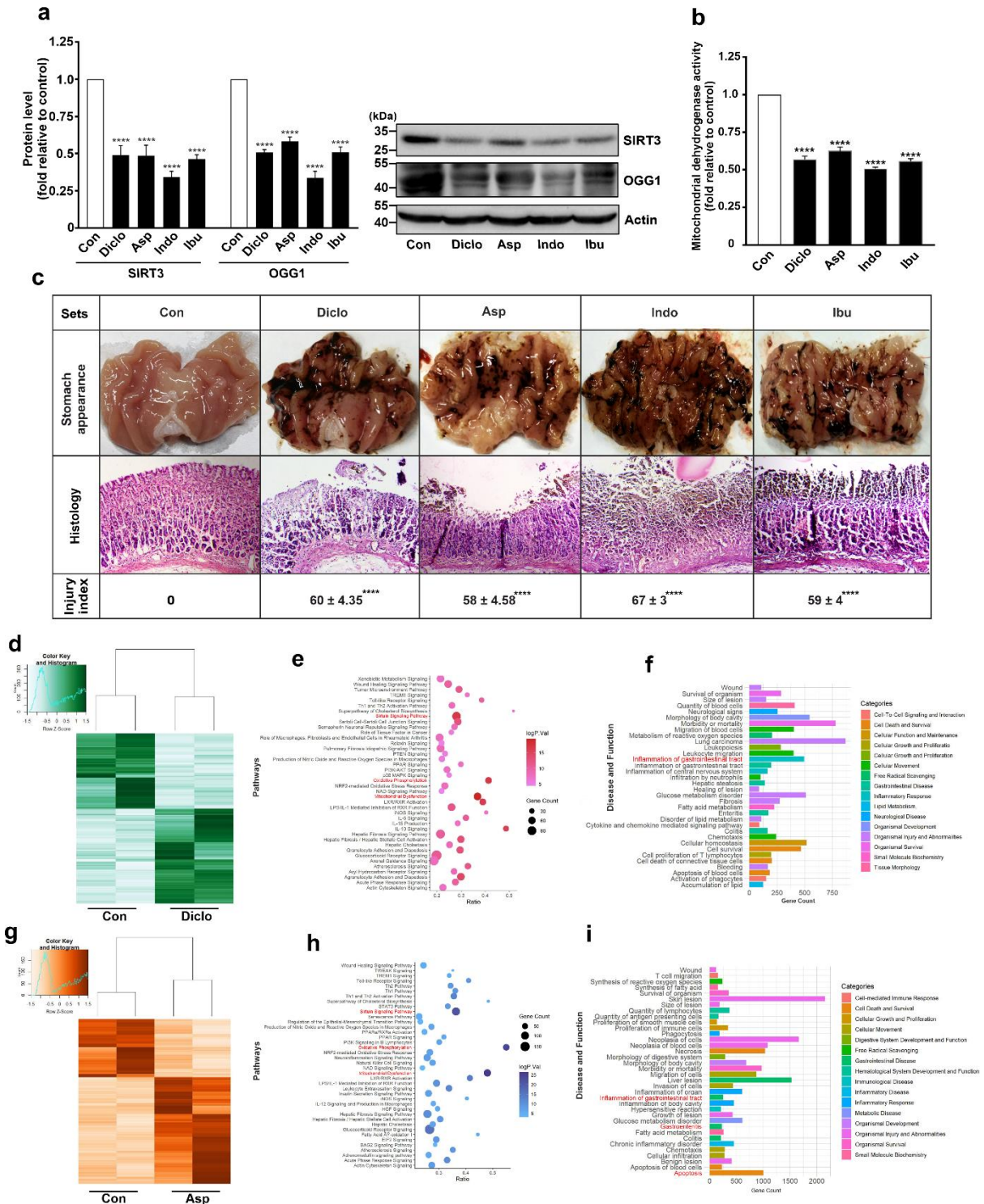
Fig. 7. **Commonly used NSAIDs decrease SIRT3 levels, leading to gastric mucosal injury and changes in gene expression. (a)** Immunoblots of SIRT3 and OGG1 in tissues from 'Con' (control), 'Diclo' (diclofenac), 'Asp' (aspirin), 'Indo' (indomethacin), and 'Ibu' (ibuprofen) groups. Actin was used as the loading control; representative blots are shown alongside the bar graphs. **(b)** Dehydrogenase activities in mitochondrial extracts from control and NSAID-treated rats. **(c)** Gastric mucosal morphology and histology stained with hematoxylin/eosin; representative images with an injury index provided. Data in **(a-b)** are presented as mean ± SD. *P < 0.05; **P <0.01; ***P < 0.001; ****P < 0.0001 compared to 'control' group, analyzed using one-way ANOVA followed by Bonferroni's post hoc test. The number of independent is 3. **(d)** Heatmap of gene expression in 'Con' and 'Diclo' (FDR ≤ 0.05). Gene expression values were analysed

using a fold change cut-off of 1.5, and the color gradient scale ranges from white (highly downregulated) to green (highly upregulated). **(e)** Dot plot showing enriched canonical pathways, with dot size indicating the proportion of genes involved and color indicating the significance level (Bonferroni corrected p values). The ratio represents the number of genes in a pathway relative to the total number of genes mapped to the same pathway. **(f)** Bar graph displaying enriched 'disease and functions' in the 'Diclo' group. **(g)** Heatmap of gene expression in 'Con' and 'Asp' groups (FDR ≤ 0.05). Gene expression values were analyzed using a fold change cut-off of 1.5, and the color gradient scale ranges from white (highly downregulated) to brown (highly upregulated). **(h)** Dot plot showing enriched canonical pathways in the 'Asp' group. **(i)** Bar graph displaying enriched 'disease and functions' in the 'Asp' group.

3.4. SIRT3 restoration averts NSAID-induced dysregulation of mtDNA-encoded ETC complex, abnormal mitochondrial quality control, mucosal inflammasome initiation and apoptosis

The impact of SIRT3 stimulation on mtDNA-encoded ETC complex components regulating bioenergy generation was investigated since SIRT3 depletion by indomethacin resulted in downregulation of OGG1, loss of mitochondrial dehydrogenase activity, and related ATP depletion. According to qRT-PCR and immunoblotting, HKL pre-treatment significantly inhibited the effects of indomethacin on the expression of the genes mt-Nd1, mt-Nd3, mt-Nd4, and NDUFB8 (complex I), mt-Cytb and UQCRC2 (complex III), mt-Co1, mt-Co2, and MTCO1 (complex IV), and mt-Atp6, mt-Atp8 and ATP5A (complex V) (Fig. 5a-b). Direct measurements of the activity of ETC complexes I and III also revealed that HKL prevented the loss of function of both complexes induced by indomethacin, ensuring proper electron transport during OXPHOS (Fig. 5c-d). Next, the condition of mitochondrial structure under both the HKL-induced SIRT3 stimulated state and the indomethacin-induced SIRT3 depletion state was analyzed since the homeostasis of mitochondrial dynamics is crucial for maintaining mitochondrial activities (Fig. 5e). It's interesting to note that HKL pre-treatment also blocked indomethacin-mediated depletion of MFN1, MFN2, OPA1, and an increase in DRP1 activation (by lowering phosphoDRP1^{ser616}), showing that mitochondrial dynamics had stabilized (Fig. 5e). The regulation of mitochondrial quality by keeping track of two important regulators of mitophagy, Parkin and PINK1 was examined. According to the data, HKL pre-treatment corrected abnormal PINK1-Parkin expression whereas indomethacin treatment caused Parkin and PINK1 to be significantly raised (Fig. 5f). Additionally, PGC1α and TOM20, the master regulators of mitochondrial biogenesis, were protected from deteriorating by HKL (Fig. 5f), preserving mitochondrial biogenesis, which is susceptible by NSAIDs. Since tissue inflammation is influenced by mitochondrial dysfunction, it was examined how HKL affected stomach inflammation and inflammasome activation. It was found that HKL greatly reduced the pro-inflammatory cytokine (Il1a, Il1b, Il6), chemokine (Cxcl3, Mcp1), and intercellular adhesion molecule (Icam1, Vcam1) increase caused by indomethacin (Fig. 5g). Additionally, it is observed that indomethacin activated the inflammasome in the stomach mucosa as demonstrated by the rise of NLRP3 and IL-1 as well as caspase 1 cleavage (Fig. 5h). However, HKL significantly inhibited the indomethacin-mediated activation of inflammasome markers (Fig. 5h). Since cell death is frequently linked to inflammatory tissue injury (49), the expression patterns of common pro- and anti-apoptotic markers was evaluated. It was observed that HKL dramatically reduced indomethacin-induced mucosal cell apoptosis by inhibiting Bcl-2 depletion and preventing PARP and caspase 3 cleavage as well as the upregulation of Bax (Fig. 5i).

3.5. Without affecting stomach acid output, HKL helps to accelerate the healing of pre-formed gastric lesions and gives gastroprotection against indomethacin.

After establishing the HKL's preventive effectiveness against NSAID gastropathy, it was investigated whether SIRT3 activation might also be utilized therapeutically to accelerate the healing of pre-formed stomach ulcers. After receiving an indomethacin treatment and being allowed to form stomach
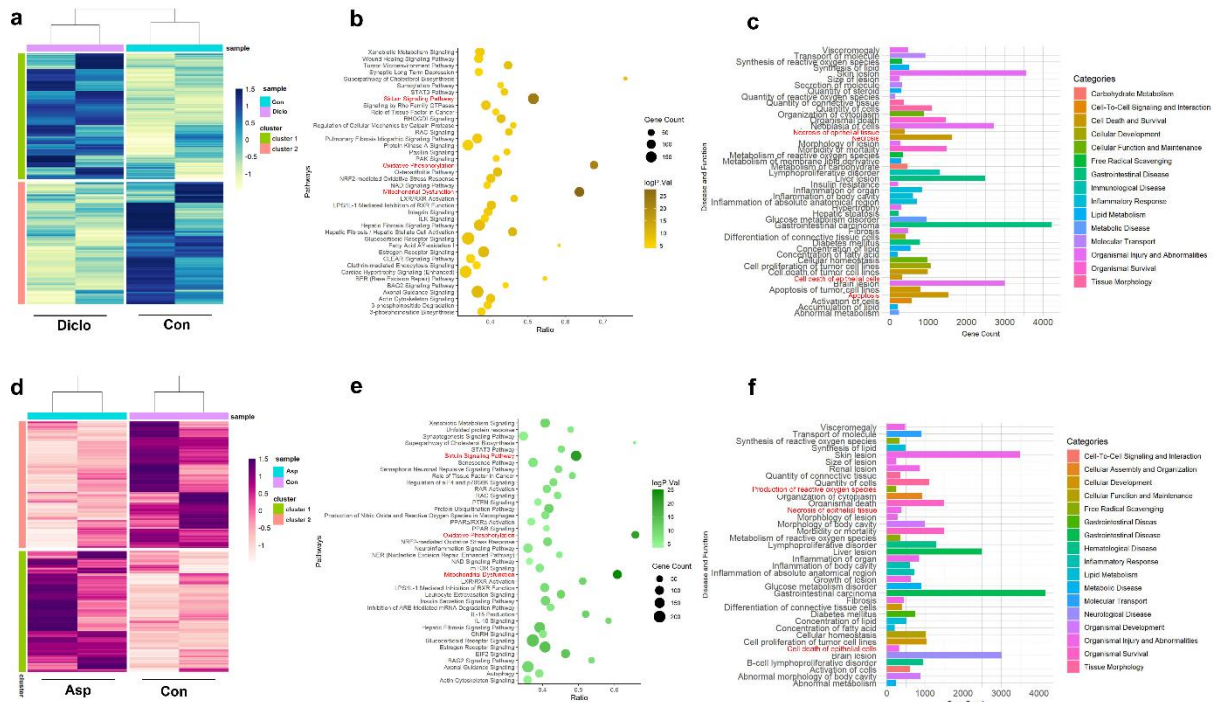
Fig. 8. Analysis of gastric mucosal transcriptome changes induced by diclofenac and aspirin using a fold change (FC) cut-off of 1.2. **(a)** Heatmap illustrating separate clustering of gene expression data from the 'Con' (control) and 'Diclo' (diclofenac) groups (FDR ≤ 0.05). The Euclidean distance metric was employed for clustering, and gene expression values were analyzed using a fold change cut-off of 1.2. The color gradient scale ranges from blue (highly upregulated) to white (highly downregulated). **(b)** Dot plot presenting enriched canonical pathways, with dot size indicating the proportion of genes involved and color representing the significance level (Bonferroni corrected p values, -log transformed). The ratio reflects the number of genes in a pathway relative to the total number of genes mapped to that pathway. **(c)** Bar graph displaying enriched 'disease and functions' in the 'Diclo' group. **(d)** Heatmap demonstrating separate clustering of gene expression data from the 'Con' and 'Asp' (aspirin) groups (FDR ≤ 0.05). The Euclidean distance metric was utilized for clustering, and gene expression values were analyzed using a fold change cut-off of 1.2. The color gradient scale ranges from magenta (highly upregulated) to white (highly downregulated). **(e)** Dot plot depicting enriched canonical pathways, with dot size indicating the proportion of genes involved and color representing the significance level (Bonferroni corrected p values, -log transformed). The ratio reflects the number of genes in a pathway relative to the total number of genes mapped to that pathway. **(f)** Bar graph presenting enriched 'disease and functions' in the 'Asp' group.

damage for 4 hours, rats were divided into two groups; one group received HKL treatment while the other group received no treatment. The level of wound clearance was compared to that of only "Indo" treated rats at time points of 0 hours, 8 hours, 12 hours, and 20 hours following HKL administration (Fig. 6). It was observed that the healing of pre-existing gastric lesions was dramatically speed up by HKL. By assessing luminal pH under baseline (unstimulated state) and 2-mercapto-1-methylimidazole-stimulated increased acid secretion condition, it was determined whether HKL treatment had an impact on gastric acid production. Strangely, unlike lansoprazole, which considerably raised the pH, HKL treatment did not affect the stomach luminal pH (Table 1). As a result, stomach acid production did not affect the HKL-dependent gastroprotection provided by HKL.

3.6. SIRT3 depletion is a generalized event caused by common NSAIDs to induce gastric mucosal injury

Finally, it was investigated whether SIRT3 depletion was exclusive to indomethacin or widespread across NSAIDs, including aspirin, diclofenac, and ibuprofen, which are often used as the main

ingredient in anti-inflammatory formulations for human therapy. Because of its cardioprotective and anti-neoplastic actions, aspirin was specifically chosen. It was observed that, like indomethacin, all of these NSAIDs dramatically reduced SIRT3 and OGG1 expression. Significantly reduced mitochondrial dehydrogenase activity and severe mucosal damage were caused by SIRT3 depletion (Fig. 7a-c). SIRT3 depletion, therefore, looked to be a common mechanism that NSAIDs target. Additionally, stomach transcriptomics of rats treated with aspirin (Figs. 7g-i and 8d-f) and diclofenac (Figs. 7d-f and 8a-c) revealed a pattern of DEGs and related gene expression programs that was comparable to indomethacin.

4. DISCUSSION

Here, SIRT3 has been identified for the first time as a new gastroprotective target that is markedly inhibited by NSAIDs thereby inflicting mitochondrial dysfunction and cellular bioenergetic dysregulation to cause gastric mucosal cell death and inflammatory tissue injury. It has been experimentally validated that NSAIDs exert a top-down control by directly inhibiting SIRT3 deacetylase activity as well as suppressing its transcriptional regulators PGC1α and ERRα to negatively affect SIRT3 expression. Interestingly, NSAID-induced aggravated redox imbalance, mitochondrial fragmentation, inflammasome activation and apoptosis are significantly blocked upon pre-treatment with a specific SIRT3 stimulator, HKL, which also prevented mucosal injury as well as hastened the resolution of pre-formed lesions in the stomach without disturbing basal acid secretion.

Even with its multiple side effects, NSAIDs are inevitable for the first-line of treatment for pain and inflammation. NSAIDs' anti-neoplastic potential is recently identified through drug-repurposing studies, which further increased their therapeutic value (50,51). It's worth noting that extra-COX pathways significantly account to the harmful actions of NSAIDs because its already proven that prostaglandin supplementation barely falls insufficient to simulate the toxic effects of NSAIDs (11). To neutralise their harmful effects and maximise their safe use, it was required to investigate newer COX-independent targets of NSAIDs. To eliminate any potential COX-1/COX-2 bias, indomethacin was employed as a prototype NSAID with very little COX-selectivity. Because NSAIDs have a particularly negative impact on the stomach, a rat model of gastric mucosal damage was used. Following NSAID treatment, sequencing-based target prediction made unbiased gene expression analysis easier. SIRT3 was revealed as a hub gene linked to a variety of metabolic effects induced by NSAIDs, including redox homeostasis, the generation of bioenergy, inflammation, and cell death. As the mitochondrial guardian, SIRT3 controls the stability of mitochondrial proteins to control metabolic processes, biogenesis, mtDNA repair, antioxidant defence, and structural dynamics. Specific target proteins that SIRT3 deacetylates include OGG1, OPA1, FOXO3a, SOD2, citrate synthase, pyruvate dehydrogenase, succinate dehydrogenase, isocitrate dehydrogenase, malate dehydrogenase (20,21). Loss of SIRT3 has been strongly linked to a number of diseases characterised by structural and functional deficiencies in the mitochondria that cause issues with metabolism and bioenergetics (21,52-54). Likewise, tissues that are metabolically active are vulnerable to SIRT3 deficiency (21,55). Despite the gut mucosa's high cellular turnover, there is no research mentioning the involvement of SIRT3 in preserving gastric mucosal integrity (56). To promote electron leakage, NSAIDs specifically target ETC complex-I. The oxygen is partially reduced by these released electrons to make $O_2^{.-}$ which then changes into additional ROS species including H_2O_2 and $\cdot OH$. SOD2 and OGG1 are two important mitochondrial antioxidants which counter oxidative stress by neutralising intra-mitochondrial $O_2^{.-}$ and removing 8-oxo-dG from mtDNA, respectively (57). Coincidentally, SIRT3 targets OGG1 and SOD2 for deacetylation. Additionally, 8-oxo-dG is a biomarker for illnesses linked to redox, such as cancer, and endogenous oxidative stress (58). MOS induction and cell death were caused by indomethacin-induced SIRT3 downregulation, which was explained by direct suppression of SIRT3 deacetylase activity, elevation of OGG1-SOD2 acetylation, and MOS induction. By enhancing antioxidant defense, SIRT3 acts as a

factor that encourages cellular lifespan (59,60). While SIRT3 overexpression significantly enhanced GSH level, SIRT3-deficient cardiomyocytes were observed to produce twice as much ROS (61). (57). Here, it is demonstrated that ATP depletion, decreased mitochondrial dehydrogenase activity, and malfunction of the ETC complex I and III caused by indomethacin-induced SIRT3 depletion resulted in a severe bioenergetic crisis. Removal of the mitochondria by ubiquitination-dependent mechanisms increased the harm. Furthermore, it is important to highlight that SIRT3 depletion-related mitochondrial toxicity and cell death seems to be similar to popular NSAIDs. When developing innovative strategies to avoid NSAID toxicity, this knowledge is essential. From a molecular standpoint, it was crucial to investigate how NSAIDs reduce SIRT3 expression. The downregulation of PGC1α and ERRα caused by indomethacin answered our question about the upstream events regulating SIRT3 expression. PGC1α-ERRα pair regulation by SIRT3 has recently been identified as a critical nuclear transcriptional axis directing a wide range of gene expressions regulating mitochondrial bioenergetics (59,62). It justifies mitochondrial depletion after SIRT3 downregulation by indomethacin because PGC1α also controls mitochondrial biogenesis (63). A significant decrease in PGC1α after indomethacin therapy in both the mitochondrial and nuclear fractions was observed. This strongly showed that NSAIDs disrupt both the nuclear and mitochondrial transcriptional activities of PGC1α in order to harm the metabolism of gastric cells overall. Additionally, SIRT3 and PGC1α depletion caused by indomethacin pointed to a mutual feedback regulation. Current research suggests that SIRT3-dependent FOXO3 deacetylation drives its nuclear translocation to upregulate PGC1α expression as a cytoprotective response, which is inhibited by SIRT3 depletion (64,65). This most likely includes the direct activation of *Sod2* transcription by PGC1α-FOXO3 (65). Numerous mitochondrial processes, such as mitosis, biogenesis, transcription, translation, OXPHOS, the TCA cycle, and the metabolism of lipids, glycosides, and amino acids are known to be regulated by SIRT3 (21). About 84 mitochondrial proteins directly interact with SIRT3 to regulate metabolism and bioenergetics. Around 20% of mitochondrial proteins are heavily acetylated (21). Through deacetylation-dependent regulation of AMPK, OPA1, FOXO3 and Lon protease, and SIRT3 also regulates mitochondrial dynamics and mitophagy (66). The expression of important mitophagy participants (Bnip3/Nix and LC3) and mediators of mitochondrial dynamics (MFN2, DRP1, and FIS1) is regulated by SIRT3 indirectly and/or directly (via FOXO3a deacetylation) (66). As a result of SIRT3 depletion and intra-mitochondrial prooxidant build-up, ETC malfunction appears to be directly attributed to indomethacin-induced MOS, mitochondrial hyper fission, and abnormal mitophagy. The pharmacological activation of SIRT3 by HKL, a specific inducer, was necessary for the functional validation of SIRT3's cytoprotective activity against indomethacin (24,67,68). It is important to note that there does not currently appear to be a synthetic SIRT3 peptide that is suitable for exogenous in vivo application, resistant to pepsin/other proteases (to protect it during systemic delivery), and mito-targeting to enable mitochondrial localization and retention for showing the deacetylase action. Therefore, the most effective and targeted pharmacological approach to test SIRT3's potential gastroprotective activity was to stimulate endogenous SIRT3 levels by the use of HKL. It's interesting to note that HKL-induced SIRT3 stimulation prevented ubiquitination and hyperacetylation of the mitochondrial proteome, which prevented cellular damage and the mitochondrial metabolic crisis caused by indomethacin. As a result, MOS was saved and ETC function was preserved. While inhibiting intra-mitochondrial $O_2^{.-}$ accumulation to stop oxidative mtDNA damage, HKL pre-treatment greatly resisted transcriptome modification by indomethacin. The expression of representative components corresponding to complex I, II, IV, and V and the direct enzymatic actions of complex I and III, which are the major sources of mitochondrial electron discharge during ETC dysfunction, made it apparent that HKL's protective action extended to almost all of the ETC complexes. If a substance protects mitochondria, it would appear essential to also provide stability and protection for the structural dynamics of mitochondria. It was evident that HKL effectively avoided the excess mitochondrial fission, abnormal mitophagy, and abrogated biogenesis caused by

indomethacin. Because various mtDAMPs, such as mtROS, oxidized mtDNA, and oxidised cardiolipin (produced after tissue damage), strongly activate NLRP3 activation, mitochondria are now thought to be the site of NLRP3 inflammasome activation (18,69). So far, there are very little evidence that NSAID-induced gastric mtDAMP production causes inflammasome activation during gastric mucosal damage. In this study, it is clearly demonstrated that HKL-induced SIRT3 activation dramatically repressed indomethacin-mediated activation of NLRP3 and the cleavage of caspase 1 to thwart IL-1 overexpression in the stomach mucosa. Concurrently, indomethacin-induced canonical inflammation and apoptosis were prevented by HKL. To support the claim that indomethacin causes mitochondrial structural and functional damage, the presented data reveals that, indomethacin downregulates SIRT3 expression and directly inhibits SIRT3 deacetylase activity. This, in turn, causes gastric mucosal inflammatory and apoptotic tissue damage. By promoting SIRT3 expression, HKL stopped the gastropathy that indomethacin causes. It is important to note that HKL is also thought to partially antagonize or activate the non-adipogenic PPAR gamma receptor in addition to its direct SIRT3-stimulating impact (70). Additionally, in mouse models, PPAR activation has been shown to provide gastroprotection and speed ulcer healing (71). Therefore, HKL's likely PPAR-agonism may also support or enhance the group's overall gastroprotective response. It is also important to note that the PPAR-PGC1α pair has previously been shown to play a significant role in controlling energy metabolism (72) and that PGC1α is likely to be favorably regulated by SIRT3 through a feedback loop. The specificity of HKL for SIRT3, a specified target among several additional off-targets, is therefore allegedly sufficient to prevent NSAID-induced stomach damage as seen here, even though HKL could have various responses. The results of this study directly support those of several earlier studies where it was revealed that SIRT3 activation by HKL preserves and maintains mitochondrial integrity, providing defense against a variety of diseases (67,73-75). So far it has been discussed how effective HKL-based SIRT3 activation is as a preventative measure against NSAID-induced gastropathy. However, a cytoprotective compound's entire effectiveness cannot be assessed without also considering its therapeutic potency. To this purpose, HKL successfully satisfied the criteria for a powerful gastroprotective molecule due to its extraordinary capacity to hasten the healing of indomethacin-induced stomach lesions. While total mucosal damage resolution in HKL-untreated sets required 72 hours following indomethacin therapy, complete wound resolution in HKL-treated sets took just 20 hours, demonstrating its powerful therapeutic activity. The relative effectiveness of HKL administered by i.p. vs. i.g. routes was also evaluated to address the potential biological application of HKL as a gastroprotective drug. The current pre-clinical work amply demonstrated that HKL can protect NSAIDs, at least in cases of indomethacin-induced mouse stomach mucosal damage, by requiring a substantially lower dosage when administered intraperitoneally (i.p.) than when administered i.g. To ensure that HKL is exploited to its full potential as a future gastroprotective drug accessible in oral formulations, more exploratory research should be conducted with a special focus on developing novel techniques to boost HKL's oral bioavailability. The majority of the anti-ulcer gastroprotective molecules now in use depend on suppressing stomach acid since it is believed that acid exacerbates harm. This must be stated before concluding. Gastric acid is not a physiological evil, notwithstanding the merits of this argument, which are apparent. Rather, acid helps to mediate protein digestion, maintain a healthy balance of the gut microbiota, protect the GI tract against opportunist pathobiont assault, and facilitate different medication and mineral absorption (76). The frequent use of anti-ulcer medications like histamine receptor antagonists or proton pump inhibitors is frequently linked to several health risks (77,78). Even though a direct link between PPI use and illness incidence is not always certain and requires substantial randomized control studies (79), excessive use of acid-suppressing medications is discouraged owing to the unavoidable need for physiological acid levels.
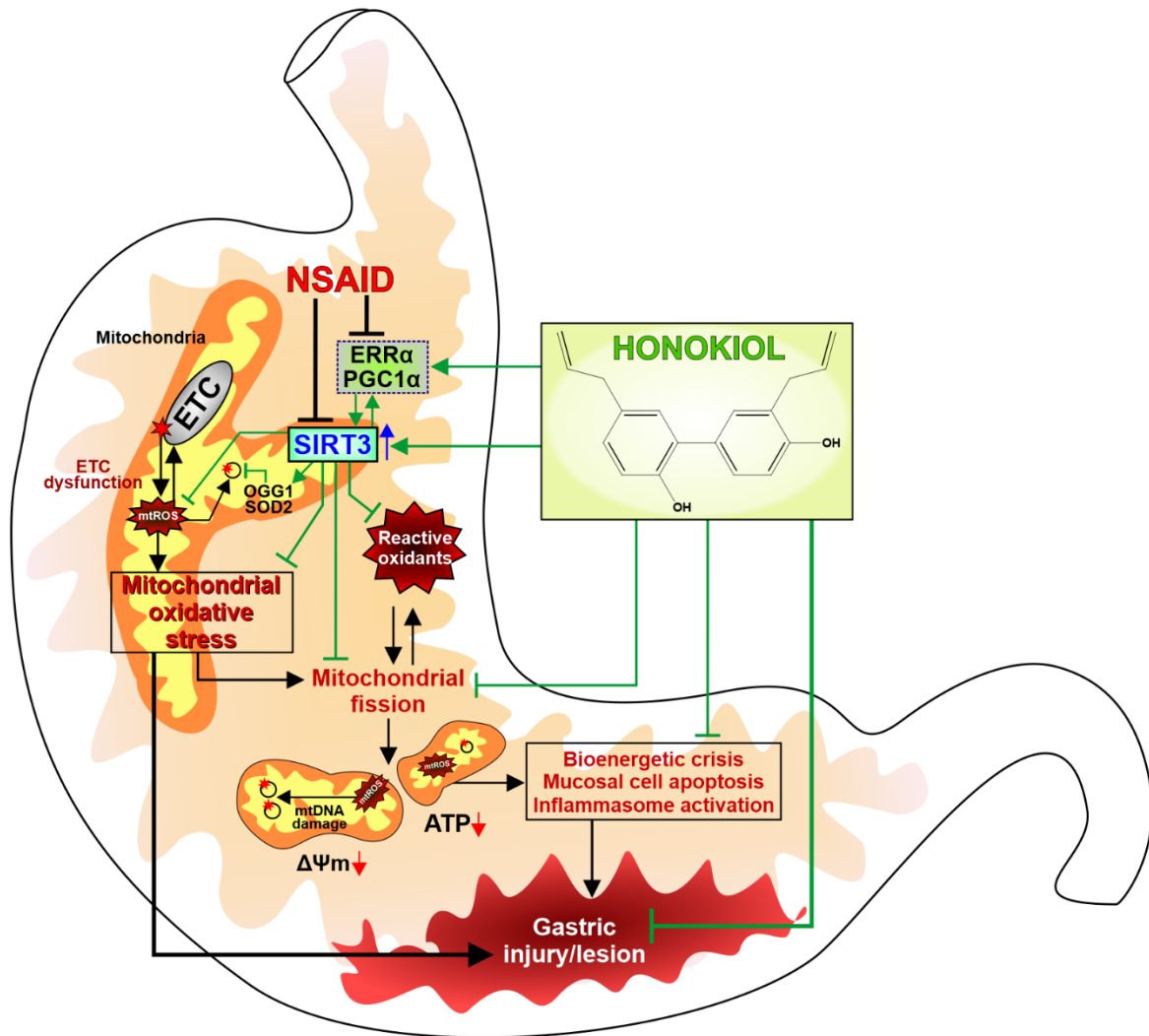
Fig. 9. Graphical representation of the mechanistic basis of SIRT3-induced protection of the gastric mucosa from NSAID-mediated mucosal injury. SIRT3 inducer, honokiol, exerts multiple level of protection by direct stimulation of SIRT3 as well as its transcriptional regulators.

Therefore, it seems rather safe if a new gastroprotective formulation specifically targets just the cytotoxic events (resulting in mucosal damage) while avoiding acid secretion. Curiously, baseline acid secretion was unaffected by HKL's anti-apoptotic and cytoprotective effects. This is advantageous because using this gastroprotective strategy, negative effects of acid suppression can be avoided, including malabsorption of specific medications, vitamin B12 deficiency, protein indigestion, gut dysbiosis, osteoporosis, rebound acid secretion, parietal cell hyperplasia and gastrinemia. In fact, current research indicates that HKL appears to be safe for intake by humans as a supplement for natural antioxidants (80). It is also important to note that SIRT3 has been described in several cancer studies as a double-edged sword because of its potential to promote cancer and/or have context-specific oncogenic or tumor suppressive properties depending on the type and metabolic needs of the tumors as well as their particular microenvironment (81). However, SIRT3 activation is largely advantageous when it comes to non-malignant diseases and provides defense against a variety of conditions triggered by inflammation, oxidative stress, mitochondrial malfunction, and energy dyshomeostasis (21,82,83). Essentially, honokiol's activation of SIRT3 neutralizes the excess ROS levels that accrued during the pathogenesis, protecting against the illness. Together, SIRT3 is revealed as a non-canonical COX-independent target of NSAIDs that is markedly downregulated following gastric mucosal damage,

resulting in mitochondrial structural and functional dysfunction. Strong gastroprotection is provided by the phyto-polyphenol SIRT3 inducer HKL while avoiding gastric acid release. Precisely leveraging this information may help create innovative gastroprotective drugs especially targeting mitochondria. Additionally, NSAID therapy combined with HKL-stimulated endogenous SIRT3 may surely aid in optimizing the therapeutic use of these "wonder medicines" while avoiding their negative effects.

5. CONCLUSION

The major finding of the work involves the identification of the mitochondrial deacetylase SIRT3 as a hitherto unknown target of NSAIDs which is downregulated to induce gastric mucosal injury. Deep transcriptome sequencing was undertaken for target mining followed by multidimensional functional validation. The study convincingly reports that SIRT3 reduction is a common cytotoxic response of major NSAIDs (including aspirin, diclofenac and ibuprofen used for human treatment purposes) to induce gastric mucosal cell death leading to the development of ulcer. Being the mitochondrial metabolic guardian, loss of SIRT3 due to NSAID treatment creates mitochondrial structural and functional havoc leading to severe fragmentation, electron transport chain dysfunction, bioenergetic crisis and consequent activation of intrinsic apoptosis. Direct evidence is provided here that NSAID concentration-dependently inhibits SIRT3 deacetylase activity. As a pharmacological tool for validation of the observed data, HKL has been strategically capitalized as an inducer of SIRT3. It was clear that endogenous SIRT3 stimulation by HKL corrected NSAID-induced transcriptomic and mitochondrial metabolic alteration to rescue inflammatory gastric injury. Another notable conclusion of the study is that HKL-induced gastroprotection is devoid of unwanted acid suppression (unlike existing antiulcer drugs). This study is extremely relevant from the biomedical perspective and it is expected that this work will certainly open up a new avenue in the field of gastroprotective drug discovery because SIRT3 is a promising druggable candidate which can be rationally exploited in a combinatorial approach to efficiently optimize NSAID usage for managing inflammatory conditions while safely bypassing their gastrotoxic effects. The study also bears a far-reaching impact owing to the damaging action of NSAIDs on other vital organs including gut, liver and heart while having protective role against diverse neoplasia. Moreover, SIRT3-inhibiting action by NSAID is a first-hand report of a new activity of NSAIDS which holds sufficient biomedical relevance. Further, SIRT3 stimulators like HKL may also qualify as new-generation safe anti-ulcer compounds as they can bypass the harmful effects of irrational acid suppression.

6. REFERENCES

1. Crofford, L. J. (2013) Use of NSAIDs in treating patients with arthritis. *Arthritis Res Ther* **15 Suppl 3**, S2
2. Ong, C. K., Lirk, P., Tan, C. H., and Seymour, R. A. (2007) An evidence-based update on nonsteroidal anti-inflammatory drugs. *Clin Med Res* **5**, 19-34
3. Kazberuk, A., Zareba, I., Palka, J., and Surazynski, A. (2020) A novel plausible mechanism of NSAIDs-induced apoptosis in cancer cells: the implication of proline oxidase and peroxisome proliferator-activated receptor. *Pharmacol Rep* **72**, 1152-1160
4. Khoo, B. L., Grenci, G., Lim, J. S. Y., Lim, Y. P., Fong, J., Yeap, W. H., Bin Lim, S., Chua, S. L., Wong, S. C., Yap, Y. S., Lee, S. C., Lim, C. T., and Han, J. (2019) Low-dose anti-inflammatory combinatorial therapy reduced cancer stem cell formation in patient-derived preclinical models for tumour relapse prevention. *Br J Cancer* **120**, 407-423
5. Cuzick, J., Otto, F., Baron, J. A., Brown, P. H., Burn, J., Greenwald, P., Jankowski, J., La Vecchia, C., Meyskens, F., Senn, H. J., and Thun, M. (2009) Aspirin and non-steroidal anti-inflammatory drugs for cancer prevention: an international consensus statement. *Lancet Oncol* **10**, 501-507

6. Bindu, S., Mazumder, S., and Bandyopadhyay, U. (2020) Non-steroidal anti-inflammatory drugs (NSAIDs) and organ damage: A current perspective. *Biochem Pharmacol* **180**, 114147

7. Sostres, C., Gargallo, C. J., and Lanas, A. (2013) Nonsteroidal anti-inflammatory drugs and upper and lower gastrointestinal mucosal damage. *Arthritis Res Ther* **15 Suppl 3**, S3

8. Whittle, B. J. (2000) COX-1 and COX-2 products in the gut: therapeutic impact of COX-2 inhibitors. *Gut* **47**, 320-325

9. Gurpinar, E., Grizzle, W. E., and Piazza, G. A. (2014) NSAIDs inhibit tumorigenesis, but how? *Clin Cancer Res* **20**, 1104-1113

10. Liggett, J. L., Zhang, X., Eling, T. E., and Baek, S. J. (2014) Anti-tumor activity of non-steroidal anti-inflammatory drugs: cyclooxygenase-independent targets. *Cancer Lett* **346**, 217-224

11. Gurpinar, E., Grizzle, W. E., and Piazza, G. A. (2013) COX-Independent Mechanisms of Cancer Chemoprevention by Anti-Inflammatory Drugs. *Front Oncol* **3**, 181

12. Kolawole, O. R., and Kashfi, K. (2022) NSAIDs and Cancer Resolution: New Paradigms beyond Cyclooxygenase. *Int J Mol Sci* **23**

13. Matsui, H., Shimokawa, O., Kaneko, T., Nagano, Y., Rai, K., and Hyodo, I. (2011) The pathophysiology of non-steroidal anti-inflammatory drug (NSAID)-induced mucosal injuries in stomach and small intestine. *J Clin Biochem Nutr* **48**, 107-111

14. Sandoval-Acuna, C., Lopez-Alarcon, C., Aliaga, M. E., and Speisky, H. (2012) Inhibition of mitochondrial complex I by various non-steroidal anti-inflammatory drugs and its protection by quercetin via a coenzyme Q-like action. *Chem Biol Interact* **199**, 18-28

15. Krause, M. M., Brand, M. D., Krauss, S., Meisel, C., Vergin, H., Burmester, G. R., and Buttgereit, F. (2003) Nonsteroidal antiinflammatory drugs and a selective cyclooxygenase 2 inhibitor uncouple mitochondria in intact cells. *Arthritis Rheum* **48**, 1438-1444

16. Suzuki, Y., Inoue, T., and Ra, C. (2010) NSAIDs, Mitochondria and Calcium Signaling: Special Focus on Aspirin/Salicylates. *Pharmaceuticals (Basel)* **3**, 1594-1613

17. Aminzadeh-Gohari, S., Weber, D. D., Vidali, S., Catalano, L., Kofler, B., and Feichtinger, R. G. (2020) From old to new - Repurposing drugs to target mitochondrial energy metabolism in cancer. *Semin Cell Dev Biol* **98**, 211-223

18. Mazumder, S., Bindu, S., De, R., Debsharma, S., Pramanik, S., and Bandyopadhyay, U. (2022) Emerging role of mitochondrial DAMPs, aberrant mitochondrial dynamics and anomalous mitophagy in gut mucosal pathogenesis. *Life Sci* **305**, 120753

19. Mazumder, S., Barman, M., Bandyopadhyay, U., and Bindu, S. (2020) Sirtuins as endogenous regulators of lung fibrosis: A current perspective. *Life Sci* **258**, 118201

20. Murugasamy, K., Munjal, A., and Sundaresan, N. R. (2022) Emerging Roles of SIRT3 in Cardiac Metabolism. *Front Cardiovasc Med* **9**, 850340

21. Zhang, J., Xiang, H., Liu, J., Chen, Y., He, R. R., and Liu, B. (2020) Mitochondrial Sirtuin 3: New emerging biological function and therapeutic target. *Theranostics* **10**, 8315-8342

22. Kim, H. S., Patel, K., Muldoon-Jacobs, K., Bisht, K. S., Aykin-Burns, N., Pennington, J. D., van der Meer, R., Nguyen, P., Savage, J., Owens, K. M., Vassilopoulos, A., Ozden, O., Park, S. H., Singh, K. K., Abdulkadir, S. A., Spitz, D. R., Deng, C. X., and Gius, D. (2010) SIRT3 is a mitochondria-localized tumor suppressor required for maintenance of mitochondrial integrity and metabolism during stress. *Cancer Cell* **17**, 41-52

23. Morigi, M., Perico, L., Rota, C., Longaretti, L., Conti, S., Rottoli, D., Novelli, R., Remuzzi, G., and Benigni, A. (2015) Sirtuin 3-dependent mitochondrial dynamic improvements protect against acute kidney injury. *J Clin Invest* **125**, 715-726

24. Pillai, V. B., Samant, S., Sundaresan, N. R., Raghuraman, H., Kim, G., Bonner, M. Y., Arbiser, J. L., Walker, D. I., Jones, D. P., Gius, D., and Gupta, M. P. (2015) Honokiol blocks and reverses cardiac hypertrophy in mice by activating mitochondrial SIRT3. *Nat Commun* **6**, 6656

25. Sun, R., Kang, X., Zhao, Y., Wang, Z., Wang, R., Fu, R., Li, Y., Hu, Y., Wang, Z., Shan, W., Zhou, J., Tian, X., and Yao, J. (2020) Sirtuin 3-mediated deacetylation of acyl-CoA synthetase family member 3 by protocatechuic acid attenuates non-alcoholic fatty liver disease. *Br J Pharmacol* **177**, 4166-4180

26. Mao, R. W., He, S. P., Lan, J. G., and Zhu, W. Z. (2022) Honokiol ameliorates cisplatin-induced acute kidney injury via inhibition of mitochondrial fission. *Br J Pharmacol* **179**, 3886-3904

27. Bindu, S., Mazumder, S., Dey, S., Pal, C., Goyal, M., Alam, A., Iqbal, M. S., Sarkar, S., Azhar Siddiqui, A., Banerjee, C., and Bandyopadhyay, U. (2013) Nonsteroidal anti-inflammatory drug induces proinflammatory damage in gastric mucosa through NF-kappaB activation and neutrophil infiltration: anti-inflammatory role of heme oxygenase-1 against nonsteroidal anti-inflammatory drug. *Free Radic Biol Med* **65**, 456-467

28. Mazumder, S., De, R., Debsharma, S., Bindu, S., Maity, P., Sarkar, S., Saha, S. J., Siddiqui, A. A., Banerjee, C., Nag, S., Saha, D., Pramanik, S., Mitra, K., and Bandyopadhyay, U. (2019) Indomethacin impairs mitochondrial dynamics by activating the PKCzeta-p38-DRP1 pathway and inducing apoptosis in gastric cancer and normal mucosal cells. *J Biol Chem* **294**, 8238-8258

29. Mazumder, S., De, R., Sarkar, S., Siddiqui, A. A., Saha, S. J., Banerjee, C., Iqbal, M. S., Nag, S., Debsharma, S., and Bandyopadhyay, U. (2016) Selective scavenging of intra-mitochondrial superoxide corrects diclofenac-induced mitochondrial dysfunction and gastric injury: A novel gastroprotective mechanism independent of gastric acid suppression. *Biochem Pharmacol* **121**, 33-51

30. Maharani, B. (2022) Screening Methods for the Evaluation of Antiulcer Drugs. in *Introduction to Basics of Pharmacology and Toxicology* (Mageshwaran Lakshmanan, D. G. S., Gerard Marshall Raj ed.). pp 371-382

31. Syed Safiullah Ghori , M. F. A. S. S. (2016) ANTIULCER POTENTIAL OF FICUS DALHOUSIAE STEM BARK METHANOLIC EXTRACT IN ALBINO RATS. *INDO AMERICAN JOURNAL OF PHARMACEUTICAL SCIENCES*

32. Raghavendran, H. R., Srinivasan, P., and Rekha, S. (2011) Immunomodulatory activity of fucoidan against aspirin-induced gastric mucosal damage in rats. *Int Immunopharmacol* **11**, 157-163

33. Wang, J., Zhai, T., and Chen, Y. (2018) Effects of Honokiol on CYP450 Activity and Transporter mRNA Expression in Type 2 Diabetic Rats. *Int J Mol Sci* **19**

34. Andrews, S. (2010) FastQC: A Quality Control Tool for High Throughput Sequence Data [Online]. *. Available online at: http://www.bioinformatics.babraham.ac.uk/projects/fastqc/*

35. Martin, M. (2011) Cutadapt Removes Adapter Sequences from High-Throughput Sequencing Reads. *EMBnet Journal* **17**, 10-12

36. Pertea, M., Kim, D., Pertea, G. M., Leek, J. T., and Salzberg, S. L. (2016) Transcript-level expression analysis of RNA-seq experiments with HISAT, StringTie and Ballgown. *Nature Protocols* **11**, 1650-1667

37. Li, H., Handsaker, B., Wysoker, A., Fennell, T., Ruan, J., Homer, N., Marth, G., Abecasis, G., Durbin, R., and Subgroup, G. P. D. P. (2009) The Sequence Alignment/Map format and SAMtools. *Bioinformatics* **25**, 2078-2079

38. Liao, Y., Smyth, G. K., and Shi, W. (2014) featureCounts: an efficient general purpose program for assigning sequence reads to genomic features. *Bioinformatics* **30**, 923-930

39. Love, M. I., Huber, W., and Anders, S. (2014) Moderated estimation of fold change and dispersion for RNA-seq data with DESeq2. *Genome Biology* **15**, 550

40. Alexander, S. P. H., Roberts, R. E., Broughton, B. R. S., Sobey, C. G., George, C. H., Stanford, S. C., Cirino, G., Docherty, J. R., Giembycz, M. A., Hoyer, D., Insel, P. A., Izzo, A. A., Ji, Y., MacEwan, D. J., Mangum, J., Wonnacott, S., and Ahluwalia, A. (2018) Goals and practicalities of immunoblotting and immunohistochemistry: A guide for submission to the British Journal of Pharmacology. *Br J Pharmacol* **175**, 407-411

41. De, R., Mazumder, S., Sarkar, S., Debsharma, S., Siddiqui, A. A., Saha, S. J., Banerjee, C., Nag, S., Saha, D., and Bandyopadhyay, U. (2017) Acute mental stress induces mitochondrial bioenergetic crisis and hyper-fission along with aberrant mitophagy in the gut mucosa in rodent model of stress-related mucosal disease. *Free Radic Biol Med* **113**, 424-438

42. Dey, S., Mazumder, S., Siddiqui, A. A., Iqbal, M. S., Banerjee, C., Sarkar, S., De, R., Goyal, M., Bindu, S., and Bandyopadhyay, U. (2014) Association of heme oxygenase 1 with the restoration of liver function after damage in murine malaria by Plasmodium yoelii. *Infect Immun* **82**, 3113-3126

43. Bindu, S., Pillai, V. B., Kanwal, A., Samant, S., Mutlu, G. M., Verdin, E., Dulin, N., and Gupta, M. P. (2017) SIRT3 blocks myofibroblast differentiation and pulmonary fibrosis by preventing mitochondrial DNA damage. *Am J Physiol Lung Cell Mol Physiol* **312**, L68-L78

44. Carrasco-Pozo, C., Gotteland, M., and Speisky, H. (2011) Apple peel polyphenol extract protects against indomethacin-induced damage in Caco-2 cells by preventing mitochondrial complex I inhibition. *J Agric Food Chem* **59**, 11501-11508

45. Spinazzi, M., Casarin, A., Pertegato, V., Salviati, L., and Angelini, C. (2012) Assessment of mitochondrial respiratory chain enzymatic activities on tissues and cultured cells. *Nat Protoc* **7**, 1235-1246

46. Curtis, M. J., Alexander, S., Cirino, G., Docherty, J. R., George, C. H., Giembycz, M. A., Hoyer, D., Insel, P. A., Izzo, A. A., Ji, Y., MacEwan, D. J., Sobey, C. G., Stanford, S. C., Teixeira, M. M., Wonnacott, S., and Ahluwalia, A. (2018) Experimental design and analysis and their reporting II: updated and simplified guidance for authors and peer reviewers. *Br J Pharmacol* **175**, 987-993

47. Bader, G. D., and Hogue, C. W. (2003) An automated method for finding molecular complexes in large protein interaction networks. *BMC bioinformatics* **4**, 2

48. Shannon, P., Markiel, A., Ozier, O., Baliga, N. S., Wang, J. T., Ramage, D., Amin, N., Schwikowski, B., and Ideker, T. (2003) Cytoscape: a software environment for integrated models of biomolecular interaction networks. *Genome research* **13**, 2498-2504

49. Rock, K. L., and Kono, H. (2008) The inflammatory response to cell death. *Annu Rev Pathol* **3**, 99-126

50. Li, L., Hu, M., Wang, T., Chen, H., and Xu, L. (2019) Repositioning Aspirin to Treat Lung and Breast Cancers and Overcome Acquired Resistance to Targeted Therapy. *Front Oncol* **9**, 1503

51. Kumar, R. (2016) Repositioning of Non-Steroidal Anti Inflammatory Drug (NSAIDs) for Cancer Treatment: Promises and Challenges. *Journal of Nanomedicine & Nanotechnology* **7**

52. Sherin, F., Gomathy, S., and Antony, S. (2021) Sirtuin3 in Neurological Disorders. *Curr Drug Res Rev* **13**, 140-147

53. Wu, J., Zeng, Z., Zhang, W., Deng, Z., Wan, Y., Zhang, Y., An, S., Huang, Q., and Chen, Z. (2019) Emerging role of SIRT3 in mitochondrial dysfunction and cardiovascular diseases. *Free Radic Res* **53**, 139-149

54. Peng, M. L., Fu, Y., Wu, C. W., Zhang, Y., Ren, H., and Zhou, S. S. (2022) Signaling Pathways Related to Oxidative Stress in Diabetic Cardiomyopathy. *Front Endocrinol (Lausanne)* **13**, 907757

55. Dittenhafer-Reed, K. E., Richards, A. L., Fan, J., Smallegan, M. J., Fotuhi Siahpirani, A., Kemmerer, Z. A., Prolla, T. A., Roy, S., Coon, J. J., and Denu, J. M. (2015) SIRT3 mediates multi-tissue coupling for metabolic fuel switching. *Cell Metab* **21**, 637-646

56. Timmons, J., Chang, E. T., Wang, J. Y., and Rao, J. N. (2012) Polyamines and Gut Mucosal Homeostasis. *J Gastrointest Dig Syst* **2**

57. Liu, J., Li, D., Zhang, T., Tong, Q., Ye, R. D., and Lin, L. (2017) SIRT3 protects hepatocytes from oxidative injury by enhancing ROS scavenging and mitochondrial integrity. *Cell Death Dis* **8**, e3158

58. Valavanidis, A., Vlachogianni, T., and Fiotakis, C. (2009) 8-hydroxy-2' -deoxyguanosine (8-OHdG): A critical biomarker of oxidative stress and carcinogenesis. *J Environ Sci Health C Environ Carcinog Ecotoxicol Rev* **27**, 120-139

59. Kincaid, B., and Bossy-Wetzel, E. (2013) Forever young: SIRT3 a shield against mitochondrial meltdown, aging, and neurodegeneration. *Front Aging Neurosci* **5**, 48

60. Merksamer, P. I., Liu, Y., He, W., Hirschey, M. D., Chen, D., and Verdin, E. (2013) The sirtuins, oxidative stress and aging: an emerging link. *Aging (Albany NY)* **5**, 144-150

61. Sundaresan, N. R., Gupta, M., Kim, G., Rajamohan, S. B., Isbatan, A., and Gupta, M. P. (2009) SIRT3 blocks the cardiac hypertrophic response by augmenting Foxo3a-dependent antioxidant defense mechanisms in mice. *J Clin Invest* **119**, 2758-2771

62. Kim, Y., and Park, C. W. (2019) Mechanisms of Adiponectin Action: Implication of Adiponectin Receptor Agonism in Diabetic Kidney Disease. *Int J Mol Sci* **20**

63. Austin, S., and St-Pierre, J. (2012) PGC1alpha and mitochondrial metabolism--emerging concepts and relevance in ageing and neurodegenerative disorders. *J Cell Sci* **125**, 4963-4971

64. Fasano, C., Disciglio, V., Bertora, S., Lepore Signorile, M., and Simone, C. (2019) FOXO3a from the Nucleus to the Mitochondria: A Round Trip in Cellular Stress Response. *Cells* **8**

65. Olmos, Y., Valle, I., Borniquel, S., Tierrez, A., Soria, E., Lamas, S., and Monsalve, M. (2009) Mutual dependence of Foxo3a and PGC-1alpha in the induction of oxidative stress genes. *J Biol Chem* **284**, 14476-14484

66. Meng, H., Yan, W. Y., Lei, Y. H., Wan, Z., Hou, Y. Y., Sun, L. K., and Zhou, J. P. (2019) SIRT3 Regulation of Mitochondrial Quality Control in Neurodegenerative Diseases. *Front Aging Neurosci* **11**, 313

67. Pillai, V. B., Kanwal, A., Fang, Y. H., Sharp, W. W., Samant, S., Arbiser, J., and Gupta, M. P. (2017) Honokiol, an activator of Sirtuin-3 (SIRT3) preserves mitochondria and protects the heart from doxorubicin-induced cardiomyopathy in mice. *Oncotarget* **8**, 34082-34098

68. Wang, J., Nisar, M., Huang, C., Pan, X., Lin, D., Zheng, G., Jin, H., Chen, D., Tian, N., Huang, Q., Duan, Y., Yan, Y., Wang, K., Wu, C., Hu, J., Zhang, X., and Wang, X. (2018) Small molecule natural compound agonist of SIRT3 as a therapeutic target for the treatment of intervertebral disc degeneration. *Exp Mol Med* **50**, 1-14

69. Liu, Q., Zhang, D., Hu, D., Zhou, X., and Zhou, Y. (2018) The role of mitochondria in NLRP3 inflammasome activation. *Mol Immunol* **103**, 115-124

70. Atanasov, A. G., Wang, J. N., Gu, S. P., Bu, J., Kramer, M. P., Baumgartner, L., Fakhrudin, N., Ladurner, A., Malainer, C., Vuorinen, A., Noha, S. M., Schwaiger, S., Rollinger, J. M., Schuster, D., Stuppner, H., Dirsch, V. M., and Heiss, E. H. (2013) Honokiol: a non-adipogenic PPARgamma agonist from nature. *Biochim Biophys Acta* **1830**, 4813-4819

71. Saha, L. (2015) Role of peroxisome proliferator-activated receptors alpha and gamma in gastric ulcer: An overview of experimental evidences. *World J Gastrointest Pharmacol Ther* **6**, 120-126

72. Kosgei, V. J., Coelho, D., Gueant-Rodriguez, R. M., and Gueant, J. L. (2020) Sirt1-PPARS Cross-Talk in Complex Metabolic Diseases and Inherited Disorders of the One Carbon Metabolism. *Cells* **9**

73. Yi, X., Guo, W., Shi, Q., Yang, Y., Zhang, W., Chen, X., Kang, P., Chen, J., Cui, T., Ma, J., Wang, H., Guo, S., Chang, Y., Liu, L., Jian, Z., Wang, L., Xiao, Q., Li, S., Gao, T., and Li, C. (2019) SIRT3-Dependent Mitochondrial Dynamics Remodeling Contributes to Oxidative Stress-Induced Melanocyte Degeneration in Vitiligo. *Theranostics* **9**, 1614-1633

74. Ramesh, S., Govindarajulu, M., Lynd, T., Briggs, G., Adamek, D., Jones, E., Heiner, J., Majrashi, M., Moore, T., Amin, R., Suppiramaniam, V., and Dhanasekaran, M. (2018) SIRT3 activator Honokiol attenuates beta-Amyloid by modulating amyloidogenic pathway. *PLoS One* **13**, e0190350

75. Quan, Y., Park, W., Jin, J., Kim, W., Park, S. K., and Kang, K. P. (2020) Sirtuin 3 Activation by Honokiol Decreases Unilateral Ureteral Obstruction-Induced Renal Inflammation and Fibrosis via Regulation of Mitochondrial Dynamics and the Renal NF-kappaBTGF-beta1/Smad Signaling Pathway. *Int J Mol Sci* **21**

76. Martinsen, T. C., Bergh, K., and Waldum, H. L. (2005) Gastric juice: a barrier against infectious diseases. *Basic Clin Pharmacol Toxicol* **96**, 94-102

77. Maffei, M., Desmeules, J., Cereda, J. M., and Hadengue, A. (2007) [Side effects of proton pump inhibitors (PPIs)]. *Rev Med Suisse* **3**, 1934-1936, 1938

78. (2012) Histamine Type-2 Receptor Antagonists (H2 Blockers). in *LiverTox: Clinical and Research Information on Drug-Induced Liver Injury*, Bethesda (MD). pp

79. Eusebi, L. H., Rabitti, S., Artesiani, M. L., Gelli, D., Montagnani, M., Zagari, R. M., and Bazzoli, F. (2017) Proton pump inhibitors: Risks of long-term use. *J Gastroenterol Hepatol* **32**, 1295-1302

80. Sarrica, A., Kirika, N., Romeo, M., Salmona, M., and Diomede, L. (2018) Safety and Toxicology of Magnolol and Honokiol. *Planta Med* **84**, 1151-1164

81. Ouyang, S., Zhang, Q., Lou, L., Zhu, K., Li, Z., Liu, P., and Zhang, X. (2022) The Double-Edged Sword of SIRT3 in Cancer and Its Therapeutic Applications. *Front Pharmacol* **13**, 871560

82. Dikalova, A. E., Pandey, A., Xiao, L., Arslanbaeva, L., Sidorova, T., Lopez, M. G., Billings, F. T. t., Verdin, E., Auwerx, J., Harrison, D. G., and Dikalov, S. I. (2020) Mitochondrial Deacetylase SIRT3 Reduces Vascular Dysfunction and Hypertension While SIRT3 Depletion in Essential Hypertension Is Linked to Vascular Inflammation and Oxidative Stress. *Circ Res* **126**, 439-452

83. Bugga, P., Alam, M. J., Kumar, R., Pal, S., Chattopadyay, N., and Banerjee, S. K. (2022) SIRT3 ameliorates mitochondrial dysfunction and oxidative stress through regulating mitochondrial biogenesis and dynamics in cardiomyoblast. *Cell Signal* **94**, 110309

NSAID, by targeting SIRT3, arrests gastric cancer cell growth through inducing mitochondrial proteome hyperacetylation and disrupting fission-fusion homeostasis

1. INTRODUCTION

Non-steroidal anti-inflammatory drugs (NSAIDs) are among the most popular over-the-counter medications enjoying a blockbuster status ever since their discovery as a result of their wide range of therapeutic benefits and growing clinical usefulness spectrum (1). The previous chapter elegantly dealt with the molecular intricacies underlying the pathogenesis of NSAID-induced gastric mucosal injury and ulceration, wherein the role of SIRT3 as a novel endogenous gastroprotective factor has been identified and validated for the first time in a *non-malignant in vivo* model of experimental gastropathy. However, owing to the anti-cancer attributes of NSAIDs, quest for identifying their precise mode of anti-neoplastic action is ever-increasing so that these wonder drugs can be more efficiently used against drug-resistant tumors and more specifically cancer stem cells which are the biggest factors for treatment failure and recurrence. Clinical researchers, through drug repurposing studies, have identified the merits of NSAIDs as promising adjuvants in anti-cancer chemotherapy (2). In addition, it is also noteworthy that patients/elderly people who have been taking NSAIDs for a long time have a relatively decreased chance of acquiring neoplasia. Additionally, using NSAIDs for a brief period after surgery has been found to help cancer patients live longer and remain disease-free (3). While the anti-angiogenic and anti-cancer properties of NSAIDs are typically linked to COX inhibition, there is mounting evidence that NSAIDs also have direct cytotoxic effects on mitochondria. Moreover, the anti-cancer effects of NSAIDs are realized at a much higher dose than required for COX suppression (4,5). But is spite of these cardinal indications, precise sub-mitochondrial targets of NSAIDs responsible for blocking cancer cell proliferation and inducing apoptosis are yet elusive.

Cancer cells' mitochondrial DNA (mtDNA) are extremely vulnerable to oxidative genotoxic stress caused by anti-cancer medications (6). The primary mitochondrial proteins that prevent oxidative damage, 8-oxoguanine DNA glycosylase (OGG1) and superoxide dismutase 2 (SOD2), are controlled by deacetylation-dependent stabilization (7). Deacetylation also controls a variety of proteins that are involved in glycolysis, TCA cycle, lipid and amino acid metabolism and redox homeostasis. Further, regulators of mitochondrial biogenesis, mitochondrial dynamics, mitochondrial permeability transition pore (mPTP), and elements of the electron transport chain (ETC) are also known to be regulated by acetylation-deacetylation (8). All these signify the importance of protein deacetylation in regulating cellular metabolism and pathogenesis. Incidentally, cancer is strongly linked to the longevity-promoting NAD^+-dependent mitochondrial deacetylase sirtuin 3 (SIRT3) (9). Notably, gastric cancer (GC) is a deadly malignancy with a poor 5-year overall survival rate and is in fact the 4th most prevalent cause of cancer fatalities accounting to 7.7% of all cancer deaths (10-11). Due to intra-tumoral molecular heterogeneity and complicated etiology, therapy options for advanced-stage GC are largely insufficient despite significant advancements in experimental and clinical anti-cancer research (12). Therefore, it is necessary to comprehend the pathological basis as well as venture effective anti-GC strategies. This brings the NSAIDs to the limelight as their anti-GC actions are poorly recognized. It has been discretely observed that NSAIDs exert mitotoxic effects on GC cells (13), but it is yet unknown whether the toxic effect of NSAIDs specifically involves SIRT3 signaling to induce cancer cell death.

In the present chapter, differential gene expression profiling of control and indomethacin-treated human gastric adenocarcinoma (AGS) cells has been done using next-generation transcriptome sequencing. Subsequently, meta-analysis of TCGA and HPA datasets was done to check the relevance of SIRT3 in GC prognosis. Putative direct interaction of SIRT3 and indomethacin as well as the nature of the interaction, *per se*, was checked by molecular dynamic simulation and deacetylase activity assay using increasing concentrations of indomethacin. The leads obtained in the observational experiments were functionally validated using specific siRNAs targeting SIRT3 as well as its upstream regulators like PGC1α and ERRα by diverse metabolic and biochemical assays in addition to gene and protein

expression analyses, high-resolution confocal imaging and flow cytometry. The transfected cells were exposed to indomethacin followed by an evaluation of molecular targets controlling mitochondrial integrity, mitochondrial dynamics, biogenesis, mitophagy and cell death in specific regards to the SIRT3 signaling axis. It was checked whether SIRT3 or PGC1α/ERRα silencing aggravated or toned down the toxic effects of indomethacin. In addition to indomethacin other popular NSAIDs used for human treatment purposes like ibuprofen, diclofenac, and aspirin were also checked for putative SIRT3 targeting for inducing cancer cell death. Finally, it was checked whether the anti-proliferative effect of indomethacin on other cancer cells like hepatocellular, colorectal and cervical carcinoma at all involved SIRT3 as a common process.

2. MATERIALS AND METHODS

2.1. Reagents

Indomethacin (Cat# I7378), diclofenac (Cat# D6899), ibuprofen (Cat# I1892), aspirin (Cat# A2093), RNase ZAP (Cat# 83930), 3-(4,5-dimethylthiazol-2-yl)-2,5-diphenyltetrazolium bromide (MTT) (Cat# CT01-5), DMSO (Cat# 276855), were procured from Sigma-Aldrich (St Louis, MO, USA). The TRIzol (Cat# 15596026), PureLink RNA Mini Kit (Cat# 12183018A), RevertAid H Minus First Strand cDNA Synthesis kit (Cat# 18091050), ATP Determination Kit (Cat#A22066), Lipofectamine RNAiMAX (Cat# 13778150), JC-1 dye (Cat# T3168), Nuclease-free water (Cat# AM9937), and PBS (Cat# 10010031) were purchased from Thermo Fisher Scientific. Mitochondria Isolation Kit (Cat# KC010100) was purchased from BioChain (Newark, USA). HT 8-oxo-dG ELISA Kit II (Cat# 4380-096-K) was procured from Trevigen (Maryland, USA) Luminata forte western HRP substrate (Cat# WBLUF0500) for ECL-based chemiluminescence, were procured from Merck Millipore (Massachusetts, USA). Sirt3 activity assay kit (Fluorometric) (Cat# ab156067), Superoxide Dismutase Activity Assay Kit (Colorimetric) (Cat# ab65354), Mitochondrial DNA Isolation Kit (Cat# ab65321) were procured from Abcam (Boston, USA). Nutrient Mixture F-12 Ham, Kaighn's Modification (Cat# AL106A), Dulbecco's Modified Eagle Medium (DMEM), High glucose (Cat# AL007S) were purchased from HIMEDIA (Maharashtra India). Opti-MEM™ Reduced Serum Medium (Cat# 31985070) was procured from Gibco. All other reagents were of analytical grade purity. siRNA for SIRT3 (Cat# sc-61555), PGC1α (Cat# sc-38884) and ERRα (Cat# sc-44706) were purchased from Santa Cruz Biotechnology (Texas, USA).

2.2. Cell culture and NSAIDs treatment

HeLa (human cervical adenocarcinoma, ATCC-CRM-CCL-2) and HCT116 (human colorectal carcinoma, ATCC-CCL-247) were kindly gifts from Dr. Kaushik Biswas. AGS cells (human gastric carcinoma cells, ATCC-CRL-1739), HepG2 (human hepatocellular carcinoma cells, ATCC HB-8065), and HCT116 (human colorectal carcinoma, ATCC-CCL (Bose Institute, India). Cells were grown as previously reported (14). Briefly stated, HepG2, HCT-116, and HeLa were cultured in DMEM whereas AGS cells were maintained in F-12 Ham-modification Kaighn's medium. Fetal bovine serum was added as a 10% addition to the culture medium. The cells were maintained at 37 °C in an incubator with 5% CO_2. Cells were divided by trypsinization once every three days. For the experiment, cells were plated at a density of $1X10^6$ and let to grow for a whole night before the fresh medium was added for the treatment. To test the impact on cell survival using a dehydrogenase activity assay, cells were exposed to escalating doses of NSAIDs. For protein expression profiling and transcriptome analysis, cells were treated with an indomethacin sublethal dosage of 0.5 mM (obtained via a viability experiment) to observe the drug's modest effects on cellular metabolism. Alkaline distilled water was used to dissolve indomethacin. In distilled water, ibuprofen and diclofenac were dissolved. DMSO was used to dissolve aspirin. The final DMSO concentration used to treat the cells was kept constant at 0.1%. Cells were

treated with diclofenac (0.5 mM), ibuprofen (2.5 mM), and aspirin (8 mM) for the SIRT3 expression profile and cell viability experiments. The studies were conducted thrice in each situation.

2.3. Cell viability assay and phase contrast microscopy for detecting cytoarchitecture

Based on the previously reported 3-(4,5-dimethylthiazol-2-yl)-2,5- diphenyl tetrazolium bromide (MTT) reduction test, cellular dehydrogenase activity was assessed to assess the vitality of AGS cells (14). In a nutshell, AGS cells were seeded in 48-well culture plates at an identical density, and allowed to grow to 60–70% confluence before being treated with NSAIDs. Following the NSAID treatment period, the cells were incubated with MTT (1 mg/mL) in PBS for 3.5 hours at 37°C with 5% CO_2, and the purple formazan was then dissolved in anhydrous DMSO. At 570 nm, the optical density was determined spectrophotometrically. After treatment, cells were washed in pre-warmed PBS and examined using an inverted phase contrast microscope to perform live cell phase contrast imaging (Leica Microsystems). A representative image has been provided, and at least five independent fields were randomly selected. Each experiment was conducted thrice.

2.4. Next-generation sequencing-based transcriptomics

Utilizing Illumina's TruSeq Stranded Total RNA Library preparation kit, total RNA sequencing libraries are created. In a nutshell, total RNA was extracted from AGS cells using Thermo's PureLink RNA Mini Kit according to the manufacturer's instructions. There were 10^7 cells per sample as the starting point. Thermo's Nanodrop 2000 and Agilent's 2100 Bioanalyzer were used to test the purity and concentration of the extracted RNA samples. Following that, samples with RIN 7.0 were utilized for library preparation. The kit's Ribo-Zero Human/Mouse/Rat depletion module was used to first deplete ribosomal RNA from an identical amount (200 ng) of RNA from each sample. This was followed by purification and divalent cation-based fragmentation. The resultant fragments underwent cDNA synthesis, A-tailing, and dual index adapter ligation after being purified. The products were then PCR enhanced and purified. The resultant RNA libraries underwent equimolar pooling, quantification, normalization, and check in Agilent 2200 TapeStation (Agilent Technologies). Finally, 100 bp paired-end massively parallel sequencing of the pooled libraries was performed on the Novaseq 6000 sequencer using a sequencing run flow cell (Illumina). The resulting Bcl files were converted to Fastq files, and FastQC v.0.11.7 was used to perform a quality check on the data (15). The Illumina Universal Adapter was then used to trim the adapter using Cutadapt v1.16(16). The trimmed reads were aligned with the Homo sapiens (human) genome assembly GRCh38 using Hisat2 2.1.0. (17). (hg38 for AGS cells). Samtools v1.19 was used to sort the Bam files (18). Gene counting was then carried out using Feature Counts (19), and differential analysis was carried out using DESeq2 (20). Filtering was done on differentially expressed genes having an expression change of 1.5 or more-fold, a p value of 0.05, and an FDR of 0.05. IPA (Ingenuity Pathway Analysis) software was then used to undertake gene enrichment and pathway analysis. To include genes affecting mitochondrial metabolism and functions, data for rat stomach mucosal samples were additionally filtered using or 1.2-fold expression change, p value, and FDR cut-off of 0.05 The sequencing was done three times. Transcriptomic data's GEO accession number is GSE202140.

2.5. SIRT3 expression analysis in human samples

Using the previously stated UALCAN, HPA, and KM plotter database analysis tools, SIRT3 expression in individual stomach samples from stomach adenocarcinoma (STAD) patients and normal samples was assessed (21). SIRT3 expression data from TCGA normal and STAD primary tumors were mined using UALCAN (http://ualcan.path.uab.edu) analysis. Transcripts per million served as a measure of the data. Multiple factors were considered when evaluating differential SIRT3 expression, including

Table 1: List of primer sequences used in q-RT-PCR reaction

Genes		Primer sequence (Human)	Annealing temperature
mt-ND1	FP	5'-CCACCTCTAGCCTAGCCGTTT-3'	52˚C
	RP	5'-GGGTCATGATGGCAGGAGTAAT-3'	
mt-ND6	FP	5'-CAAACAATGTTCAACCAGTAACCACTAC-3'	52˚C
	RP	5'-ATATACTACAGCGATGGCTATTGAGGA-3'	
mt-CO1	FP	5'-GACGTAGACACACGAGCATATTTCA-3'	52˚C
	RP	5'-AGGACATAGTGGAAGTGAGCTACAAC-3'	
mt-ATP6	FP	5'-TAGCCATACACAACACTAAAGGACGA-3'	52˚C
	RP	5'-GGGCATTTTTAATCTTAGAGCGAAA-3'	
mt-CYT-B	FP	5'-ATCACTCGAGACGTAAATTATGGCT-3'	52˚C
	RP	5'-TGAACTAGGTCTGTCCCAATGTATG-3'	
SIRT3	FP	5'-AGAAGAGATGCGGGACCTTG-3'	52˚C
	RP	5'-GGTCCATCAAGCCTAGAGCAG-3'	
GAPDH	FP	5'-CCTCAACTACATGGTTTACA-3'	52˚C
	RP	5'-CTCCTGGAAGATGGTGAT-3'	

sample types (normal, n=34, and primary tumour, n=415), individual cancer stages (stage 1, n=18, stage 2, n=123, stage 3, n=169, and stage 4, n=41), and histological subtypes (adenocarcinoma NOS, n=155, adenocarcinoma diffuse, n=69, adenocarcinoma). SIRT3 expression was evaluated in individual stomach samples from stomach adenocarcinoma (STAD) patients and normal samples using the aforementioned UALCAN, HPA, and KM plotter database analysis methods (21). Utilizing UALCAN analysis, SIRT3 expression data from TCGA normal and STAD primary tumors were mined. The data were measured in transcripts per million. Individual cancer stages (stage 1, n=18, stage 2, n=123, stage 3, n=169, and stage 4) and histological subtypes (adenocarcinoma NOS, n=155, adenocarcinoma diffuse, n=69, and adenocarcinoma, n=41) were also taken into account when examining differential SIRT3 expression. Kaplan-Meier Plotter Database Analysis (http://kmplot.com/analysis/) was used to determine the prognostic importance of SIRT3 concerning GC survival (22). To determine the odds of overall survival (OS) associated with low and high SIRT3 expressions, the KM plotter for Gastric Cancer module was utilized. It has been determined that a hazard ratio (HR) with a 95% confidence interval and a p value of 0.05 is statistically significant. SIRT3's Affy id/Gene symbol was 221913, and 875 patient sample data were used in the analysis. The survival plot in the figure's inset showed the median survival values for cohorts with low and high SIRT3 expression levels. The OGG1 Affy ID/Gene symbol is 205760 s at, and the same parameters were used for Kaplan-Meier Plotter OS analysis of the OGG1 low and high expression cohorts.

2.6. RNA isolation and real-time RT-PCR
Following the manufacturer's instructions, total RNA was extracted using TRIzol (Invitrogen, Carlsbad, CA) and quantified using a Maestrogen nano Spectrophotometer (Life Teb Gen co, Tehran-Iran). Utilizing Thermo's RevertAid H Minus first strand cDNA synthesis kit, obtained total RNA (2 μg)) was reverse transcribed using an oligo-dT18 primer. This was followed by rDNAse treatment. After suitable dilution, the generated cDNAs were utilized for qPCR using primers from Integrated DNA Technologies Inc (Table 1). The qPCR was conducted using a Roche LightCycler 96 qPCR equipment and SYBR green master mix under the following cycle conditions: initially denaturing at 95°C for 10 minutes, then denaturing at 72°C for 15 seconds for 40 cycles, then annealing for 30 seconds at the given annealing temperatures (Table 1). And then extension at 72°C for 25 sec. As previously noted,

relative gene expression was determined using the $2^{-\Delta\Delta Cq}$ calculation, and the results were reported as a fold relative to control. The internal control employed was Gapdh.

2.7. Immunoblot analysis

Total protein was extracted from AGS cells using pre-chilled mammalian cell lysis buffer for immunoblot analysis (supplemented with protease and phosphatase inhibitors). Using a commercial kit from Biochain, mitochondria were extracted from AGS cells. Isolated mitochondria were lysed in the cell lysis buffer with the addition of nicotinamide (50 mM) and trichostatin A (10 µM) to examine the acetylation of mitochondrial proteins. By using Lowry's technique for protein quantification, identical amounts of proteins were combined with SDS loading buffer and resolved in 10% polyacrylamide-SDS gels. The resolved proteins were then electroblotted and transferred to a nitrocellulose membrane (0.22 µM). The membrane was blocked using either 5% skim milk or 5% BSA solution, which was then followed by overnight incubation with primary antibodies (Table 2). The blots were then incubated in an HRP-conjugated secondary antibody for two hours at room temperature after being rinsed in TBS solution with 0.1% Tween 20 added. Finally, the blots were washed, and the Bio-Rad Chemidoc system created immuno-reactive bands. Every blot was cleaned using stripping buffer (Cat#T7135A, TAKARA), then it was re-probed to ensure that the loading controls for total protein and mitochondrial protein, respectively, ACTIN and TOM20, had been applied. Using ImageJ software, densitometric analyses were performed, and findings were shown as fold changes relative to control. The experiments were carried out three times in each case.

2.8. Isolation of mitochondria

Mitochondria were isolated from cells using a BioChain mitochondria isolation kit according to the manufacturer's instructions. Briefly, mitochondria were isolated from 2×10^8 AGS cells each from a different experimental set. In a Dounce homogenizer set up on ice, each sample was gently homogenized. The samples were then centrifuged at 600 g for 10 min to remove the cell fragments and nuclei. The mitochondrial fraction was obtained by collecting the supernatant and centrifuging it once more at 12,000 g for 15 min. The respiratory chain complex and dehydrogenase tests or lysing for immunoblotting, if necessary, were performed using the resulting pellets (about 99% pure), which were obtained after the mitochondrial pellets were rinsed three times in the mitochondria separation buffer. The studies were conducted three times in each situation.

2.9. Isolation of mitochondrial DNA and measurement of 8-oxo-dG by ELISA

Using the phenol-chloroform technique, the DNA from the isolated mitochondrial pellets from AGS cells was extracted. In a nutshell, the mitochondrial pellet was resuspended in 100 µL of lysis solution supplemented with Proteinase K and incubated at 50°C for 3 hours before being added to and well mixed with 200 µL of phenol-chloroform. To separate the phases, the contents were centrifuged at 10,000 rpm. After collecting the aqueous phase, 500 mL of ethanol and 200 mL of 7.5 µM ammonium acetate were added. For two hours, the tubes were held at -20°C. The samples were then centrifuged for 30 minutes at 10,000 g. The pellets were then cleaned with 500 µL of 70% ethanol before being dissolved in 30 µL of TB buffer. Using spectrophotometry, the mtDNA was estimated. After that, identical amounts of mtDNA from each experimental set were obtained for 8-oxo-dG quantification via ELISA utilizing a commercially available HT 8-oxo-dG ELISA Kit II from Trevigen. The studies were conducted three times in each situation.

Table 2: List of antibodies used for immunoblotting and immunofluorescent studies

Antibodies	Supplier	Species	Catalog number	RRID
Sirt3	Cell Signaling Technology	Rabbit	2627	AB_2188622
OGG1	Novus Biologicals	Rabbit	NB100-106	AB_10104097
PGC1α	Abcam	Rabbit	Ab54481	AB_881987
ERRα	Cell Signaling Technology	Rabbit	13826	AB_2750873
Acetylated lysine	Cell Signaling Technology	Rabbit	9814	AB_10544700
Acetylated OGG1	Abcam	Rabbit	ab93670	AB_10562267
Acetylated SOD2	Abcam	Rabbit	Ab137037	AB_2784527
Phospho-DRP1 (Ser637)	Cell Signaling Technology	Rabbit	4867	AB_10622027
pAMPKα	Abcam	Rabbit	ab133448	AB_2923300
AMPK	Abcam	Rabbit	ab32047	AB_722764
Parkin	Sigma	Mouse	P6248	AB_477384
PINK1	Novus Biologicals	Rabbit	BC100-494	AB_10127658
TOM20	Santa Cruz Biotechnology	Rabbit	sc-11415	AB_2207533
Cleaved Caspase 9	Cell Signaling Technology	Rabbit	9505	AB_2290727
Bax	Santa Cruz Biotechnology	Mouse	sc-7480	AB_626729
Cytochrome C	Abcam	Rabbit	ab53056	AB_869315
Bcl-xL	Cell Signaling Technology	Rabbit	2764	AB_2228008
Cleaved caspase 3	Cell Signaling Technology	Rabbit	9664	AB_2070042
Cleaved PARP	Cell Signaling Technology	Rabbit	5625	AB_10699459
Anti-DNA/RNA Damage antibody [15A3]	Abcam	Mouse	ab62623	AB_940049
Actin	Cell Signaling Technology	Mouse	3700	AB_2242334
OPA1	Abcam	Rabbit	ab42364	AB_944549
MFN1	Abcam	Rabbit	ab104585	AB_10712602
MFF	Abcam	Rabbit	ab81127	AB_1860496
DRP1	Abcam	Rabbit	ab184247	AB_2895215
p-DRP1^{S616}	Cell Signaling Technology	Rabbit	4494	AB_11178659
Rabbit anti-mouse IgG	Sigma	Mouse	A9044	AB_258431
Goat anti-mouse IgG	Sigma	Rabbit	A0545	AB_257896
Alexa Fluor 647	Invitrogen	Mouse	A-21235	AB_2535804
Alexa Fluor 488	Invitrogen	Rabbit	A-11034	AB_2576217

2.10. Superoxide dismutase-2 (SOD2) activity assay

The activity of mitochondrial superoxide dismutase (SOD) was measured using the commercially available superoxide dismutase (SOD) activity test kit ab65354 (Abcam). In a nutshell, cells treated with indomethacin and control cells had their mitochondria separated. After being lysed in ice-cold 0.1M Tris/HCl, pH 7.4, 0.5% Triton X-100, 5 mM -ME, and 0.1 mg/ml PMSF, the mitochondrial pellets were then tested for their superoxide dismutase (SOD) activity by the manufacturer's instructions. The information is displayed as a ratio of 100%, which represents the control mitochondrial fraction's SOD activity. By measuring the protein content in each mitochondrial compartment, the relative SOD activity was adjusted. The experiments were carried out three times in each case.

2.11. Analysis of mitochondrial transmembrane potential ($\Delta\Psi m$)

3×10^6 cells were employed for JC-1 staining, followed by flow cytometry, for $\Delta\Psi m$ analysis in AGS cells. After the treatment, the cells were washed in medium that had been preheated to 37 °C, and then they were incubated with JC-1 (5 µg/mL) for 15 min at 37 °C/5% CO_2 in complete darkness. Following incubation, the cells were separated, diluted in PBS to a density of 10^6 cells/mL, and analyzed on a FACS-LSR Fortessa, BD, using the FACS DIVA software under the recommended conditions. The studies were run three times with 10^4 cells in each set.

2.12. Measurement of ATP content

Following the manufacturer's instructions, the ATP content of AGS cells was determined using an ATP measurement kit (Invitrogen Corp., Carlsbad, CA, USA). Briefly, 10^7 cells per experimental set were lysed in cold cell lysis solution at the same rate (supplemented with Triton X-100). The clear supernatants obtained after centrifuging the lysates were utilized. A luminometer was used to test ATP content (BioTek). Each sample's ATP content was scaled to its corresponding protein concentration. The experiments were carried out three times in each case.

2.13. Small interfering RNA (siRNA) transfection

Following the established transfection methodology, siRNA-based reverse transfection was used to silence the expression of SIRT3, ERRα, and PGC1α (14). In a nutshell, lyophilized siRNA duplexes were reconstituted to a final concentration of 10 µM in the nuclease-free resuspension buffer (10 µM Tris-HCl, 20 mM NaCl, 1 mM EDTA, pH 8.0). 50–60% of confluent cells were treated to the appropriate siRNAs or scrambled siRNA (control siRNA). OptiMEM was used to dilute 75 pmol of siRNA and Lipofectamine RNAiMAX (Thermo) before they were combined and fed to the cells that had already become used to it. Each time, transfections using control siRNAs that were scrambled were carried out. The transfection medium was used to sustain the cells for 16–18 hours, after which full growth medium was added. Indomethacin 0.5 mM was applied to the transfected cells for 24 hours. The experiments were carried out three times in each case.

2.14. Confocal microscopy for mitochondrial structure analysis and immunocytochemistry

After treatment, cells were washed in pre-warmed medium and stained for 20 minutes with MitoTracker Red CMX ROS (100 nM) to assess the mitochondrial structure. Hoechst 33342 was utilized to stain the nuclei. After staining, the cells were rinsed in pre-warmed medium and examined with a 63X oil immersion lens and a thermo-regulated stage in a 5% CO_2 atmosphere using a Leica TCS-SP8 confocal microscope (Leica Microsystems, Wetzlar, Germany). To prevent laser-induced toxicity to the cells, light intensity was kept below 2%. As previously noted, treated cells were frozen (2% paraformaldehyde), permeabilized, and blocked in 5% BSA solution in PBS for the immunofluorescent labeling of 8-Oxo-dG. (14). Primary antibodies against 8-oxo-dG (anti DNA/RNA damage antibody) and TOM20 (for identifying mitochondria) were diluted in the blocking solution and incubated

overnight. The cells were then washed and exposed to secondary antibodies against TOM20 (Alexa fluor 647-conjugated anti-rabbit IgG) and 8-oxo-dG (Alexa fluor 488-conjugated anti-mouse IgG) the next day. The coverslips were cleaned before mounting them on glass slides so they could be seen with a 63X oil immersion lens. Digital zooming was used when necessary, and each experimental set had at least 100 cells inspected. To give sample photos, at least 5 independent fields were randomly selected. The pictures are examples of experiments that were independently repeated. The experiments were carried out three times in each case. Adobe Photoshop was used to trim the images, make general brightness/contrast changes, and combine them. Adobe Photoshop was used to trim the images and do general brightness/contrast adjustments, and CorelDraw X7 was used to put them together.

2.15. Measurement of mitochondrial superoxide
To evaluate the accumulation of reactive pro-oxidants in mitochondria in AGS cells, mitoSox staining was done. Following treatment, the cells were dissociated and washed with pre-warmed PBS. The cells were then stained with MitoSox by the manufacturer's instructions. Cells were examined in BD's FACS LSR Fortessa after being washed three times with pre-warmed PBS. Software called FACS DIVA was used to evaluate the data under predetermined conditions. Each batch of 10^4 cells was examined, and the experiment was run three times.

2.16. FITC-Annexin V staining for cell death determination
As previously mentioned, annexin V/propidium iodide (PI) dual staining was used to measure the apoptosis of AGS cells (14). In a nutshell, the cells were separated following treatment. Following the manufacturer's instructions, the cells were then removed from the annexin V binding buffer (Abcam) and stained with FITC-annexin V and PI (propidium iodide). Then, cells were analyzed in BD's FACS LSR Fortessa. The FACS DIVA program was used to evaluate the data under prescribed conditions. The studies were run three times with 10^4 cells in each set.

2.17. Cell cycle analysis
The cell cycle was studied using the flow cytometric method. AGS cells were cultured in 6-well plates, collected after the treatment, and fixed with chilled ethanol (70% v/v) using a gentle vortex. The cells were then maintained at 4°C overnight. The next day, the fixed cells were washed in PBS and stained for 15 minutes at room temperature in PBS containing 100 µg/ml propidium iodide (P-4170, Sigma) and 20 µg/ml RNase A (catalog No. 12091-039, Invitrogen). Software called BD FACS Diva 6.2 was used to analyze BD LSR Fortessa. The studies were run three times with 10^4 cells in each set.

2.18. Determination of SIRT3 deacetylase activity
The deacetylase activity of SIRT3 was measured in the presence or absence of indomethacin using the SIRT3 fluorometric activity assay kit (Abcam, ab156067). As instructed by the manufacturer, the experiment was carried out. In a nutshell, the activity of purified human recombinant SIRT3 was evaluated in the presence of increasing concentrations of indomethacin (0.1-0.5 mM) using kinetic measurements every two minutes for 45 minutes in a BioTek Synergy H1 Hybrid Multi-Mode Reader with excitation at 350 nm and emission at 450 nm. The experiment was done three times, with each reaction being carried out in duplicate following the kit instructions.

2.19. Molecular simulation to explore SIRT3-indomethacin interaction
PubChem was used to determine the chemical composition of indomethacin (PubChem CID: 3715), diclofenac (PubChem CID: 3033), ibuprofen (PubChem CID: 3672), and aspirin (PubChem CID: 2244). From the Protein Data Bank (PDB) or PDB-REDO repositories, 31 crystal structures of Sirtuin 3 (UniProtKB: SIR3 HUMAN) were downloaded on September 1, 2022 (Table 3) (23). 22 crystal

structures with good geometries and electron density map fitting were chosen for docking investigations based on the model attributes (as stated in the wwPDB validation report accessible on the PDB website)

Table 3: Computed binding energies of indomethacin (kcal/mol) with different crystal structures of SIRT3[†]

Receptor\Ligand	Indomethacin	Diclofenac	Ibuprofen	Aspirin
pdb4jt8	-10.06	-7.64	-7.75	-6.00
redo3glt	-9.73	-8.50	-8.01	-6.86
redo4bvf	-9.63	-8.57	-8.09	-6.82
pdb5z93	-9.27	-8.67	-8.13	-6.49
pdb4bve	-9.23	-8.61	-8.12	-6.98
redo4jsr	-9.05	-7.86	-7.55	-6.27
redo5bwo	-9.02	-8.12	-7.39	-6.31
redo3gls	-8.80	-7.54	-7.17	-6.11
redo4bvh	-8.75	-7.61	-8.15	-7.40
pdb5z94	-8.62	-7.99	-6.81	-6.33
redo4fz3	-8.51	-6.97	-6.21	-5.44
pdb4c7b	-8.39	-7.33	-6.71	-6.08
redo4fvt	-8.33	-7.06	-6.67	-6.07
redo3glu	-8.29	-7.94	-7.22	-5.98
pdb5ytk	-8.07	-7.97	-7.39	-5.97
redo5zgc	-7.81	-7.06	-6.40	-6.27
pdb5d7n	-7.79	-7.02	-7.06	-6.22
redo4hd8	-7.67	-6.78	-6.42	-5.44
pdb4bv3	-7.40	-7.26	-8.06	-7.20
pdb4bn4	-7.36	-6.78	-7.61	-7.63
redo4bv3	-7.05	-8.20	-7.99	-6.94
pdb4bvb	-6.71	-7.85	-8.09	-7.30
Mean	**-8.43±0.89**	**-7.70±0.61**	**-7.41±0.65**	**-6.46±0.60**

[†]*Crystal structures taken from PDB or REDO repositories are indicated by the pdb or redo prefix to the PDB accession code of the protein.*

(Table 3 and Table 4). Molecular docking simulations were carried out using AutoDock Vina following protocol (24). Crystallographic water molecules and any associated ligands were taken out of the protein crystal structures. PDB Hydro was used to fill in the protein's missing side chains (25). Alternative atom placements were eliminated. Polar hydrogens were added with AutoDockTools (26). Atom types for AutoDock4 were allocated. The preparation of ligand structures was done similarly. The ligands' whole set of rotatable bonds were liberated. The free, NAD$^+$-bound, and indomethacin-bound SIRT3 was subjected to a set of time- and temperature-dependent molecular

Table 4: Available crystal structures of Sirtuin 3, their qualities‡ and bound ligand information

PDB ID	Model Quality	Data Fit Quality	Quality Average	Redo Model Quality	Redo Data Fit Quality	Redo Average	Ligands
4bv3	81	81	81	2	0	1	OCZ,APR,NAD
5d7n	80	79	80	0	0	0	1PE,PG4
4bn4	70	81	75	0	1	0.5	OP2,AR6
5z93	92	55	73	-1	0	-0.5	KHB
4bvb	74	71	73	1	1	1	OCZ,AR6
5z94	89	54	72	0	0	0	CIT,KHB
5ytk	80	58	69	1	1	1	
4jt8	70	60	65	1	1	1	1NR
4bve	48	79	63	1	0	0.5	FZN
4c7b	68	50	59	1	0	0.5	BVB,FDL
4jt9	44	64	54	1	0	0.5	1NS
3glt	47	58	52	2	1	1.5	FZN
4hd8	42	61	51	2	0	1	PIT,FDL
4bvf	33	70	51	2	0	1	FZN
4jsr	36	62	49	2	1	1.5	1NQ
4c78	39	40	40	1	0	0.5	ALY,BVB
3glr	33	45	39	0	1	0.5	ALY
4o8z	47	26	37	1	0	0.5	BBI
3glu	21	52	36	2	1	1.5	
4fvt	45	26	36	2	1	1.5	ALY,CNA,NLE
5y4h	39	31	35	1	1	1	8QF,ALY
3gls	17	53	35	2	1	1.5	
6iso	34	28	31	1	0	0.5	
4bvg	22	34	28	1	0	0.5	XYQ
4bvh	37	17	27	2	1	1.5	OCZ,AR6,OAD
5bwn	29	21	25	-1	1	0	MYK
4bn5	8	42	25	1	0	0.5	SR7,CNA
5zgc	23	21	22	2	1	1.5	KHB
4fz3	20	20	20	2	0	1	ALY,MCM
5bwo	20	1	11	2	2	2	PLM
5h4d	17	1	9	1	0	0.5	BBI,FDL,NAD

‡REDO model and data fit qualities are given on an arbitrary scale of -2 (worst) to 2 (best).

dynamics (MD) simulations (300 K, 1 bar and 240 ns, respectively, in this study). In MD simulation, the protein or protein-ligand complex atomic model is put in an explicit aqueous environment, and the entire system is incubated for a certain amount of time at a specified temperature and pressure. The atoms become mobile due to temperature, and Brownian movements allow for the unrestricted movement of molecules in water. Thus, it takes into account how solvents and the flexibility of receptors may affect ligand interactions. You can see any structural alterations that the ligand binding causes in the protein. For the MD simulation, lower energy and higher frequency bound conformations were used. As previously indicated, MD was carried out in a water environment using a basic point-charge force field called OPLS (optimal potentials for liquid simulations) (27). Schrodinger Maestro was used to extract structural information from the simulation trajectories, including secondary structural characteristics, time-correlated interactions, root mean square deviations (RMSD), residue-wise fluctuations in terms of root mean square deviations (RMSF), and interaction energies (Academic Release 2020-4).

2.20. Statistical analyses

Every experiment was performed at least thrice. Experiment-related data were provided as mean standard deviation. One-way ANOVA followed by Bonferroni's Multiple-Comparison test was used for comparisons of more than two experimental groups, and unpaired t-test (with Welch correction) was used to determine the degree of significance when comparing two experimental groups. A P value of less than 0.05 (P<0.05) was taken into account for statistical significance. GraphPad Prism 8 and Microsoft Office Excel 2019 were used to statistically analyze the data.

3. RESULTS

3.1. Indomethacin triggers gastric cancer cell death in dose and time-dependent manner
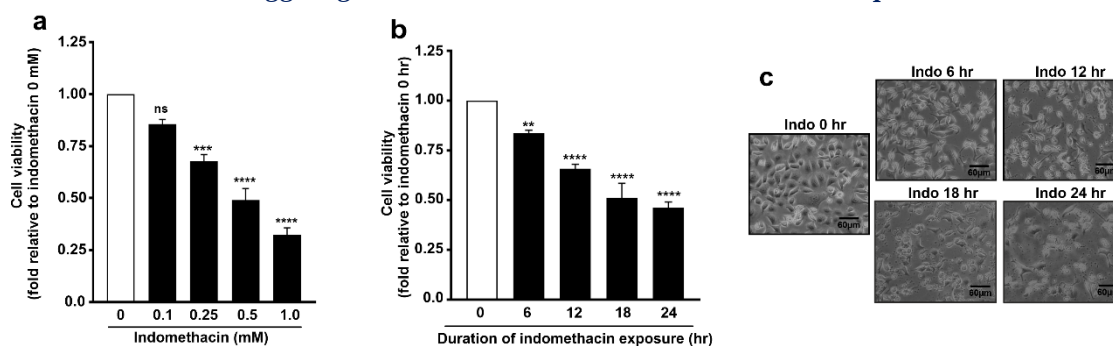
Fig. 1. Kinetics of indomethacin-induced gastric cancer cell death. (**a**) Bar graph showing dose response of indomethacin, checked as cell viability (by following MTT reduction), in AGS cells. (**b**) Cell viability as measured by MTT reduction assay in indomethacin-treated cells. (**c**) Phase contrast micrographs (representative images) of AGS cells treated with indicated indomethacin for indicated duration (in hours). The number of independent experiments is 3. (**a, c**) Data are mean ± SD. *$P < 0.05$; **$P < 0.01$; ***$P < 0.001$; ****$P < 0.0001$ versus 'indomethacin 0hr' calculated by one-way ANOVA followed by Bonferroni's post hoc test. Number of independent experiments: 3.

AGS cells were treated with indomethacin at different concentrations (0.1 mM to 1 mM) to follow the cytotoxic effect of the drug. Cellular dehydrogenase activity revealed that at 0.5 mM, indomethacin reduced cellular metabolism by ≈50% compared to control (Fig. 1a). Because 0.5 mM indomethacin-induced a sub-lethal effect on the gastric cells, this dose was used for all subsequent experiments to take into account the subtle effects of the drugs which otherwise might get unnoticed at a higher concentration due to the increased susceptibility of mitochondria to higher concentrations of a cytotoxic compound. Moreover, at 0.5 mM (dose) dose, indomethacin inhibited AGS cell proliferation in time-dependent mummer (Fig. 1b). Phase contrast microscopy of the AGS cells treated with indomethacin

also revealed a remarkable deterioration of cellular architecture in a time-dependent manner (Fig. 1c) similar to the reduction of cell proliferation.
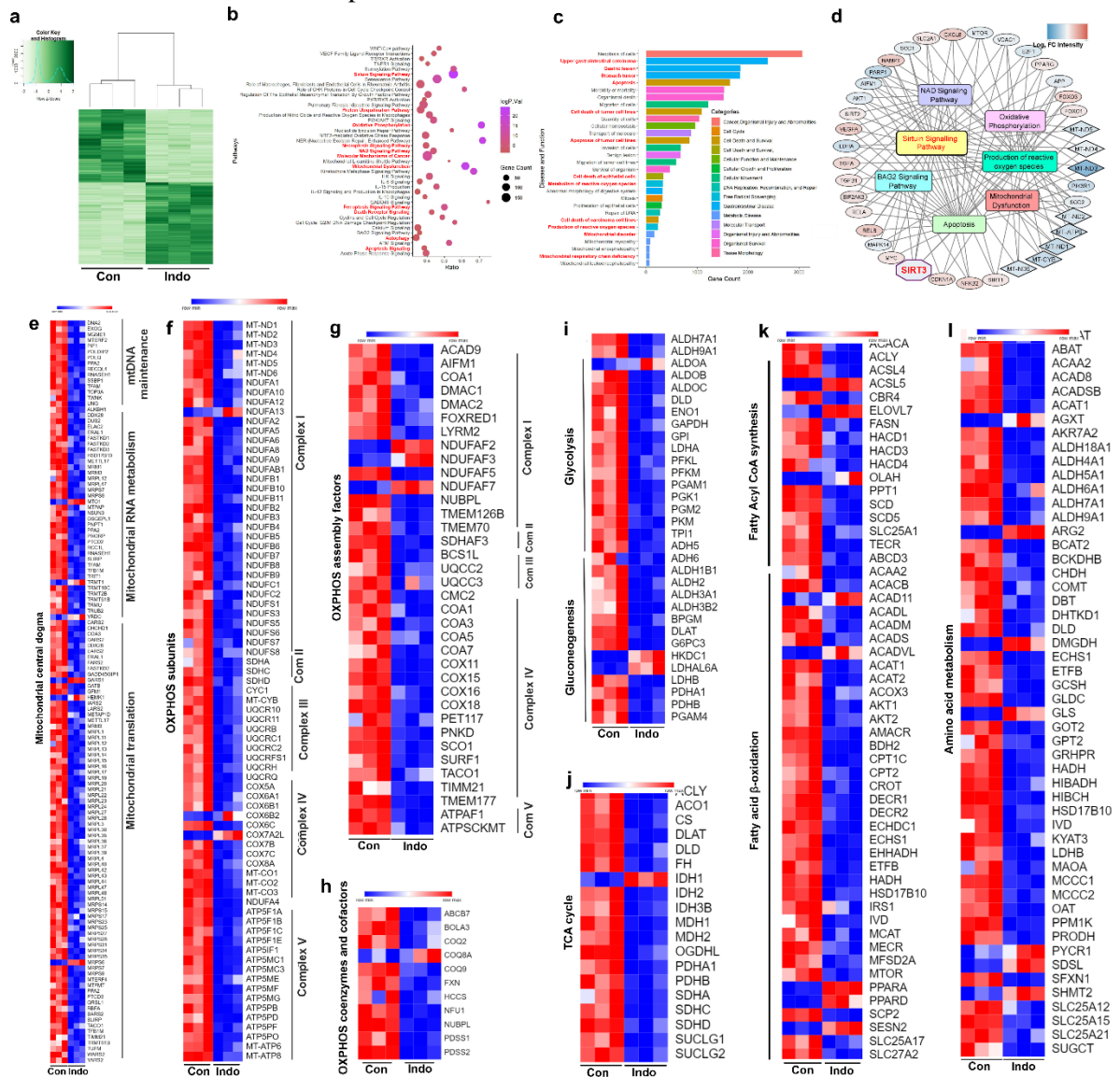
Fig. 2. Indomethacin detrimentally alters gastric cancer cell transcriptome indicating cellular metabolic crisis and mitochondrial dysfunction (a) Heatmap shows separate clustering of 'Con' and 'Indo' (FDR ≤ 0.05). Euclidean distance metric was used while clustering the gene expression data. The expression value of genes analyzed with fold change cut off of 1.5; colour gradient scale with white being highly downregulated to green being highly up-regulated. (**b**) Dot plot showing enriched canonical pathways. The size of dots represents the proportion of genes involved in the particular signaling/pathway while the range of colour indicates Bonferroni corrected p values (-log transformed). The ratio represents the number of genes in fraction with respect to the total number of genes that map to the same pathway. (**c**) Bar graph showing the disease and functions enriched in the 'Indo' set. (**d**) Hub gene network. The expression values of genes are represented with colour gradient scale with blue being highly downregulated to red being highly up-regulated. **e-i.** Heatmap shows the association of a subset of DEGs with mitochondrial central dogma including 'mtDNA maintenance', 'mtRNA metabolism' and 'mitochondrial translation' **(e),** OXPHOS subunits including genes for complex I (CI), complex II (CII), complex III (CIII), complex IV (CIV) and complex V (CV) **(f),** OXPHOS assembly factors including genes for complex I (CI), complex II (CII), complex III (CIII), complex IV (CIV) and complex V (CV) **(g),** OXPHOS enzymes and cofactors **(h),** 'glycolysis' and 'gluconeogenesis' **(i),** 'TCA cycle' **(j),** 'fatty acyl CoA synthesis' and fatty acid β-oxidation' **(k), '**amino acid metabolism' **(l)** between 'Con' and 'Indo' (FDR ≤ 0.05). The expression value of genes analyzed with fold change cut off of 1.5; colour gradient scale with blue: downregulated to red: up-regulated (**e-l**). All sequencing were done in triplicates.

3.2. Transcriptome analysis revealed SIRT3 as a major hub gene targeted by indomethacin to affect multiple metabolic pathways in AGS cells

High-depth transcriptome sequencing data revealed that indomethacin-treated cells had 3984 upregulated and 4474 downregulated genes compared to "control" cells, as represented through heat map (Fig. 2a) of the DEGs (analyzed using a log FC cut-off of 1.5, FDR 0.05) (GSE202140). Interestingly, "Sirtuin signaling pathway" and related DEGs got identified as important gene expression programs upon gene enrichment analysis using IPA (ingenuity pathway analysis) (Fig. 2b-c). Next, the gene interaction network was constructed using Cytoscape's MCODE plugin to screen for the hub gene/s controlling mitochondrial metabolism and cellular integrity. SIRT3 was found as a connecting node/main hub gene associated with several signaling pathways. Additionally, other important regulators of mitochondrial metabolism including ETC complex subunits, SOD, FOXO3/1, VDAC1, MTOR, and NF-κB subunits were also highlighted (Fig. 2d). Co-incidentally, SIRT3 is linked with majority of these players, according to IPA-based interactome research. These data tempted us to delve deeper into the functional properties of SIRT3 owing to its probable connection with NSAID-related GC cell death as evident in transcriptome data. The heatmaps were further zoomed in to examine the particular gene expression profiles affected by indomethacin, such as "mitochondrial central dogma" (Fig. 2e), "OXPHOS" (Fig. 2f–h), and the main components of cancer metabolism, including carbohydrate (Fig. 2i–j), fatty acid (Fig. 2k), and amino acid metabolism (Fig. 2l). The majority of the DEGs, incidentally, showed a substantial gross downregulation after indomethacin treatment, thereby highlighting the multifaceted detrimental sub-cellular changes triggered by indomethacin.

3.3. Human dataset mining revealed the prognostic relevance of SIRT3 in GC

After identifying SIRT3 as a major lead in the transcriptomics data, I quickly inquired about the lead's applicability to patient-derived STAD samples. The TCGA samples were compared for differences in SIRT3 gene expression between primary gastric tumor (n=415) and normal tissues (n=34) (Fig. 3a). According to ULCAN analysis, tumor samples had considerably more median (40.549 transcripts per million) SIRT3 transcripts than normal samples do (19.018 transcripts per million). Additionally, I examined whether the gene expression pattern and SIRT3 protein expression were consistent. SIRT3 was found to be highly expressed in tumor cells compared to glandular cells in immunohistochemical archives of typical normal and GC samples from the Human Protein Atlas database (stained with the antibody CAB037142) (Fig. 3b). In the graphic, the patient samples representative picture denotes the intestine type GC. Then, UALCAN analysis of SIRT3 expression based on the pathological staging of GC showed that SIRT3 expression is higher in late-stage tumors, indicating a possible link with tumor invasion and progression (Fig. 3c). Additionally, as shown by the TCGA patient data, elevated SIRT3 expression was also identified in the major histological subtypes of GC (Fig. 3d). SIRT3 expression was examined in patient data from Caucasian, African-American, and Asian samples because the prevalence of GC differs by race. It was observed that while there is a significant difference in SIRT3 expression between normal and tumor samples, there was no apparent significant difference between the races, suggesting that elevated SIRT3 expression is a common feature of gastric malignancies (Fig. 3e). To investigate the prognostic significance of increased SIRT3 transcripts, all these correlations logically deserved investigation. Indeed, high SIRT3 expression is linked to a shorter median OS of 24.6 months as compared to 99.4 months in low SIRT3 expression, according to Kaplan-Meier survival curves (Fig. 3f) (HR=1.99, log rank P=3e-11). This finding suggests a poor prognosis. SIRT3 expression may serve as a predictive marker of death, according to the TCGA data collected together.
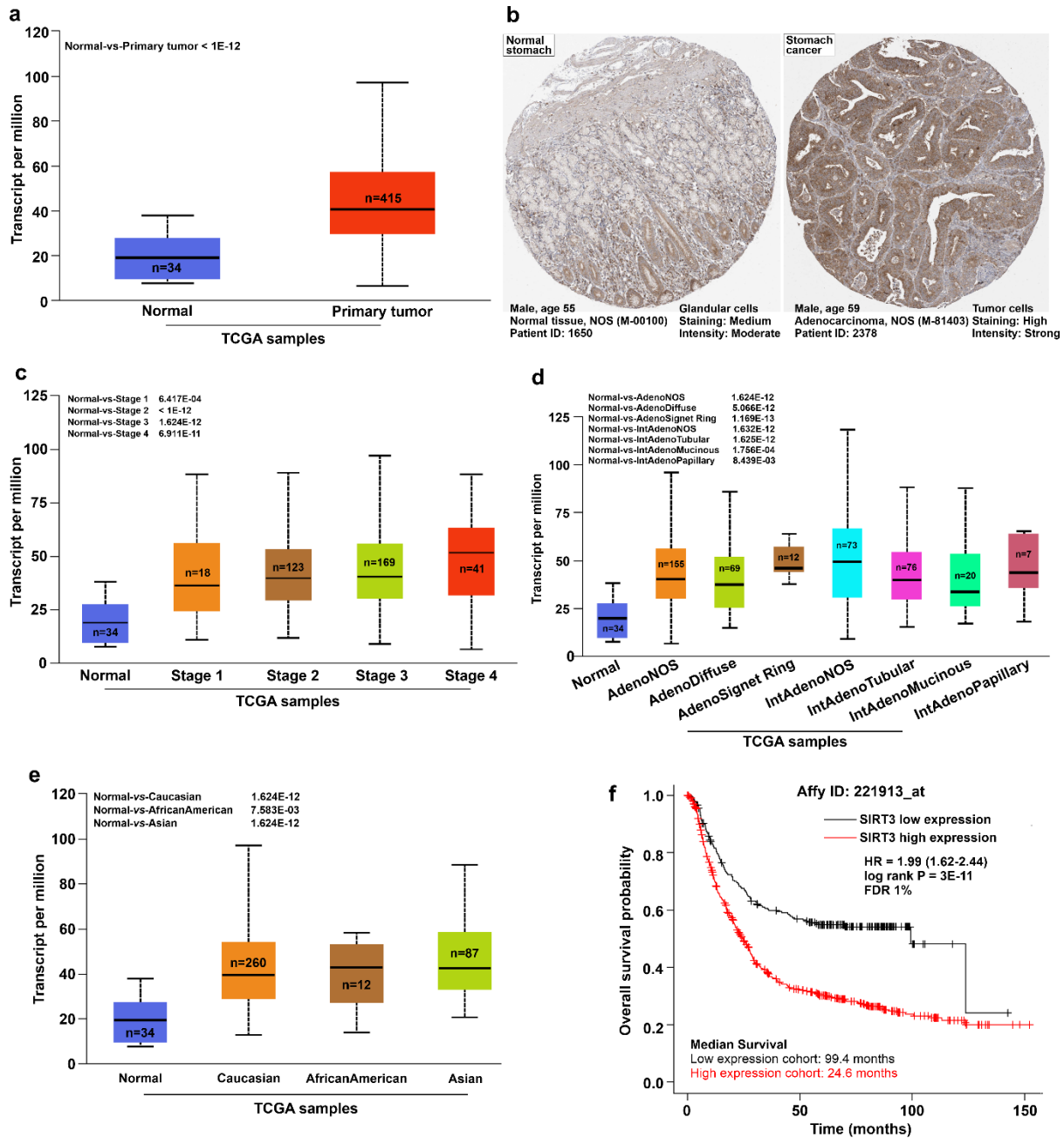
Fig. 3. High SIRT3 expression is associated with poor prognosis of GC (**a**) UALCAN analysis for the correlation between SIRT3 mRNA expression and human gastric adenocarcinoma; p< 1E-12 for Normal-vs-Primary tumor. (**b**) SIRT3 expression in gastric cancer and normal tissues from the Human Protein Atlas (HPA) database. Immunohistochemical staining done with antibody CAB037142. (**c**) UALCAN analysis for the correlation between SIRT3 mRNA expression and pathological stages of human gastric adenocarcinoma; N-vs-S1 6.417E-04, N-vs-S2 <1E-12, N-vs-S3 1.624E-12, N-vs-S4 6.911E-11. (**d**) UALCAN analysis for the correlation between *Sirt3* mRNA expression and histological subtypes (Adenocarcinoma NOS, Adenocarcinoma Diffuse, Adenocarcinoma SignetRing, Intestinal Adenocarcinoma NOS, Intestinal Adenocarcinoma Tubular, Intestinal Adenocarcinoma Mucinous, Intestinal Adenocarcinoma Papillary) of human gastric adenocarcinoma; *p* 1.62458935193399E-12 for Normal-vs-Adenocarcinoma (NOS), 5.06639175057444E-12 for Normal-vs-Adenocarcinoma (Diffuse), 1.16906484493029E-13 for Normal-vs-Adenocarcinoma(Signet Ring), 1.63247193540883E-12 for Normal-vs-Intestinal Adenocarcinoma (NOS), 1.6251444634463E-12 for Normal-vs-Intestinal Adenocarcinoma(Tubular), 1.756760E-04 for Normal-vs-Intestinal Adenocarcinoma(Mucinous), 8.439600E-03 for Normal-vs-Intestinal Adenocarcinoma(Papillary).

> **(e)** UALCAN analysis for the correlation between SIRT3 mRNA expression and human races (Caucasian, African-American and Asian); *p* 1.62436730732907E-12 for Normal-vs-Caucasian, 7.583800E-03 for Normal-vs-African American, 1.62447832963153E-12 for Normal-vs-Asian. (**f**) Kaplan-Meier survival curve comparing the high and low expressions of SIRT3 (n=875) in overall survival (OS) checked with mRNA gene chip Affy ID: 221913_at; HR: 1.99 (1.62-2.44), log rank P: 3.0E-11, FDR: 1%

3.4. Indomethacin-induced SIRT3 downregulation in GC cells underlies ETC complex gene downregulation, mitochondrial fragmentation, mitophagy and cell death via PGC-1α/AMPK-dependent signaling

Sequencing results showing downregulation of SIRT3 were confirmed by qPCR (Fig. 4a), which was followed by protein-level evaluation. Depletion of SIRT3 was caused by indomethacin dose-dependently (Fig. 4b). Additionally, indomethacin steadily deteriorated cytoarchitecture and cell survival while decreasing both SIRT3 and OGG1, the primary base excision repair protein fixing mtDNA damage (Fig. 4c). Then the functional impact of SIRT3 depletion was examined on the acetylation state of the mitochondrial proteome, with a focus on its two main targets, OGG1 and SOD2. Along with an elevation in the quantity of 8-oxoguanine (8-oxo-dG) in mtDNA, the acetylation of the mitochondrial proteome (Fig. 4d), notably that of OGG1 and SOD2 (Fig. 4e), was also dramatically increased (Fig. 4f). This was observed simultaneously with a considerable decline in SOD2 enzyme activity (Fig. 4g), pointing to mtDNA damage and a coordinated downregulation of the mitochondrial antioxidant defense. Significant mitochondrial depolarization (Fig. 4h) and ATP depletion were further signs of mitochondrial dysfunction in cells treated with indomethacin (Fig. 4i). Since OGG1 downregulation, ATP depletion, and reduced cell viability were all associated with indomethacin-dependent SIRT3 reduction, the condition of mtDNA-encoded ETC subunits were examined.

Following indomethacin treatment, MT-ND1, MT-ND6, MT-ATP6, MT-CYTB, and MT-CO1 that correspond to complexes I, V, III, and IV were found downregulated (Table. 5). Then, I examined structural dynamics and mitophagy to assess the quality control of the mitochondria. Fusogenic OPA1 and MFN1 as well as phospho-DRP1^{ser637} were significantly downregulated, but total DRP1 and phospho-DRP1^{ser616} were significantly upregulated. Additionally, during indomethacin-mediated SIRT3 depletion, increase of the mitophagy markers PINK1 and Parkin (Fig. 4j-k) were also observed. Because of increased mitophagy, the decrease in TOM20 (Fig. 4k) plainly showed mitochondrial depletion. The detrimental impact of indomethacin-induced mitopathology was reflected in immunoblot data indicating cell death as confirmed by BAX elevation and PARP cleavage while BCL-xL depletion (Fig. 4l).

Table 5: Gene expression profile of mitochondrial ETC complex subunits in AGS cells

	MT-ND1	MT-ND6	MT-ATP6	MT-CYTB	MT-CO1
Control	1	1	1	1	1
Indomethacin	0.036 ± 0.03****	0.02 ± 0.01****	0.01 ± 0.01****	0.02 ± 0.02****	0.03 ± 0.02****

*Gene expression analysis for MT-ND1, MT-ND6, MT-CYTB, MT-CO1, and MT-ATP6 by quantitative RT-PCR in AGS cells treated with 0.5 mM indomethacin for 24 hr. Table values indicate fold change in gene expression upon indomethacin treatment relative to 'control' (after normalization by Gapdh). Data are mean ± SD. *P < 0.05; ***P < 0.001, ****P < 0.0001 versus control calculated by unpaired Student's t test with Welch correction. The number of independent experiments is 3.*

Direct mitochondrial involvement, via activation of intrinsic apoptosis, was further evident from elevation of cleaved caspase 9 and 3 as well as cytochrome c (Fig. 4m). I then examined whether indomethacin targets the upstream transcriptional control on SIRT3 expression as induced by peroxisome proliferator-activated receptor gamma coactivator 1 alpha (PGC1α) and estrogen receptor related receptor (ERRα) to understand the mechanistic basis of NSAID-induced SIRT3 depletion. It was observed that indomethacin significantly decreased PGC1α and ERRα expression (Fig. 4n). Data
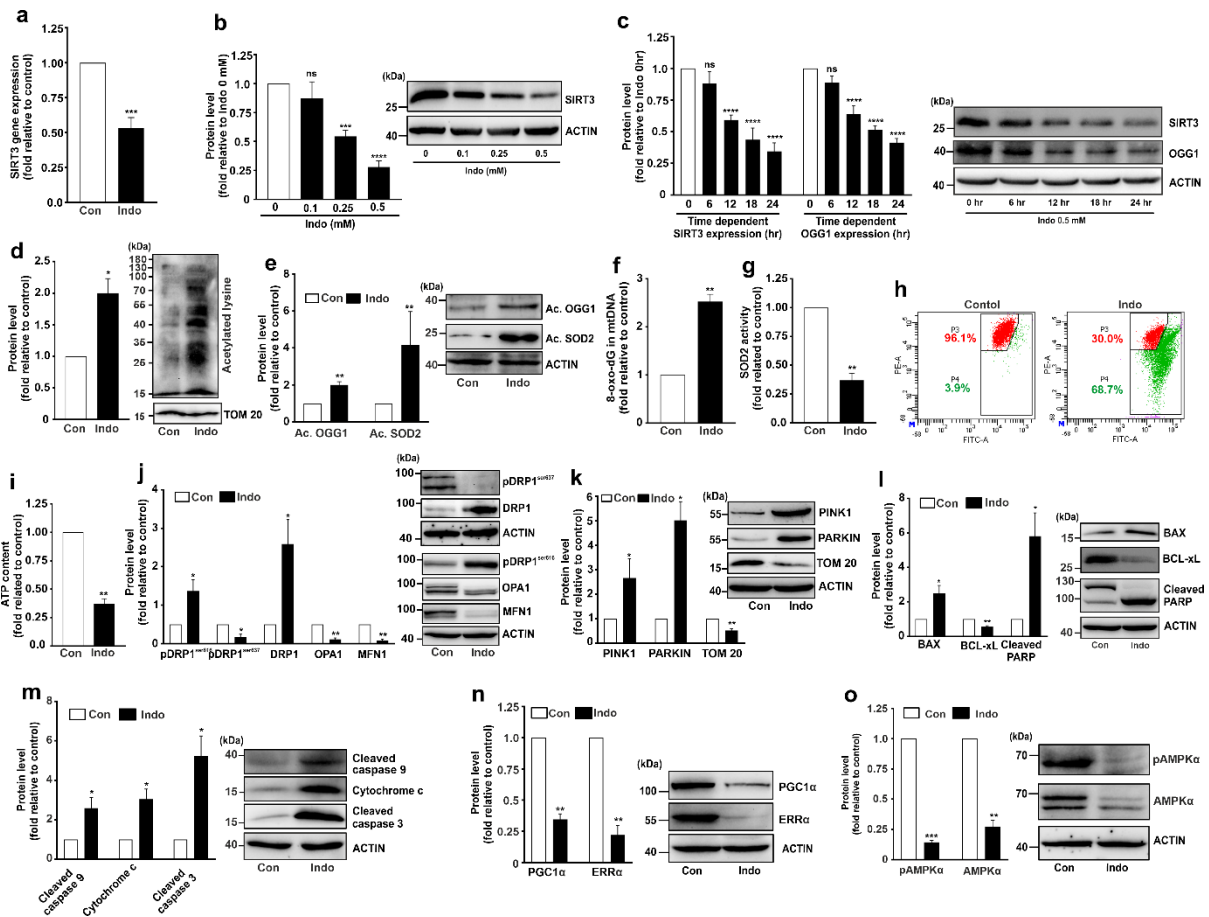
Fig. 4. Reduction of SIRT3 by indomethacin triggers mtDNA-encoded ETC complex gene downregulation, mitochondrial hyperfission and cell death (**a**) Quantitative RT-PCR for SIRT3 gene expression in control and indomethacin-treated cells; bar graph indicates fold change in gene expression relative to control (after normalization by GAPDH). (**b**) Immunoblot of SIRT3 in AGS cells treated with indomethacin at indicated concentrations for 24 hr. (**c**) Immunoblots of SIRT3 and OGG1 in AGS cells treated with 0.5 mM indomethacin for the indicated duration. ACTIN was used as the loading control (**b-c**). (**d**) Immunoblot of acetylated lysine in the mitochondrial fraction of AGS cells treated with 0.5 mM indomethacin for 24 hr. TOM20 was used as the loading control. (**e**) Immunoblots of acetylated OGG1 and acetylated SOD2 in AGS cells treated with 0.5 mM indomethacin for 24 hr. ACTIN was used as the loading control. (**f**) mtDNA damage as measured by 8-oxo-dG ELISA and (**g**) mitochondrial SOD2 activity in AGS cells treated with 0.5 mM indomethacin for 24 hr. (**h**) Flowcytometric detection of ΔΨm. 10,000 cells were checked per set and numerical values within the quadrants indicate the percentage of cells therein. (**i**) Bar graph showing ATP content in 'con' and 'indo'-treated AGS cells for 24 hr. (**j-m**) Immunoblots of pDRP1^{ser637}, DRP1, pDRP1^{ser616}, OPA1, MFN1 (**j**), PINK1, PARKIN, TOM 20 (**k**), BAX, BCL-xL, cleaved PARP (**l**), cleaved caspase 9, cytochrome c and cleaved caspase 3 (**m**) in 'con' and 'indo'-treated AGS cells with 0.5 mM indomethacin for 24 hr. ACTIN was used as the loading control. (**n-o**) Immunoblots for PGC1α, ERRα (**n**), pAMPKα and AMPKα (**o**) in 'con' and 'indo'-treated AGS cells with 0.5 mM indomethacin for 24 hr. ACTIN was used as the loading control. The number of independent experiments is 3 (**a-o**). Representative blot alongside of bar graph (**b-e, j-o**). (**a, d-o**), Data are mean ± SD. *$P < 0.05$; **$P < 0.01$; ***$P < 0.001$ versus control calculated by unpaired Student's t test with Welch correction. (**b-c**) Data are mean ± SD. ***$P < 0.001$; ****$P < 0.0001$ versus 'Indo 0h' calculated by one-way ANOVA followed by Bonferroni's post hoc test. ns: non-significant. The number of independently repeated experiments is 3 in every experiments.

also showed that indomethacin inhibited 5' AMP-activated protein kinase (AMPK) activity (Fig. 4o), therefore influencing the AMPK/PGC-1α /SIRT3 signaling axis, which is likely to function in a feedback loop (30).
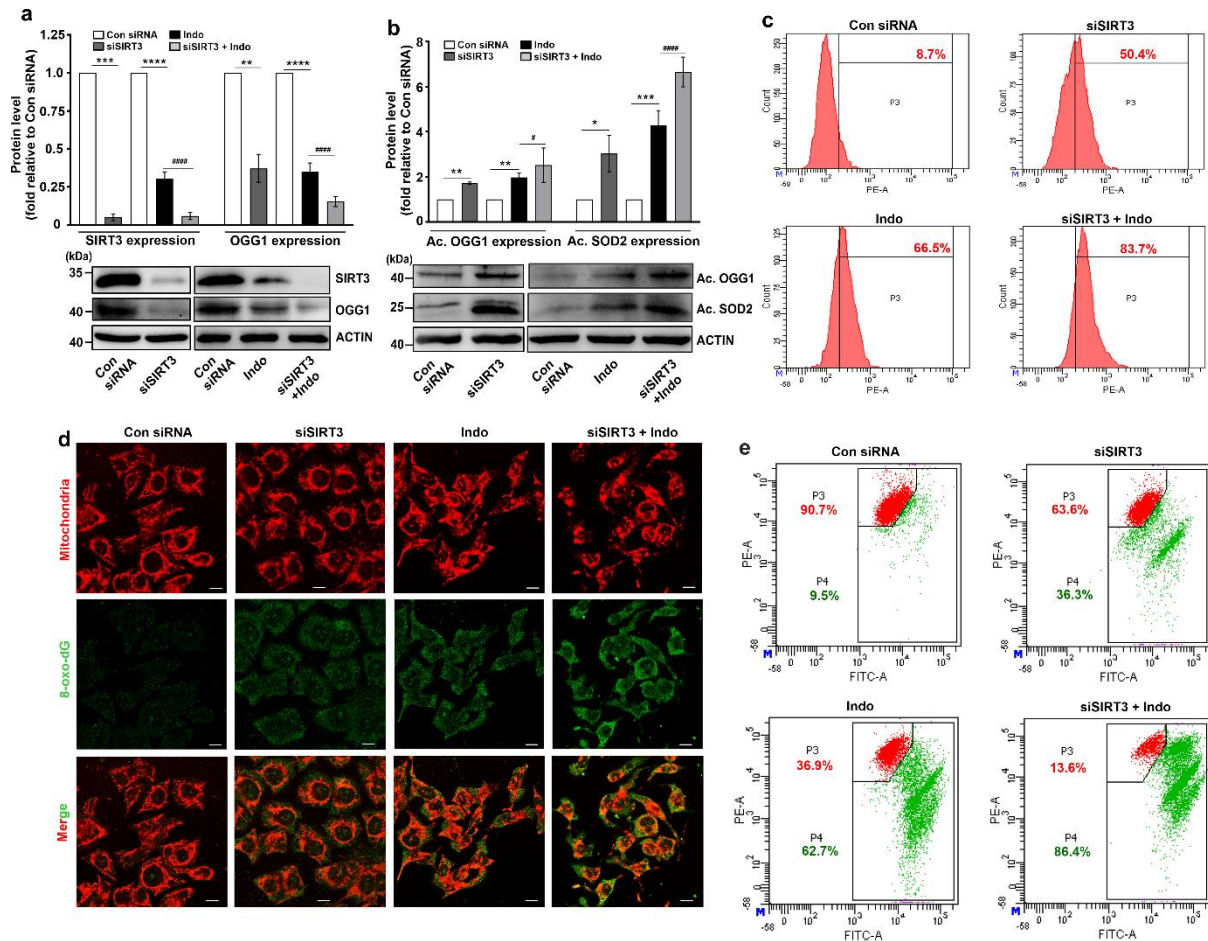
Fig. 5. SIRT3 silencing aggravates indomethacin-induced SOD2 and OGG1 acetylation as well as oxidative stress and mitochondrial depolarization (**a**) Immunoblot of SIRT3 and OGG1 in SIRT3-silenced AGS cells treated with indomethacin for 24 hr. (**b**) Immunoblot of acetylated OGG1 and SOD2 in SIRT3-silenced AGS cells treated with indomethacin for 24 hr. For (**a-b**) representative blots presented below the bar graphs. (**c**) Flowcytometric detection of mitochondrial superoxide ion (O_2^-) accumulation in SIRT3-silenced AGS cells treated with indomethacin (0.5 mM) for 24 hr. (**d**) Confocal immunofluorescent micrographs showing 8-oxo-dG (green) and TOM20 (red) in SIRT3-silenced AGS cells treated with indomethacin (0.5 mM) for 24 hr. (**e**) Flowcytometric detection of ΔΨm (mitochondrial membrane potential) in SIRT3-silenced AGS cells treated with indomethacin (0.5 mM) for 24 hr; 10,000 cell were checked per set and numerical values within the quadrants indicate the percentage of cells therein. Data are mean ± SD. *P < 0.05; **P < 0.01; ***P < 0.001; ****P < 0.0001 versus 'Con siRNA' and #P < 0.05; ####P < 0.0001 versus 'Indo' calculated by one-way ANOVA followed by Bonferroni's post hoc test. For confocal microscopy, at least 3 randomly selected fields were captured and a representative image has been provided. The number of independently repeated experiments is 3 in every case.

3.5. SIRT3 knockdown aggravates indomethacin-induced mitochondrial damage and cytopathology

Given the fact that SIRT3 is crucial for regulating cellular and mitochondrial metabolism, it was next asked what might actually happen if indomethacin is supplemented in SIRT3-silenced cells. The downregulation of SIRT3 and OGG1, caused by indomethacin, was worsened by SIRT3 knockdown, which also enhanced the acetylation of OGG1 and SOD2 (Fig. 5a-b). Functional impact of SIRT3 knockdown was observed in flowcytometric data indicating intra-mitochondrial superoxide ion (O_2^-) elevation (Fig. 5c). By indicating intracellular 8-oxo-dG accumulation, confocal micrographs further substantiated the impact of OGG1 downregulation (Fig. 5d). Indomethacin treatment increased mitochondrial depolarization in SIRT3-silenced cells compared to siSIRT3 or indomethacin treatment
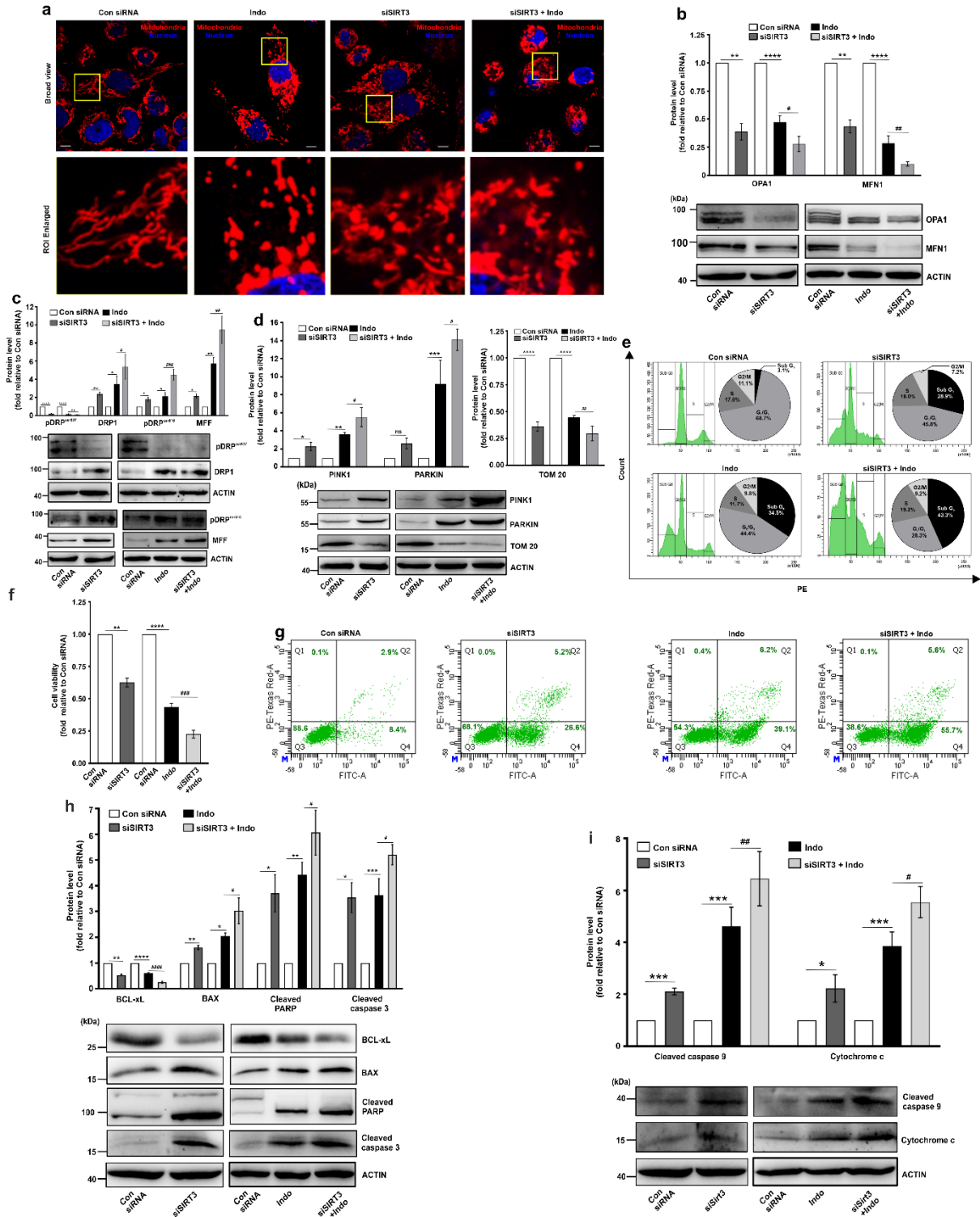
Fig. 6. SIRT3 silencing exacerbates indomethacin-induced mitochondrial dysfunction and cytotoxic responses (a) Live-cell confocal immunofluorescent micrographs showing MitoTracker red-stained mitochondria and Hoechst 33342-stained nuclei for depicting mitochondrial structural dynamics. The size bar indicates 10 µm. At least 3 randomly selected fields were captured and representative micrographs are presented. **(b-d)** Immunoblots of OPA1, MFN1 (**b**), pDRP1^{ser637}, total DRP1, pDRP1^{ser616}, MFF (**c**) and PINK1, PARKIN and TOM20 (**d**) in SIRT3-silenced AGS cells treated with indomethacin (0.5 mM) for 24 hr. ACTIN was used as the loading control. For (**b-d**) representative blots below the bar graphs. (**e**) Flowcytometry analysis of cell cycle in SIRT3-silenced AGS cells treated with indomethacin for 24 hr. 10,000 cell were checked per set; pie-charts presented as insets in the respective histograms. **(f)** Cell viability

was measured by MTT reduction assay in SIRT3-silenced cells treated with indomethacin (0.5 mM) for 24 hr. (**g**) Flowcytometric detection of Annexin V/PI (propidium iodide)-stained cells for measuring apoptosis in SIRT3-silenced AGS cells treated with indomethacin; 10,000 cells were checked per set. Numerical values within the quadrants indicate the percentage of cells therein. (**h-i**) Immunoblots of BCL-xL, BAX, cleaved PARP and cleaved caspase 3 (**h**) and cleaved caspase 9, and cytochrome c (**i**) in SIRT3-silenced AGS cells treated with indomethacin (0.5 mM) for 24 hrs. ACTIN was used as the loading control. For (**h-i**) representative blots are presented alongside the bar graphs. Data are mean ± SD. *$P < 0.05$; **$P < 0.01$; ***$P < 0.001$; ****$P < 0.0001$ versus 'Con siRNA' and #$P < 0.05$; ##$P < 0.01$; ###$P < 0.001$ versus 'Indo' calculated by one-way ANOVA followed by Bonferroni's post hoc test. ns: non-significant. The number of independently repeated experiments is 3 in every case.

alone, demonstrating that increased mitochondrial oxidative stress also translated into loss of mitochondrial integrity (Fig. 5e).

Further, high-resolution confocal micrographs revealed loss of mitochondrial structural integrity concurrent with mitochondrial functional abrogation as observed above. Indomethacin-treated cells exhibited extensively fragmented and punctate-clustered mitochondria compared to filamentous mitochondria in control-siRNA-treated cells. Furthermore, SIRT3 knockdown accelerated mitochondrial disintegration, clumping, and shrinkage (Fig. 6a). OPA1, MFN1, and phospho-DRP1^{ser637} decrease, whereas MFF, phospho-DRP1^{ser616}, and DRP1 elevation, also provided evidence of mitochondrial fragmentation (Fig. 6b-c). In fact, hyperfission progressed synchronously with mitochondrial depletion and aberrant mitophagy (in the absence of any compensatory rescuing effect of mitochondrial biogenesis), as evident from the coordinated upregulation of major mitophagy regulators (PINK1 and PARKIN) while downregulation of TOM20 (Fig. 6d).

As a result of the cumulative effects of mitochondrial dysfunction, triggered by indomethacin treatment in a SIRT3-silenced state, the cell cycle intensely worsened (as evident from significant increase in the sub-G$_0$ population) (Fig. 6e), along with an aggravated loss of cell viability (Fig. 6f), and elevation in cell death (Fig. 6g-h). A rise in caspase 9 and cytochrome C specifically made the involvement of intrinsic apoptosis obvious (Fig. 6i). When compared to either siSIRT3 or indomethacin treatment alone, the combined negative effects of "siSIRT3 + indomethacin" were considerably greater.

3.6. Indomethacin downregulates transcriptional regulators of SIRT3 and blocks the feed-back loop of AMPK/PGC-1α/SIRT3 signalling

So far, it has been observed that inhibition of the AMPK/PGC-1α /SIRT3 signaling axis contributes to indomethacin-induced mitochondrial dysfunction and AGS cell death. For further confirmation, it was checked whether inhibiting SIRT3 transcriptional regulators, *per se*, had any impact on indomethacin treatment. The expression of SIRT3 was found depleted when PGC1α or ERRα are silenced. Additionally, indomethacin treatment exacerbated the SIRT3-downregulating impact of PGC1α or ERRα knockdown (Fig. 7a-b), which made the cytoarchitectural damage (Supplementary Fig. S3) and cell viability decline much worse (Fig. 7c-d). Additionally, to further support the inhibitory effect on the feed-back loop of AMPK/PGC-1α/SIRT3 signaling, SIRT3 knockdown significantly exacerbated the direct inhibitory effect of indomethacin on PGC1α and ERRα as well as activation of AMPK (Fig. 7e-f).

3.7. Indomethacin competitively inhibited the deacetylase activity of purified SIRT3 by binding to NAD site

Next, the possible mechanism for the suppression of SIRT3 deacetylase activity was ventured to investigate the degree to which indomethacin interferes with SIRT3 signaling. Data mainly showed that indomethacin decreased human recombinant SIRT3's deacetylase activity (Fig. 8a). I used a molecular docking approach to find the thermodynamically most stable complexes of the ligands under study with SIRT3 in silico using a stochastic algorithm to further clarify the mode of inhibition
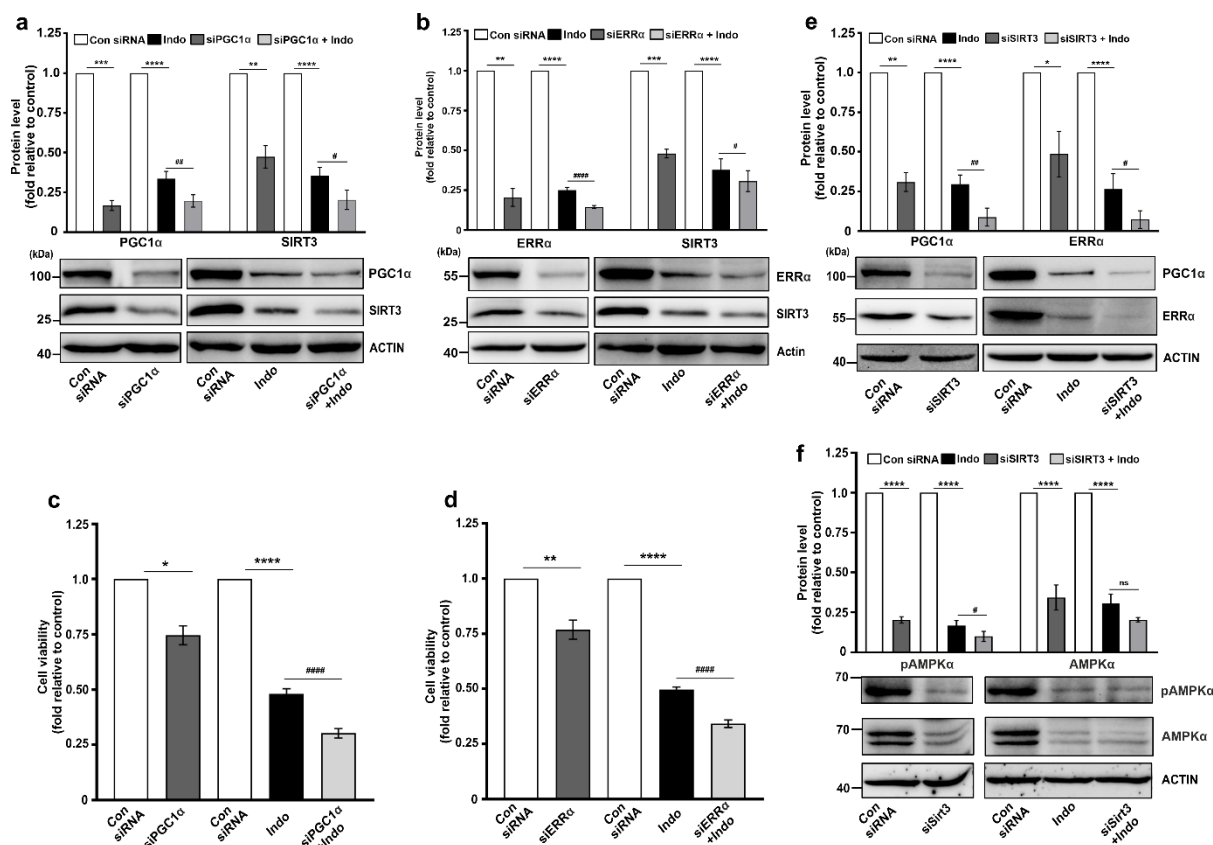
Fig. 7. Indomethacin downregulates transcriptional regulators of SIRT3 and reduces AMPK phosphorylation. (a) Immunoblots of PGC1α and SIRT3 in PGC1α-silenced AGS cells treated with 0.5 mM indomethacin. **(b)** Immunoblots of ERRα and SIRT3 in ERRα-silenced AGS cells treated with indomethacin. ACTIN was used as the loading control; representative blots are shown below the bar graphs **(a-b)**. **(c-d)** Cell viability was measured by MTT reduction assay in PGC1α-silenced **(c)** and ERRα-silenced AGS cells treated with 0.5 mM indomethacin for 24 hr. **(e-f)** Immunoblots of PGC1α and ERRα **(e)** and pAMPKα and AMPKα **(f)** in SIRT3-silenced AGS cells treated with indomethacin (0.5 mM). ACTIN was used as the loading control; representative blots are shown below the bar graphs. Data are mean ± SD. *$P < 0.05$; **$P < 0.01$; ***$P < 0.001$; ****$P < 0.0001$ versus 'Con siRNA' and #$P < 0.05$; ##$P < 0.01$; ####$P < 0.0001$ versus 'Indo' calculated by one-way ANOVA followed by Bonferroni's post hoc test. ns: non-significant. The number of independently repeated experiments is 3 in every case.

and identify the crucial amino acid residues responsible for the interaction between SIRT3 and indomethacin (randomly screening through several possible configurations and repeating the process until convergence is achieved). The four ligands with SIRT3 conformers so produced by molecular docking are given with their lowest binding free energy (Table 3). Compared to other NSAIDs, indomethacin consistently showed lower binding energy with diverse SIRT3 conformations, making it appear as the most effective ligand. Indomethacin's mean binding energy is significantly lower (-8.430.89 kcal/mol) (Table 4). Most likely binding mechanisms for indomethacin are shown based on the clustering of binding patterns (Fig. 8b). When compared with NAD-binding, indomethacin-binding indicates a competitive mode of interaction with NAD because of binding site overlap. NAD and ADP-D-ribose had similar binding energies to indomethacin at -10.14 kcal/mol and -9.07 kcal/mol, respectively. This suggests that indomethacin and NAD may compete for the same binding site. Four low-energy/high-frequency bound indomethacin conformers were employed in MD simulation to study the stability of the binding modes and understand the specific interactions involved (Fig. 8b). As a starting point, the apo and NAD-bound holo conformations of SIRT3 were examined.
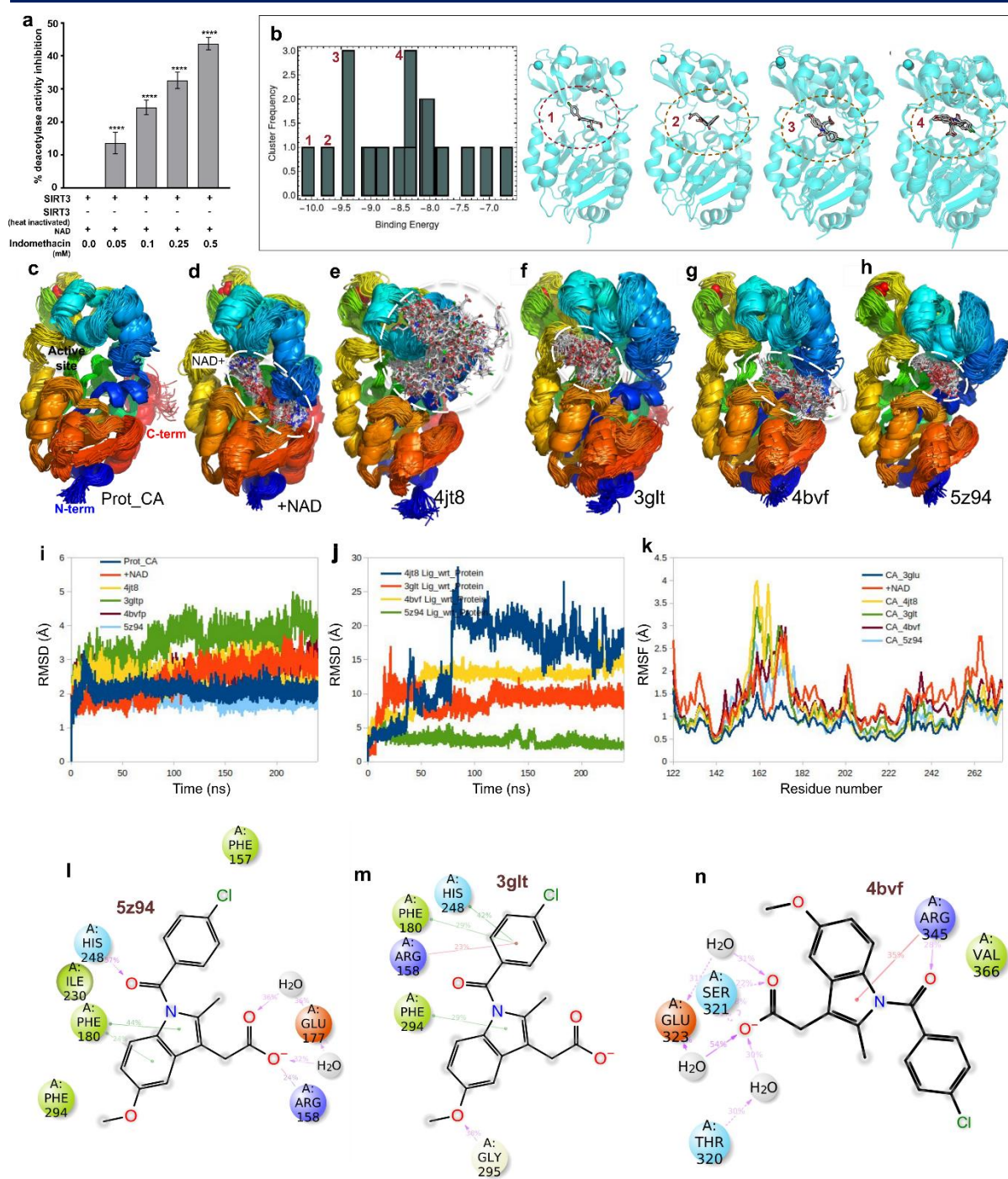
Fig. 8. Indomethacin inhibits deacetylase activity of SIRT3 and shows competitive inhibition through binding-site overlap with NAD. (a) Dose dependent inhibition of SIRT3 deacetylase activity by indomethacin. Data are mean ± SD. ****$P < 0.0001$ versus indomethacin 0 mM calculated using one-way ANOVA with Bonferroni's post hoc test. (**b**) Clustering of binding modes of indomethacin with SIRT3 as obtained by molecular docking. Low energy and high frequency modes **(1-4)** are shown, which corresponds to the binding with pdb4jt8, redo3glt, redo4bvf, pdb5z94 structures, respectively. Sirtuin is shown in a cyan cartoon model. Indomethacin is shown in white stick model with standard color codes for N, O and Cl. (**c-h**) Stability of indomethacin binding with SIRT3 as obtained from 240 ns molecular dynamics simulation. **c.** Apo enzyme (PDB: 3glu) control in SPC water under OPLS-AA force field for 240 ns. 100 snapshots at 2.4 ns intervals are superimposed. Protein is shown in ribbon representation and N-terminal to C-terminal is colored in rainbow (blue to red). Active site is labelled. (**d**) NAD+ bound holoenzyme (PDB: 4bv3) control. NAD$^+$ in white stick model is labeled and the binding region is encircled with white dashed line. (**e**) 4jt8 indomethacin complex. Indomethacin is shown in white stick model and the binding region is encircled with

105

white dashed line. (**f**) 3glt indomethacin complex. (**g**) 4bvf indomethacin complex. (**h**) 5z94 indomethacin complex. (**i**) Protein backbone C_α RMSD for apoenzyme, holoenzyme and all the indomethacin bound complexes of apoenzyme with respect to the initial conformations. (**j**) RMSD of indomethacin in all the four bound complexes with respect to the initial conformation of the complexes. (**k**) Residue-wise fluctuations (RMSF) in protein backbone for apo, holo and indomethacin bound conditions. (**l-n**) Time average interaction of indomethacin with sirtuin 3 (5z94, 3glt. 5bvf) as obtained from molecular dynamics simulations. Three possible conformations are shown. 5z94 and 3glt shows binding near the active site His248. 4bvf shows binding in the distal part of NAD+ binding channel. (**l**) In 5z94, catalytic His248 forms a hydrogen bond (pink arrow from H donor to acceptor) with the amide carbonyl moiety of indomethacin. Phe180 showed pi-stacking interaction (green lines) with the indole ring of indomethacin. Carboxylate group of indomethacin formed two water bridges through H bonds (pink arrows) with Glu177 and a salt bridge (red/blue line) with the positively charged Arg158. Phe157, Phe294 and Ile230 formed hydrophobic contacts with chlorobenzene, indole and methoxy moieties, respectively. (**m**) 3glt shows another stable bound conformation of indomethacin within the active site of the enzyme. In this conformation catalytic His248 forms pi-stacking with chlorobenzene moiety of indomethacin along with Phe180 (green lines). Positively charged Arg158 forms cation-pi interaction (red line) with chlorobenzene. Phe294 forms pi-pi stacking (green line) with the indole moiety of indomethacin. Gly295 forms a hydrogen bond (pink arrow from H donor to acceptor). (**n**) 4bvf shows yet another stable bound conformation in the distal part of NAD+ binding tunnel. In this conformation, the carboxylate group of indomethacin forms water bridges with Thr320 and Glu323 and a direct hydrogen bond (pink arrows) with Ser321. Arg345 forms a cation-pi interaction with the indole and a H bond with the amide carbonyl of indomethacin. Val366 forms hydrophobic contacts with chlorobenzene moiety.

Snapshots of the protein/protein-ligand complex structures are provided (Fig. 8c-h) and stacked for comparison to provide a qualitative knowledge of the stability of apo, holo and indomethacin-bound complexes. Additionally, a quantitative representation is shown (Fig. 8i–k) using standard deviations that are time-correlated or time-averaged (RMSD and RMSF, respectively). Both the apoprotein and the holoprotein linked to NAD exhibit flawless structural integrity in water. The first 2-3 rise in RMSD is seen as a result of the crystal structure relaxing in the solvent environment (Fig. 8i). Both the apoprotein and the holoprotein maintained a constant shape once they had reached equilibrium for the duration of the simulation. The most stable of the four possible indomethacin complexes was the 5z94 complex, which was followed by the 3glt complex. The ligand migrated to the distal end of the NAD-binding tunnel and reached a stable conformation in the case of the 4bvf complex. The ligand dissolved from the binding site in 4jt8, as evidenced by a sharp rise in RMSD at around 80 ns (Fig. 8j). Although the ligand remained coupled to the enzyme's surface for the remainder of the simulation track, no stable contact could be seen. The elevated C RMSF also exhibits this (Fig. 8k). For the three most stable conformers (5z94, 3glt, and 4bvf), significant SIRT3-ligand interactions were seen at least 20% of the time during the simulation (Fig. 8l-n). Similar interactions occur upon binding around the catalytic His248 residue in 5z94 and 3glt. His248 can interact with indomethacin's chlorobenzene moiety via a pi-stacking interaction (42%) or a hydrogen bond (57%) with the amide carbonyl. Additionally, Phe180 and Phe294 participate in the pi-stacking interaction of indomethacin's indole ring (44%) or chlorobenzene (29%). The carboxylate group of indomethacin was observed to create a salt bridge (24% of the time) with Arg158, a crucial NAD-binding residue. Additionally, it has a 23% chance of forming a cation-pi contact with the chlorobenzene group. It was discovered that two water bridges allow the carboxylate group of indomethacin to bind with the protein's Glu177 (36%). Gly295 donates a hydrogen bond to the methoxy group, stabilizing it (38%). In addition to these particular interactions, Phe157, Phe294 and Ile230 made hydrophobic contacts with the corresponding moieties of chlorobenzene, indole, and methoxy (Fig. 7L-M). However, 4bvf has an indomethacin-bound conformation that is stable in the distal portion of the NAD binding tunnel (Fig. 8o). In this conformation, the carboxylate group of indomethacin forms water bridges with Thr320 and Glu323 and a direct hydrogen bond with Ser321. Arg345 forms a cation-pi interaction with the indole and a hydrogen bond with the amide carbonyl of indomethacin. Val366 forms hydrophobic contact with chlorobenzene. Thus, the amide
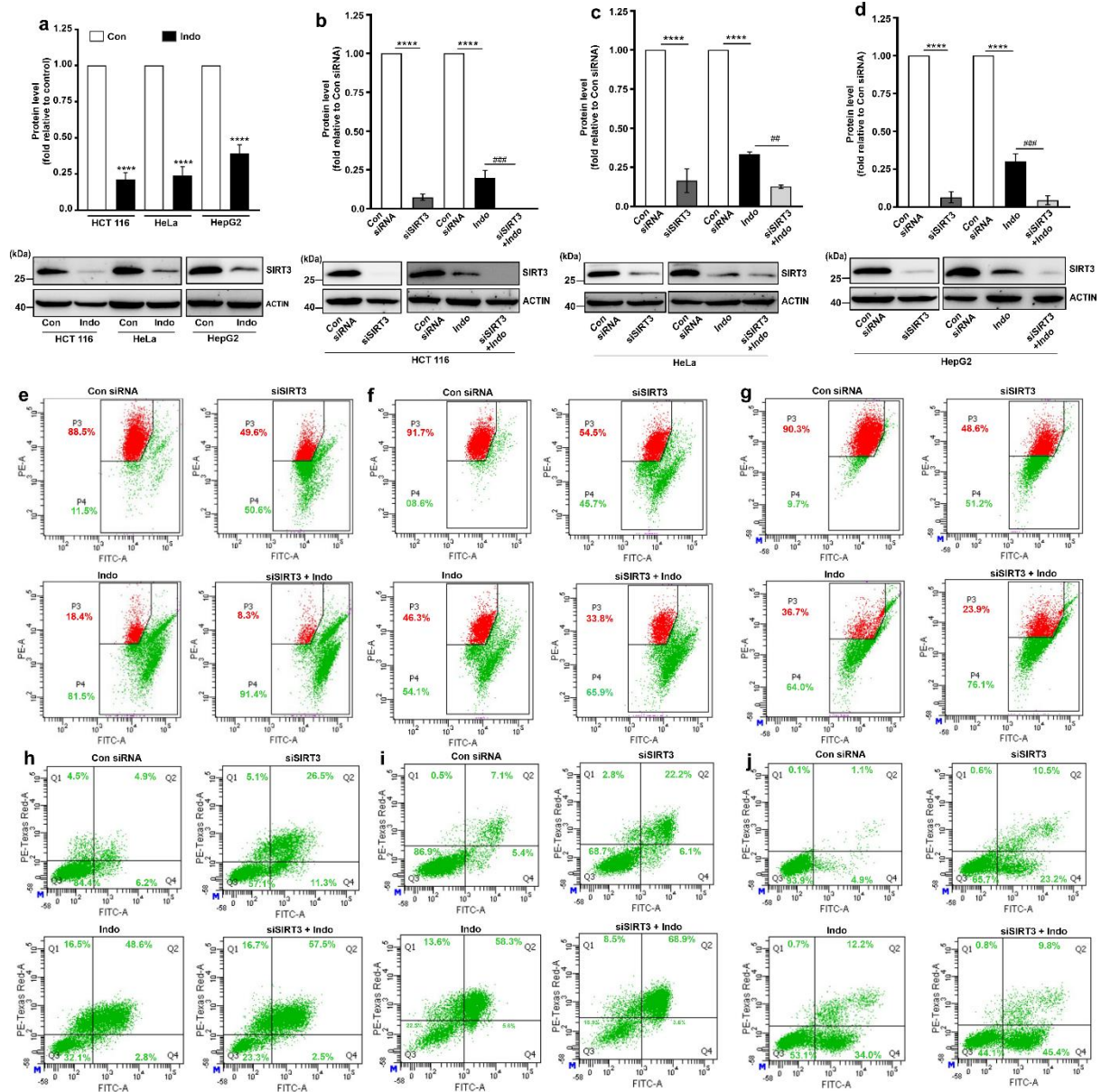
Fig. 9. Downregulation of SIRT3 is associated with indomethacin-induced toxicity in colon, cervical, and hepatocellular carcinoma cells. (a) Immunoblots of SIRT3 in HCT-116, HeLa, HepG2 cell lines treated with 0.5 mM of indomethacin for 24 hr. **(b-d)** Immunoblots of SIRT3 in SIRT3-silenced HCT-116 cells **(b),** HeLa cells **(c)** and HepG2 cells **(d)** treated with 0.5 mM indomethacin for 24 hr. ACTIN was used as loading control and representative blots presented below the bar graphs **(a-d).** **(e-g)** Flowcytometric detection of ΔΨm (mitochondrial membrane potential) in SIRT3-silenced HCT-116 cells **(e),** HeLa cells **(f)** and HepG2 cells **(g)** treated with indomethacin for 24 hr. **(h-j)** Flowcytometric detection of Annexin V/PI (propidium iodide)-stained cells for measuring apoptosis in SIRT3-silenced HCT-116 cells **(h),** HeLa cells **(i),** and HepG2 **(j)** cells treated with indomethacin for 24 hr. 10,000 cells were checked per set. Numerical values within the quadrants indicate the percentage of cells therein. Data are mean ± SD. ****$P < 0.0001$ versus 'Con siRNA' and ##$P < 0.01$; ###$P < 0.001$ versus 'Indo' calculated by one-way ANOVA followed by Bonferroni's post hoc test. The number of independently repeated experiments is 3 in every case.

carboxylate group of indomethacin forms water bridges with Thr320 and Glu323 and a direct hydrogen bond with Ser321. Arg345 forms a cation-pi interaction with the indole and a hydrogen bond with the amide carbonyl of indomethacin. Val366 forms hydrophobic contacts with chlorobenzene moiety. Thus, the amide carbonyl, indole, carboxylate, chlorobenzene as well as the methoxy moiety of indomethacin were found to play significant roles in the interaction with SIRT3.
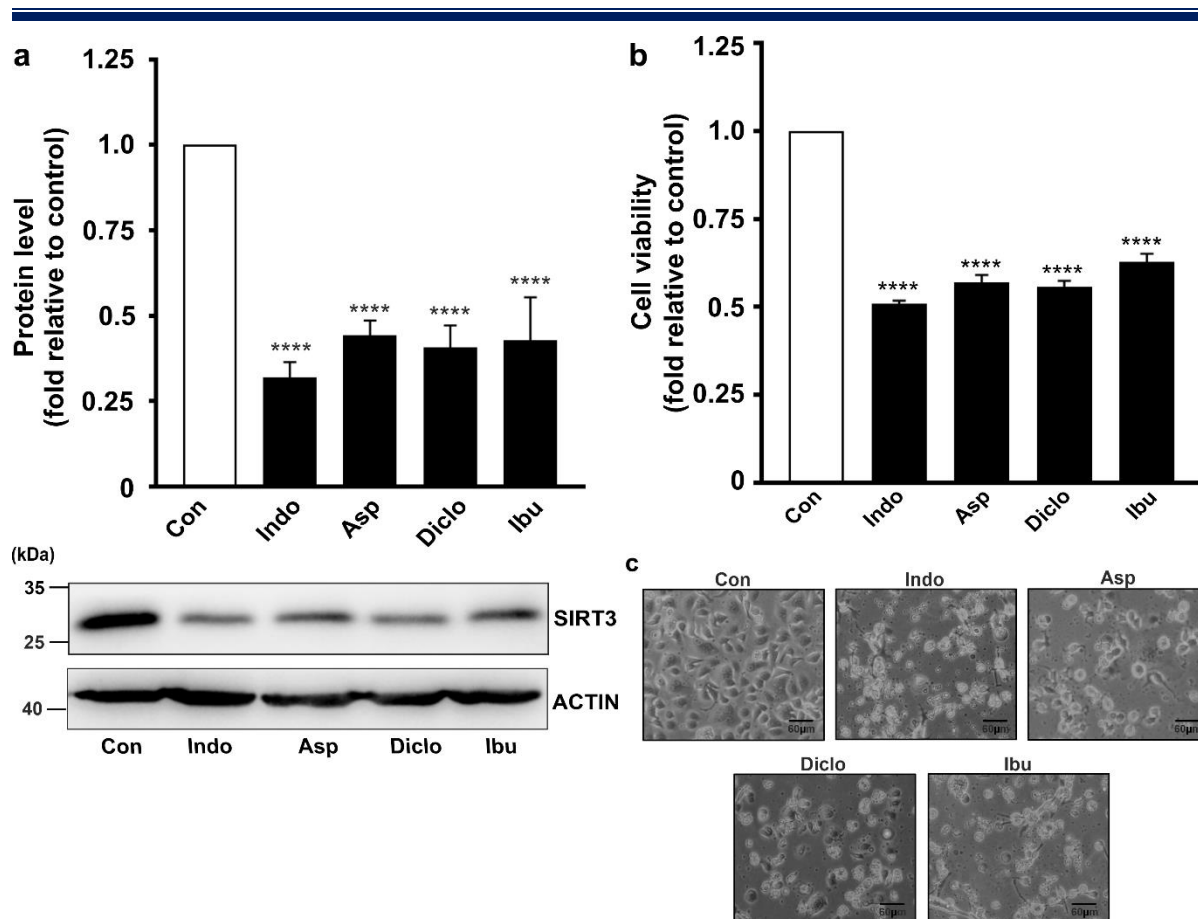
Fig. 10. Downregulation of SIRT3 is associated with the anti-cancer property of popular NSAIDs including diclofenac, aspirin and ibuprofen. (a) Immunoblot of SIRT3 in AGS cells treated with Indo (0.5 mM), Asp (8mM), Diclo (0.5 mM), and Ibu (2.5 mM) for 24 hr. ACTIN was used as the loading control; representative blots below the bar graph. **(b)** Cell viability represented as dehydrogenase activity in the control and NSAID-treated cells. **(c)** Phase-contrast micrographs of AGS cells treated with indicated NSAIDs. At least 3 randomly selected fields were captured and representative micrographs are presented. Data **(a-b)**, are mean $\pm$ SD ****$P < 0.0001$ versus 'control' calculated by one-way ANOVA followed by Bonferroni's post hoc test. The number of independently repeated experiments is 3 in every case.

3.8. SIRT3 downregulation by indomethacin accounts for mitochondrial damage and apoptosis in colon, cervical and hepatocellular carcinoma cells

Next, it was investigated whether the toxic effects of indomethacin involved SIRT3 in non-GC cells because NSAIDs have anti-cancer effects in a variety of malignancies (31), utilizing cell lines from three different carcinomas, namely HCT-116 (colorectal), HeLa (cervical), and HepG2 (hepatocellular). According to data, indomethacin treatment significantly decreased SIRT3 expression in HCT-116, HeLa, and HepG2 cells (Fig. 9a), and SIRT3 knockdown made the impact worse (Fig. 9b-d). Additionally, much like in the AGS cells, the indomethacin-induced mitochondrial depolarization and cell death were exacerbated by SIRT3 downregulation (Fig. 9e-g) (Fig. 9h-j). Thus, it appears that SIRT3 decrease is a crucial and widespread reaction responsible for the anti-neoplastic effect of indomethacin against a variety of cancer cells.

3.9. SIRT3 reduction is a common cytotoxic action triggered by popular NSAIDs to induce cancer cell death.

Finally, I investigated whether SIRT3 downregulation was unique to indomethacin or universal to well-known NSAIDS including diclofenac, aspirin, and ibuprofen, which also have anti-inflammatory

properties and anti-tumor activity. Data showed that all three of these NSAIDs dramatically decreased SIRT3 expression while also reducing cell viability and destroying the cytoarchitecture (Fig. 10a) (Fig. 10b-c). Since the effects were generally equivalent to those of indomethacin, SIRT3 depletion may be a frequent occurrence underpinning the harmful effects of NSAIDs.

4. DISCUSSION

In this chapter, it is reported how indomethacin (an NSAID) targets SIRT3 to show its antineoplastic effect against GC. Transcriptome sequencing of control and indomethacin-treated AGS cells identified SIRT3 as a prominent target that is markedly downregulated by NSAIDs. The antioxidant protein SIRT3 is downregulated, which destroys the redox equilibrium of the cell and causes oxidative stress, mitochondrial damage, and apoptosis. While I demonstrate the mechanism by which indomethacin decreases SIRT3 expression together with its upstream regulators (PGC1α and ERRα), it also inhibits AMPK activity, which together suppresses the AMPK-PGC1α -SIRT3 signaling axis. Additionally, SIRT3 knockdown exacerbates NSAID-induced cytotoxicity by escalating mitochondrial oxidative damage and cellular bioenergetic crisis. Due to its probable binding site overlap with NAD, indomethacin competitively suppresses SIRT3 activity, which has a direct impact on SIRT3 activity. Additionally, SIRT3 decrease appears to be a widespread impact of common NSAIDs and may even be a consistent cytotoxic effect, which may explain the NSAID-induced mortality of colon, cervical, and hepatocellular cancer cell lines. A very aggressive cancer, GC has a complicated pathophysiology, genetic heterogeneity, and few effective treatment choices, particularly for those with advanced tumors and numerous metastases (32). Notably, the prognosis for GC is made worse by the fact that it is nearly never identified until it has progressed. According to Lauren's criteria, GC is divided into intestinal and diffuse types even though 90% of gastric tumors are adenocarcinomas (33). The precise biological characteristic of a tumor is frequently determined using additional metrics or a combination of a few parameters. As of now, the list of actionable molecular targets includes HER2, VEGF, EGFR, FGFR2, CDH1, CTLA-4, and PD-1/PD-L1 (34). However, the search for fresh molecular targets with greater actionability is always growing. High age, male sex, tobacco use, race, familial history, inactivity, radiation exposure, and fiber intake are risk factors that are common to both non-cardia and cardia GCs; however, *Helicobacter pylori* infection, radiation exposure, high intake of salty and smoked food are specific risk factors for non-cardia GC; and obesity and GERD are specific risk factors for cardia GC (35). Geographically speaking, South and Central America, East Asia, Eastern Europe, and North America all have higher rates of GC than Africa and North America do. Additionally, in terms of racial variance, white Americans are twice as likely to have cardia GC, whereas Asian/Pacific islanders, Black people, and Hispanics are more likely to have non-cardia GC, which emphasizes the regulatory impacts of environmental variables (35). Precise knowledge about tumor biology and risk factors is therefore crucial while strategizing treatment plans. With regard to treatment, emerging reports on drug repurposing of NSAIDs in cancer have highlighted their anti-neoplastic potential in GCs (36-38). The COX-independent effects of NSAIDs predominantly involve the induction of severe mitochondrial damage (39). However, precise sub-mitochondrial targets of NSAIDs, specifically in the aggressive-phenotype GC cells, remain yet to be identified. Therefore, using indomethacin as a standard NSAID with negligible COX selectivity (to rule out COX-1/COX-2 bias), I primarily undertook deep transcriptomic sequencing of treated AGS cells for unbiased identification of any novel actionable sub-mitochondrial target. It is worth mentioning at this point that indomethacin is also used against human malignancies besides treating pain/inflammation (40,41). While avoiding any interfering metabolic effects that would be anticipated in vivo, AGS cells made it simple to explore the mechanisms behind and functionally validate the direct lethal effects of NSAIDs on a pure gastric cancer cell line. In this study, a relatively low indomethacin dose (IC$_{50}$) was employed to study the subtle sub-cellular processes

that could have been challenging to observe at a greater lethal level. Indomethacin generated considerable cytotoxicity, as seen by increased MOS and apoptosis, even at a sub-lethal dosage. Transcriptomics based on sequencing allowed for an impartial investigation of NSAID-induced DEGs. In cells treated with NSAIDs, a distinct separation of gene sets was observed. Pathway analysis and network clustering revealed a coordinated upregulation of metabolic pathways involving carbohydrate, amino acid, and fatty acid metabolism as well as mitochondrial central dogma, specifically OXPHOS, and downregulation of pathways involving protein ubiquitination, cell death, and ROS metabolism. SIRT3 was found to have considerably lower expression than the other highlighted DEGs. SIRT3 is an important connection between many metabolic pathways, the antioxidant defense of the mitochondria, and the integrity of cellular bioenergetics. SIRT3, often referred to as the "guardian of mitochondria," controls a variety of mitochondrial proteins, including those involved in the TCA cycle, mitochondrial biogenesis, and mitochondrial dynamics (42). Through the deacetylation-dependent control of transcriptional regulators like FOXO3 and LKB1, SIRT3 also controls gene expression. In particular, SOD2 and OGG1, which have been linked to a variety of diseases, including cancer, are the main deacetylation targets of SIRT3 (43). It's interesting to note that the NSAID-induced downregulation of SIRT3 and OGG1 in AGS cells in our work is consistent with the TCGA data, which also shows that SIRT3 and SOD2 are significantly expressed in GC. Additionally, Kaplan-Meier survival curves show that SIRT3 and OGG1 high-expressing groups have shorter median overall survival times (99.4 and 77.2 months, respectively) than low-expressing groups. Furthermore, although GC has a varied racial incidence depending on race, GCs from diverse races such Caucasian, African American, and Asian have considerably high SIRT3 expression. SIRT3 thus appears to be a significant mitochondrial target linked to a poor prognosis in GC. In this regard, I found that indomethacin specifically targeted SIRT3 at multiple levels by downregulating SIRT3 transcriptional regulators ERRα and PGC1α, decreasing SIRT3 gene and protein expression, blocking SIRT3 deacetylase activity, increasing mitochondrial protein acetylation, and specifically acetylating OGG1 and SOD2. Additionally, indomethacin decreased AMPK activity to obstruct the AMPK- PGC1α -SIRT3 signaling pathway. Treatment with indomethacin in AGS cells resulted in a decrease in total AMPK and phosphorylated AMPK levels in conjunction with ATP depletion, SIRT3 downregulation, and PGC1α downregulation. This is consistent with findings that indicate SIRT3 indirectly controls PGC1α expression through FOXO3 deacetylation and AMPK activation (44), and AMPK- PGC1α signaling boosts SIRT3 expression while also maintaining mitochondrial structural and functional integrity (45). Furthermore, because PGC1α is a strong regulator of mitochondrial biogenesis, it further supports the idea that mitochondrial depletion occurs while NSAIDs are acting. Consequently, increased mitochondrial fission and clearance of injured mitochondria with high ROS load are linked to SIRT3 loss following indomethacin therapy. In fact, it was discovered that SIRT3 knockdown made this impact worse. This is consistent with other studies that linked SIRT3 depletion to mitochondrial DNA damage in illnesses (46). In this situation, I observed that NSAID treatment of SIRT3-silenced cells significantly enhanced intra-mitochondrial superoxide load and 8-oxo-dG accumulation, demonstrating the rapid negative effects of acetylated SOD2 and OGG1 depletion. All of these consequences result in reduced viability of AGS cells, with decreased SIRT3 being responsible for severe mitochondrial depolarization and subsequent death. Additionally, SIRT3 was downregulated and cell viability was decreased as a result of indomethacin-induced depletion of ERRα and PGC1α, elucidating the mechanism by which NSAIDs inhibit SIRT3 at the gene level.

 Although SIRT3 is known to prefer OXPHOS over glycolysis in the context of cancer (42), tumor-specific actions of SIRT3 cannot be overlooked due to its high expression and effects that promote glycolysis and assure cell proliferation (47). This suggests that SIRT3 may have an oncogenic function in cancers that are dependent on glycolysis but less OXPHOS-dependent. To satisfy their energy needs for maintaining their maximum survival in a damaged tumor microenvironment, cancer cells really actively adapt to shifting surroundings by switching between glycolysis and OXPHOS (48-50). There
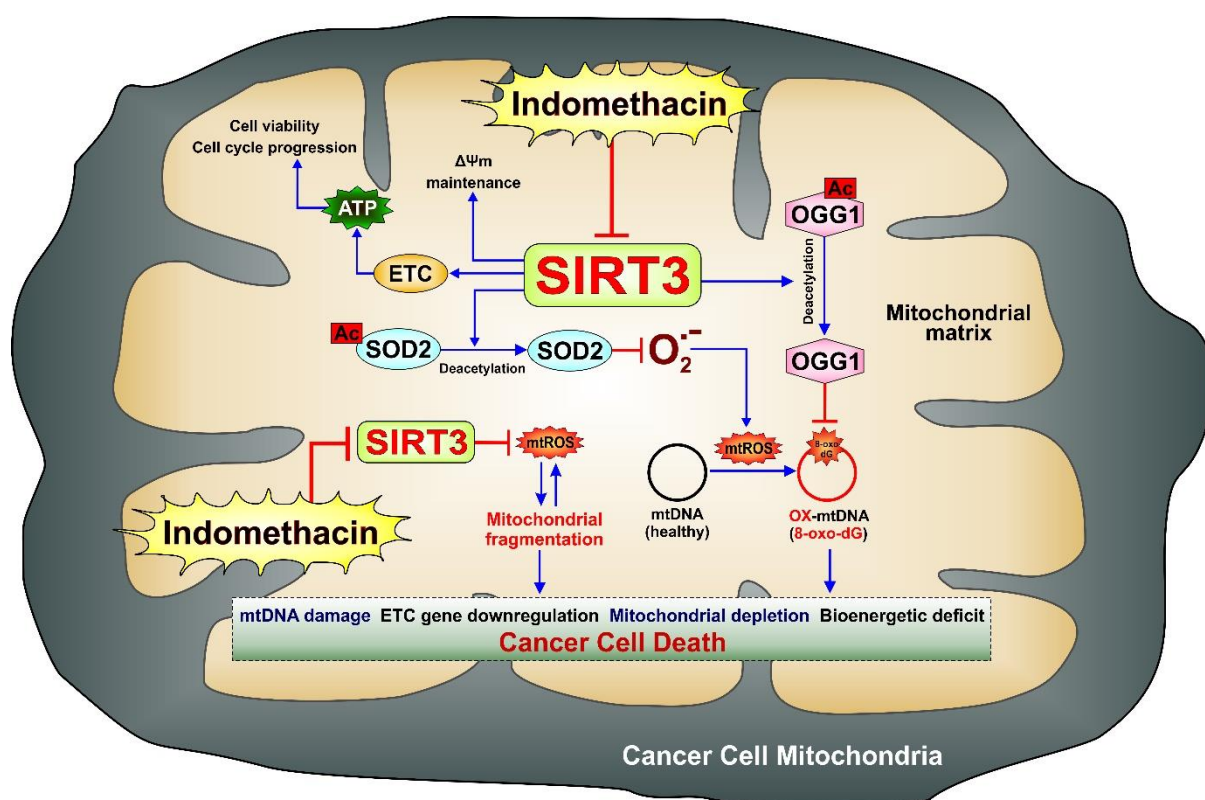
Fig 11. Graphical representation of the mechanistic basis of NSAID-induced SIRT3reduction and its consequence on mitochondrial functional integrity and hence cancer cell viability.

is a lot of evidence for SIRT3's tumor-suppressing and oncogenic effects in many cancers (42). But I distinctly found that SIRT3 downregulation made NSAID-induced AGS cell death substantially worse. Due to SIRT3's significance in maintaining cellular integrity under resting settings, I also observed that silencing it had a little negative impact on cell viability (47). Similar to SIRT3 silencing, ectopic SIRT3 overexpression may also be dangerous for cancer cells since it would cause CypD to become dissociated from the VDAC complex due to hyperactivated SIRT3 deacetylating it. In turn, released CypD would prevent Hexokinase II (HK2) from attaching to VDAC, resulting in VDAC's separation from the mitochondrial inner membrane. The anti-neoplastic cytoprotective action of mitochondrial membrane-bound HK2 is achieved by reducing the buildup of mitochondrial BAX (51). In fact, it has been discovered that HK2 blocks the release of cytochrome c and the activation of caspase 3 that are brought on by indomethacin (52). Additionally, SIRT3 overexpression may negatively impact redox equilibrium in cancer cells by excessively suppressing ROS levels (as a result of its multifaceted antioxidant actions). As a result, I logically decided against using SIRT3 overexpression as a validation strategy in our work since preserving cancer cells' integrity requires an optimal SIRT3 level, which is incredibly challenging in an ectopic overexpression system. It was shown that indomethacin has a potential binding-site overlap with NAD to plausibly induce competitive suppression of SIRT3 deacetylase activity. This finding relates to the molecular basis of SIRT3 inhibition. Based on molecular docking, it was determined that indomethacin and NAD may compete for stable SIRT3 binding with the least amount of conformational distortion. Additionally, detailed structural analysis was based on molecular dynamics simulation, which showed that indomethacin's amide carbonyl, indole, carboxylate, chlorobenzene, and methoxy moieties contribute significantly to the binding of SIRT3 to His248. Phe180. Phe294. Arg158. Glu177. Gly295. Phe157. Phe294. Ile230. Thr320. Glu323. Ser321. and Arg345. Indomethacin appeared to be the best ligand with the lowest binding free energy when

compared to other NSAIDs including diclofenac, ibuprofen, and aspirin, making it a potential SIRT3 inhibitor that may be used in the development of NSAID-based anti-cancer drugs that particularly target SIRT3. The advantage of indomethacin over diclofenac, ibuprofen, and aspirin in terms of SIRT3 binding was demonstrated by in silico data, but I examined the impact of these NSAIDs on SIRT3 expression, which may work independently of direct protein-binding effectiveness. Notably, SIRT3 expression was markedly downregulated together with the loss of cell viability, highlighting the significance of SIRT3 suppression as a widespread side effect of well-known NSAIDs used to treat human illnesses. Ultimately, the observation that indomethacin-induced death of other diverse cancer cells like colon, cervical, and hepatocellular carcinomas also significantly involve SIRT3 depletion-associated loss of mitochondrial integrity proved the significance of SIRT3 as a pivotal and undisputed regulator of anti-cancer effects of NSAIDs. Targeted SIRT3 knockdown in these cell lines significantly exacerbated the harmful effects of indomethacin, similar to gastric cancer.

5. CONCLUSION

The major finding of the work involves documenting the inhibitory action of NSAIDs on SIRT3 in cancer cells leading to metabolic and bioenergetic crisis consequent with the induction of apoptosis. High-depth next-generation transcriptome sequencing was used for unbiased probing of indomethacin-induced differential gene expressions accounting for gastric cancer (GC) cell death. Target prediction followed by multidimensional functional validations revealed that SIRT3 gets significantly downregulated, both at the gene and protein expression levels, in the indomethacin-treated cells leading to mitochondrial structural and functional damage. In fact, TCGA stomach adenocarcinoma data mining also suggested that high SIRT3 expression in GC patients is associated with poor prognosis and low median overall survival. Mitochondrial pathology due to indomethacin-induced SIRT3 reduction was found to crucially involve augmented intra-mitochondrial superoxide anions and 8-oxo-dG content as direct consequence of SOD2 and OGG1 hyperacetylation and depletion. Consequent elevation in pro-oxidant burden contributed to mitochondrial depolarization, fragmentation, respiratory chain failure, bioenergetic crisis and ultimately cell death in cancer cells. I provided first-hand report about the mechanism of inhibition of SIRT3 deacetylase activity by indomethacin wherein indomethacin exerts competitive inhibition due to biding site overlap with NAD+. Mechanistically, I showed that indomethacin downregulates SIRT3 transcriptional regulators, PGC1α and ERRα, as well as reduces AMPK activation to block AMPK/PGC1α/SIRT3 signaling axis in GC cells. The resultant effect of SIRT3 signaling blockage translates into mitochondrial hyperacetylation, mtDNA damage, ETC complex gene downregulation, mitochondrial fragmentation and elevated mitophagy. Functional validation relied on specific SIRT3 silencing, which significantly intensified the mitotoxic effects of indomethacin in addition to blocking cell cycle progression, aggravating intra-mitochondrial superoxide ions accumulation and increasing GC cell death. Therefore, it can be concluded that SIRT3 downregulation is a pivotal event in controlling cell death by NSAIDs. This information has enormous translational value since SIRT3 silencing combined with NSAID therapy can be used as a successful antineoplastic approach against malignancies that are resistant to therapy and have poor prognosis.

6. REFERENCES

1. Bindu, S., Mazumder, S., and Bandyopadhyay, U. (2020) Non-steroidal anti-inflammatory drugs (NSAIDs) and organ damage: A current perspective. *Biochem Pharmacol* **180**, 114147
2. Tuynman, J. B., Buskens, C. J., Kemper, K., ten Kate, F. J., Offerhaus, G. J., Richel, D. J., and van Lanschot, J. J. (2005) Neoadjuvant selective COX-2 inhibition down-regulates important oncogenic pathways in patients with esophageal adenocarcinoma. *Ann Surg* **242**, 840-849, discussion 849-850

3. Shaji, S., Smith, C., and Forget, P. (2021) Perioperative NSAIDs and Long-Term Outcomes After cancer Surgery: a Systematic Review and Meta-analysis. *Curr Oncol Rep* **23**, 146

4. Ahnen, D. J. (1998) Colon cancer prevention by NSAIDs: what is the mechanism of action? *Eur J Surg Suppl*, 111-114

5. Rigas, B., and Shiff, S. J. (2000) Is inhibition of cyclooxygenase required for the chemopreventive effect of NSAIDs in colon cancer? A model reconciling the current contradiction. *Med Hypotheses* **54**, 210-215

6. Huang, M., Myers, C. R., Wang, Y., and You, M. (2021) Mitochondria as a Novel Target for Cancer Chemoprevention: Emergence of Mitochondrial-targeting Agents. *Cancer Prev Res (Phila)* **14**, 285-306

7. Ansari, A., Rahman, M. S., Saha, S. K., Saikot, F. K., Deep, A., and Kim, K. H. (2017) Function of the SIRT3 mitochondrial deacetylase in cellular physiology, cancer, and neurodegenerative disease. *Aging Cell* **16**, 4-16

8. Kumar, S., and Lombard, D. B. (2015) Mitochondrial sirtuins and their relationships with metabolic disease and cancer. *Antioxid Redox Signal* **22**, 1060-1077

9. Carafa, V., Rotili, D., Forgione, M., Cuomo, F., Serretiello, E., Hailu, G. S., Jarho, E., Lahtela-Kakkonen, M., Mai, A., and Altucci, L. (2016) Sirtuin functions and modulation: from chemistry to the clinic. *Clin Epigenetics* **8**, 61

10. Sung, H., Ferlay, J., Siegel, R. L., Laversanne, M., Soerjomataram, I., Jemal, A., and Bray, F. (2021) Global Cancer Statistics 2020: GLOBOCAN Estimates of Incidence and Mortality Worldwide for 36 Cancers in 185 Countries. *CA Cancer J Clin* **71**, 209-249

11. Li, Y., Feng, A., Zheng, S., Chen, C., and Lyu, J. (2022) Recent Estimates and Predictions of 5-Year Survival in Patients with Gastric Cancer: A Model-Based Period Analysis. *Cancer Control* **29**, 10732748221099227

12. Kumar, V., Soni, P., Garg, M., Kamholz, S., and Chandra, A. B. (2018) Emerging Therapies in the Management of Advanced-Stage Gastric Cancer. *Front Pharmacol* **9**, 404

13. Wen, B., Wei, Y. T., Mu, L. L., Wen, G. R., and Zhao, K. (2020) The molecular mechanisms of celecoxib in tumor development. *Medicine (Baltimore)* **99**, e22544

14. De, R., Sarkar, S., Mazumder, S., Debsharma, S., Siddiqui, A. A., Saha, S. J., Banerjee, C., Nag, S., Saha, D., Pramanik, S., and Bandyopadhyay, U. (2018) Macrophage migration inhibitory factor regulates mitochondrial dynamics and cell growth of human cancer cell lines through CD74-NF-kappaB signaling. *J Biol Chem* **293**, 19740-19760

15. Andrews, S. (2010) FastQC: A Quality Control Tool for High Throughput Sequence Data [Online]. . *Available online at: http://www.bioinformatics.babraham.ac.uk/projects/fastqc/*

16. Martin, M. (2011) Cutadapt Removes Adapter Sequences from High-Throughput Sequencing Reads. *EMBnet Journal* **17**, 10-12

17. Pertea, M., Kim, D., Pertea, G. M., Leek, J. T., and Salzberg, S. L. (2016) Transcript-level expression analysis of RNA-seq experiments with HISAT, StringTie and Ballgown. *Nature Protocols* **11**, 1650-1667

18. Li, H., Handsaker, B., Wysoker, A., Fennell, T., Ruan, J., Homer, N., Marth, G., Abecasis, G., Durbin, R., and Subgroup, G. P. D. P. (2009) The Sequence Alignment/Map format and SAMtools. *Bioinformatics* **25**, 2078-2079

19. Liao, Y., Smyth, G. K., and Shi, W. (2014) featureCounts: an efficient general purpose program for assigning sequence reads to genomic features. *Bioinformatics* **30**, 923-930

20. Love, M. I., Huber, W., and Anders, S. (2014) Moderated estimation of fold change and dispersion for RNA-seq data with DESeq2. *Genome Biology* **15**, 550

21. Huo, Q., Li, Z., Cheng, L., Yang, F., and Xie, N. (2020) SIRT7 Is a Prognostic Biomarker Associated With Immune Infiltration in Luminal Breast Cancer. *Front Oncol* **10**, 621

22. Szasz, A. M., Lanczky, A., Nagy, A., Forster, S., Hark, K., Green, J. E., Boussioutas, A., Busuttil, R., Szabo, A., and Gyorffy, B. (2016) Cross-validation of survival associated biomarkers in gastric cancer using transcriptomic data of 1,065 patients. *Oncotarget* **7**, 49322-49333

23. Joosten, R. P., Womack, T., Vriend, G., and Bricogne, G. (2009) Re-refinement from deposited X-ray data can deliver improved models for most PDB entries. *Acta Crystallogr D Biol Crystallogr* **65**, 176-185

24. Trott, O., and Olson, A. J. (2010) AutoDock Vina: improving the speed and accuracy of docking with a new scoring function, efficient optimization, and multithreading. *J Comput Chem* **31**, 455-461

25. Azuara, C., Lindahl, E., Koehl, P., Orland, H., and Delarue, M. (2006) PDB_Hydro: incorporating dipolar solvents with variable density in the Poisson-Boltzmann treatment of macromolecule electrostatics. *Nucleic Acids Res* **34**, W38-42

26. Morris, G. M., Huey, R., Lindstrom, W., Sanner, M. F., Belew, R. K., Goodsell, D. S., and Olson, A. J. (2009) AutoDock4 and AutoDockTools4: Automated docking with selective receptor flexibility. *J Comput Chem* **30**, 2785-2791

27. Pal, U., Pramanik, S. K., Bhattacharya, B., Banerji, B., and N, C. M. (2016) Binding interaction of a gamma-aminobutyric acid derivative with serum albumin: an insight by fluorescence and molecular modeling analysis. *Springerplus* **5**, 1121

28. Bader, G. D., and Hogue, C. W. (2003) An automated method for finding molecular complexes in large protein interaction networks. *BMC bioinformatics* **4**, 2

29. Shannon, P., Markiel, A., Ozier, O., Baliga, N. S., Wang, J. T., Ramage, D., Amin, N., Schwikowski, B., and Ideker, T. (2003) Cytoscape: a software environment for integrated models of biomolecular interaction networks. *Genome research* **13**, 2498-2504

30. Wang, Y., Li, X., and Zhao, F. (2021) MCU-Dependent mROS Generation Regulates Cell Metabolism and Cell Death Modulated by the AMPK/PGC-1alpha/SIRT3 Signaling Pathway. *Front Med (Lausanne)* **8**, 674986

31. Zhang, Z., Chen, F., and Shang, L. (2018) Advances in antitumor effects of NSAIDs. *Cancer Manag Res* **10**, 4631-4640

32. Selim, J. H., Shaheen, S., Sheu, W. C., and Hsueh, C. T. (2019) Targeted and novel therapy in advanced gastric cancer. *Exp Hematol Oncol* **8**, 25

33. Ma, J., Shen, H., Kapesa, L., and Zeng, S. (2016) Lauren classification and individualized chemotherapy in gastric cancer. *Oncol Lett* **11**, 2959-2964

34. Bin, Y. L., Hu, H. S., Tian, F., Wen, Z. H., Yang, M. F., Wu, B. H., Wang, L. S., Yao, J., and Li, D. F. (2021) Metabolic Reprogramming in Gastric Cancer: Trojan Horse Effect. *Front Oncol* **11**, 745209

35. Karimi, P., Islami, F., Anandasabapathy, S., Freedman, N. D., and Kamangar, F. (2014) Gastric cancer: descriptive epidemiology, risk factors, screening, and prevention. *Cancer Epidemiol Biomarkers Prev* **23**, 700-713

36. Brusselaers, N., and Lagergren, J. (2018) Maintenance use of non-steroidal anti-inflammatory drugs and risk of gastrointestinal cancer in a nationwide population-based cohort study in Sweden. *BMJ Open* **8**, e021869

37. Li, L., Hu, M., Wang, T., Chen, H., and Xu, L. (2019) Repositioning Aspirin to Treat Lung and Breast Cancers and Overcome Acquired Resistance to Targeted Therapy. *Front Oncol* **9**, 1503

38. Kumar, R. (2016) Repositioning of Non-Steroidal Anti Inflammatory Drug (NSAIDs) for Cancer Treatment: Promises and Challenges. *Journal of Nanomedicine & Nanotechnology* **7**

39. Brandolini, L., Antonosante, A., Giorgio, C., Bagnasco, M., d'Angelo, M., Castelli, V., Benedetti, E., Cimini, A., and Allegretti, M. (2020) NSAIDs-dependent adaption of the mitochondria-proteasome system in immortalized human cardiomyocytes. *Sci Rep* **10**, 18337

40. Woo, J. K., Kang, J. H., Jang, Y. S., Ro, S., Cho, J. M., Kim, H. M., Lee, S. J., and Oh, S. H. (2015) Evaluation of preventive and therapeutic activity of novel non-steroidal anti-inflammatory drug, CG100649, in colon cancer: Increased expression of TNF-related apoptosis-inducing ligand receptors enhance the apoptotic response to combination treatment with TRAIL. *Oncol Rep* **33**, 1947-1955

41. Lai, S. W., and Liao, K. F. (2013) Aspirin use after diagnosis improves survival in older adults with colon cancer. *J Am Geriatr Soc* **61**, 843-844

42. Zhang, J., Xiang, H., Liu, J., Chen, Y., He, R. R., and Liu, B. (2020) Mitochondrial Sirtuin 3: New emerging biological function and therapeutic target. *Theranostics* **10**, 8315-8342

43. Torrens-Mas, M., Oliver, J., Roca, P., and Sastre-Serra, J. (2017) SIRT3: Oncogene and Tumor Suppressor in Cancer. *Cancers (Basel)* **9**

44. Li, Y., Wang, Q., Li, J., Shi, B., Liu, Y., and Wang, P. (2021) SIRT3 affects mitochondrial metabolic reprogramming via the AMPK-PGC-1alpha axis in the development of benign prostatic hyperplasia. *Prostate* **81**, 1135-1148

45. Yu, L., Gong, B., Duan, W., Fan, C., Zhang, J., Li, Z., Xue, X., Xu, Y., Meng, D., Li, B., Zhang, M., Bin, Z., Jin, Z., Yu, S., Yang, Y., and Wang, H. (2017) Melatonin ameliorates myocardial ischemia/reperfusion injury in type 1 diabetic rats by preserving mitochondrial function: role of AMPK-PGC-1alpha-SIRT3 signaling. *Sci Rep* **7**, 41337

46. Pillai, V. B., Bindu, S., Sharp, W., Fang, Y. H., Kim, G., Gupta, M., Samant, S., and Gupta, M. P. (2016) Sirt3 protects mitochondrial DNA damage and blocks the development of doxorubicin-induced cardiomyopathy in mice. *Am J Physiol Heart Circ Physiol* **310**, H962-972

47. Cui, Y., Qin, L., Wu, J., Qu, X., Hou, C., Sun, W., Li, S., Vaughan, A. T., Li, J. J., and Liu, J. (2015) SIRT3 Enhances Glycolysis and Proliferation in SIRT3-Expressing Gastric Cancer Cells. *PLoS One* **10**, e0129834

48. Shiratori, R., Furuichi, K., Yamaguchi, M., Miyazaki, N., Aoki, H., Chibana, H., Ito, K., and Aoki, S. (2019) Glycolytic suppression dramatically changes the intracellular metabolic profile of multiple cancer cell lines in a mitochondrial metabolism-dependent manner. *Sci Rep* **9**, 18699

49. Lasche, M., Emons, G., and Grundker, C. (2020) Shedding New Light on Cancer Metabolism: A Metabolic Tightrope Between Life and Death. *Front Oncol* **10**, 409

50. Jose, C., Bellance, N., and Rossignol, R. (2011) Choosing between glycolysis and oxidative phosphorylation: a tumor's dilemma? *Biochim Biophys Acta* **1807**, 552-561

51. Schoeniger, A., Wolf, P., and Edlich, F. (2022) How Do Hexokinases Inhibit Receptor-Mediated Apoptosis? *Biology (Basel)* **11**

52. Pastorino, J. G., Shulga, N., and Hoek, J. B. (2002) Mitochondrial binding of hexokinase II inhibits Bax-induced cytochrome c release and apoptosis. *J Biol Chem* **277**, 7610-7618

SUMMARY OF WORK

SUMMARY OF WORK

Non-steroidal anti-inflammatory drugs (NSAIDs) are a unique class of over-the-counter anti-nociceptive agents/medicines which are distinct from acetaminophen due to their remarkable property of cyclooxygenase inhibition and prostaglandin suppression thereby preventing as well as ameliorating inflammation-associated myriad non-malignant and malignant pathologies. In spite of their broad range of therapeutic utilities, long term NSAID usage accompanies several side effects of which gastric mucosal injury and ulceration demands foremost mention. Although prostaglandin suppression apparently seems to be the most important factor contributing to the toxic effects of NSAIDs, research over decades have convincingly established that there are several cyclooxygenase/prostaglandin-independent signaling pathways which are directly activated upon NSAID treatment leading to cell death. Quest for precise knowledge about these cyclooxygenase/prostaglandin-independent sub-cellular targets of NSAIDs are ever increasing. The work in the present thesis is specifically directed to address this relevant issue and identify novel, actionable target/s of NSAIDs. Amidst various sub-cellular targets of NSAIDs, mitochondria demand foremost weightage owing to the fact that NSAIDs have been observed to directly bind to a site adjacent to complex-I of the electron transport chain resulting in electron leakage and generation of superoxide anions, the progenitor reactive oxygen species. The superoxide ions eventually transform into other detrimental ROS including hydrogen peroxide and hydroxyl radicals which collectively inflict 'mitochondrial oxidative stress', the fundamental event responsible for cellular redox dyshomeostasis, bioenergetic crisis and cell death. Gastric mucosal injury by NSAIDs evidently involves MOS and abrogated mitochondrial structural dynamic homeostasis in a cyclooxygenase/prostaglandin-independent manner. However, the intricate sub-mitochondrial events, activated by NSAIDs, leading to cell death are only beginning to be revealed. The work in this thesis is specifically targeted towards identifying specific sub-mitochondrial target/s of NSAIDs which are directly responsible for inducing bioenergetic crisis and cell death so that these wonder drugs can be rationally utilized upon taming their detrimental effects while optimizing the benefits.

In the first experimental chapter, a rodent model of acute gastric mucosal injury by NSAIDs has been used to study the effect on gastric mucosal mitochondrial metabolism. Indomethacin was selected due to its cyclooxygenase non-selective nature and rampant usage both in experimental studies as well as clinical trials. High-depth next generation transcriptome sequencing data revealed that SIRT3 was significantly down regulated in the gastric mucosa of indomethacin-treated rats compared to control. Gene expression data correlated with protein expression pattern of SIRT3 as well as its major target OGG1. In fact, it was also observed that indomethacin directly inhibited SIRT3 deacetylase activity in a dose-dependent pattern. A direct impact of SIRT3 downregulation was realized from increased acetylation of mitochondrial proteome and specific acetylation of OGG1 and SOD2 thereby indicating disruption of cellular redox homeostasis and induction of oxidative stress. This was further evident from increased 8-oxo-dG level in the indomethacin-treated gastric samples. Indomethacin-dependent SIRT3 reduction was found to trigger mtDNA damage, respiratory chain defect and severe mitochondrial fragmentation leading to cell death and inflammatory tissue injury. Interestingly, a specific SIRT3 stimulator, Honokiol, significantly resisted indomethacin-induced SIRT3 depletion and mitochondrial dysfunctions thereby preventing gastric mucosal injury in a dose dependent manner. Honokiol also blocked indomethacin-induced downregulation of SIRT3 regulators, PGC1α and ERRα, as well as accelerated the healing of pre-formed gastric lesions by indomethacin but did not interfere with basal and MMI-stimulated gastric acid secretion unlike lansoprazole. Thus, SIRT3 was identified as a new target of NSAIDs wherein endogenous SIRT3 stimulation by phytopolyphenols like honokiol qualified as a potent gastroprotective agent which may be rationally utilized in producing new generation gastroprotective formulation (**Chapter 1**).

Having established the novel gastroprotective role of SIRT3 in non-malignant gastropathy by NSAIDs, it became extremely pertinent to explore, next, whether NSAID-induced gastric cancer cell death at all

involved SIRT3. The second experimental chapter precisely dealt with detailed mechanistic exploration of how indomethacin triggered mitochondrial bioenergetic crisis and apoptosis in gastric cancer using human gastric adenocarcinoma cell line (AGS). Here again, transcriptome sequencing was primarily undertaken to check the differential gene expression profiles in the control and indomethacin-treated AGS cells. A wide array of genes associated with cellular metabolism was found severely downregulated along with SIRT3 upon indomethacin treatment. Sequencing data rationally paved the way for in depth association studies which identified that indomethacin directly interacted with SIRT3 with a binding-site overlap with NAD to exert competitive inhibition of SIRT3 deacetylase activity. A direct relevance of the study was further tested by meta-analysis of the TCGA data set which revealed that high SIRT3 expression was associated with poor prognosis in gastric cancer. It was clearly observed that indomethacin severely jeopardized cellular redox homeostasis by augmenting acetylation of SOD2 and OGG1 as well as fragmenting the mitochondrial filament network. In fact, specific knockdown of SIRT3 expression as well as expression of its transcriptional regulators PGC1α and ERRα severely aggravated the mitochondrial toxic effects of indomethacin to amplify cell death and deter cell proliferation. The AMPK/PGC1α/SIRT3 axis was identified as the dominant pathway underlying indomethacin-induced gastric cancer cell death. Interestingly, other popular NSAIDs like diclofenac, aspirin and ibuprofen also involved SIRT3 downregulation to induce gastric cancer cell death thereby functionally establishing SIRT3 as a dominant target of NSAIDs to induce cancer cell death. These data hold immense relevance because SIRT3 knockdown supplemented with NSAID treatment may be ventured as a more effective anti-cancer strategy against drug-resistant tumors with bad prognosis (**Chapter 2**).

Collectively, the study for the first time identified SIRT3 as a predominant target of NSAIDs which is severely downregulated as well as inhibited by these wonder drugs to exert their toxic effect against normal gastric mucosal cells as well as gastric adenocarcinoma cells. Being the mitochondrial metabolic guardian, SIRT3 is quintessential in maintaining cellular integrity wherein the SIRT3 stimulator honokiol qualified as a potent gastroprotective agent which significantly resists mitochondrial damage and inflammatory tissue injury by NSAIDs without affecting basal acid suppression unlike existing anti-ulcer drugs. Moreover, being the metabolic fulcrum of a cell, SIRT3 depletion by NSAIDs severely hits the bioenergetic homeostasis to deter cancer cell proliferation, thereby explaining the basis of the anti-neoplastic action of NSAIDs which are being increasingly used in anti-cancer therapeutics.

LIST OF PUBLICATIONS

List of publications

1. **Honokiol, an inducer of Sirtuin 3, protects against NSAID-induced gastric mucosal mitochondrial pathology, apoptosis and inflammatory tissue injury**. **Subhashis Debsharma**, Saikat Pramanik, Samik Bindu, Somnath Mazumder, Troyee Das, Debanjan Saha, Rudranil De, Shiladitya Nag, Chinmoy Banerjee, Asim Azhar Siddiqui, Zhumur Ghosh, Uday Bandyopadhyay.*, British Journal of Pharmacology, PMID: 36914615, 2023*

2. **Indomethacin impairs mitochondrial dynamics by activating the PKCζ-p38-DRP1 pathway and inducing apoptosis in gastric cancer and normal mucosal cells.** Somnath Mazumder, Rudranil De, **Subhashis Debsharma**, Samik Bindu, Pallab Maity, Souvik Sarkar, Shubhra Jyoti Saha, Asim Azhar Siddiqui, Chinmoy Banerjee, Shiladitya Nag, Debanjan Saha, Saikat Pramanik, Kalyan Mitra, Uday Bandyopadhyay. *J Biol Chem; PMID: 30940726, 2019*

3. **Emerging role of mitochondrial DAMPs, aberrant mitochondrial dynamics and anomalous mitophagy in gut mucosal pathogenesis.** Somnath Mazumder, Samik Bindu, Rudranil De, **Subhashis Debsharma**, Saikat Pramanik, Uday Bandyopadhyay, *Life Sci. PMID: 35787999, 2022*

4. **Macrophage migration inhibitory factor regulates mitochondrial dynamics and cell growth of human cancer cell lines through CD74-NF-κB signaling.** Rudranil De, Souvik Sarkar, Somnath Mazumder, **Subhashis Debsharma**, Asim Azhar Siddiqui, Shubhra Jyoti Saha, Chinmoy Banerjee, Shiladitya Nag, Debanjan Saha, Saikat Pramanik, Uday Bandyopadhyay *J Biol Chem, PMID: 30366984, 2018*

5. **Acute mental stress induces mitochondrial bioenergetic crisis and hyper-fission along with aberrant mitophagy in the gut mucosa in rodent model of stress-related mucosal disease.** Rudranil De, Somnath Mazumder, Souvik Sarkar, **Subhashis Debsharma**, Asim Azhar Siddiqui, Shubhra Jyoti Saha, Chinmoy Banerjee, Shiladitya Nag, Debanjan Saha and Uday Bandyopadhyay *(2017) Free Radical Biology & Medicine, PMID: 28993273*

6. **Hydrazonophenol, a Food Vacuole-Targeted and Ferriprotoporphyrin IX-Interacting Chemotype Prevents Drug-Resistant Malaria.** Shubhra Jyoti Saha, Asim Azhar Siddiqui, Saikat Pramanik, Debanjan Saha, Rudranil De, Somnath Mazumder, **Subhashis Debsharma**, Shiladitya Nag, Chinmoy Banerjee, and Uday Bandyopadhyay *ACS Infect Dis. PMID: 30472841, 2019*

7. **Selective scavenging of intra-mitochondrial superoxide corrects diclofenac-induced mitochondrial dysfunction and gastric injury: A novel gastroprotective mechanism independent of gastric acid suppression.** Somnath Mazumder, Rudranil De, Souvik Sarkar, Asim Azhar Siddiqui, Shubhra Jyoti Saha, Chinmoy Banerjee, Mohd. Shameel Iqbal, Shiladitya Nag, **Subhashis Debsharma**, Uday Bandyopadhyay*, Biochemical Pharmacology, PMID: 27693316, 2016*

8. **Nuclease activity of Plasmodium falciparum Alba family protein PfAlba3**. Chinmoy Banerjee, Shiladitya Nag, Manish Goyal, Debanjan Saha, Asim Azhar Siddiqui, Somnath Mazumder, **Subhashis Debsharma**, Saikat Pramanik, Uday Bandyopadhyay. *Cell Reports, PMID: 36947546, 2023*

9. **Rab7 of Plasmodium falciparum is involved in its retromer complex assembly near the digestive vacuole.** Asim Azhar Siddiqui, Debanjan Saha, Mohd Shameel Iqbal, Shubhra Jyoti Saha, Souvik Sarkar, Chinmoy Banerjee, Shiladitya Nag, Somnath Mazumder, Rudranil De, Saikat Pramanik,

Subhashis Debsharma, Uday Bandyopadhyay. *Biochim Biophys Acta Gen Subj*, *PMID: 32512169*, *2020*

Manuscripts under review

1. **SIRT3, a target of non-steroidal anti-inflammatory drug to trigger mitochondrial dysfunction and gastric cancer cell death. Subhashis Debsharma**, Saikat Pramanik, Samik Bindu, Somnath Mazumder, Troyee Das, Uttam Pal, Rudranil De, Shiladitya Nag, Chinmoy Banerjee, Nakul Chandra Maiti, Zhumur Ghosh, Uday Bandyopadhyay [**under revision**]

2. **Tyrosine28 plays an essential role in the DNase activity of P. falciparum Alba6.** Shiladitya Nag; Chinmoy Banerjee; Manish Goyal; Asim Azhar Siddiqui; Debanjan Saha; Somnath Mazumder; **Subhashis Debsharma**; Shubhra Jyoti Saha; Saikat Pramanik; Rudranil De; Uday Bandyopadhyay [**under revision**]

Conference

<u>**Oral presentation**</u>

Title: Aberrant mitochondrial dynamics: a new therapeutic target for the management of pain killer-induced gastropathy

Conference: India International Science Festival (IISF) 2020, **Date:** 22.12.2020 - 24.12.2020 (Certificate attached)

<u>**Poster presentation**</u>

Title: Non-steroidal anti-inflammatory drugs induce mitochondrial hyperfission and bioenergetic crisis to induce gastric cancer cell death

Conference: FRONTIERS IN CANCER SCIENCE 2021, **Date:** 01.11.2021 - 03.11.2021 (Participation certificate attached)

<u>**As a co-author**</u>

Title: Selective scavenging of intra-mitochondrial prooxidants corrects non-steroidal anti-inflammatory drug-induced gastropathy: an acid secretion-independent novel gastroprotective strategy.

Conference details: Mechanistic and Therapeutic Approaches in Human and Animal Health, 2021; 6-8th December 2021, Dept. of Zoology, Cooch Behar Panchanan Barma University, India

Title: Non-steroidal anti-inflammatory drug, Indomethacin, impairs mitochondrial dynamics and cellular respiration to induce death in gastric cancer cells: the central effect targeting cellular metabolic hub

Conference details: India International Science Festival (IISF) 2019, 5-8th November 2019, Biswa Bangla Convention Centre & Science City, Kolkata, India

RESEARCH ARTICLE

Honokiol, an inducer of sirtuin-3, protects against non-steroidal anti-inflammatory drug-induced gastric mucosal mitochondrial pathology, apoptosis and inflammatory tissue injury

Subhashis Debsharma[1] | Saikat Pramanik[1] | Samik Bindu[2] |
Somnath Mazumder[3] | Troyee Das[4] | Debanjan Saha[1] | Rudranil De[5] |
Shiladitya Nag[1] | Chinmoy Banerjee[1] | Asim Azhar Siddiqui[1] | Zhumur Ghosh[4] |
Uday Bandyopadhyay[1,6] [ORCID]

[1]Division of Infectious Diseases and Immunology, CSIR-Indian Institute of Chemical Biology, Kolkata, West Bengal, India

[2]Department of Zoology, Cooch Behar Panchanan Barma University, Cooch Behar, West Bengal, India

[3]Department of Zoology, Raja Peary Mohan College, Uttarpara, West Bengal, India

[4]Division of Bioinformatics, Bose Institute, Kolkata, West Bengal, India

[5]Amity Institute of Biotechnology, Amity University, Kolkata, Kolkata, West Bengal, India

[6]Division of Molecular Medicine, Bose Institute, Kolkata, West Bengal, India

Correspondence
Dr Uday Bandyopadhyay, Division of Molecular Medicine, Bose Institute, EN 80, Sector V, Bidhan Nagar, Kolkata, West Bengal 700091, India.
Email: ubandyo_1964@yahoo.com; udayb@jcbose.ac.in

Funding information
Department of Biotechnology, Ministry of Science and Technology, India; Science and Engineering Research Board, Grant/Award Number: SB/S2/JCB-54/2014

Background and Purpose: Mitochondrial oxidative stress, inflammation and apoptosis primarily underlie gastric mucosal injury caused by the widely used non-steroidal anti-inflammatory drugs (NSAIDs). Alternative gastroprotective strategies are therefore needed. Sirtuin-3 pivotally maintains mitochondrial structural integrity and metabolism while preventing oxidative stress; however, its relevance to gastric injury was never explored. Here, we have investigated whether and how sirtuin-3 stimulation by the phytochemical, honokiol, could rescue NSAID-induced gastric injury.

Experimental Approach: Gastric injury in rats induced by indomethacin was used to assess the effects of honokiol. Next-generation sequencing-based transcriptomics followed by functional validation identified the gastroprotective function of sirtuin-3. Flow cytometry, immunoblotting, qRT-PCR and immunohistochemistry were used measure effects on oxidative stress, mitochondrial dynamics, electron transport chain function, and markers of inflammation and apoptosis. Sirtuin-3 deacetylase activity was also estimated and gastric luminal pH was measured.

Key Results: Indomethacin down-regulated sirtuin-3 to induce oxidative stress, mitochondrial hyperacetylation, 8-oxoguanine DNA glycosylase 1 depletion, mitochondrial DNA damage, respiratory chain defect and mitochondrial fragmentation leading to severe mucosal injury. Indomethacin dose-dependently inhibited sirtuin-3 deacetylase activity. Honokiol prevented mitochondrial oxidative damage and inflammatory tissue injury by attenuating indomethacin-induced depletion of both sirtuin-3 and its transcriptional regulators PGC1α and ERRα. Honokiol also accelerated gastric wound healing but did not alter gastric acid secretion, unlike lansoprazole.

Conclusions and Implications: Sirtuin-3 stimulation by honokiol prevented and reversed NSAID-induced gastric injury through maintaining mitochondrial integrity.

Honokiol did not affect gastric acid secretion. Sirtuin-3 stimulation by honokiol may be utilized as a mitochondria-based, acid-independent novel gastroprotective strategy against NSAIDs.

KEYWORDS

apoptosis, gastric injury, honokiol, mitochondria, non-steroidal anti-inflammatory drugs, Sirtuin-3

1 | INTRODUCTION

Non-steroidal anti-inflammatory drugs (NSAIDs) are widely used for managing diverse inflammatory disorders (Crofford, 2013; Ong et al., 2007). Furthermore, drug repurposing studies have shown NSAIDs to exhibit potent anticancer activities, as long-term NSAID users have a relatively lower risk of developing cancers in the GI tract, breast, prostate and lung (Cuzick et al., 2009; Kazberuk et al., 2020; Khoo et al., 2019). In spite of such a wide spectrum of therapeutic utility, prolonged usage of NSAIDs appears risky owing to their toxic effects on multiple organs, with the GI tract being the most severely affected (Bindu et al., 2020; Sostres et al., 2013). Therefore, precise knowledge about the subcellular target(s) of NSAIDs is crucial for optimizing their clinical usage while rationally avoiding their toxicity. NSAIDs are standard **cyclooxygenase 1/2** (COX1/2) inhibitors (Bindu et al., 2020; Whittle, 2000), although COX-independent effects are equally shown (Gurpinar et al., 2013; Gurpinar et al., 2014; Kolawole & Kashfi, 2022; Liggett et al., 2014). In this regard, mitochondrial oxidative stress (MOS) and intrinsic apoptosis constitute the major COX-independent NSAID actions, accounting for gut mucosal injury (Matsui et al., 2011). NSAIDs directly target mitochondria to jeopardize mitochondrial metabolism (Aminzadeh-Gohari et al., 2020; Bindu et al., 2020; Krause et al., 2003; Mazumder et al., 2022; Sandoval-Acuna et al., 2012; Suzuki et al., 2010). Therefore, it is logical that endogenous cytoprotective factors would promptly respond to combat the stress.

Mitochondrial antioxidants such as superoxide dismutase (SOD2) and the base excision repair enzyme, **8-oxoguanine DNA glycosylase 1 (OGG1)**, as well as mitochondrial electron transport chain (ETC) complex proteins and mitochondria-resident key enzymes in metabolic pathways, are regulated by deacetylation (Mazumder et al., 2020; Murugasamy et al., 2022; Zhang et al., 2020). Moreover, mitochondrial structural dynamics regulating outer membrane fusion GTPase, optic atrophy 1 (OPA1) and the master regulator of mitochondrial biogenesis, **PPAR-γ coactivator 1α (PGC1α)** are also stabilized by deacetylation. Such deacetylation is carried out by the NAD$^+$-dependent class III histone deacetylase **sirtuin-3 (Sirt3)**, functioning as a gatekeeper of mitochondrial integrity against stress (H. S. Kim et al., 2010; Mazumder et al., 2020). Thus, in Sirt3 knockout (KO) mice, there is a marked increase in acetylated mitochondrial proteins (Murugasamy et al., 2022). Further, Sirt3 depletion has been observed in several organ pathologies (Mao et al., 2022; Morigi et al., 2015; Pillai et al., 2015; Sun et al., 2020). However, there is no

What is already known

- Despite their gastrodamaging side-effects, NSAIDs appear unavoidable owing to their anti-inflammatory effects in diverse pathologies.
- NSAIDs target mitochondria, COX-independently, inducing apoptosis. However, precise sub-mitochondrial target(s) of NSAIDs are not known.

What does this study add

- Sirt3 is a new target of NSAIDs which is down-regulated during development of gastric injury.
- Honokiol-induced Sirt3 stimulation prevents indomethacin-induced mitochondrial pathology and inflammatory gastric injury without affecting acid secretion.

Clinical significance

- Sirt3 is a non-canonical COX-independent target of NSAIDs to induce gastric mucosal injury.
- Sirt3 stimulation represents a promising gastroprotective strategy that may benefit NSAIDs usage bypassing their side-effects.

report about any involvement of Sirt3 in NSAID-induced GI pathology or whether Sirt3 can be targeted as a possible gastroprotective strategy.

We therefore used an unbiased forward approach of target mining by next-generation sequencing of the gastric transcriptome in NSAID-treated rats. Interestingly, Sirt3 appeared as a prominent lead, and specific stimulation of Sirt3, by the phyto-polyphenol **honokiol** clearly prevented NSAID-induced mitochondrial damage and gastropathy without affecting basal gastric acid secretion, unlike existing anti-ulcer compounds. We compared the efficacy of intraperitoneal (i.p.) with that of intragastric (i.g.) administration of honokiol and found that a much lower dose was sufficient to provide significant

gastroprotection when administered i.p. Further, we extensively investigated the specific mitoprotective mode of action of honokiol in the gastric mucosa of NSAID-treated rats. Our findings identify Sirt3 as a hitherto unreported, dominant gastroprotective target, while revealing the potency of honokiol as a new generation gastroprotective agent. These findings will certainly provide novel therapeutic insights into NSAID-based treatment modalities, in which targeted stimulation of Sirt3 may help to avoid the toxic effects of NSAIDs, while strategically optimizing the benefits.

2 | METHODS

2.1 | In vivo model of NSAID-induced gastric mucosal damage

All animal care and experimental procedures were carried out with strict adherence to the approved guidelines of ARRIVE and the institutional animal ethics committee, registered with the Committee for the Purpose of Control and Supervision of Experiments on Animals (CPCSEA), India (Permit No. 147/1999/CPCSEA). Utmost care was taken to minimize the pain and suffering of the rats during experimental handling. Animal studies are reported in compliance with the ARRIVE guidelines (Percie du Sert et al., 2020) and with the recommendations made by the *British Journal of Pharmacology* (Lilley et al., 2020).

Sprague–Dawley rats (180–220 g) were provided by the institutional animal facility of CSIR-Indian Institute of Chemical Biology. Animals were maintained at $24 \pm 2°C$ with 12-h light–dark cycles and provided with standard rat chow and ad libitum access to water. Before the experiments, the rats were subjected to fasting for 24 h with free access to water. Rats of either sex were used for all in vivo experiments. However, in any specific experiment, rats from only a single sex have been used.

Gastric mucosal injury was induced by NSAIDs given by oral administration. Indomethacin (48 mg·kg^{-1}) was dissolved in distilled water supplemented with minimal volumes of alkali (Na_2CO_3), as mentioned previously (Bindu et al., 2013; Mazumder et al., 2019). The pH of the resultant solution was checked before administration. Diclofenac (75 mg·kg^{-1}) and ibuprofen (400 mg·kg^{-1}) were obtained as sodium salts and hence dissolved in distilled water; aspirin (400 mg·kg^{-1}) was administered as suspension in 1% carboxymethylcellulose, as mentioned previously (Ghori et al., 2016; Maharani, 2022; Mazumder et al., 2016; Raghavendran et al., 2011). A separate group of rats (n = 5) were also treated with vehicles (1% carboxymethylcellulose or alkaline water). No detectable gastric mucosal injury was observed. The gastric injury was allowed to develop, and after 4 h, the rats were humanely killed (asphyxiation with >90% CO_2 followed by cervical dislocation) and gastric mucosal samples were collected for subsequent experiments. For the honokiol-induced protection set (HKL + Indo), rats were pre-treated with honokiol i.p. (40 mg·kg^{-1}), followed by oral administration of indomethacin after 30 min. For i.p. administration, honokiol was dissolved in peanut oil and injected as described previously (Pillai et al., 2015). The ED$_{50}$ of honokiol was derived from a dose–response study ranging from 5 to 60 mg·kg^{-1}. A separate group of rats (n = 5) were also treated with the vehicle (peanut oil) followed by oral administration of indomethacin. No detectable protection was observed in the vehicle-treated group, and the extent of mucosal injury was comparable with that after indomethacin treatment. Honokiol, at different doses (20, 40, 60 and 80 mg·kg^{-1} bw), was also given i.g. in a separate group of rats 30 min prior to indomethacin administration as mentioned above, to compare the efficacy of i.p. with that of i.g. administration. For i.g. administration, honokiol was suspended in a solution of carboxymethylcellulose sodium salt (0.5%), as described previously (Wang, Zhai, & Chen, 2018). Gastric injury was allowed to develop. After 4 h, the rats were humanely killed and the gastric mucosa examined to determine the injury index (II) scores and comparison of efficacy between ip and ig administration of honokiol. A separate group of rats (n = 5) were treated i.g. with 0.5% carboxymethylcellulose solution followed by oral administration of indomethacin. No detectable protection was observed in the vehicle-treated group.

For gastric mucosal wound healing studies, 2 sets of rats (20 rats per set) were treated with indomethacin and mucosal injury was allowed to develop for 4 h. After 4 h, 1 set of rats (n = 20) was treated once with honokiol and samples were collected, after humane killing, at different time points, namely, 0, 8, 12 and 20 h following honokiol injection. Thus, 0 h of healing corresponds to 4 h of indomethacin treatment when the injury is at the peak. A parallel set of rats (n = 20) were treated with the vehicle (instead of honokiol) and maintained in the same way to compare the efficacy of honokiol-induced healing and spontaneous healing. Vehicle-treated rats were also used for sample collection at identical time points to that of honokiol-treated rats. In every group, the number of rats was maintained at n = 5.

Scores of mucosal injury (II) were generated by an individual unaware of the treatment condition, to avoid bias. The II was calculated as the percentage of the injured area in the stomach formed by bleeding lesions, blood clots and visible hyperaemia. Mean II was calculated as the sum of the total scores in each group of rats divided by the number of rats in that respective group. Tissue samples for next-generation sequencing and PCR-based gene expression profiling were preserved by storing in RNAlater (Cat# R0901, Sigma-Aldrich), whereas tissues for protein expression profiling were snap-frozen and stored until further use. For mitochondrial preparation, tissue samples were subjected to subcellular fractionation using a commercially available mitochondria isolation kit, as described below.

2.2 | Histological study of gastric mucosa

Semi-thin (5 μm) sections were prepared from buffered formalin-fixed and paraffin-embedded gastric mucosal tissues. The semi-thin sections were collected on a glass slide, deparaffinized and passed through

graded solutions of ethanol for double staining with haematoxylin and eosin. The stained sections were examined under a microscope (Leica DM-2500, Leica Microsystems, Wetzlar, Germany).

2.3 | Next-generation sequencing-based transcriptomics

Total RNA sequencing library preparations were generated, using TruSeq Stranded Total RNA Library preparation kit from Illumina. Briefly, total RNA was isolated from the tissue or cell samples using PureLink RNA Mini Kit (Thermo Fisher Scientific) following the manufacturer's guidelines. The starting material was 45 mg of tissue. The quality and concentration of the isolated RNA samples were checked in Nanodrop 2000 (Thermo Fisher Scientific) and Agilent 2100 Bioanalyzer. Samples with RNA integrity number (RIN) ≥ 7.0 were subsequently used for library preparation. An equal amount (200 ng) of RNA from each sample was first subjected to ribosomal RNA depletion using the Ribo-Zero Human/Mouse/Rat depletion module of the kit followed by purification and divalent cation-based fragmentation. The resulting fragments were purified and subjected to cDNA synthesis, A-tailing and dual index adapter ligation. The products were subsequently purified and PCR enriched. The resulting RNA libraries were checked in Agilent 2200 TapeStation (Agilent Technologies), quantified, normalized and subjected to equimolar pooling. The pooled libraries were finally loaded on a sequencing run flow cell (Illumina) and subjected to 100-bp paired-end massively parallel sequencing in NovaSeq 6000 sequencer (Illumina). Resulting Bcl files were converted to Fastq files and the data were subjected to a quality check using FastQC v0.11.7 (Andrews, 2010). This was followed by adapter trimming with Cutadapt v1.16 (Martin, 2011) using Illumina Universal Adapter. Hisat2 v2.1.0 (Pertea et al., 2016) was used to align the trimmed reads with Rat Rno6 reference genome (for rat samples). Sorting of Bam files was performed with SAMtools v1.19 (H. Li et al., 2009) Next, gene count was performed with FeatureCounts (Liao et al., 2014) followed by differential analysis using DESeq2 (Love et al., 2014). Differentially expressed genes (DEGs) with ≥1.5- or ≤1.5-fold expression change and P value ≤ 0.05 and false discovery rate (FDR) ≤ 0.05 were filtered. Finally, gene-enrichment and pathway analyses were performed with IPA (Ingenuity Pathway Analysis) software. For rat gastric mucosal samples, data were also filtered with ≥1.2- or ≤1.2-fold expression change and P value ≤ 0.05 and FDR cut-off ≤ 0.05 to include genes regulating mitochondrial metabolism and functions. The Gene Expression Omnibus (GEO) accession number for rat transcriptomic data is GSE201565.

2.4 | Isolation of mitochondria

Mitochondria were isolated from tissue samples using the Mitochondria Isolation Kit (Cat# KC010100, purchased from BioChain) following the manufacturer's guidelines. Mitochondrial isolation used here, in principle, depends on two-step differential centrifugations. The tissue after mechanical disruption (in hypotonic lysis buffer

supplemented with protease inhibitors) by homogenization is subjected to low-speed centrifugation for removal of precipitated debris, unfragmented cells and large cellular organelles. Subsequently, high-speed centrifugation of the supernatant (of the first step) is performed to isolate viable and enzymatically active mitochondria. A pure mitochondrial fraction is obtained by repeated washing of the final pellet. In the present study, an equal amount of gastric mucosal tissues (200 mg) from each experimental set was subjected to mitochondria isolation. Mild homogenization of the samples was carried out with a Dounce homogenizer, on ice. Nuclei and cell debris were removed by centrifugation at 600 x g for 10 min and the supernatant was collected, which was further centrifuged at 12,000 x g for 15 min to obtain the mitochondrial fraction. The mitochondrial pellets were washed three times in mitochondria isolation buffer, and the resultant pellets (approximately 99% pure) were either used for respiratory chain complex and dehydrogenase assays or lysed for immunoblotting, as described earlier (Mazumder et al., 2019).

2.5 | Immunoblot analysis

For immunoblot analysis, total protein was extracted from gastric mucosal tissues by homogenization of samples in pre-chilled mammalian cell lysis buffer (supplemented with protease and phosphatase inhibitors), as described previously (Mazumder et al., 2019). Mitochondrial extracts were prepared by subcellular fractionation of tissue samples as mentioned above. For analysis of mitochondrial protein acetylation, mitochondria isolation and lysis buffers were supplemented with nicotinamide (50 mM) and trichostatin A (10 μM). Protein was quantified by Lowry's method, and an equal amount of protein was loaded in each well of the 10% polyacrylamide–SDS gels and subjected to electrophoresis followed by wet transfer-based immunoblotting using nitrocellulose membrane. Blots were blocked in 5% skimmed milk or 5% BSA solution followed by incubation in primary antibodies (Table S1) overnight as per the manufacturer's guidelines. The blots were washed in Tris-buffered saline (TBS) solution supplemented with 0.1% Tween 20 and subsequently incubated in HRP-conjugated secondary antibody for 2 h at room temperature. The blots were finally washed in TBS solution supplemented with 0.1% Tween 20, and immuno-reactive bands were developed in Bio-Rad ChemiDoc system. Actin and TOM20 were used as the loading controls for total protein and mitochondrial protein, respectively. Densitometric analyses were carried out using ImageJ software, and data are represented as fold change (FC) relative to control. The experimental procedures provided here conform with the *BJP* guidelines (Alexander et al., 2018).

2.6 | Analysis of mitochondrial transmembrane potential (ΔΨm)

ΔΨm was measured using JC-1. In principle, JC-1 is a cationic lipophilic dye (naturally showing green fluorescence) that enters

mitochondria, accumulates there in a concentration-dependent manner and starts forming reversible complexes, known as J aggregates (exhibiting excitation and emission in the red spectrum, maximum at ~590 nm). Thus, in a healthy cells with mitochondria having normal $\Delta\Psi m$, JC-1 enters in mitochondria (negatively charged) and accumulates there forming red fluorescent J aggregates. On the contrary, in unhealthy cells or mitochondria, the JC-1 entry is greatly reduced owing to the loss of mitochondrial transmembrane electrochemical potential, which renders the mitochondrial inner membrane less negative. Under this condition, JC-1 fails to reach its threshold level for the formation of J aggregates, resulting in the maintenance of its monomeric, green fluorescent state. In the present study, $\Delta\Psi m$ was measured in the mitochondria isolated from control and treated stomachs, using a F-7000 Fluorescence Spectrophotometer (Hitachi High-Technologies Corporation). Equal amounts of mucosal tissue from each sample were used for mitochondria isolation followed by protein estimation to use equal amounts of mitochondria for $\Delta\Psi m$ analysis. Mitochondria were incubated in darkness for 15 min in 500 μl of ATP-supplemented JC-1 assay buffer containing 300 nM of JC-1. A single-excitation–dual-emission format was used for analysing JC-1 monomers and aggregates at 530 and 590 nm, respectively. $\Delta\Psi m$ was expressed as fluorescence ratio of 590 nm/530 nm, as described previously (Mazumder et al., 2019).

2.7 | Measurement of ATP content

ATP content of gastric mucosal tissue was measured to follow the bioenergetic state of the mucosal cells upon treatment with indomethacin. Because tissue ATP production is mostly attributed to functional mitochondria with integrity, depletion in ATP would reflect mitochondrial dysfunction and resultant bioenergetic deficit of the affected tissue. ATP determination kit (A22066; Thermo Fisher Scientific) was used to measure gastric mucosal ATP level in control and treated rats by following the manufacturer's instructions. This is a bioluminescence-based assay kit and it contains recombinant firefly luciferase and its substrate D-luciferin. The principle of the assay is based upon the ATP requirement of luciferase enzyme for the production of the light (emission maximum of ~560 nm at pH 7.8). The greater the amount of ATP present in the tissue extract, the greater the amount of light emitted from the reaction, as follows.

$$\text{Luciferin} + \text{ATP} + O_2 \xrightarrow{\text{Mg}^{2+} \text{ and luciferase}} \text{Oxyluciferin} + \text{AMP} + \text{Pyrophosphate} + CO_2 + \text{Light}$$

Briefly, an equal amount of tissue (50 mg) from each sample was minced and lysed in 5% sulfosalicylic acid solution (for sample deproteinization). The lysates were centrifuged at 12,000 x g and the supernatants were used for ATP measurement in a luminometer (BioTek). The values were normalized by protein concentrations of the respective samples, as described previously (De et al., 2017; Mazumder et al., 2016).

2.8 | RNA isolation and quantitative real-time PCR (qRT-PCR)

Total RNA was isolated by using TRIzol (Thermo Fisher Scientific), following the manufacturer's protocol, and estimated using Maestrogen Spectrophotometer (MaestroGen Inc., Taiwan). The obtained total RNA (2 μg) was reverse transcribed with oligo-dT18 primer using RevertAid H Minus First Strand cDNA Synthesis Kit (Thermo Fisher Scientific) followed by rDNAse treatment. The resultant cDNAs were used for qPCR after proper dilution by using primers (Table S2) obtained from Integrated DNA Technologies Inc. (San Diego, CA, USA). The Roche LightCycler 96 qPCR system was used for performing the qPCR by using SYBR green mastermix (Roche) in following the as-mentioned cycle conditions: initial denaturation temperature at 95°C/10 min followed by 40 cycles of denaturation at 95°C/15 s, annealing (at indicated annealing temperatures; Table S2) for 30 s and extension at 72°C/25 s. Relative gene expression was calculated using $2^{-\Delta\Delta Cq}$ method and the data were represented as FC relative to control, as described previously (De et al., 2017; Dey et al., 2014; Mazumder et al., 2019). *Gapdh* was used as the internal control.

2.9 | Determination of Sirt3 deacetylase activity

Sirt3 fluorometric activity assay kit (Abcam, ab156067) was used to measure deacetylase activity of Sirt3, with or without indomethacin. The experiment was performed as per the manufacturer's protocol. Briefly, in presence of increasing concentrations of indomethacin (100–500 μM), the activity of purified human recombinant Sirt3 was assessed, taking the kinetic measurement at 2-min intervals till 45 min, in a BioTek Synergy H1 Hybrid Multi-Mode Reader with excitation at 350 nm and emission at 450 nm.

2.10 | Mitochondrial dehydrogenase assay

Mitochondrial metabolic integrity in tissue samples was measured by analysing mitochondrial dehydrogenase activity, which can reduce MTT into a purple-coloured formazan that can be solubilized and quantified spectrophotometrically at 570 nm. An equal amount of gastric tissue (200 mg) from different experimental sets was used for mitochondria isolation, and the resultant fractions were incubated in MTT solution (1 mg·ml^{-1} in PBS) for 3.5 h at 37°C/5% CO_2. Samples were centrifuged and pellets were solubilized in equal volumes of anhydrous DMSO. The absorbance of the purple solution was measured spectrophotometrically at 570 nm, as described previously (De et al., 2017; Mazumder et al., 2019). Mitochondrial protein from every fraction was estimated and used for normalization of the ODs corresponding to the respective samples.

2.11 | Isolation of mtDNA and measurement of 8-oxo-7,8-dihydro-2′-deoxyguanosine by ELISA

DNA from the isolated mitochondrial pellets was extracted by the phenol-chloroform method. Briefly, the mitochondrial pellet was resuspended in 100 μl of Proteinase K-supplemented lysis buffer and incubated at 50°C for 3 h, following which 200 μl of phenol-chloroform was added and mixed thoroughly. The contents were centrifuged at 11,000 x g for 10 minutes at 25^0C to separate the phases. The aqueous phase was collected and 200 μl of 7.5-M ammonium acetate and 500 μl of ethanol were added. The tubes were kept at $-20°$C for 2 h. The samples were next centrifuged at 10,000 x g for 30 min. The pellets were washed with 500 μl of 70% ethanol and, finally, the DNA pellets were dissolved in 30 μl of Tris-EDTA buffer. The mtDNA was spectrophotometrically estimated. An equal amount of mtDNA from each experimental set was then taken for assay of OGG1 activity, by measuring levels of 8-oxo-7,8-dihydro-2′-deoxyguanosine (8-oxo- dG) with a commercially available HT 8-oxo-dG ELISA Kit II from Trevigen, as described by Bindu et al. (2017).

2.12 | Confocal immunohistochemical analysis

The accumulation of 8-oxo-dG content in gastric mucosal tissue of Con, Indo and HKL + Indo rats was followed by confocal fluorescent immunohistochemical analyses. Formalin-fixed and paraffinized tissue sections were deparaffinized, rehydrated and subjected to antigen retrieval by heating in sodium citrate buffer. Next, the tissue sections were blocked with 10% goat serum and 1% BSA in TBS for 2 h. The tissue sections were incubated overnight in primary antibody solution containing 8-oxo-dG (anti-DNA/RNA damage antibody) (Table S1). The slides were washed and incubated in Alexa Fluor 647-tagged anti-mouse secondary antibody. The slides were again washed. 4′,6-Diamidino-2-phenylindole (DAPI) was used for nuclear staining. The washed slides were mounted in 30% glycerol in PBS and observed under a microscope. Confocal images were taken in the Leica TCS-SP8 confocal microscope (Leica Microsystems, Wetzlar, Germany) using Leica Application Suite X (LAS X) software. All experiments were repeated three times and the confocal images presented are randomly picked up portions of the gastric mucosal sections. Image cropping and global adjustments for brightness/contrast were done in Adobe Photoshop and assembled in CorelDraw X7, as mentioned previously (De et al., 2017; Mazumder et al., 2019). The experimental procedure provided herein duly conforms with the *BJP* guidelines (Alexander et al., 2018).

2.13 | Detection of mitochondrial superoxide anion ($O_2^{•-}$)

MitoSox staining was used to detect the presence of mitochondrial $O_2^{•-}$ in isolated gastric mucosal cells, as described by De et al., (2017). Briefly, gastric mucosal scrapings were washed in pre-warmed

Hanks Balanced Salt Solution (HBSS) and incubated in a pre-aerated solution containing 100 units·ml^{-1} penicillin and 100 μg·ml^{-1} streptomycin supplemented with 0.05% hyaluronidase and 0.1% collagenase for 80 min, with shaking, at 37°C/5% CO_2. The cell suspension was aseptically filtered using 50-μm cell strainers. The filtered cells were washed thrice in pre-warmed HBSS and resuspended in PBS. The cells were next checked for viability (using the Trypan blue exclusion method). Viable cells were counted and 10^6 cells from each set were incubated with MitoSox Red (Thermo Fisher Scientific) at 37°C for 30 min. Next, the cells were washed three times and analysed by flow cytometry in FACS, LSRFortessa, BD. Data were analysed in FACS DIVA software under standard parameters; 10^4 cells were evaluated per set and experiments were repeated three times.

2.14 | Assay of mitochondrial ETC complex I and III activities

Mitochondrial ETC complex I (NADH:ubiquinone oxidoreductase) and complex III (decylubiquinol cytochrome c oxidoreductase) activities were spectrophotometrically quantified through the rate of oxidation of NADH (measured as change in OD$_{340 nm}$) and reduction of cytochrome c (measured as change in OD$_{550 nm}$), as described elsewhere (Carrasco-Pozo et al., 2011; Spinazzi et al., 2012). Briefly, an equal amount of isolated mitochondria (15 μg of protein) was lysed in a hypotonic buffer before using for enzymatic assays. For complex I assay, NADH and ubiquinone were used as substrates. Specific complex I activity was derived by estimating the rotenone-sensitive NADH–ubiquinone oxidoreductase action of the mitochondrial extract from control and treated samples. For the complex III assay, oxidized cytochrome c and ubiquinol were used as substrates. The specific complex III activity was derived by estimating the antimycin A-sensitive decylubiquinol cytochrome c oxidoreductase action of the mitochondrial extract. In either case, the rate of enzymatic activity was recorded for 2 min.

2.15 | Measurement of gastric luminal pH

Rats were fasted for 24 h with free access to water. On the day of the experiment, rats were injected with **lansoprazole** (20 mg·kg^{-1}, i.p.) or honokiol (40 mg·kg^{-1}, i.p.) 30 min prior to administration of 2-mercapto-1-methylimidazole (MMI) (40 mg·kg^{-1}, i.p.), as described previously (Mazumder et al., 2016). This set was indicated as 'stimulated' because MMI stimulates acid secretion. The second set of starved rats was treated with lansoprazole or honokiol without MMI injection. This set was denoted as 'unstimulated (basal)'. At 4 h after treatment, rats were humanely killed, the abdomen opened and the oesophageal and pyloric ends of the stomach were tied with a thread to prevent the escape of gastric secretions. A small incision was made at the cardiac end of the stomach and the contents were flushed with 2 ml of 0.9% saline and the clear supernatant was collected after centrifugation (5000 x *g* for 10 minutes at 25^0C).

The pH of the fluid was then measured with a hand-held pH meter.

2.16 | Data and statistical analysis

The data and statistical analysis comply with the recommendations of the *British Journal of Pharmacology* on experimental design and analysis, and experiments have been designed to generate groups of equal size, using randomization and blinded analysis (Curtis et al., 2022). All animal studies were done with randomly segregated rats. For every set, the animal number was maintained at 5 (n = 5), as standardized and reported previously (Bindu et al., 2013; Mazumder et al., 2016; Mazumder et al., 2019). The in vitro experiments were done in triplicate. All experiments were repeated at least three times. Experimental data are shown as means ± SD. When comparing two experimental groups, unpaired *t* test (with Welch's correction) was done to calculate the level of significance, whereas one-way analysis of variance (ANOVA) followed by Bonferroni's multiple-comparison test was done for comparing more than two groups. For all data, *P* value < 0.05 was considered statistically significant. The group size mentioned here is the number of independent values, and that statistical analysis was done using these independent values. Statistical analysis of data was done using GraphPad Prism 8 and Microsoft Office Excel 2019 software.

2.17 | Materials

Indomethacin (Cat# I7378), ibuprofen (Cat# I1892), diclofenac (Cat# D6899), aspirin (Cat# A5376), honokiol (Cat# 384620), 2-mercapto-1-methylimidazole (MMI, Cat#301507), lansoprazole (Cat# L8533), RNase ZAP 3-(4,5-dimethylthiazol-2-yl)-2,5-diphenyltetrazolium bromide (MTT) (Cat# CT01-5), carboxymethylcellulose sodium salt (Cat# C5678), bovine serum albumin (BSA) (Cat# A7906) and DMSO were procured from Sigma (St. Louis, MO, USA). TRIzol (Cat# 15596026), PureLink RNA Mini Kit (Cat# 12183018A), RevertAid H Minus First Strand cDNA Synthesis Kit (Cat# 18091050), ATP Determination Kit (Cat# A22066), PowerUp™ SYBR™ Green Master Mix (Cat# A25742), 5,5′,6,6′-tetrachloro-1,1′,3,3′-tetraethylbenzimi-dazoylcarbocyanineiodide (JC-1) dye (Cat# T3168), MitoSOX™ mitochondrial superoxide indicator (Cat# M36008), nuclease-free water (Cat# AM9937), Hoechst 33342 (Cat# H3570) and phosphate-buffered saline (PBS) (Cat# 10010031) were purchased from Thermo Fisher Scientific (Waltham, MA USA). Mitochondria Isolation Kit (Cat# KC010100) was purchased from BioChain (Newark, CA, USA). HT 8-oxo-dG enzyme-linked immunosorbent assay (ELISA) Kit II (Cat# 4380-096-K) was procured from Trevigen (Bio-Techne, Minneapolis, USA). Luminata Forte Western horseradish peroxidase (HRP) substrate (Cat# WBLUF0500) for electrochemiluminescence (ECL)-based chemiluminescence was procured from Merck Millipore (Burlington, MA, USA). Sirt3 activity assay kit (Fluorometric) (Cat# ab156067) and Mitochondrial DNA (mtDNA) Isolation Kit (Cat# ab65321) were purchased from Abcam (Boston, MA, USA). BioTrace NT nitrocellulose transfer membrane (Cat# 66485) was procured from Pall Corporation (Port Washington, NY, USA). Blotting-Grade Blocker (Cat# 1706404) was procured from Bio-Rad Laboratories, Inc. (Hercules, CA, USA). All other reagents were of analytical grade purity.

2.18 | Nomenclature of targets and ligands

Key protein targets and ligands in this article are hyperlinked to corresponding entries in http://www.guidetopharmacology.org and are permanently archived in the Concise Guide to PHARMACOLOGY 2021/2022 (Alexander, Cidlowski et al., 2021; Alexander, Fabbro, Kelly, Mathie, Peters, Veale, Armstrong, Faccenda, Harding, Pawson, Southan, Davies, Beuve et al., 2021; Alexander, Fabbro, Kelly, Mathie, Peters, Veale, Armstrong, Faccenda, Harding, Pawson, Southan, Davies, Boison et al., 2021; Alexander, Kelly et al., 2021).

3 | RESULTS

3.1 | Transcriptome analysis revealed the association of Sirt3 in NSAID-induced gastric mucosal injury

As the stomach is the organ most severely affected by the toxic effects of NSAIDs, we undertook high-depth transcriptome sequencing of control and indomethacin-treated rat gastric mucosa to comprehensively explore the alterations in gene expression, during gastropathy. Indomethacin was used as a prototype COX non-selective NSAID. Tissues for transcriptome sequencing were collected from control and indomethacin-treated samples with high-grade mucosal injury (Figure 1a). Heat map analysis revealed the DEG set with 885 up-regulated and 211 down-regulated genes in 'indomethacin' compared with 'control' when filtered with log FC cut-off of 1.5, *P* value ≤ 0.05 and FDR ≤ 0.05 (Figure 1b and File S1a–c) (GSE201565). Gene-enrichment analysis using 'ingenuity pathway analysis' revealed the prominent pathways and 'disease and function' involved in indomethacin-induced gastric cytotoxicity (Figure 1c,d). 'Apoptosis and death receptor signalling', 'TNFR signalling', 'p38 MAPK signalling', 'interferon signalling', 'granulocyte and agranulocyte adhesion and diapedesis', 'acute phase signalling' and 'NRF2-mediated oxidative stress response' appeared as prominently highlighted pathways (Figure 1c), whereas 'gastroenteritis', 'synthesis, production and metabolism of reactive oxygen species', 'cell cycle progression', 'apoptosis', 'bleeding', 'inflammation of gastrointestinal tract', 'inflammatory bowel disease', 'fibrosis', 'colitis' and 'phagocyte and macrophage activation' appeared as predominant class of 'disease and function', significantly contributing to the DEG counts (Figure 1d). Because mitochondria are associated with a wide array of pathways and functions identified in the transcriptome data, we checked caspase 9 and caspase 3, as well as cytochrome c, as terminal markers of intrinsic apoptosis due to mitochondrial dysfunction. We also measured ΔΨm and ATP content. Data indicated significant
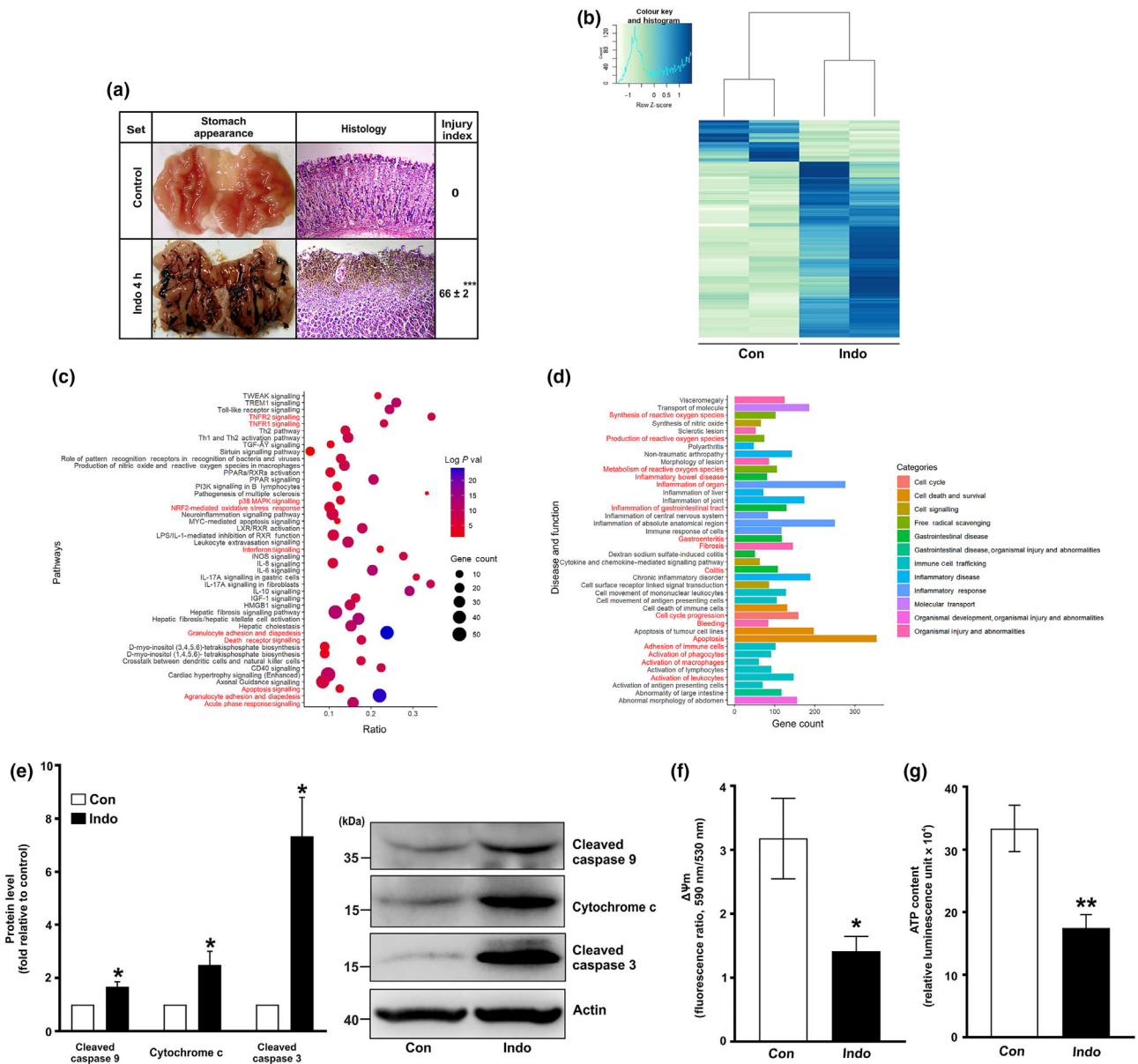
FIGURE 1 Indomethacin induces transcriptome alteration, intrinsic apoptosis and mitochondrial dysfunction in gastric mucosa. (a) Gastric mucosal morphology and haematoxylin/eosin-stained histology of control (Con) and indomethacin-treated (Indo) rats (n = 5). Representative images are provided. (b) Heatmap shows separate clustering of samples corresponding to control 'Con' and indomethacin 'Indo' (false discovery rate [FDR] ≤ 0.05). Euclidean distance metric was used while clustering the gene expression data of the differentially expressed genes (DEGs). Euclidean distance metric was used while clustering the gene expression data. The expression value of genes analysed with fold change cut-off of 1.5; colour gradient scale with white being highly down-regulated to blue being highly up-regulated. (c) Dot plot showing enriched canonical pathways. The size of dots represents the proportion of genes involved in the particular signalling pathway, whereas the range of colour indicates Bonferroni corrected P values (−log transformed). The ratio represents the number of genes in fraction with respect to the total number of genes that map to the same pathway. (d) Bar graph showing the disease and functions enriched in the 'indomethacin' set. (e) Immunoblots of cleaved caspase 9, cytochrome c and cleaved caspase 3 in gastric mucosal tissues from control and indomethacin-treated rats (n = 5). Actin was used as the loading control. Representative blots are shown on the right. (f) Mitochondrial transmembrane potential (ΔΨm) in gastric mucosal tissues from control and indomethacin-treated rats (n = 5). (g) ATP content in gastric mucosal tissues from control and indomethacin-treated rats. Indomethacin treatment: 48 mg·kg^{-1} for 4 h. Data (a, e–g) are mean ± SD, n = 5. *$P < 0.05$, significantly different from control; unpaired Student's t test with Welch's correction. The number of independent experiments is 3.

elevation of cleaved caspase 9 and 3 as well as cytochrome c along with drastic mitochondrial depolarization and ATP depletion in the indomethacin-treated tissues (Figure 1e–g).

As immunoblotting indicated mitochondrial dysfunction, we delved deeper into the transcriptome data to check for crucial genes regulating ETC and mitochondrial metabolism (Figure 2). ETC
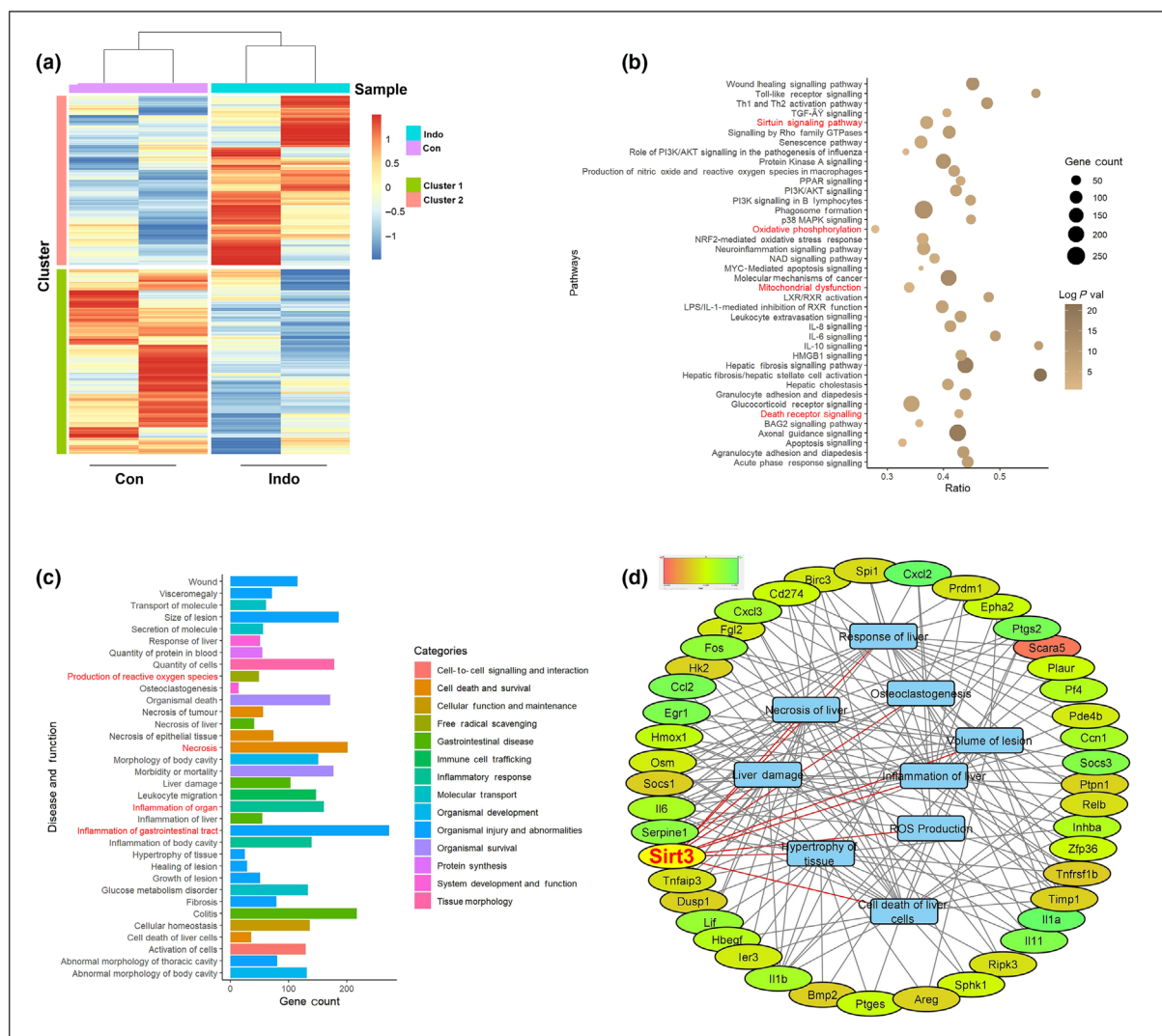
FIGURE 2 Indomethacin alters gene expression programmes that regulate mitochondrial functions and sirtuin signalling. (a) Heatmap shows separate clustering of samples corresponding to control (Con) and indomethacin –treated (Indo) rats. Euclidean distance metric was used while clustering the gene expression data of the differentially expressed genes (DEGs). The expression value of genes analysed with fold change cut-off of 1.2; colour gradient scale with blue being highly down-regulated to red being highly up-regulated. (b) The dot plot shows enriched canonical pathways. The size of dots represents the proportion of genes involved in the particular signalling/pathway, whereas the range of colour indicates Bonferroni corrected P values ($-$log transformed). Ratio represents the number of genes in fraction with respect to the total number of genes that map to the same pathway. (c) The bar graph shows the disease and functions enriched in the indomethacin-treated set. (d) Hub gene network; gene names represented in oval shapes whereas associated functions are represented by rectangular boxes. The expression value of genes represented with colour gradient scale with red being highly down-regulated to green being highly up-regulated. Grey lines indicate the association of genes with associated functions, whereas red lines indicate the association of sirtuin-3 (Sirt3), the hub gene, with respective associated functions.

complex genes however did not show up in the transcriptome data when analysed with an FC cut-off of 1.5, even with evident mito-pathology and ATP depletion in the indomethacin-treated tissues. Therefore, we rationally relaxed the standard FC cut-off (of 1.5) slightly to 1.2 to check for DEGs regulating mitochondrial functions (Figure 2a and File S1d). Interestingly, 'mitochondrial dysfunction' and 'oxidative phosphorylation' were significantly reflected as important pathways (Figure 2b and File S1e). ETC complex-related gene expression was severely compromised along with elevation of proapoptotic and down-regulation of antioxidant and anti-apoptotic

markers (File S1e). Functional enrichment analysis revealed the association of 272 DEGs with GI inflammation, 160 DEGs with organ inflammation, 147 DEGs with leukocyte migration, 74 DEGs with epithelial tissue necrosis and 49 DEGs with reactive oxygen species (ROS) production (File S1e). Interestingly, the 'sirtuin signal-ling pathway' was highlighted with Sirt3, turning out as a common gene associated with several categories of disease and functions including 'gastrointestinal disease', 'free radical scavenging', 'inflammatory response', 'cell death and survival', 'cellular function and maintenance', 'cell-to-cell signalling and interaction', 'molecular

transport', 'protein synthesis', 'tissue morphology', 'organismal development' and 'injury and abnormalities' (Figure 2c and File S1f). We subsequently used Molecular Complex Detection (MCODE) (Bader & Hogue, 2003) plugin in Cytoscape (Shannon et al., 2003) to build the gene interaction network and screened the hub gene(s) regulating mitochondrial metabolism and cellular integrity. *Sirt3* appeared as a top hub gene controlling myriad signalling processes, regulating mitochondrial metabolism and cellular integrity (Figure 2d). Because there are no reports linking Sirt3 with NSAID-induced bioenergetic crisis and gastric injury, we explored the functional correlation of this protein in NSAID-induced gastric injury in our model.

3.2 | NSAID impairs Sirt3 expression, thereby inducing gastric mucosal cell injury, and inhibits deacetylase activity of purified Sirt3

Sirt3 down-regulation directed us to follow its mechanistic aspects. Validation of the transcriptome data by qRT-PCR and immunoblotting revealed significant depletion of Sirt3 during maximum tissue injury (Figure 3a,b). Functional relevance of Sirt3 was evident from depletion of OGG1 in the injured mucosa (Figure 3b). To understand the pattern of Sirt3 expression in the course of injury induction followed by spontaneous resolution, we checked the kinetics of Sirt3 expression. Both Sirt3 and OGG1 followed a concerted temporal depletion with the progression of mucosal damage from 0 to 4 h of indomethacin treatment followed by gradual restoration by 72 h when the lesions spontaneously healed, as evident from tissue restitution (Figure 3c,d). To check whether indomethacin has any direct effect on the deacetylase activity of Sirt3, we evaluated the deacetylase activity of Sirt3 in presence of increasing concentration of indomethacin. Data indicated that indomethacin dose-dependently inhibited the deacetylase activity of purified Sirt3 (Figure 3e). In addition, we observed that indomethacin treatment significantly elevated mitochondrial proteome acetylation (Figure 3f) along with profound 8-oxo-dG accumulation in mtDNA, implying oxidative damage to mtDNA (Figure 3g). Even in the transcriptome sequencing data, it was clear that several Sirt3 targets, including *Ogg1*, *Xrcc6*, *Pdha1*, *Aco1*, *Idh1*, *Sdhb*, *Mdh1*, *Ndufa9*, *Glud1* and *Acadl* exhibited prominent down-regulation (File S1d). Further, we observed a concurrent reduction in mitochondrial dehydrogenase activity (Figure 3h) and elevation of mitochondrial proteome ubiquitination (Figure 3i), suggesting mitochondrial dysfunction due to Sirt3 depletion followed by increased clearance of damaged mitochondria.

So far, we documented how Sirt3 deficiency could account for indomethacin-induced mitopathology and cell death. But how did the NSAID actually cause Sirt3 down-regulation? As indomethacin depleted Sirt3 gene expression, we asked whether indomethacin targets any upstream transcriptional regulator/s. Surprisingly, we found significant depletion of both PGC1α and the **oestrogen-related receptor α (ERRα)** in the injured mucosa, thereby revealing the basis of transcriptional depletion of Sirt3 (Figure 3j).

3.3 | Sirt3 induction by honokiol prevents NSAID-induced transcriptome alteration and mitochondrial pathology to avert mucosal cell death and attenuate gastric mucosal injury

We next asked whether Sirt3 stimulation can prevent NSAID-induced gastric cell death and mucosal injury. Rats were pre-treated with honokiol, a specific pharmacological Sirt3 inducer (Pillai et al., 2015), given i.p.. The dose–response study indicated 40 mg·kg^{-1} as the optimum gastroprotective dose, against indomethacin, with an ED_{50} of 12.32 mg·kg^{-1} (Figure 4a,b). Following these data, we next asked whether i.g. administration of honokiol would exhibit any gastroprotective effect against indomethacin. This might also reflect any better clinical relevance as such a non-invasive route of administration is certainly more advantageous in terms of drug delivery. To compare the different effects of i.p. and i.g. routes of honokiol administration, four doses of honokiol (20, 40, 60 and 80 mg·kg^{-1}) were selected, based on the data obtained after i.p. administration. The dose–response study (Figure 4c) clearly indicated that i.g. administration of honokiol at 80 mg·kg^{-1} offered gastroprotection, comparable to that after i.p. administration of honokiol at 40 mg·kg^{-1}. To avoid administration of the higher doses of honokiol to the rats, we opted for the i.p. route in the subsequent experiments.

Next, we checked the gastric transcriptome profiles of honokiol-pre-treated indomethacin-treated (HKL + Indo) rats. Sequencing data revealed that gene expression pattern in HKL + Indo group was largely similar to that in the control group and significantly opposed to the pattern in the Indo only group (Figure 4d–g). DEG analysis (at FC cut-off of 1.5) revealed 417 up-regulated and 815 down-regulated genes in HKL + Indo, compared with Indo, out of which 505 up-regulated and 85 down-regulated genes found in Indo group showed reversed expression relative to those in the HKL + Indo group, suggesting a protective effect of honokiol-induced Sirt3 stimulation (Figure 4e). At FC cut-off of 1.2, 4215 up-regulated and 3176 down-regulated genes in the Indo group showed reversed expression relative to those in the HKL + Indo group (Figure 4f,g). Significant DEGs mostly constituted genes controlling mitochondrial functions and those implicated in gastric injury, inflammatory and apoptotic pathways (File S2a,b). *Hmox1*, *Txnrd1*, *Sod1*, *Mmp13*, *Mmp3*, *Tnf1b*, *Ccl2*, *Cxcl2*, *Icam1*, *Vcam1*, *Hif1a*, *Cxcl3*, *Il6*, *Il1b*, *Il1a*, *Nfkb2*, *Nfkb1*, *Nlrp3*, *Fas*, *Bcl2* and *Tlr9* were prominently observed, thereby indicating that honokiol treatment decreased MOS and inflammation. Notably, the expression of *Sirt3* in the HKL + Indo group was comparable to that in the control group. The protective effect of honokiol against indomethacin was clearly evident from the restoration of Sirt3 expression (Figure 4h,i). Further, we could also show a stimulatory action of honokiol on the expression of tricarboxylic acid (TCA) cycle enzymes, such as like *Aco1* and *Idh1*, which are important targets of Sirt3 (File S2b).

To understand the mechanistic basis of honokiol-dependent Sirt3 stimulation and prevention of NSAID-induced gastropathy, we checked the status of Sirt3 targets and acetylation status of the mitochondrial proteome. We found that honokiol pre-treatment prevented indomethacin-induced OGG1 depletion (Figure 4i) and rescued Sirt3
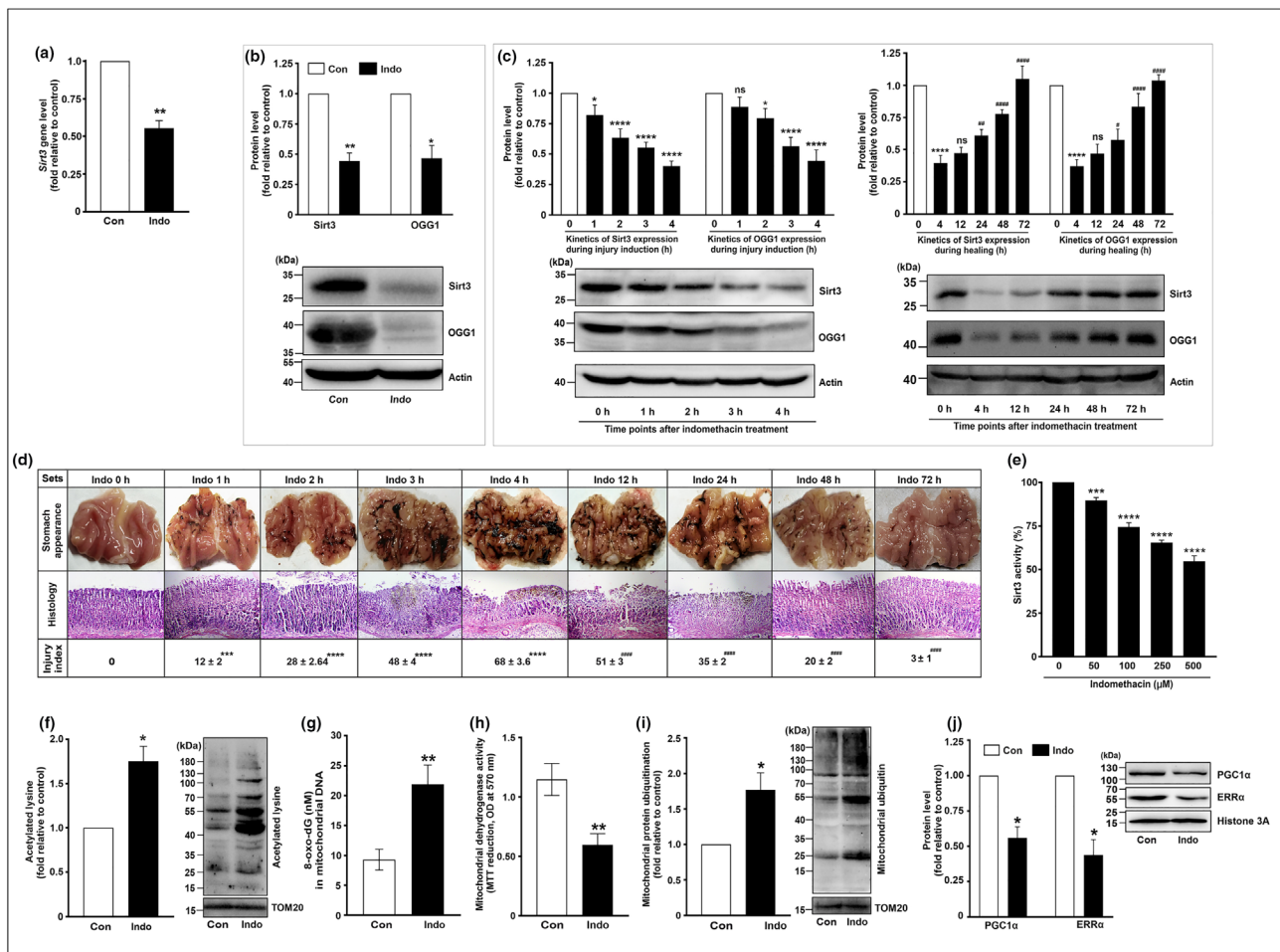
FIGURE 3 Impaired sirtuin-3 (Sirt3) expression and activity are associated with indomethacin-induced gastric mucosal cell damage. (a) *Sirt3* gene expression analysis in gastric mucosal tissues from control (Con) and indomethacin –treated (Indo) rats by qPCR; bar graph indicates fold change in gene expression relative to control (after normalization by *Gapdh*). (b) Immunoblots of Sirt3 and 8-oxoguanine DNA glycosylase 1 (OGG1) in gastric mucosal tissues from control and indomethacin –treated rats. Representative blots are shown below the bar graph. (c) Immunoblots of Sirt3 and OGG1 in indomethacin –treated rats at indicated time points. Representative blots are below the bar graphs. Actin: loading control (b, c). (d) Gastric mucosal morphology and haematoxylin/eosin-stained histology from indomethacin –treated rats (n = 5) at indicated time points; representative images and micrographs are shown. (e) Deacetylase activity of purified Sirt3 measured in presence of increasing concentrations of indomethacin. (f) Immunoblot of acetylated lysine in the mitochondrial fraction of gastric mucosal tissues from control and indomethacin –treated rats. TOM20: loading control. (g) Mitochondrial DNA (mtDNA) damage measured by 8-oxo-dG enzyme-linked immunosorbent assay (ELISA) in gastric mucosal tissues from control and indomethacin –treated rats. (h) Mitochondrial dehydrogenase activity, measured by MTT reduction assay, in the mitochondrial fraction of gastric mucosal tissues from control and indomethacin –treated rats. (i) Immunoblot of ubiquitination in the mitochondrial fraction from control and indomethacin –treated rats. TOM20: loading control. (j) Immunoblot of PGC1α and ERRα in the nuclear fraction from control and indomethacin –treated rats. Histone 3A: loading control. Representative blots are presented alongside the bar graphs (f, i, j). Data (c, d) are mean ± SD, n = 5. *$P < 0.05$, significantly different from Indo 0 h; #$P < 0.05$, significantly different from Indo 4 h; one-way ANOVA followed by Bonferroni's post hoc test. Data (e) are mean ± SD, n = 5. *$P < 0.05$, significantly different from Indo 0 μM; one-way ANOVA followed by Bonferroni's post hoc test. Unpaired Student's *t* test with Welch's correction (for comparing two groups) was used for analysing the data in (a, b, f–j). ns, non-significant. The number of independent experiments is 3.

activity as evident from attenuation of mitochondrial proteome hyper-acetylation (Figure 4j) and specific acetylation of OGG1 and SOD2 (Figure 4k). Prevention of OGG1 deactivation was further reflected through reduction of indomethacin-induced 8-oxo-dG accumulation in mtDNA, as shown by ELISA (Figure 4l) and immunohistochemical analysis (Figure 4m) of tissue levels of 8-oxo-dG in situ. Because 8-oxo-dG accumulation is a direct consequence of mtDNA oxidation,

we checked the level of the progenitor ROS molecule, superoxide ($O_2^{\bullet-}$), in the gastric mucosal cells isolated from rats treated with indomethacin, with and without honokiol, through MitoSox-based flow cytometry. Pre-treatment with honokiol blocked NSAID-induced intracellular $O_2^{\bullet-}$ accumulation (Figure 4n) coupled with restoration of ΔΨm, preservation of mitochondrial dehydrogenase activity and prevention of bioenergetic crisis (Figure 4o–q). In The honokiol-
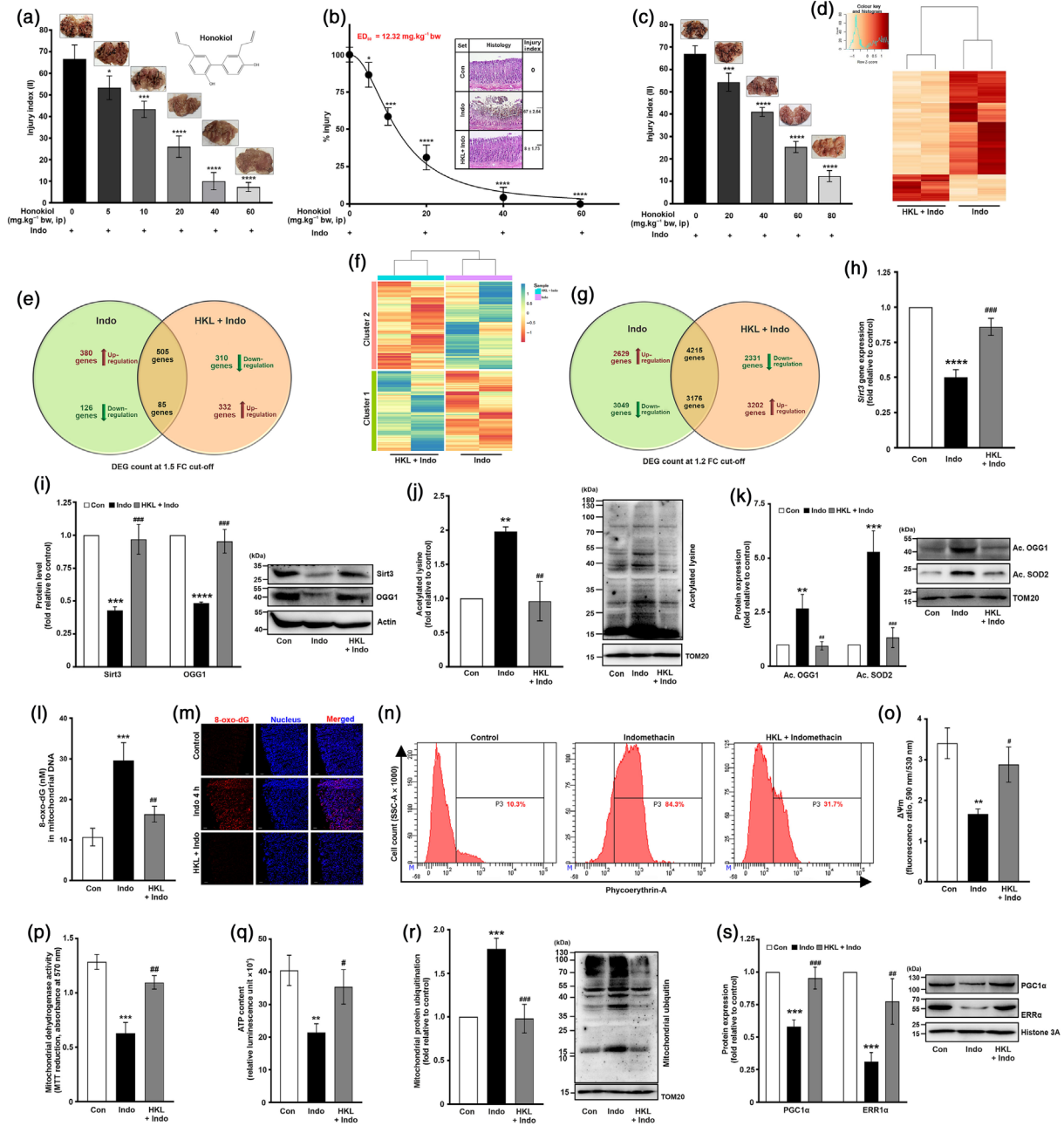
FIGURE 4 Legend on next page.

dependent Sirt3 stimulation also significantly prevented indomethacin-induced mitochondrial ubiquitination (Figure 4r). From a mechanistic perspective, we observed that endogenous Sirt3 stimulation by honokiol significantly reversed the down-regulation of PGC1α and ERRα induced by indomethacin (Figure 4s), revealing a feedback regulation.

3.4 | Sirt3 induction prevents NSAID-induced altered expression of mtDNA-encoded ETC complex, aberrant mitochondrial quality control, mucosal inflammasome activation and apoptosis

Because Sirt3 depletion by indomethacin involved down-regulation of OGG1, reduction of mitochondrial dehydrogenase activity and associated ATP depletion, we checked the effect of Sirt3 stimulation on mtDNA-encoded ETC complex subunits controlling bioenergy production. qRT-PCR and immunoblotting revealed that Sirt3 stimulation by pre-treatment with honokiol, significantly prevented indomethacin-induced down-regulation of mt-Nd1, mt-Nd3, mt-Nd4 and NDUFB8 (complex I), mt-Cytb and UQCRC2 (complex III), mt-Co1, mt-Co2 and MTCO1 (complex IV) and mt-Atp6, mt-Atp8 and ATP5A (complex V) (Figure 5a,b). Direct measurement of ETC complex I and III activities also indicated that honokiol prevented indomethacin-induced deterioration of both complexes, thereby ensuring proper electron flow during OXPHOS (Figure 5c,d). Because mitochondrial functions critically depend on the homeostasis of mitochondrial dynamics, we next checked the mitochondrial structure under the indomethacin-induced, Sirt3 depleted state and during honokiol-induced Sirt3 stimulation (Figure 5e). Interestingly, honokiol pre-treatment also prevented indomethacin-induced depletion of mitofusin (MFN)1, MFN2 and OPA1 and increase of DRP1 activation (through reducing phospho-DRP1-Ser616), thereby indicating stabilization of mitochondrial dynamics (Figure 5e). We also checked mitochondrial quality control by following two key mitophagy regulators, Parkin and PINK1. Data revealed that Parkin and PINK1 were highly elevated during indomethacin treatment whereas honokiol pre-treatment restored aberrant PINK1–Parkin expression (Figure 5f). In addition, honokiol also prevented the decrease in the mitochondrial biogenesis master-regulator PGC1α and TOM20 (Figure 5f) to maintain mitochondrial biogenesis, which is jeopardized by NSAID treatment.

As mitochondrial pathology affects the inflammatory status of the tissue, we checked the effect of honokiol on gastric inflammation and inflammasome activation. We found that the indomethacin-induced elevation of pro-inflammatory cytokines (Il1a, Il1b and Il6), chemokines (Cxcl3 and Mcp1) and intercellular adhesion molecules (Icam1 and Vcam1) was prevented by honokiol pre-treatment (Figure 5g). Moreover, we also observed that indomethacin triggered inflammasome activation in the gastric mucosa, shown by raised levels of NLRP3 and IL-1β, along with caspase 1 cleavage (Figure 5h).

FIGURE 4 Stimulation of sirtuin-3 (Sirt3) prevents indomethacin-induced gastric transcriptome alteration, mitochondrial dysfunctions and tissue injury. (a) Bar graph showing the dose-response of honokiol (HKL; given i.p.) pre-treatment on indomethacin-induced (Indo) gastric mucosal injury. Representative image of the gastric mucosal morphology corresponding to indicated dose of honokiol is shown as inset (on respective bars). Chemical structure of honokiol is shown as inset. (b) Dose–response curve of honokiol showing effective dose (ED$_{50}$) and haematoxylin/eosin-stained gastric mucosal histology from control (Con), indomethacin (Indo) and HKL + Indo treated rats; representative micrographs presented. (c) Bar graph showing the intragastric (ig) dose response of honokiol pre-treatment on indomethacin-induced gastric mucosal injury. Representative image of the gastric mucosal morphology corresponding to indicated dose of honokiol has been shown as inset (on respective bars). (d) Heatmap shows separate clustering of samples from HKL + Indo and Indo treated rats (false discovery rate [FDR] ≤ 0.05). Euclidean distance metric was used while clustering gene expression data. The expression value of genes analysed with fold change (FC) cut-off of 1.5; colour gradient scale: white being highly down-regulated to brown being highly up-regulated. (e) Venn diagram of differentially expressed gene (DEG) count in Indo (compared with control) and HKL + Indo (compared with Indo) when analysed with an FC cut-off of 1.5. (f) Heatmap for samples from HKL + Indo'and Indo treated rats after analysis with FC cut-off of 1.2; colour gradient scale: red being highly down-regulated to blue being highly up-regulated. (g) Venn diagram of DEG count in Indo (compared with control) and HKL + Indo (compared with Indo) treated rats, when analysed with an FC cut-off of 1.2 for better resolution of genes controlling mitochondrial functions. Brown upward and green downward arrows (along with corresponding DEG counts) indicate up-regulation and down-regulation of gene expression, respectively, DEG counts in the intersection regions of the Venn diagrams indicate common genes that were up-regulated/down-regulated with Indo treatment (compared with control) whereas their expression was reversed with HKL + Indo treatment (when compared with Indo). (h) Sirt3 gene expression analysis in gastric mucosal tissues from Con, Indo and HKL + Indo by qPCR; bar graph indicates FC in gene expression relative to control (after normalization to Gapdh). (i) Immunoblots of Sirt3 and 8-oxoguanine DNA glycosylase 1 (OGG1) in tissues from Con, Indo and HKL + Indo treated rats. Actin: loading control. (j, k) Immunoblots of acetylated lysine (j), acetylated OGG1 and acetylated superoxide dismutase (SOD2) (k) in the mitochondrial fraction of tissues from Con, Indo and HKL + Indo treated rats. TOM20: loading control. (l) mtDNA damage as measured by 8-oxo-dG levels, with ELISA. (m) Confocal immunohistochemical staining showing 8-oxo-dG (green) and nucleus (blue) in Con, Indo and HKL + Indo treated rats. (n) Flow cytometry for mitochondrial superoxide accumulation in Con, Indo and HKL + Indo treated rats. (o) Mitochondrial transmembrane potential (ΔΨm). (p) Mitochondrial dehydrogenase activity. (q) ATP content. (r) Immunoblot of ubiquitination in the mitochondrial fraction of tissues from Con, Indo and HKL + Indo treated rats. TOM20: loading control. (s) Immunoblot of PGC1α and ERRα in the nuclear fraction of tissues from Con, Indo and HKL + Indo treated rats. Histone 3A: loading control. Representative blots are presented alongside the bar graphs (i–k, r, s). Data are mean ± SD, n = 5. *P < 0.05, significantly different from HKL 0 mg·kg^{-1}; one-way ANOVA followed by Bonferroni's post hoc test. Number of independent experiments: 3 (a–c). Data are mean ± SD, n = 5. *P < 0.05, significantly different from Con; #P < 0.05, significantly different from Indo; one-way ANOVA followed by Bonferroni's post hoc test (b, h–l, o–s). The number of independent experiments is 3.
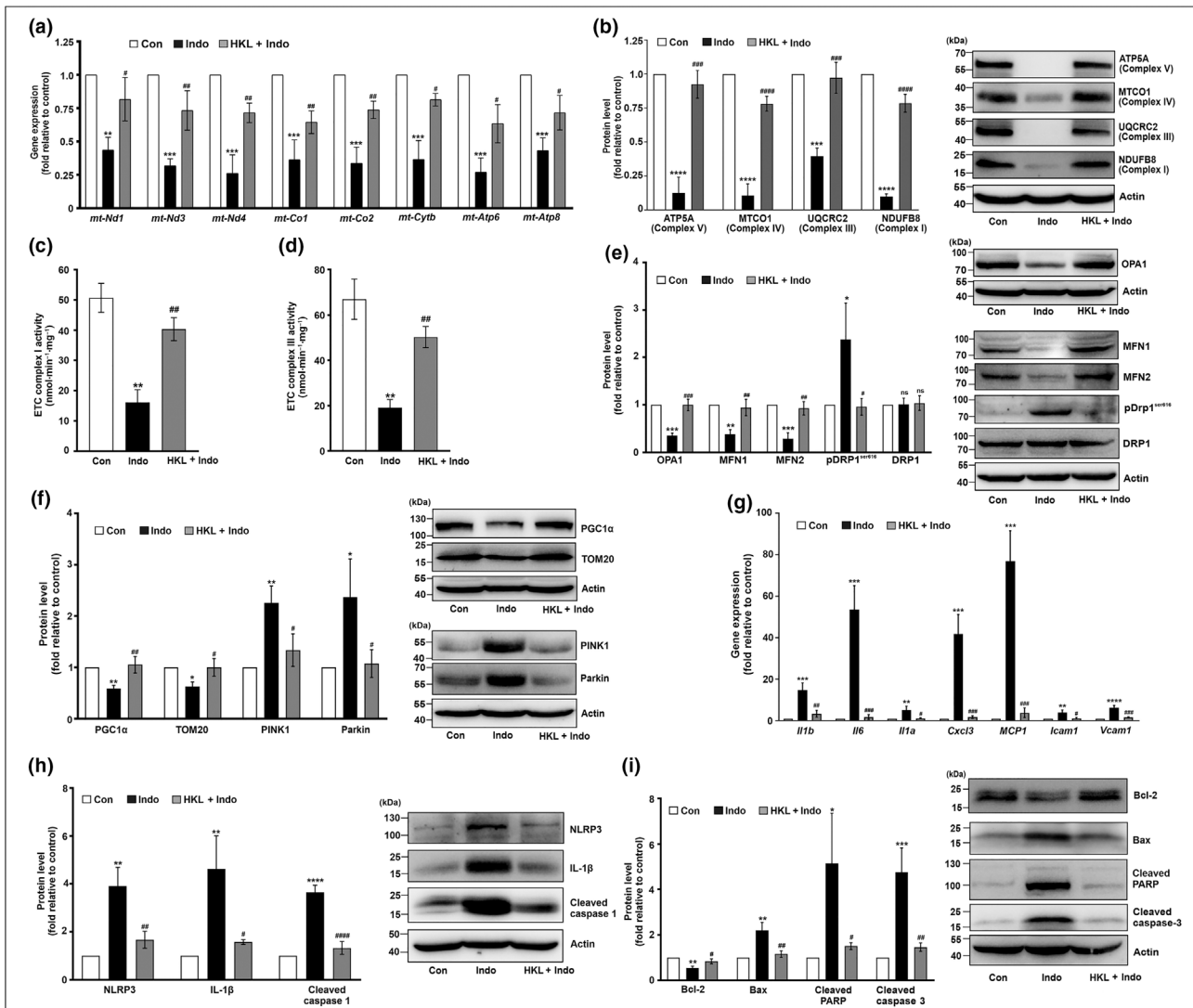
FIGURE 5 Stimulation of sirtuin-3 (Sirt3) prevents indomethacin-induced block of electron transport chain (ETC) complex gene expression, aberrant mitochondrial dynamics, mucosal inflammation and apoptosis. (a) Gene expression analysis for *mt-Nd1*, *mt-Nd3*, *mt-Nd4*, *mt-Cytb*, *mt-Co1*, *mt-Co2*, *mt-Atp6* and *mt-Atp8* by qRT-PCR) in control (Con), indomethacin (Indo) and honokiol+indomethacin (HKL + Indo) treated rats. Bar graphs indicate fold change in gene expression relative to control (after normalization by *Gapdh*). (b) Immunoblots of ATP5A, MTCO1, UQCRC2 and NDUFB8 in tissues from Con, Indo and HKL + Indo treated rats. (c) ETC complex I activity and (d) ETC complex III activity in the mitochondrial fraction of tissues from Con, Indo and HKL + Indo treated rats. (e) Immunoblots of MFN1, MFN2 OPA1, pDRP1^{ser616} and DRP1 in tissues from Con, Indo and HKL + Indo treated rats. (f) Immunoblots of PGC1α, TOM20, PINK1 and Parkin in tissues from Con, Indo and HKL + Indo treated rats. (g) Gene expression analysis for *Il1b*, *Il6*, *Il1a*, *Cxcl3*, *Mcp1*, *Icam1* and *Vcam1* by qRT-PCR in samples from Con, Indo and HKL + Indo treated rats. Bar graphs indicate fold change in gene expression relative to control (after normalization by *Gapdh*). (h) Immunoblots of NLRP3, IL-1β and cleaved caspase 1 in tissues from Con, Indo and HKL + Indo treated rats. (i) Immunoblots of Bcl-2, Bax, cleaved PARP and cleaved caspase 3 in tissues from Con, Indo and HKL + Indo treated rats. Actin was used as the loading control; representative blots are presented alongside the bar graphs (b, e, f, h, i). Data are mean ± SD, n = 5. *$P < 0.05$, significantly different from control; #$P < 0.05$, significantly different from Indo-treated rats; one-way ANOVA followed by Bonferroni's post hoc test. The number of independent experiments is 3.

However, honokiol significantly prevented indomethacin-induced up-regulation of inflammasome markers (Figure 5h). Because inflammatory tissue damage is often associated with cell death (Rock & Kono, 2008), we finally checked the expression profiles of typical pro-apoptotic and anti-apoptotic markers and found that honokiol significantly attenuated indomethacin-induced mucosal cell apoptosis through blocking the depletion of **Bcl-2** while preventing **PARP** and caspase 3 cleavage, as well as the up-regulation of **Bax** (Figure 5i).

3.5 | Honokiol accelerates the healing of pre-formed gastric lesions and offers gastroprotection against indomethacin without affecting gastric acid secretion

After documenting the prophylactic potency of honokiol against NSAID gastropathy, we checked whether Sirt3 stimulation could be used as a therapeutic strategy to accelerate the healing of pre-formed
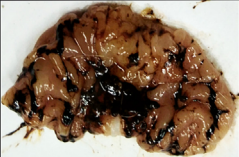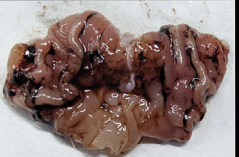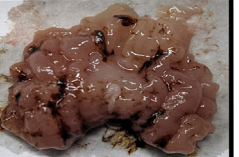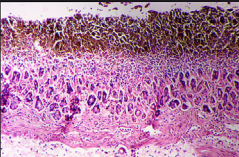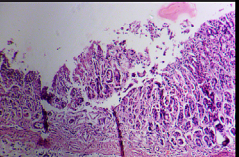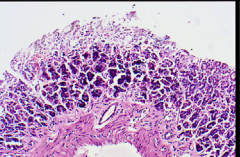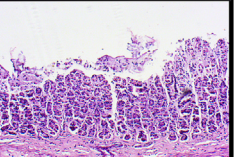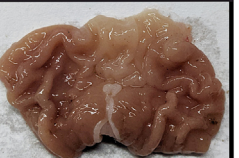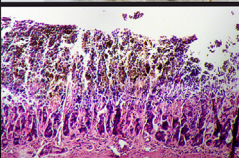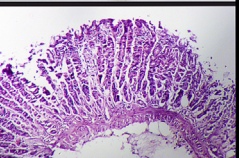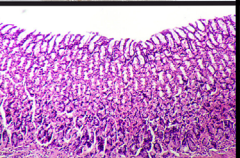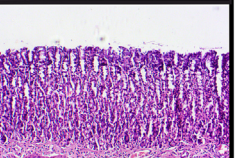
Experimental conditions		0 h	8 h	12 h	20 h
Indo	Stomach appearance				
	Histology				
	Injury index	67	52 ± 3**	41 ± 3.60****	32 ± 3.60****
HKL + Indo	Stomach appearance				
	Histology				
	Injury index	68	28 ± 2****	11 ± 1****	04 ± 1****

FIGURE 6 Honokiol (HKL) accelerates the healing of pre-formed gastric lesions induced by indomethacin. Stomach morphology and histology of indomethacin (Indo)–treated rats (upper panel) and HKL + Indo-treated rats (lower panel).

gastric lesions. Rats were treated with indomethacin and allowed to develop gastric injury for 4 h after which one set of rats was treated with honokiol and the other set was left untreated. At 0, 8, 12 and 20 h after treatment with honokiol, the extent of wound resolution was compared with that in rats treated with indomethacin only, at the same time point (Figure 6). We observed that honokiol significantly accelerated the healing of pre-formed gastric lesions.

We next checked whether honokiol treatment affected gastric acid production by measuring luminal pH under states of basal (unstimulated) and elevated (MMI-stimulated) acid secretion. Interestingly, honokiol treatment did not change gastric luminal pH significantly, unlike lansoprazole, which drastically elevated the pH (Table 1). Thus, the gastroprotection provided by honokiol was not mediated by altered gastric acid production.

3.6 | Sirt3 depletion is a generalized response elicited by common NSAIDs to trigger gastric mucosal injury

Finally, we checked whether Sirt3 depletion was specific to indomethacin or common to NSAIDs such as diclofenac, ibuprofen and aspirin, frequently found as principal components in typical anti-inflammatory

TABLE 1 pH of gastric luminal secretion of different experimental groups of rats.

Experimental set	Stomach luminal pH
Control	2.73 ± 0.45
Control + honokiol	2.48 ± 0.17ns
Control + lansoprazole	7.09 ± 0.26****
MMI	1.63 ± 0.15*
MMI + honokiol	1.83 ± 0.35*
MMI + Lansoprazole	6.61 ± 0.52****

Note: Data shown represent gastric luminal pH in control, control + honokiol', control + lansoprazole, 2-mercapto-1-methylimidazole (MMI), MMI + honokiol and MMI + lansoprazole-treated rats (n = 5). Data are mean ± SD. The number of independent experiments is 3. $*P < 0.05$, significantly different from control, ns, non-significant; one-way ANOVA followed by Bonferroni's post hoc test.

formulations for humans. Aspirin was particularly selected because of its cardioprotective and anti-neoplastic effects. We observed that all these NSAIDs significantly down-regulated Sirt3 and OGG1, similar to the effects of indomethacin. Sirt3 depletion led to significantly compromised mitochondrial dehydrogenase activity and severe mucosal injury (Figure 7a–c). Hence, Sirt3 depletion appeared a common
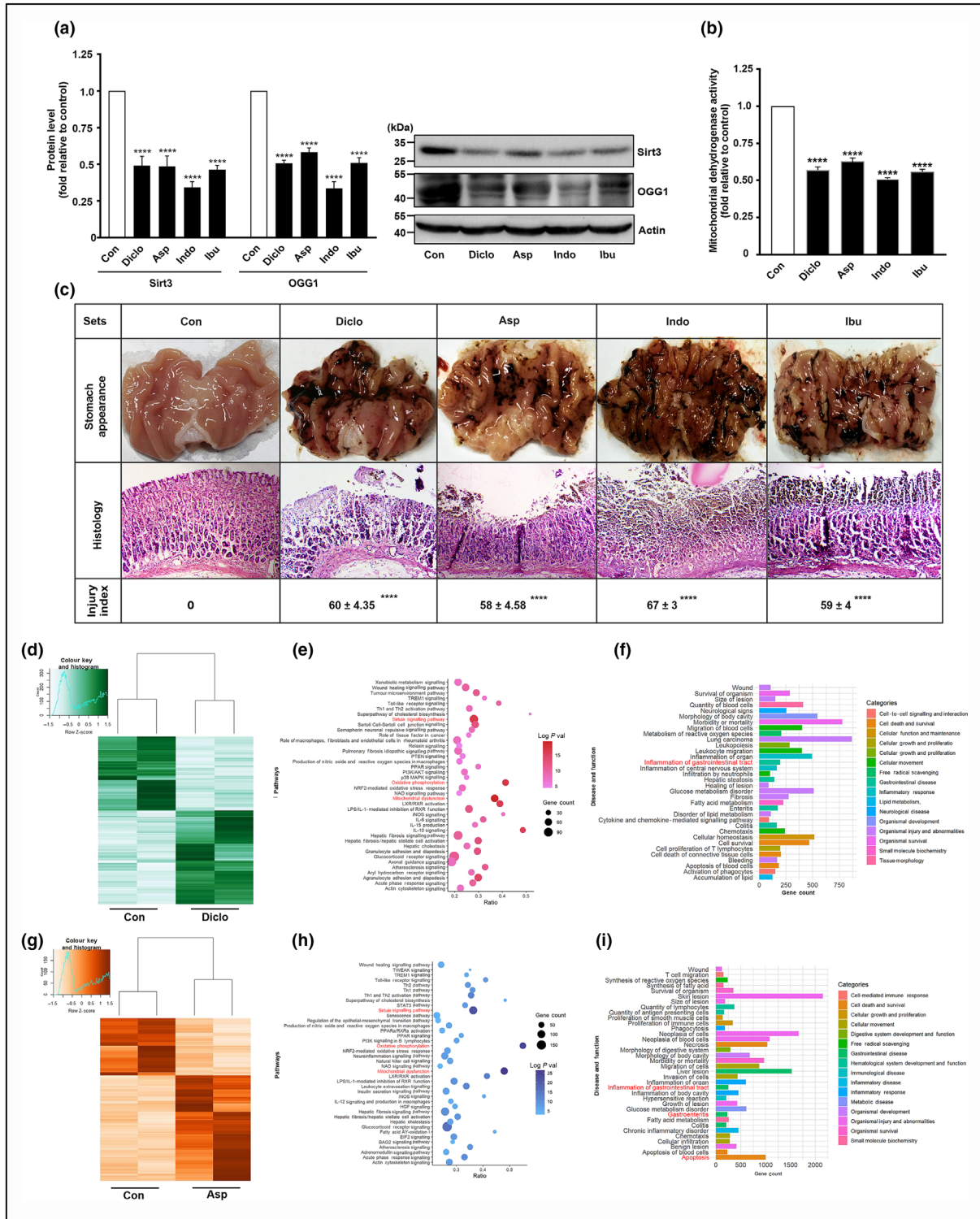
FIGURE 7 Legend on next page.

pathway targeted by NSAIDs. Further, gastric transcriptomics of diclo-fenac (Figures 7d–f and 8a–c) and aspirin (Figures 7g–i and 8d–f)-treated rats revealed patterns of DEGs and associated gene expression programmes, similar to those in rats treated with indomethacin (Files S3a–f and S4a–f).

4 | DISCUSSION

Here, we have identified Sirt3 as a novel gastroprotective target, which is severely down-regulated by NSAIDs to activate mitochondrial oxidative damage and a consequent cellular bioenergetic crisis, in gastric mucosal cells, leading to apoptosis and inflammatory tissue injury. We showed that NSAID directly inhibited Sirt3 deacetylase activity and suppressed its transcriptional regulators PGC1α and ERRα to exert a top-down suppression. Most notably, Sirt3 stimulation by honokiol markedly blocked NSAID-induced mitochondrial fragmentation, the exacerbated redox perturbation, inflammasome activation and apoptosis to prevent mucosal injury, besides accelerating the healing of pre-formed gastric lesions without affecting basal gastric acid secretion.

Despite their toxic side-effects, NSAIDs are still widely used as the first-line medicines against pain and inflammation. Emerging reports on drug repurposing of NSAIDs, which revealed their anti-neoplastic potential, have further expanded their clinical utility (Kumar, 2016; L. Li et al., 2019). Interestingly, supplementation with prostaglandins actually fails to completely ameliorate the toxic effects of NSAIDs, thereby indicating towards the involvement of extra-COX actions (Gurpinar et al., 2013). Therefore, we were keen to explore newer, COX-independent, target(s) of NSAIDs, which may be utilized for neutralizing their toxic effects while optimizing their safer usage. We used indomethacin as a prototype NSAID with negligible COX selectivity to rule out potential COX1/COX2 bias. A gastric mucosal injury model in rats was used because the gut is most severely affected by NSAIDs.

Sequencing-based target prediction was used for unbiased gene expression profiling upon NSAID treatment. Sirt3 was identified as a hub gene associated with diverse metabolic effects elicited by NSAIDs including redox homeostasis, bioenergy production, inflammation and cell death. As the mitochondrial guardian, Sirt3 controls mitochondrial protein stability to regulate antioxidant defence, structural dynamics, biogenesis, mtDNA repair and metabolism primarily through the deacetylation of target proteins including FOXO3a, OGG1, OPA1, SOD2, pyruvate dehydrogenase, citrate synthase, aconitase, isocitrate dehydrogenase, succinate dehydrogenase, malate dehydrogenase, succinate dehydrogenase, Ku70, GSK3β, mitochondrial trifunctional protein and phosphofructokinase (Murugasamy et al., 2022; Zhang et al., 2020). Loss of Sirt3 has been critically implicated in diverse pathologies involving mitochondrial structural and functional defects, leading to metabolic and bioenergetic problems (Peng et al., 2022; Sherin et al., 2021; Wu et al., 2019; Zhang et al., 2020). As a result, metabolically active tissues are susceptible to Sirt3 deficiency (Dittenhafer-Reed et al., 2015; Zhang et al., 2020). However, there is no report citing the role of Sirt3 in maintaining gastric mucosal integrity, in spite of gut mucosa having a rapid cellular turnover (Timmons et al., 2012). NSAIDs directly target the ETC complex I to cause electron leakage. These leaked electrons trigger partial reduction of oxygen to produce $O_2^{\bullet-}$, which subsequently transforms into other ROS species such as H_2O_2 and $\bullet OH$. In this context, SOD2 and OGG1 are major mitochondrial antioxidant arsenals controlling oxidative stress through neutralizing intra-mitochondrial $O_2^{\bullet-}$ and excising 8-oxo-dG in mtDNA (J. Liu et al., 2017). Coincidentally, both OGG1 and SOD2 are deacetylation targets of Sirt3. Moreover, 8-oxo-dG also serves as a biomarker for endogenous oxidative stress and redox-associated pathologies including cancer (Valavanidis et al., 2009). Indomethacin-induced Sirt3 down-regulation along with direct inhibition of Sirt3 deacetylase activity and elevation of OGG1–SOD2 acetylation explained the basis of MOS induction and cell death. Sirt3 serves as a cellular longevity promoting factor by boosting the antioxidant defences (Kincaid & Bossy-Wetzel, 2013; Merksamer et al., 2013). Sirt3-deficient cardiomyocytes produce double the amount of ROS (Sundaresan et al., 2009), whereas Sirt3 overexpression significantly increased glutathione (GSH) levels (J. Liu et al., 2017). Here, we show that indomethacin-induced Sirt3 depletion resulted in a severe bioenergetic crisis through attenuated mitochondrial dehydrogenase activity, ETC complex I and III dysfunction and ATP depletion. Ubiquitination-dependent mitochondrial elimination further potentiated the damage. Moreover, it is noteworthy that Sirt3 depletion-

FIGURE 7 Popular NSAIDs deplete Sirtuin-3 (Sirt3) to induce gastric mucosal injury and transcriptomic alteration. (a) Immunoblots of Sirt3 and 8-oxoguanine DNA glycosylase 1 (OGG1) in tissues from samples from control (Con), diclofenac (Diclo), aspirin (Asp), indomethacin (Indo) and ibuprofen (Ibu) treated rats. Actin: loading control; representative blots alongside the bar graphs. (b) Dehydrogenase activities in the mitochondrial extracts from control and indicated NSAIDs-treated rats. (c) Gastric mucosal morphology and haematoxylin/eosin-stained histology; representative images provided with injury index. Data shown in (a, b) are means ± SD; n = 5. *P < 0.05 significantly different from control; one-way ANOVA, followed by Bonferroni's post hoc test. The number of independent experiments is 3. (d) Heatmap of samples from control (Con) and diclofenac (Diclo) treated rats (false discovery rate [FDR] ≤ 0.05). Euclidean distance metric was used while clustering the gene expression data. The expression value of genes analysed with fold change (FC) cut-off of 1.5; colour gradient scale: white being highly down-regulated to green being highly up-regulated. (e) Dot plot showing enriched canonical pathways. Dot size: proportion of genes involved in a particular signalling pathway; colour range: Bonferroni corrected P values (−log transformed). Ratio: number of genes in fraction with respect to the total number of genes that map to the same pathway. (f) Bar graph showing 'disease and functions' enriched in diclofenac- treated rats. (g) Heatmap of from control (Con) and aspirin (Asp) treated rats (FDR ≤ 0.05). The expression value of genes analysed with FC cut-off of 1.5; colour gradient scale with white being highly down-regulated to brown being highly up-regulated. (h) The dot plot shows enriched canonical pathways. (i) Bar graph showing 'disease and functions' enriched in aspirin-treated rats.
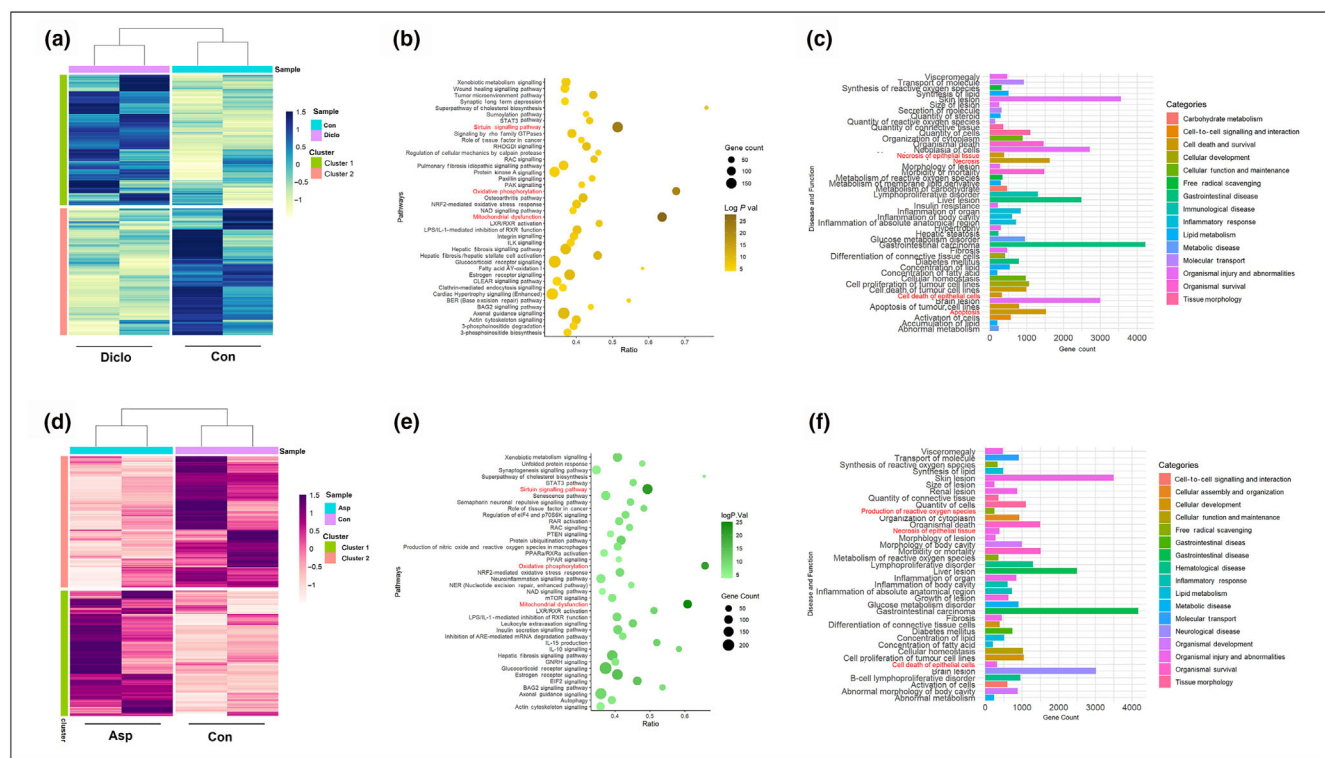
FIGURE 8   Gastric mucosal transcriptome alteration by diclofenac and aspirin after analysis at 1.2 fold change (FC) cut-off. (a) Heatmap shows separate clustering of samples from control (Con) and diclofenac (Diclo) treated rats (false discovery rate [FDR] ≤ 0.05). Euclidean distance metric was used while clustering the gene expression data. Expression value of genes analysed with FC cut-off of 1.2; colour gradient scale with blue being highly up-regulated to white being highly down-regulated. (b) Dot plot shows enriched canonical pathways. Size of dots: proportion of genes involved in particular signalling/pathway; colour range: Bonferroni corrected P values (−log transformed). Ratio represents the number of genes in fraction with respect to the total number of genes that map to the same pathway. (c) Bar graph showing 'disease and functions' enriched in diclofenac-treated rats. (d) Heatmap shows separate clustering of samples from control (Con) and aspirin (Asp) treated rats (FDR ≤ 0.05). Euclidean distance metric was used while clustering the gene expression data. Expression value of genes analysed with FC cut-off of 1.2; colour gradient scale with magenta being highly up-regulated to white being highly down-regulated. (e) Dot plot shows enriched canonical pathways. Size of dots: proportion of genes involved in particular signalling/pathway; colour range: Bonferroni corrected P values (−log transformed). Ratio represents the number of genes in fraction with respect to the total number of genes that map to the same pathway. (f) Bar graph showing 'disease and functions' enriched in aspirin-treated rats.

associated mitochondrial toxicity and cell death appeared to be a common side-effect of popular NSAIDs. This information is crucial while devising novel approaches to avoid NSAID toxicity.

From a mechanistic perspective, it was imperative to explore how NSAIDs down-regulate Sirt3. Therefore, we checked the upstream events controlling Sirt3 expression, and found that indomethacin induced the down-regulation of PGC1α and ERRα. The action of Sirt3 in regulating the PGC1α–ERRα duo has recently emerged as a pivotal nuclear transcriptional axis, orchestrating several gene expressions controlling mitochondrial bioenergetics (Y. Kim & Park, 2019; Kincaid & Bossy-Wetzel, 2013). Coincidentally, PGC1α also regulates mitochondrial biogenesis (Austin & St-Pierre, 2012), which justified mitochondrial depletion during Sirt3 down-regulation by indomethacin. Upon indomethacin treatment, we observed prominent depletion of PGC1α in both nuclear and mitochondrial fractions. This clearly suggested that NSAID blocks both nuclear and mitochondrial transcriptional activities of PGC1α to exert a comprehensive detrimental effect on gastric cell metabolism. Moreover, indomethacin-induced

Sirt3 and PGC1α depletion also implied a mutual feedback regulation. Existing reports suggest that Sirt3-dependent FOXO3 deacetylation induces its nuclear translocation to up-regulate PGC1α expression as a cytoprotective response (Fasano et al., 2019; Olmos et al., 2009) that is blunted by Sirt3 depletion. This is likely to involve direct PGC1α–FOXO3 interaction to activate *Sod2* transcription (Olmos et al., 2009). Sirt3 is noted for regulating diverse mitochondrial functions including mitosis, biogenesis, transcription, translation, OXPHOS, TCA cycle, and lipid, glycoside and amino acid metabolism (Zhang et al., 2020). Around 20% of mitochondrial proteins are highly acetylated and Sirt3 directly interacts with about 84 mitochondrial proteins to control metabolism and bioenergetics (Zhang et al., 2020). Sirt3 also controls mitochondrial dynamics and mitophagy through deacetylation-dependent regulation of OPA1, AMPK, Lon protease and FOXO3 (Meng et al., 2019). Sirt3 indirectly and/or directly (through FOXO3a deacetylation) regulates the expression of mediators of mitochondrial dynamics, such as MFN2, DRP1 and FIS1, and key mitophagy players, such as Bnip3/Nix and LC3 (Meng

et al., 2019). In this regard, indomethacin-induced MOS, mitochondrial hyperfission and aberrant mitophagy appear as direct attributes of Sirt3 depletion and intra-mitochondrial pro-oxidant accumulation to trigger ETC dysfunction.

Functional validation of the cytoprotective action of Sirt3 against indomethacin specifically relied on pharmacological Sirt3 stimulation by honokiol, a specific inducer (Pillai et al., 2015; Pillai et al., 2017; Wang, Nisar, et al., 2018). It is worth mentioning that, at present, there is apparently no commercially available synthetic Sirt3 peptide suitable for use in vivo, which would exhibit resistance against pepsin/other proteases (to protect it during systemic delivery) and be cell-permeable and mito-targeting, to allow intra-mitochondrial localization and retention for expressing the deacetylase activity. Therefore, honokiol-induced stimulation of endogenous Sirt3 levels served as the most suitable and specific pharmacological strategy to check the putative gastroprotective action of Sirt3. This approach also had the benefit of providing a novel gastroprotective strategy, specifically relying on pharmacological Sirt3 stimulation, because of the ease of this mode of intervention strategy, compared with the more precise but elaborate and highly expensive genetic manipulation-based intervention strategies while considering from a real-life therapeutic point of view. Interestingly, honokiol-induced Sirt3 stimulation corrected indomethacin-induced mitochondrial metabolic crisis and cellular damage through salvaging MOS and preserving ETC function as a consequence of attenuating mitochondrial proteome hyperacetylation and ubiquitination. honokiol pre-treatment significantly diminished transcriptome alteration by indomethacin while blocking intra-mitochondrial $O_2^{\bullet-}$ accumulation to prevent oxidative mtDNA damage. In fact, it was remarkable to find that the protective actions of honokiol extended to almost all the ETC complexes, as shown from the expressions of representative components corresponding to complex I, II, IV and V as well as direct enzymatic activities of complex I and III, which serve as major sources of mitochondrial electron leakage during ETC dysfunction. If a compound safeguards mitochondria, it seems imperative to offer protection and stability to mitochondrial structural dynamics. It was clear that the excess mitochondrial fission, aberrant mitophagy and inhibited biogenesis, induced by indomethacin, were markedly prevented by honokiol. Recently, mitochondria have been considered as epicentre of NLRP3 inflammasome activation because several mtDAMPs, including mtROS, oxidized mtDNA and oxidized cardiolipin (released during tissue injury), potently trigger NLRP3 activation (Q. Liu et al., 2018; Mazumder et al., 2022). So far, there is negligible evidence of NSAID-induced gastric mtDAMP release leading to inflammasome activation during gastric mucosal injury. Here, we clearly observed for the first time that honokiol-induced Sirt3 stimulation significantly prevented indomethacin-mediated NLRP3 activation and caspase 1 cleavage to block IL-1β up-regulation in the gastric mucosa. This was concurrent with honokiol-induced prevention of canonical inflammation and apoptosis, triggered by indomethacin. Therefore, we provide evidence that indomethacin down-regulated Sirt3 expression along with directly inhibiting Sirt3 deacetylase activity to inflict mitochondrial structural and functional damage for triggering gastric mucosal inflammatory and apoptotic

tissue damage. Honokiol, by stimulating Sirt3 expression, prevented indomethacin-induced gastropathy. It is worth mentioning that in addition to its direct Sirt3-stimulating effect, honokiol is also credited with partial agonism or activation of non-adipogenic PPARγ (Atanasov et al., 2013). Moreover, PPARγ activation has also been reported to offer gastroprotection and hasten ulcer healing in rodent models (Saha, 2015). Therefore, possible PPARγ agonism by honokiol may also contribute to or synergize its collective gastroprotective response. However, it is also noteworthy that the PPARγ–PGC1α couple has already been shown to crucially regulate energy metabolism (Kosgei et al., 2020), in a process where PGC1α is likely to be positively regulated by Sirt3 through a feedback loop. Therefore, although honokiol might have multiple responses, specificity of honokiol for Sirt3, as a defined target amongst many other off-targets, is supposedly good enough to prevent NSAID-induced gastric injury, as observed here. The observations in the present study are in direct agreement with several other studies where Sirt3 stimulation by honokiol has been found to preserve and maintain mitochondrial integrity, leading to protection against diverse pathologies (Pillai et al., 2017; Quan et al., 2020; Ramesh et al., 2018; Yi et al., 2019).

So far, we have considered the prophylactic effects of honokiol-induced Sirt3 stimulation, against NSAID gastropathy. However, a comprehensive efficacy of a cytoprotective compound stands incomplete without assessment of its therapeutic potency. In this context, honokiol also qualified as a potent gastroprotective compound because of its remarkable ability to accelerate the healing of preformed gastric lesions by indomethacin. Whereas untreated rats took 72 h after indomethacin treatment for complete resolution of mucosal injury, rats given honokiol treatment after developing profuse mucosal injury, had a shorter time (20 h) to complete wound resolution, thereby revealing its potent therapeutic efficacy. We also checked the comparative efficacy of i.p. and i.g. routes of honokiol administration, in an attempt to address the applied biomedical relevance of considering honokiol as a potential gastroprotective compound. It was clear, in the present study, that i.p. administration of honokiol required a much lower dose compared with i.g. administration, in order to provide protection against NSAIDs, at least in terms of the indomethacin-induced gastric mucosal injury in rodents. This certainly warrants further exploratory studies, specifically focused on formulating newer strategies to enhance oral bioavailability of honokiol, for ensuring its optimal utilization as a future gastroprotective drug available in oral formulations. Finally, it is imperative to state that most of the existing anti-ulcer gastroprotective compounds rely on gastric acid suppression, because acid aggravates injury. Although this logic definitely has a merit, however, it is undeniable that gastric acid is not a physiological evil. Rather, acid safeguards the GI tract from opportunist pathobiont attack besides maintaining normal gut microbiota balance, facilitating the absorption of various drug and minerals and, most notably, mediating protein digestion (Martinsen et al., 2005). Extensive usage of anti-ulcer formulations such as the proton pump inhibitors (PPIs) or histamine receptor antagonists, are often associated with several health hazards (Histamine Type-2 Receptor Antagonists (H2 Blockers), 2018; Maffei et al., 2007). Although a direct relation

between PPI intake and disease occurrence is not absolutely certain in every case and demands extensive randomized control trials (Eusebi et al., 2017), the over-usage of acid-suppressing drugs is not encouraged due to the need for physiological levels of acid. Therefore, it would be beneficial if a novel gastroprotective formulation directly targeted only the cytotoxic events (causing mucosal injury) while avoiding effects on acid secretion. Interestingly, the anti-apoptotic and cytoprotective action of honokiol did not affect basal acid secretion. This is an advantage because the harmful effects of acid suppression (such as gut dysbiosis, malabsorption of certain medicines, protein indigestion, vitamin B12 deficiency, osteoporosis, rebound acid secretion, gastrinemia and parietal cell hyperplasia) can be avoided using this gastroprotective strategy. Indeed, a recent report suggests that honokiol is apparently safe for human consumption as a natural antioxidant supplement (Sarrica et al., 2018). Further, it is also worth mentioning that several studies on cancers have projected Sirt3 as a double-edged sword, reflecting its cancer and/or context-specific oncogenic or tumour-suppressive attributes, depending on the nature and metabolic requirements of the tumours and their unique microenvironment (Ouyang et al., 2022). However, in regard to non-malignant pathologies, Sirt3 stimulation is mostly beneficial and offers protection against a range of pathologies associated with inflammation, oxidative stress, mitochondrial dysfunction and energy dyshomeostasis (Bugga et al., 2022; Dikalova et al., 2020; Zhang et al., 2020). The excess level of ROS accumulated in course of the pathogenesis is neutralized by Sirt3 stimulation by honokiol, leading to protection from the disease.

Taken together, our data showed Sirt3 to be a non-canonical, COX-independent, target of NSAIDs, which is severely down-regulated leading to mitochondrial structural and functional disorder during gastric mucosal injury. The phyto-polyphenol, honokiol, acting as a Sirt3 inducer, offers strong gastroprotection while not affecting gastric acid secretion. Precisely exploiting this knowledge may lead to the design of novel gastroprotective compounds, specifically targeting mitochondria. Furthermore, NSAID treatment, coupled with endogenous Sirt3 stimulation by honokiol, may definitely help to optimize the therapeutic usage of these 'wonder drugs', while avoiding their side effects.

AUTHOR CONTRIBUTIONS

ACKNOWLEDGEMENTS

CONFLICT OF INTEREST STATEMENT

The authors declare no competing interests with any part of the manuscript.

DECLARATION OF TRANSPARENCY AND SCIENTIFIC RIGOUR

This Declaration acknowledges that this paper adheres to the principles for transparent reporting and scientific rigour of preclinical research as stated in the *BJP* guidelines for Design & Analysis, Immunoblotting and Immunochemistry, and Animal Experimentation, and as recommended by funding agencies, publishers and other organizations engaged with supporting research.

DATA AVAILABILITY STATEMENT

Processed and raw RNA-seq data generated in this study are available in the GEO with accession number GSE201565 for rat transcriptomics data. All data pertaining to this study are provided in the manuscript and supporting information.

ORCID

Uday Bandyopadhyay https://orcid.org/0000-0002-5928-6790

REFERENCES

Alexander, S. P., Cidlowski, J. A., Kelly, E., Mathie, A., Peters, J. A., Veale, E. L., Armstrong, J. F., Faccenda, E., Harding, S. D., Pawson, A. J., Southan, C., Davies, J. A., Coons, L., Fuller, P. J., Korach, K. S., & Young, M. J. (2021). THE CONCISE GUIDE TO PHARMACOLOGY 2021/22: Nuclear hormone receptors. *British Journal of Pharmacology*, *178*(S1), S246–S263. https://doi.org/10.1111/bph.15540

14765381, 0, Downloaded from https://bpspubs.onlinelibrary.wiley.com/doi/10.1111/bph.16070 by Indian Institution Of Chem Biology, Wiley Online Library on [17/05/2023]. See the Terms and Conditions (https://onlinelibrary.wiley.com/terms-and-conditions) on Wiley Online Library for rules of use; OA articles are governed by the applicable Creative Commons License

Alexander, S. P., Fabbro, D., Kelly, E., Mathie, A., Peters, J. A., Veale, E. L., Armstrong, J. F., Faccenda, E., Harding, S. D., Pawson, A. J., Southan, C., Davies, J. A., Beuve, A., Brouckaert, P., Bryant, C., Burnett, J. C., Farndale, R. W., Friebe, A., Garthwaite, J., … Waldman, S. A. (2021). THE CONCISE GUIDE TO PHARMACOLOGY 2021/22: Catalytic receptors. *British Journal of Pharmacology*, *178*(S1), S264–S312. https://doi.org/10.1111/bph.15541

Alexander, S. P., Fabbro, D., Kelly, E., Mathie, A., Peters, J. A., Veale, E. L., Armstrong, J. F., Faccenda, E., Harding, S. D., Pawson, A. J., Southan, C., Davies, J. A., Boison, D., Burns, K. E., Dessauer, C., Gertsch, J., Helsby, N. A., Izzo, A. A., Koesling, D., … Wong, S. S. (2021). THE CONCISE GUIDE TO PHARMACOLOGY 2021/22: Enzymes. *British Journal of Pharmacology*, *178*(S1), S313–S411. https://doi.org/10.1111/bph.15542

Alexander, S. P., Kelly, E., Mathie, A., Peters, J. A., Veale, E. L., Armstrong, J. F., Faccenda, E., Harding, S. D., Pawson, A. J., Southan, C., Buneman, O. P., Cidlowski, J. A., Christopoulos, A., Davenport, A. P., Fabbro, D., Spedding, M., Striessnig, J., Davies, J. A., Ahlers-Dannen, K. E., … Zolghadri, Y. (2021). THE CONCISE GUIDE TO PHARMACOLOGY 2021/22: Other Protein Targets. *British Journal of Pharmacology*, *178*(S1), S1–S26. https://doi.org/10.1111/bph.15537

Alexander, S. P. H., Roberts, R. E., Broughton, B. R. S., Sobey, C. G., George, C. H., Stanford, S. C., Cirino, G., Docherty, J. R., Giembycz, M. A., Hoyer, D., Insel, P. A., Izzo, A. A., Ji, Y., MacEwan, D. J., Mangum, J., Wonnacott, S., & Ahluwalia, A. (2018). Goals and practicalities of immunoblotting and immunohistochemistry: A guide for submission to the *British Journal of Pharmacology*. *British Journal of Pharmacology*, *175*, 407–411. https://doi.org/10.1111/bph.14112

Aminzadeh-Gohari, S., Weber, D. D., Vidali, S., Catalano, L., Kofler, B., & Feichtinger, R. G. (2020). From old to new—Repurposing drugs to target mitochondrial energy metabolism in cancer. *Seminars in Cell & Developmental Biology*, *98*, 211–223. https://doi.org/10.1016/j.semcdb.2019.05.025

Andrews, S. (2010). FastQC: A quality control tool for high throughput sequence data [Online]. Available online at: http://www.bioinformatics.babraham.ac.uk/projects/fastqc/

Atanasov, A. G., Wang, J. N., Gu, S. P., Bu, J., Kramer, M. P., Baumgartner, L., Fakhrudin, N., Ladurner, A., Malainer, C., Vuorinen, A., Noha, S. M., Schwaiger, S., Rollinger, J. M., Schuster, D., Stuppner, H., Dirsch, V. M., & Heiss, E. H. (2013). Honokiol: A non-adipogenic PPARγ agonist from nature. *Biochimica et Biophysica Acta*, *1830*, 4813–4819. https://doi.org/10.1016/j.bbagen.2013.06.021

Austin, S., & St-Pierre, J. (2012). PGC1α and mitochondrial metabolism—Emerging concepts and relevance in ageing and neurodegenerative disorders. *Journal of Cell Science*, *125*, 4963–4971. https://doi.org/10.1242/jcs.113662

Bader, G. D., & Hogue, C. W. (2003). An automated method for finding molecular complexes in large protein interaction networks. *BMC Bioinformatics*, *4*, 2. https://doi.org/10.1186/1471-2105-4-2

Bindu, S., Mazumder, S., & Bandyopadhyay, U. (2020). Non-steroidal anti-inflammatory drugs (NSAIDs) and organ damage: A current perspective. *Biochemical Pharmacology*, *180*, 114147. https://doi.org/10.1016/j.bcp.2020.114147

Bindu, S., Mazumder, S., Dey, S., Pal, C., Goyal, M., Alam, A., Iqbal, M. S., Sarkar, S., Azhar Siddiqui, A., Banerjee, C., & Bandyopadhyay, U. (2013). Nonsteroidal anti-inflammatory drug induces proinflammatory damage in gastric mucosa through NF-κB activation and neutrophil infiltration: Anti-inflammatory role of heme oxygenase-1 against nonsteroidal anti-inflammatory drug. *Free Radical Biology & Medicine*, *65*, 456–467. https://doi.org/10.1016/j.freeradbiomed.2013.07.027

Bindu, S., Pillai, V. B., Kanwal, A., Samant, S., Mutlu, G. M., Verdin, E., Dulin, N., & Gupta, M. P. (2017). SIRT3 blocks myofibroblast differentiation and pulmonary fibrosis by preventing mitochondrial DNA damage. *American Journal of Physiology. Lung Cellular and Molecular Physiology*, *312*, L68–L78. https://doi.org/10.1152/ajplung.00188.2016

Bugga, P., Alam, M. J., Kumar, R., Pal, S., Chattopadyay, N., & Banerjee, S. K. (2022). Sirt3 ameliorates mitochondrial dysfunction and oxidative stress through regulating mitochondrial biogenesis and dynamics in cardiomyoblast. *Cellular Signalling*, *94*, 110309. https://doi.org/10.1016/j.cellsig.2022.110309

Carrasco-Pozo, C., Gotteland, M., & Speisky, H. (2011). Apple peel polyphenol extract protects against indomethacin-induced damage in Caco-2 cells by preventing mitochondrial complex I inhibition. *Journal of Agricultural and Food Chemistry*, *59*, 11501–11508. https://doi.org/10.1021/jf202621d

Crofford, L. J. (2013). Use of NSAIDs in treating patients with arthritis. *Arthritis Research & Therapy*, *15*(Suppl 3), S2. https://doi.org/10.1186/ar4174

Curtis, M. J., Alexander, S. P. H., Cirino, G., George, C. H., Kendall, D. A., Insel, P. A., Izzo, A. A., Ji, Y., Panettieri, R. A., Patel, H. H., Sobey, C. G., Stanford, S. C., Stanley, P., Stefanska, B., Stephens, G. J., Teixeira, M. M., Vergnolle, N., & Ahluwalia, A. (2022). Planning experiments: Updated guidance on experimental design and analysis and their reporting III. *British Journal of Pharmacology*, *179*, 3907–3913. https://doi.org/10.1111/bph.15868

Cuzick, J., Otto, F., Baron, J. A., Brown, P. H., Burn, J., Greenwald, P., Jankowski, J., La Vecchia, C., Meyskens, F., Senn, H. J., & Thun, M. (2009). Aspirin and non-steroidal anti-inflammatory drugs for cancer prevention: An international consensus statement. *The Lancet Oncology*, *10*, 501–507. https://doi.org/10.1016/S1470-2045(09)70035-X

De, R., Mazumder, S., Sarkar, S., Debsharma, S., Siddiqui, A. A., Saha, S. J., Banerjee, C., Nag, S., Saha, D., & Bandyopadhyay, U. (2017). Acute mental stress induces mitochondrial bioenergetic crisis and hyperfission along with aberrant mitophagy in the gut mucosa in rodent model of stress-related mucosal disease. *Free Radical Biology & Medicine*, *113*, 424–438. https://doi.org/10.1016/j.freeradbiomed.2017.10.009

Dey, S., Mazumder, S., Siddiqui, A. A., Iqbal, M. S., Banerjee, C., Sarkar, S., De, R., Goyal, M., Bindu, S., & Bandyopadhyay, U. (2014). Association of heme oxygenase 1 with the restoration of liver function after damage in murine malaria by *Plasmodium yoelii*. *Infection and Immunity*, *82*, 3113–3126. https://doi.org/10.1128/IAI.01598-14

Dikalova, A. E., Pandey, A., Xiao, L., Arslanbaeva, L., Sidorova, T., Lopez, M. G., Billings, F. T., Verdin, E., Auwerx, J., Harrison, D. G., & Dikalov, S. I. (2020). Mitochondrial deacetylase Sirt3 reduces vascular dysfunction and hypertension while Sirt3 depletion in essential hypertension is linked to vascular inflammation and oxidative stress. *Circulation Research*, *126*, 439–452. https://doi.org/10.1161/CIRCRESAHA.119.315767

Dittenhafer-Reed, K. E., Richards, A. L., Fan, J., Smallegan, M. J., Fotuhi Siahpirani, A., Kemmerer, Z. A., Prolla, T. A., Roy, S., Coon, J. J., & Denu, J. M. (2015). SIRT3 mediates multi-tissue coupling for metabolic fuel switching. *Cell Metabolism*, *21*, 637–646. https://doi.org/10.1016/j.cmet.2015.03.007

Eusebi, L. H., Rabitti, S., Artesiani, M. L., Gelli, D., Montagnani, M., Zagari, R. M., & Bazzoli, F. (2017). Proton pump inhibitors: Risks of long-term use. *Journal of Gastroenterology and Hepatology*, *32*, 1295–1302. https://doi.org/10.1111/jgh.13737

Fasano, C., Disciglio, V., Bertora, S., Lepore Signorile, M., & Simone, C. (2019). FOXO3a from the nucleus to the mitochondria: A round trip in cellular stress response. *Cell*, *8*(9), 1110.

Ghori, S. S., Amer, M. F., & Siddiqa, S. (2016). Antiulcer potential of *Ficus dalhousiae* stem bark methanolic extract in albino rats. *Indo American Journal of Pharmaceutical Sciences*, *3*(10), 1096–1101.

Gurpinar, E., Grizzle, W. E., & Piazza, G. A. (2013). COX-independent mechanisms of cancer chemoprevention by anti-inflammatory drugs.

Frontiers in Oncology, *3*, 181. https://doi.org/10.3389/fonc.2013.00181

Gurpinar, E., Grizzle, W. E., & Piazza, G. A. (2014). NSAIDs inhibit tumorigenesis, but how? *Clinical Cancer Research*, *20*, 1104–1113. https://doi.org/10.1158/1078-0432.CCR-13-1573

Histamine type-2 receptor antagonists (H2 blockers). (2018). In *LiverTox: Clinical and research information on drug-induced liver injury*. National Institute of Diabetes and Digestive and Kidney Diseases.

Kazberuk, A., Zareba, I., Palka, J., & Surazynski, A. (2020). A novel plausible mechanism of NSAIDs-induced apoptosis in cancer cells: The implication of proline oxidase and peroxisome proliferator-activated receptor. *Pharmacological Reports*, *72*, 1152–1160. https://doi.org/10.1007/s43440-020-00140-z

Khoo, B. L., Grenci, G., Lim, J. S. Y., Lim, Y. P., Fong, J., Yeap, W. H., Bin Lim, S., Chua, S. L., Wong, S. C., Yap, Y. S., Lee, S. C., Lim, C. T., & Han, J. (2019). Low-dose anti-inflammatory combinatorial therapy reduced cancer stem cell formation in patient-derived preclinical models for tumour relapse prevention. *British Journal of Cancer*, *120*, 407–423. https://doi.org/10.1038/s41416-018-0301-9

Kim, H. S., Patel, K., Muldoon-Jacobs, K., Bisht, K. S., Aykin-Burns, N., Pennington, J. D., van der Meer, R., Nguyen, P., Savage, J., Owens, K. M., Vassilopoulos, A., Ozden, O., Park, S. H., Singh, K. K., Abdulkadir, S. A., Spitz, D. R., Deng, C. X., & Gius, D. (2010). SIRT3 is a mitochondria-localized tumor suppressor required for maintenance of mitochondrial integrity and metabolism during stress. *Cancer Cell*, *17*, 41–52. https://doi.org/10.1016/j.ccr.2009.11.023

Kim, Y., & Park, C. W. (2019). Mechanisms of adiponectin action: Implication of adiponectin receptor agonism in diabetic kidney disease. *International Journal of Molecular Sciences*, *20*, 1782. https://doi.org/10.3390/ijms20071782

Kincaid, B., & Bossy-Wetzel, E. (2013). Forever young: SIRT3 a shield against mitochondrial meltdown, aging, and neurodegeneration. *Frontiers in Aging Neuroscience*, *5*, 48. https://doi.org/10.3389/fnagi.2013.00048

Kolawole, O. R., & Kashfi, K. (2022). NSAIDs and cancer resolution: New paradigms beyond cyclooxygenase. *International Journal of Molecular Sciences*, *23*, 1432. https://doi.org/10.3390/ijms23031432

Kosgei, V. J., Coelho, D., Gueant-Rodriguez, R. M., & Gueant, J. L. (2020). Sirt1-PPARS cross-talk in complex metabolic diseases and inherited disorders of the one carbon metabolism. *Cell*, *9*, 1882. https://doi.org/10.3390/cells9081882

Krause, M. M., Brand, M. D., Krauss, S., Meisel, C., Vergin, H., Burmester, G. R., & Buttgereit, F. (2003). Nonsteroidal antiinflammatory drugs and a selective cyclooxygenase 2 inhibitor uncouple mitochondria in intact cells. *Arthritis and Rheumatism*, *48*, 1438–1444. https://doi.org/10.1002/art.10969

Kumar, R. (2016). Repositioning of non-steroidal anti inflammatory drug (NSAIDs) for cancer treatment: Promises and challenges. *Journal of Nanomedicine & Nanotechnology*, *7*, 1000e140. https://doi.org/10.4172/2157-7439.1000e140

Li, H., Handsaker, B., Wysoker, A., Fennell, T., Ruan, J., Homer, N., Marth, G., Abecasis, G., Durbin, R., & Subgroup, G. P. D. P. (2009). The sequence alignment/map format and SAMtools. *Bioinformatics*, *25*, 2078–2079. https://doi.org/10.1093/bioinformatics/btp352

Li, L., Hu, M., Wang, T., Chen, H., & Xu, L. (2019). Repositioning aspirin to treat lung and breast cancers and overcome acquired resistance to targeted therapy. *Frontiers in Oncology*, *9*, 1503. https://doi.org/10.3389/fonc.2019.01503

Liao, Y., Smyth, G. K., & Shi, W. (2014). featureCounts: An efficient general purpose program for assigning sequence reads to genomic features. *Bioinformatics*, *30*, 923–930. https://doi.org/10.1093/bioinformatics/btt656

Liggett, J. L., Zhang, X., Eling, T. E., & Baek, S. J. (2014). Anti-tumor activity of non-steroidal anti-inflammatory drugs: Cyclooxygenase-

independent targets. *Cancer Letters*, *346*, 217–224. https://doi.org/10.1016/j.canlet.2014.01.021

Lilley, E., Stanford, S. C., Kendall, D. E., Alexander, S. P. H., Cirino, G., Docherty, J. R., George, C. H., Insel, P. A., Izzo, A. A., Ji, Y., Panettieri, R. A., Sobey, C. G., Stefanska, B., Stephens, G., Teixeira, M. M., & Ahluwalia, A. (2020). ARRIVE 2.0 and the British Journal of Pharmacology: Updated guidance for 2020. *British Journal of Pharmacology*, *177*, 3611–3616. https://doi.org/10.1111/bph.15178

Liu, J., Li, D., Zhang, T., Tong, Q., Ye, R. D., & Lin, L. (2017). SIRT3 protects hepatocytes from oxidative injury by enhancing ROS scavenging and mitochondrial integrity. *Cell Death & Disease*, *8*, e3158. https://doi.org/10.1038/cddis.2017.564

Liu, Q., Zhang, D., Hu, D., Zhou, X., & Zhou, Y. (2018). The role of mitochondria in NLRP3 inflammasome activation. *Molecular Immunology*, *103*, 115–124. https://doi.org/10.1016/j.molimm.2018.09.010

Love, M. I., Huber, W., & Anders, S. (2014). Moderated estimation of fold change and dispersion for RNA-seq data with DESeq2. *Genome Biology*, *15*, 550. https://doi.org/10.1186/s13059-014-0550-8

Maffei, M., Desmeules, J., Cereda, J. M., & Hadengue, A. (2007, 1938). Side effects of proton pump inhibitors (PPIs). *Revue Médicale Suisse*, *3*, 1934–1936.

Maharani, B. (2022). Screening methods for the evaluation of antiulcer drugs. In D. G. S. Mageshwaran Lakshmanan & G. M. Raj (Eds.), *Introduction to basics of pharmacology and toxicology* (pp. 371–382). Springer Nature.

Mao, R. W., He, S. P., Lan, J. G., & Zhu, W. Z. (2022). Honokiol ameliorates cisplatin-induced acute kidney injury via inhibition of mitochondrial fission. *British Journal of Pharmacology*, *179*, 3886–3904. https://doi.org/10.1111/bph.15837

Martin, M. (2011). Cutadapt removes adapter sequences from high-throughput sequencing reads. *EMBnet Journal*, *17*, 10–12. https://doi.org/10.14806/ej.17.1.200

Martinsen, T. C., Bergh, K., & Waldum, H. L. (2005). Gastric juice: A barrier against infectious diseases. *Basic & Clinical Pharmacology & Toxicology*, *96*, 94–102. https://doi.org/10.1111/j.1742-7843.2005.pto960202.x

Matsui, H., Shimokawa, O., Kaneko, T., Nagano, Y., Rai, K., & Hyodo, I. (2011). The pathophysiology of non-steroidal anti-inflammatory drug (NSAID)-induced mucosal injuries in stomach and small intestine. *Journal of Clinical Biochemistry and Nutrition*, *48*, 107–111. https://doi.org/10.3164/jcbn.10-79

Mazumder, S., Barman, M., Bandyopadhyay, U., & Bindu, S. (2020). Sirtuins as endogenous regulators of lung fibrosis: A current perspective. *Life Sciences*, *258*, 118201. https://doi.org/10.1016/j.lfs.2020.118201

Mazumder, S., Bindu, S., De, R., Debsharma, S., Pramanik, S., & Bandyopadhyay, U. (2022). Emerging role of mitochondrial DAMPs, aberrant mitochondrial dynamics and anomalous mitophagy in gut mucosal pathogenesis. *Life Sciences*, *305*, 120753. https://doi.org/10.1016/j.lfs.2022.120753

Mazumder, S., De, R., Debsharma, S., Bindu, S., Maity, P., Sarkar, S., Saha, S. J., Siddiqui, A. A., Banerjee, C., Nag, S., Saha, D., Pramanik, S., Mitra, K., & Bandyopadhyay, U. (2019). Indomethacin impairs mitochondrial dynamics by activating the PKCζ-p38-DRP1 pathway and inducing apoptosis in gastric cancer and normal mucosal cells. *The Journal of Biological Chemistry*, *294*, 8238–8258. https://doi.org/10.1074/jbc.RA118.004415

Mazumder, S., De, R., Sarkar, S., Siddiqui, A. A., Saha, S. J., Banerjee, C., Iqbal, M. S., Nag, S., Debsharma, S., & Bandyopadhyay, U. (2016). Selective scavenging of intra-mitochondrial superoxide corrects diclofenac-induced mitochondrial dysfunction and gastric injury: A novel gastroprotective mechanism independent of gastric acid

suppression. *Biochemical Pharmacology*, *121*, 33–51. https://doi.org/10.1016/j.bcp.2016.09.027

Meng, H., Yan, W. Y., Lei, Y. H., Wan, Z., Hou, Y. Y., Sun, L. K., & Zhou, J. P. (2019). SIRT3 regulation of mitochondrial quality control in neurodegenerative diseases. *Frontiers in Aging Neuroscience*, *11*, 313. https://doi.org/10.3389/fnagi.2019.00313

Merksamer, P. I., Liu, Y., He, W., Hirschey, M. D., Chen, D., & Verdin, E. (2013). The sirtuins, oxidative stress and aging: An emerging link. *Aging (Albany NY)*, *5*, 144–150. https://doi.org/10.18632/aging.100544

Morigi, M., Perico, L., Rota, C., Longaretti, L., Conti, S., Rottoli, D., Novelli, R., Remuzzi, G., & Benigni, A. (2015). Sirtuin 3-dependent mitochondrial dynamic improvements protect against acute kidney injury. *The Journal of Clinical Investigation*, *125*, 715–726. https://doi.org/10.1172/JCI77632

Murugasamy, K., Munjal, A., & Sundaresan, N. R. (2022). Emerging roles of SIRT3 in cardiac metabolism. *Frontiers in Cardiovascular Medicine*, *9*, 850340. https://doi.org/10.3389/fcvm.2022.850340

Olmos, Y., Valle, I., Borniquel, S., Tierrez, A., Soria, E., Lamas, S., & Monsalve, M. (2009). Mutual dependence of Foxo3a and PGC-1α in the induction of oxidative stress genes. *The Journal of Biological Chemistry*, *284*, 14476–14484. https://doi.org/10.1074/jbc.M807397200

Ong, C. K., Lirk, P., Tan, C. H., & Seymour, R. A. (2007). An evidence-based update on nonsteroidal anti-inflammatory drugs. *Clinical Medicine & Research*, *5*, 19–34. https://doi.org/10.3121/cmr.2007.698

Ouyang, S., Zhang, Q., Lou, L., Zhu, K., Li, Z., Liu, P., & Zhang, X. (2022). The double-edged sword of SIRT3 in cancer and its therapeutic applications. *Frontiers in Pharmacology*, *13*, 871560. https://doi.org/10.3389/fphar.2022.871560

Peng, M. L., Fu, Y., Wu, C. W., Zhang, Y., Ren, H., & Zhou, S. S. (2022). Signaling pathways related to oxidative stress in diabetic cardiomyopathy. *Frontiers in Endocrinology (Lausanne)*, *13*, 907757. https://doi.org/10.3389/fendo.2022.907757

Percie du Sert, N., Hurst, V., Ahluwalia, A., Alam, S., Avey, M. T., Baker, M., Browne, W. J., Clark, A., Cuthill, I. C., Dirnagl, U., Emerson, M., Garner, P., Holgate, S. T., Howells, D. W., Karp, N. A., Lazic, S. E., Lidster, K., MacCallum, C. J., Macleod, M., … Würbel, H. (2020). The ARRIVE guidelines 2.0: updated guidelines for reporting animal research. *PLoS Biology*, *18*, e3000410.

Pertea, M., Kim, D., Pertea, G. M., Leek, J. T., & Salzberg, S. L. (2016). Transcript-level expression analysis of RNA-seq experiments with HISAT, StringTie and Ballgown. *Nature Protocols*, *11*, 1650–1667. https://doi.org/10.1038/nprot.2016.095

Pillai, V. B., Kanwal, A., Fang, Y. H., Sharp, W. W., Samant, S., Arbiser, J., & Gupta, M. P. (2017). Honokiol, an activator of Sirtuin-3 (SIRT3) preserves mitochondria and protects the heart from doxorubicin-induced cardiomyopathy in mice. *Oncotarget*, *8*, 34082–34098. https://doi.org/10.18632/oncotarget.16133

Pillai, V. B., Samant, S., Sundaresan, N. R., Raghuraman, H., Kim, G., Bonner, M. Y., Arbiser, J. L., Walker, D. I., Jones, D. P., Gius, D., & Gupta, M. P. (2015). Honokiol blocks and reverses cardiac hypertrophy in mice by activating mitochondrial Sirt3. *Nature Communications*, *6*, 6656. https://doi.org/10.1038/ncomms7656

Quan, Y., Park, W., Jin, J., Kim, W., Park, S. K., & Kang, K. P. (2020). Sirtuin 3 activation by honokiol decreases unilateral ureteral obstruction-induced renal inflammation and fibrosis via regulation of mitochondrial dynamics and the renal NF-κB-TGF-β1/Smad signaling pathway. *International Journal of Molecular Sciences*, *21*, 402. https://doi.org/10.3390/ijms21020402

Raghavendran, H. R., Srinivasan, P., & Rekha, S. (2011). Immunomodulatory activity of fucoidan against aspirin-induced gastric mucosal damage in rats. *International Immunopharmacology*, *11*, 157–163. https://doi.org/10.1016/j.intimp.2010.11.002

Ramesh, S., Govindarajulu, M., Lynd, T., Briggs, G., Adamek, D., Jones, E., Heiner, J., Majrashi, M., Moore, T., Amin, R., Suppiramaniam, V., &

Dhanasekaran, M. (2018). SIRT3 activator Honokiol attenuates β-Amyloid by modulating amyloidogenic pathway. *PLoS ONE*, *13*, e0190350. https://doi.org/10.1371/journal.pone.0190350

Rock, K. L., & Kono, H. (2008). The inflammatory response to cell death. *Annual Review of Pathology*, *3*, 99–126. https://doi.org/10.1146/annurev.pathmechdis.3.121806.151456

Saha, L. (2015). Role of peroxisome proliferator-activated receptors alpha and gamma in gastric ulcer: An overview of experimental evidences. *World Journal of Gastrointestinal Pharmacology and Therapeutics*, *6*, 120–126. https://doi.org/10.4292/wjgpt.v6.i4.120

Sandoval-Acuna, C., Lopez-Alarcon, C., Aliaga, M. E., & Speisky, H. (2012). Inhibition of mitochondrial complex I by various non-steroidal anti-inflammatory drugs and its protection by quercetin via a coenzyme Q-like action. *Chemico-Biological Interactions*, *199*, 18–28. https://doi.org/10.1016/j.cbi.2012.05.006

Sarrica, A., Kirika, N., Romeo, M., Salmona, M., & Diomede, L. (2018). Safety and toxicology of magnolol and honokiol. *Planta Medica*, *84*, 1151–1164. https://doi.org/10.1055/a-0642-1966

Shannon, P., Markiel, A., Ozier, O., Baliga, N. S., Wang, J. T., Ramage, D., Amin, N., Schwikowski, B., & Ideker, T. (2003). Cytoscape: A software environment for integrated models of biomolecular interaction networks. *Genome Research*, *13*, 2498–2504. https://doi.org/10.1101/gr.1239303

Sherin, F., Gomathy, S., & Antony, S. (2021). Sirtuin3 in neurological disorders. *Current Drug Research Reviews*, *13*, 140–147. https://doi.org/10.2174/2589977512666201207200626

Sostres, C., Gargallo, C. J., & Lanas, A. (2013). Nonsteroidal anti-inflammatory drugs and upper and lower gastrointestinal mucosal damage. *Arthritis Research & Therapy*, *15*(Suppl 3), S3. https://doi.org/10.1186/ar4175

Spinazzi, M., Casarin, A., Pertegato, V., Salviati, L., & Angelini, C. (2012). Assessment of mitochondrial respiratory chain enzymatic activities on tissues and cultured cells. *Nature Protocols*, *7*, 1235–1246. https://doi.org/10.1038/nprot.2012.058

Sun, R., Kang, X., Zhao, Y., Wang, Z., Wang, R., Fu, R., Li, Y., Hu, Y., Wang, Z., Shan, W., Zhou, J., Tian, X., & Yao, J. (2020). Sirtuin 3-mediated deacetylation of acyl-CoA synthetase family member 3 by protocatechuic acid attenuates non-alcoholic fatty liver disease. *British Journal of Pharmacology*, *177*, 4166–4180. https://doi.org/10.1111/bph.15159

Sundaresan, N. R., Gupta, M., Kim, G., Rajamohan, S. B., Isbatan, A., & Gupta, M. P. (2009). Sirt3 blocks the cardiac hypertrophic response by augmenting Foxo3a-dependent antioxidant defense mechanisms in mice. *The Journal of Clinical Investigation*, *119*, 2758–2771. https://doi.org/10.1172/JCI39162

Suzuki, Y., Inoue, T., & Ra, C. (2010). NSAIDs, mitochondria and calcium signaling: Special focus on aspirin/salicylates. *Pharmaceuticals (Basel)*, *3*, 1594–1613. https://doi.org/10.3390/ph3051594

Timmons, J., Chang, E. T., Wang, J. Y., & Rao, J. N. (2012). Polyamines and gut mucosal homeostasis. *Journal of Gastrointestinal & Digestive System*, *2*, 001. https://doi.org/10.4172/2161-069X.S7-001

Valavanidis, A., Vlachogianni, T., & Fiotakis, C. (2009). 8-hydroxy-2′-deoxyguanosine (8-OHdG): A critical biomarker of oxidative stress and carcinogenesis. *Journal of Environmental Science and Health. Part C, Environmental Carcinogenesis & Ecotoxicology Reviews*, *27*, 120–139. https://doi.org/10.1080/10590500902885684

Wang, J., Nisar, M., Huang, C., Pan, X., Lin, D., Zheng, G., Jin, H., Chen, D., Tian, N., Huang, Q., Duan, Y., Yan, Y., Wang, K., Wu, C., Hu, J., Zhang, X., & Wang, X. (2018). Small molecule natural compound agonist of SIRT3 as a therapeutic target for the treatment of intervertebral disc degeneration. *Experimental & Molecular Medicine*, *50*, 1–14. https://doi.org/10.1038/s12276-018-0173-3

Wang, J., Zhai, T., & Chen, Y. (2018). Effects of honokiol on CYP450 activity and transporter mRNA expression in type 2 diabetic rats.

International Journal of Molecular Sciences, *19*, 815. https://doi.org/10.3390/ijms19030815

Whittle, B. J. (2000). COX-1 and COX-2 products in the gut: Therapeutic impact of COX-2 inhibitors. *Gut*, *47*, 320–325. https://doi.org/10.1136/gut.47.3.320

Wu, J., Zeng, Z., Zhang, W., Deng, Z., Wan, Y., Zhang, Y., An, S., Huang, Q., & Chen, Z. (2019). Emerging role of SIRT3 in mitochondrial dysfunction and cardiovascular diseases. *Free Radical Research*, *53*, 139–149. https://doi.org/10.1080/10715762.2018.1549732

Yi, X., Guo, W., Shi, Q., Yang, Y., Zhang, W., Chen, X., Kang, P., Chen, J., Cui, T., Ma, J., Wang, H., Guo, S., Chang, Y., Liu, L., Jian, Z., Wang, L., Xiao, Q., Li, S., Gao, T., & Li, C. (2019). SIRT3-dependent mitochondrial dynamics remodeling contributes to oxidative stress-induced melanocyte degeneration in vitiligo. *Theranostics*, *9*, 1614–1633. https://doi.org/10.7150/thno.30398

Zhang, J., Xiang, H., Liu, J., Chen, Y., He, R. R., & Liu, B. (2020). Mitochondrial Sirtuin 3: New emerging biological function and therapeutic target. *Theranostics*, *10*, 8315–8342. https://doi.org/10.7150/thno.45922

SUPPORTING INFORMATION

Additional supporting information can be found online in the Supporting Information section at the end of this article.

How to cite this article: Debsharma, S., Pramanik, S., Bindu, S., Mazumder, S., Das, T., Saha, D., De, R., Nag, S., Banerjee, C., Siddiqui, A. A., Ghosh, Z., & Bandyopadhyay, U. (2023). Honokiol, an inducer of sirtuin-3, protects against non-steroidal anti-inflammatory drug-induced gastric mucosal mitochondrial pathology, apoptosis and inflammatory tissue injury. *British Journal of Pharmacology*, 1–24. https://doi.org/10.1111/bph.16070

Indomethacin impairs mitochondrial dynamics by activating the PKCζ–p38–DRP1 pathway and inducing apoptosis in gastric cancer and normal mucosal cells

Somnath Mazumder[‡1], **Rudranil De**[‡1], **Subhashis Debsharma**[‡], **Samik Bindu**[§], **Pallab Maity**[‡], **Souvik Sarkar**[‡], **Shubhra Jyoti Saha**[‡], **Asim Azhar Siddiqui**[‡], **Chinmoy Banerjee**[‡], **Shiladitya Nag**[‡], **Debanjan Saha**[‡], **Saikat Pramanik**[‡], **Kalyan Mitra**[¶], and ⓘ **Uday Bandyopadhyay**[‡2]

From the ‡Division of Infectious Diseases and Immunology, CSIR-Indian Institute of Chemical Biology, Kolkata, West Bengal 700032, the §Department of Zoology, Cooch Behar Panchanan Barma University, Cooch Behar, West Bengal 736101, and the ¶Sophisticated Analytical Instrument Facility, CSIR-Central Drug Research Institute, Sector 10, Jankipuram Extension, Sitapur Road, Lucknow 226031, Uttar Pradesh, India

Edited by Luke O'Neill

The subcellular mechanism by which nonsteroidal anti-inflammatory drugs (NSAIDs) induce apoptosis in gastric cancer and normal mucosal cells is elusive because of the diverse cyclooxygenase-independent effects of these drugs. Using human gastric carcinoma cells (AGSs) and a rat gastric injury model, here we report that the NSAID indomethacin activates the protein kinase Cζ (PKCζ)–p38 MAPK (p38)–dynamin-related protein 1 (DRP1) pathway and thereby disrupts the physiological balance of mitochondrial dynamics by promoting mitochondrial hyper-fission and dysfunction leading to apoptosis. Notably, DRP1 knockdown or SB203580-induced p38 inhibition reduced indomethacin-induced damage to AGSs. Indomethacin impaired mitochondrial dynamics by promoting fissogenic activation and mitochondrial recruitment of DRP1 and down-regulating fusogenic optic atrophy 1 (OPA1) and mitofusins in rat gastric mucosa. Consistent with OPA1 maintaining cristae architecture, its down-regulation resulted in EM-detectable cristae deformity. Deregulated mitochondrial dynamics resulting in defective mitochondria were evident from enhanced Parkin expression and mitochondrial proteome ubiquitination. Indomethacin ultimately induced mitochondrial metabolic and bioenergetic crises in the rat stomach, indicated by compromised fatty acid oxidation, reduced complex I–associated electron transport chain activity, and ATP depletion. Interestingly, Mdivi-1, a fission-preventing mito-protective drug, reversed indomethacin-induced DRP1 phosphorylation on Ser-616, mitochondrial proteome ubiquitination, and mitochondrial metabolic crisis. Mdivi-1 also prevented indomethacin-induced mitochondrial macromolecular damage, caspase activation, mucosal inflammation, and gastric mucosal injury. Our results identify mitochondrial hyper-fission as a critical and common subcellular event triggered by indomethacin that promotes apoptosis in both gastric cancer and normal mucosal cells, thereby contributing to mucosal injury.

Nonsteroidal anti-inflammatory drugs (NSAIDs)[3] are the most effective medicines for treating pain and inflammation (1, 2). In addition to their anti-nociceptive action, NSAIDs are also gaining significant importance because of their anti-neoplastic effects against a wide spectrum of cancers. In fact, prolonged NSAID users are at lower risk of developing cancers (3, 4), and these noncanonical anti-cancer drugs are now included in a combination–chemotherapy regimen as they potentiate chemotherapy and radiotherapy (5). Although prostaglandin depletion due to cyclooxygenase (COX) inhibition is primarily responsible for both anti-inflammatory as well as cytotoxic anti-cancer action of NSAIDs (6), COX-independent targets, including cGMP phosphodiesterase, peroxisome proliferator-activated receptors, retinoid X receptor, IKKβ, AMP kinase, and other targets of these drugs as well as their metabolites (7), help to trigger cell death by apoptosis while blocking proliferation. Hence, NSAIDs are gaining immense importance and have been under exploration in various diseases, including cancer (7–10). Despite their multidimensional health benefits, the toxic actions of NSAIDs are observed against various normal cells of the body that compromise metabolic homeostasis and tissue integrity (6, 11, 12). Of the several organs affected by long-term NSAID usage (13–16), the gastrointestinal system

---

[3] The abbreviations used are: NSAID, nonsteroidal anti-inflammatory drug; MFF, mitochondrial fission factor; MTT, 3-(4,5-dimethylthiazol-2-yl)-2,5-diphenyltetrazolium bromide; STED, stimulated emission depletion microscopy; ETC, electron transport chain; ROS, reactive oxygen species; OCR, oxygen consumption ratio; ANOVA, analysis of variance; TEM, transmission EM; COX, cyclooxygenase; IMM, inner mitochondrial membrane; MOS, mitochondrial oxidative stress; RCR, respiratory control ratio; qPCR, quantitative PCR; NAO, nonyl acridine orange; AGS, human gastric epithelial cell; PSI, pseudo-substrate inhibitor; FCCP, carbonyl cyanide p-trifluoromethoxyphenylhydrazone; II, injury index; ROI, region of interest; MAPK, mitogen-activated protein kinase; ERK, extracellular signal-regulated kinase; JNK, c-Jun N-terminal kinase; PG, prostaglandin; FtMt, mitochondrial ferritin; DAPI, 4′,6-diamidino-2-phenylindole; DAB, 3,3′-diaminobenzidine.

Review article

Emerging role of mitochondrial DAMPs, aberrant mitochondrial dynamics and anomalous mitophagy in gut mucosal pathogenesis

Somnath Mazumder [a,1], Samik Bindu [b,1], Rudranil De [c], Subhashis Debsharma [d], Saikat Pramanik [d], Uday Bandyopadhyay [d,e,*]

[a] *Department of Zoology, Raja Peary Mohan College, 1 Acharya Dhruba Pal Road, Uttarpara, West Bengal 712258, India*
[b] *Department of Zoology, Cooch Behar Panchanan Barma University, Cooch Behar, West Bengal 736101, India*
[c] *Amity Institute of Biotechnology, Amity University, Kolkata, Plot No: 36, 37 & 38, Major Arterial Road, Action Area II, Kadampukur Village, Newtown, Kolkata, West Bengal 700135, India*
[d] *Division of Infectious Diseases and Immunology, CSIR-Indian Institute of Chemical Biology, 4 Raja S.C. Mullick Road, Kolkata, West Bengal 700032, India*
[e] *Division of Molecular Medicine, Bose Institute, EN 80, Sector V, Bidhan Nagar, Kolkata, West Bengal 700091, India*

A B S T R A C T

Gastroduodenal inflammation and ulcerative injuries are increasing due to expanding socio-economic stress, unhealthy food habits-lifestyle, smoking, alcoholism and usage of medicines like non-steroidal anti-inflammatory drugs. In fact, gastrointestinal (GI) complications, associated with the prevailing COVID-19 pandemic, further, poses a challenge to global healthcare towards safeguarding the GI tract. Emerging evidences have discretely identified mitochondrial dysfunctions as common etiological denominators in diseases. However, it is worth realizing that mitochondrial dysfunctions are not just consequences of diseases. Rather, damaged mitochondria severely aggravate the pathogenesis thereby qualifying as perpetrable factors worth of prophylactic and therapeutic targeting. Oxidative and nitrosative stress due to endogenous and exogenous stimuli triggers mitochondrial injury causing production of mitochondrial damage associated molecular patterns (mtDAMPs), which, in a feed-forward loop, inflicts inflammatory tissue damage. Mitochondrial structural dynamics and mitophagy are crucial quality control parameters determining the extent of mitopathology and disease outcomes. Interestingly, apart from endogenous factors, mitochondria also crosstalk and in turn get detrimentally affected by gut pathobionts colonized during luminal dysbiosis. Although mitopathology is documented in various pre-clinical/ clinical studies, a comprehensive account appreciating the mitochondrial basis of GI mucosal pathogenesis is largely lacking. Here we critically discuss the molecular events impinging on mitochondria along with the interplay of mitochondria-derived factors in fueling mucosal damage. We specifically emphasize on the potential role of aberrant mitochondrial dynamics, anomalous mitophagy, mitochondrial lipoxidation and ferroptosis as emerging regulators of GI mucosal pathogenesis. We finally discuss about the prospect of mitochondrial targeting for next-generation drug discovery against GI disorders.

1. Introduction

Gastrointestinal (GI) disorders are escalating worldwide owing to multiple factors including stress, trauma, excess cigarette smoking, alcohol abuse, increasing inclination towards painkiller (non-steroidal anti-inflammatory drugs, NSAIDs) usage, *Helicobacter pylori* infection and of course increasing influence of gluten-enriched diet (which significantly alters the normal gut microbiota composition to instate a chronic basal inflammation) [1,2]. Mucosal inflammation, a central denominator in major GI pathologies, is a multifactorial phenomenon where mitochondrial structural and functional aberrance critically compromises the tissue integrity besides triggering a maladaptive immunological regulation of the pathogenesis [3–5]. Owing to the high energy requirement for maintaining intestinal barrier functions as well as cellular turnover, to replenish the constantly denuding GI mucosal surface, mitochondrial health is quintessential for maintaining GI integrity. Mitopathology is therefore likely to fuel the occurrence and/or recurrence of GI disorders. Clinical manifestations of mitochondrial

---

Macrophage migration inhibitory factor regulates mitochondrial dynamics and cell growth of human cancer cell lines through CD74–NF-κB signaling

Rudranil De[1], Souvik Sarkar[1], Somnath Mazumder, Subhashis Debsharma, Asim Azhar Siddiqui, Shubhra Jyoti Saha, Chinmoy Banerjee, Shiladitya Nag, Debanjan Saha, Saikat Pramanik, and ⓘ Uday Bandyopadhyay[2]

From the Division of Infectious Diseases and Immunology, CSIR-Indian Institute of Chemical Biology, Jadavpur, Kolkata 700032, West Bengal, India

Edited by Luke O'Neill

The indispensable role of macrophage migration inhibitory factor (MIF) in cancer cell proliferation is unambiguous, although which specific roles the cytokine plays to block apoptosis by preserving cell growth is still obscure. Using different cancer cell lines (AGS, HepG2, HCT116, and HeLa), here we report that the silencing of MIF severely deregulated mitochondrial structural dynamics by shifting the balance toward excess fission, besides inducing apoptosis with increasing sub-G_0 cells. Furthermore, enhanced mitochondrial Bax translocation along with cytochrome c release, down-regulation of Bcl-xL, and Bcl-2 as well as up-regulation of Bad, Bax, and p53 indicated the activation of a mitochondrial pathway of apoptosis upon MIF silencing. The data also indicate a concerted down-regulation of Opa1 and Mfn1 along with a significant elevation of Drp1, cumulatively causing mitochondrial fragmentation upon MIF silencing. Up-regulation of Drp1 was found to be further coupled with fissogenic serine 616 phosphorylation and serine 637 dephosphorylation, thus ensuring enhanced mitochondrial translocation. Interestingly, MIF silencing was found to be associated with decreased NF-κB activation. In fact, NF-κB knockdown in turn increased mitochondrial fission and cell death. In addition, the silencing of CD74, the cognate receptor of MIF, remarkably increased mitochondrial fragmentation in addition to preventing cell proliferation, inducing mitochondrial depolarization, and increasing apoptotic cell death. This indicates the active operation of a MIF-regulated CD74–NF-κB signaling axis for maintaining mitochondrial stability and cell growth. Thus, we propose that MIF, through CD74, constitutively activates NF-κB to control mitochondrial dynamics and stability for promoting carcinogenesis via averting apoptosis.

Macrophage migration inhibitory factor (MIF)[3] is a pluripotent inflammatory marker, which is widely known for its proinflammatory role in generating immune response by activating macrophages and T cells (1). MIF has been shown to promote tumorigenesis in many models of colorectal adenomas, intestinal tumors, ovarian cancer, and hepatocellular carcinoma (2, 3). MIF is high in both serum and epithelial cells of gastric cancer patients (4, 5). The intricate association of up-regulated MIF expression in gastrointestinal tract malignancies makes MIF a biomarker for gastric cancer as well as a potential target in anti-cancer therapies. Despite its significance in cancer, the precise role of MIF in carcinogenesis is still elusive, although some critical MIF-mediated pathways including P115 (6), inactivation of p53 (7), and stimulation of angiogenesis (2) have been investigated. The literature also suggests that CD74, the cognate receptor of MIF, upon stimulation activates NF-κB, a key molecular player in cancer and inflammation, which triggers the entry of stimulated cells into the S-phase, elevates DNA synthesis and cell division and augments BCL-X_L expression (8). CD74-MIF signaling is suspected to play a vital prognostic role in many malignancies (9). Notably, clinical immunotherapies are also being conducted targeting CD74 by milatuzumab, the monoclonal anti-CD74 antibody, in malignancies like B-cell lymphomas (10) and multiple myeloma (11).

Mitochondria are organelles that provide the majority of the energy in most cells by synthesizing ATP (12). As mitochondria are dynamic organelles that continuously undergo fission and fusion (12), mitochondrial structural integrity plays a critical role in metabolic functions (13). Severe defects in either mitochondrial fusion or fission lead to mitochondrial dysfunction (14). The Warburg effect proposes redundancy of mitochondrial oxidative phosphorylation as a major source of cellular bioenergy production; however the heterogeneity of cancer

[3] The abbreviations used are: MIF, macrophage migration inhibitory factor; MTT, 3-(4,5-dimethylthiazol-2-yl)-2,5-diphenyl tetrazolium bromide; PI, propidium iodide; AGS, human gastric adenocarcinoma (cells); DMEM, Dulbecco's modified Eagle's medium; JC-1, 5,5',6,6'-tetrachloro-1,1',3,3'-tetraethylbenzimidazolylcarbocyanine iodide; RLU, relative light unit; STED, stimulated emission depletion (microscopy); qPCR, real-time quantitative PCR; ANOVA, analysis of variance; ROI, region of interest; KD, knockdown; L-DOPA, L-Dopachrome methyl ester.

Original article

Acute mental stress induces mitochondrial bioenergetic crisis and hyper-fission along with aberrant mitophagy in the gut mucosa in rodent model of stress-related mucosal disease

Rudranil De, Somnath Mazumder, Souvik Sarkar, Subhashis Debsharma, Asim Azhar Siddiqui, Shubhra Jyoti Saha, Chinmoy Banerjee, Shiladitya Nag, Debanjan Saha, Uday Bandyopadhyay*

Division of Infectious Diseases and Immunology, CSIR-Indian Institute of Chemical Biology, 4, Raja S. C. Mullick Road, Jadavpur, Kolkata 700032, West Bengal, India

A B S T R A C T

Psychological stress, depression and anxiety lead to multiple organ dysfunctions wherein stress-related mucosal disease (SRMD) is common to people experiencing stress and also occur as a side effect in patients admitted to intensive care units; however the underlying molecular aetiology is still obscure. We report that in rat-SRMD model, cold restraint-stress severely damaged gut mitochondrial functions to generate superoxide anion ($O_2^{\bullet-}$), depleted ATP and shifted mitochondrial fission-fusion dynamics towards enhanced fission to induce mucosal injury. Activation of mitophagy to clear damaged and fragmented mitochondria was evident from mitochondrial translocation of Parkin and PINK1 along with enhanced mitochondrial proteome ubiquitination, depletion of mitochondrial DNA copy number and TOM 20. However, excess and sustained accumulation of $O_2^{\bullet-}$-generating defective mitochondria overpowered the mitophagic machinery, ultimately triggering Bax-dependent apoptosis and NF-κB-intervened pro-inflammatory mucosal injury. We further observed that stress-induced enhanced serum corticosterone stimulated mitochondrial recruitment of glucocorticoid receptor (GR), which contributed to gut mitochondrial dysfunctions as documented from reduced ETC complex 1 activity, mitochondrial $O_2^{\bullet-}$ accumulation, depolarization and hyper-fission. GR-antagonism by RU486 or specific scavenging of mitochondrial $O_2^{\bullet-}$ by a mitochondrially targeted antioxidant mitoTEMPO ameliorated stress-induced mucosal damage. Gut mitopathology and mucosal injury were also averted when the perception of mental stress was blocked by pre-treatment with a sedative or antipsychotic. Altogether, we suggest the role of mitochondrial GR-$O_2^{\bullet-}$-fission cohort in brain-mitochondria cross-talk during acute mental stress and advocate the utilization of this pathway as a potential target to prevent mitochondrial unrest and gastropathy bypassing central nervous system.

1. Introduction

Sustained mental ailments like anxiety and depression significantly affect our health by altering physiological homeostasis [1–3]. Stress-related mucosal disease (SRMD) is one such manifestation documented worldwide in patients experiencing stress [4]. Moderate to acute mucosal bleeding in critically ill patients of Intensive Care Unit (ICU) is one of the critical stress-associated phenomena and the mortality rate is significantly high (40–50%) [5,6]. Stomach houses a semi-autonomous nervous system (enteric nervous system, ENS) consisting of five hundred million nerves in the lining of the human gut. It is also the source and/or the depository of many neurotransmitters. ENS is sometimes called the "second brain," and it arises from the same tissue as the central nervous system (CNS) during development. CNS and ENS continue to influence each other lifelong and interestingly the stress

response is manifested through ENS more promptly than any other organ leading to functional gastrointestinal disorders, mucosal bleeding, inflammation, pain, and other bowel symptoms. On the other hand poor gut health has been implicated in various psychophysical disorders [7].

Being the cellular powerhouse, mitochondrial health, biogenesis and protein quality control are matters of critical concern; imbalance of mitochondrial metabolism is associated with oxidative stress and various cytopathologies [8,9]. Mitochondrial structural dynamics [10] is delicately tuned with outer environment. While mild stress induces organellar hyperfusion, moderate to acute stress evokes fragmentation followed by mitophagy in eukaryotes [11,12]. Several quality control proteases like PINK1, PARL and Parkin constantly monitor mitochondrial integrity and ensure timely clearance of damaged organelles [13,14]. Apart from its roles in mitophagy, PINK1 also participates in

Hydrazonophenol, a Food Vacuole-Targeted and Ferriprotoporphyrin IX-Interacting Chemotype Prevents Drug-Resistant Malaria

Shubhra Jyoti Saha,[ORCID] Asim Azhar Siddiqui,[ORCID] Saikat Pramanik, Debanjan Saha,[ORCID] Rudranil De, Somnath Mazumder, Subhashis Debsharma, Shiladitya Nag, Chinmoy Banerjee, and Uday Bandyopadhyay*[ORCID]

Division of Infectious Diseases and Immunology, CSIR - Indian Institute of Chemical Biology, 4 Raja S. C. Mullick Road, Jadavpur, Kolkata 700032, West Bengal, India

Ⓢ Supporting Information

ABSTRACT: The rapid emergence of resistance against frontline antimalarial drugs essentially warrants the identification of new-generation antimalarials. Here, we describe the synthesis of (E)-2-isopropyl-5-methyl-4-((2-(pyridin-4-yl)hydrazono)methyl)phenol (**18**), which binds ferriprotoporphyrin-IX (Fe^{III}-PPIX) (K_d = 33 nM) and offers antimalarial activity against chloroquine-resistant and sensitive strains of *Plasmodium falciparum* in vitro. Structure−function analysis reveals that compound **18** binds Fe^{III}-PPIX through the −C=N−NH− moiety and 2-pyridyl substitution at the hydrazine counterpart plays a critical role in antimalarial efficacy. Live cell confocal imaging using a fluorophore-tagged compound confirms its accumulation inside the acidic food vacuole (FV) of *P. falciparum*. Furthermore, this compound concentration-dependently elevates the pH in FV, implicating a plausible interference with Fe^{III}-PPIX crystallization (hemozoin formation) by a dual function: increasing the pH and binding free Fe^{III}-PPIX. Different off-target bioassays reduce the possibility of the promiscuous nature of compound **18**. Compound **18** also exhibits potent in vivo antimalarial activity against chloroquine-resistant *P. yoelii* and *P. berghei* ANKA (causing cerebral malaria) in mice with negligible toxicity.

KEYWORDS: *Plasmodium, malaria, hemozoin, food vacuole, parasite metabolism*
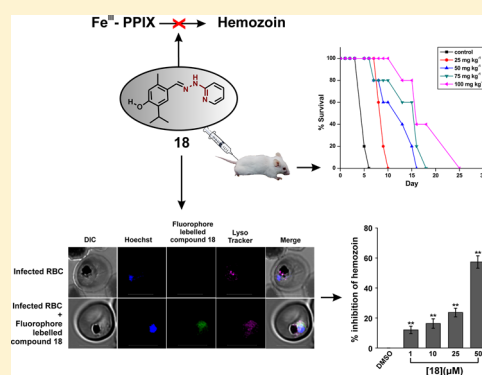
The adverse effect of malaria across the globe demands serious attention due to the increasing number of reports of multi-drug-resistant (MDR) strains posing a severe threat to human life and productivity.[1,2] Reports of 216 million cases with 445 000 deaths in 2016 repeatedly accentuate the desideratum of new antimalarial chemotherapeutics against MDR strains.[3] Moreover, the emergence of drug resistance against artemisinin partner drugs such as piperaquine and mefloquine has resulted in a significant failure of artemisinin combination therapy (ACT) on the Thai−Cambodian border, where chloroquine (CQ) resistance was developed almost 50 years ago.[4] The spread of resistance therefore needs to be dealt with in the identification of new antimalarial chemotypes that are efficacious against MDR malaria in the most unfortified regions.[1,5]

Intraerythrocytic stages of *P. falciparum* are responsible for its clinical symptoms, and during these stages, the parasite digests hemoglobin in the acidic food vacuole (FV) and thereby releases heme (Fe^{III}-PPIX), a nonprotein constituent of hemoglobin as a byproduct.[6,7] This free Fe^{III}-PPIX, a well-known pro-oxidant, may cause severe oxidative damage to the lipid bilayers of the parasitic cell membrane, leading to

membrane lesion.[8−10] In order to evade the detrimental consequences of free Fe^{III}-PPIX accumulation, *Plasmodium* crystallizes it into nontoxic inert hemozoin (Hz).[11,12] It was found that the development of CQ resistance in parasites was mainly due to multiple mutations in the *P. falciparum* CQ resistance transporter (*Pf*CRT) that results in structure-specific efflux of the drug from FV.[13] Despite this resistance, the Hz crystallization pathway within the parasite is still essential, and thus it may be used as a sustainable drug target.[14] Thus, scaffolds which bind to free Fe^{III}-PPIX and inhibit Hz crystallization can be detrimental to parasites due to free Fe^{III}-PPIX accumulation within the FV and have merit as potent antimalarials.

In the search for new antimalarial chemotypes, we focused our study on Fe^{III}-PPIX binding moieties that are capable of interacting with high affinity. A novel class of chiral gallium(III) complexes of amine-phenol ligand and schiff-base phenol ligand were reported to possess decent efficacy against CQ-sensitive and -resistant strains.[15] These cationic

Contents lists available at ScienceDirect

Biochemical Pharmacology

Selective scavenging of intra-mitochondrial superoxide corrects diclofenac-induced mitochondrial dysfunction and gastric injury: A novel gastroprotective mechanism independent of gastric acid suppression

CrossMark

Somnath Mazumder, Rudranil De, Souvik Sarkar, Asim Azhar Siddiqui, Shubhra Jyoti Saha, Chinmoy Banerjee, Mohd. Shameel Iqbal, Shiladitya Nag, Subhashis Debsharma, Uday Bandyopadhyay *

Division of Infectious Diseases and Immunology, CSIR-Indian Institute of Chemical Biology, West Bengal, India

A B S T R A C T

Non-steroidal anti-inflammatory drugs (NSAIDs) are widely used to treat multiple inflammatory diseases and pain but severe gastric mucosal damage is the worst outcome of NSAID-therapy. Here we report that mitoTEMPO, a mitochondrially targeted superoxide (O_2^-) scavenger protected as well as healed gastric injury induced by diclofenac (DCF), the most commonly used NSAID. Common existing therapy against gastric injury involves suppression of gastric acid secretion by proton pump inhibitors and histamine H_2 receptor antagonists; however, dyspepsia, vitamin B12 deficiency and gastric microfloral dysbalance are the major drawbacks of acid suppression. Interestingly, mitoTEMPO did not inhibit gastric acid secretion but offered gastroprotection by preventing DCF-induced generation of O_2^- due to mitochondrial respiratory chain failure and by preventing mitochondrial oxidative stress (MOS)-mediated mitopathology. MitoTEMPO even restored DCF-stimulated reduced fatty acid oxidation, mitochondrial depolarization and bioenergetic crisis in gastric mucosa. MitoTEMPO also prevented the activation of mitochondrial pathway of apoptosis and MOS-mediated proinflammatory signaling through NF-κB by DCF. Furthermore, mitoTEMPO when administered in rats with preformed gastric lesions expedited the healing of gastric injury and the healed stomach exhibited its normal physiology as evident from gastric acid and pepsin secretions under basal or stimulated conditions. Thus, in contrast to the existing antiulcer drugs, mitochondrially targeted O_2^- scavengers like mitoTEMPO may represent a novel class of gastroprotective molecules that does not affect gastric acid secretion and may be used in combination with DCF, keeping its anti-inflammatory action intact, while reducing its gastrodamaging effects.

© 2016 Elsevier Inc. All rights reserved.

1. Introduction

Around 30 million people consume NSAIDs globally every day [1]. However, severe gastrointestinal disorder accompanied by gas-

tric mucosal perforation and bleeding is a major concern as well as the worst outcome of prolonged NSAID-therapy [2]. Diclofenac (DCF), an anthranilic acid derivative with pKa of 4.0 [3] is the most widely prescribed NSAID for treating several forms of pain and inflammation [4]. An estimated 16,500 NSAID-associated deaths occurring annually in the United States exclusively account for the arthritis patients and about 107,000 patients affected with NSAID-induced gastropathy are annually admitted to hospitals [5–7]. Although several NSAIDs have been withdrawn from the market owing to their negative health effects, DCF is still in the market and finds application against a diverse spectrum of human pathologies [4] ranging from rheumatic and non-rheumatic diseases, pain, fever, chronic inflammation, dysmenorrhea to several

---

Article

Nuclease activity of *Plasmodium falciparum* Alba family protein PfAlba3

Chinmoy Banerjee,[1] Shiladitya Nag,[1] Manish Goyal,[1] Debanjan Saha,[1] Asim Azhar Siddiqui,[1] Somnath Mazumder,[1] Subhashis Debsharma,[1] Saikat Pramanik,[1] and Uday Bandyopadhyay[1,2,3,*]

[1]Division of Infectious Diseases and Immunology, CSIR-Indian Institute of Chemical Biology, 4, Raja S. C. Mullick Road, Jadavpur, Kolkata, West Bengal 700032, India
[2]Division of Molecular Medicine, Bose Institute, EN 80, Sector V, Bidhan Nagar Kolkata, 700091, West Bengal, India
[3]Lead contact
*Correspondence: ubandyo_1964@yahoo.com
https://doi.org/10.1016/j.celrep.2023.112292

SUMMARY

Plasmodium falciparum Alba domain-containing protein Alba3 (PfAlba3) is ubiquitously expressed in intra-erythrocytic stages of *Plasmodium falciparum*, but the function of this protein is not yet established. Here, we report an apurinic/apyrimidinic site-driven intrinsic nuclease activity of PfAlba3 assisted by divalent metal ions. Surface plasmon resonance and atomic force microscopy confirm sequence non-specific DNA binding by PfAlba3. Upon binding, PfAlba3 cleaves double-stranded DNA (dsDNA) hydrolytically. Mutational studies coupled with mass spectrometric analysis indicate that K23 is the essential residue in modulating the binding to DNA through acetylation-deacetylation. We further demonstrate that PfSir2a interacts and deacetylates K23-acetylated PfAlba3 in favoring DNA binding. Hence, K23 serves as a putative molecular switch regulating the nuclease activity of PfAlba3. Thus, the nuclease activity of PfAlba3, along with its apurinic/apyrimidinic (AP) endonuclease feature identified in this study, indicates a role of PfAlba3 in DNA-damage response that may have a far-reaching consequence in *Plasmodium* pathogenicity.

INTRODUCTION

Nucleases play a fundamental role in a growing number of biological pathways ranging from cellular defense, nutrient regeneration, and apoptosis to nucleic acid metabolism.[1] *Plasmodium falciparum*, the etiological agent of human malignant malaria, has mastered the art of survival by capitalizing on its complex life cycle and intriguingly specialized metabolism to counter host-defense strategies. The oxidative environment under which its intra-erythrocytic stage perpetuates poses a lethal threat to its vulnerable AT-biased genome.[2] Oxidative stress, an inevitable consequence of the parasites' metabolism along with the host immune system as a countermeasure, inflicts DNA damage as a consequence of its interaction with reactive oxygen species (ROS), specifically the hydroxyl radical. Among the several DNA lesions associated, apurinic/apyrimidinic (AP) sites formed due to spontaneous hydrolysis or specific excision of inappropriate or damaged bases by DNA *N*-glycosylases are one of the most frequent to be observed.[3,4] It is estimated that in mammalian cells, around 10,000 bases are lost per day.[5,6] The subsequent loss of an encoding base in the DNA template may end up blocking the DNA and RNA polymerases, thereby stalling DNA replication and transcription. Moreover, translesional DNA synthesis may further culminate into single-nucleotide replacements or deletions/insertions leading to mutations. AP sites are crucial, owing to their high chemical reactivity, and may enhance the production of DNA breaks as well as render DNA-protein and DNA-DNA crosslink. These AP sites, if left untreated, can have deleterious consequences, as they are highly mutagenic and cytotoxic.[7,8] Hence, for maintaining genome integrity, the repair of AP sites is a major mechanism wherein AP endonucleases serve as key enzymes to initiate the repair process. Out of the four nucleobases, adenine and guanine exhibit maximum propensity for impromptu base loss. Considering the fact that the *Plasmodium falciparum* genome exhibits unusually high adenine (A) and thymine (T) content (~80%) and spontaneous de-adenination of DNA occurs naturally, it is quite apparent that an active AP repair process is prevalent. Ten DNA endonucleases encoded by the genome of *Plasmodium falciparum* 3D7 clone have been identified, of which seven are predicted to harbor an endonuclease/exonuclease/phosphatase (IPR005135) domain that plays a crucial role in DNA catalysis.[9] The repair of nuclear DNA in *Plasmodium falciparum* has been proposed to involve homologous recombination, mismatch repair (MMR) pathways, and alternative end joining.[10,11] Putative proteins involved in nucleotide excision repair have also been reported.[12] Base excision repair (BER) in *Plasmodium falciparum* is mediated via long patch repair mechanism by class II AP endonucleases present in the parasite lysate. Recent studies have identified two mitochondrial AP endonucleases in *Plasmodium falciparum*.[13,14] Apart from these two mitochondrial AP endonucleases, three more enzymes (uracil DNA glycosylase, flap endonuclease 1,
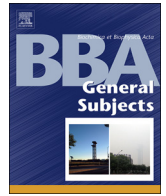
Rab7 of *Plasmodium falciparum* is involved in its retromer complex assembly near the digestive vacuole

Asim Azhar Siddiqui, Debanjan Saha, Mohd Shameel Iqbal, Shubhra Jyoti Saha, Souvik Sarkar, Chinmoy Banerjee, Shiladitya Nag, Somnath Mazumder, Rudranil De, Saikat Pramanik, Subhashis Debsharma, Uday Bandyopadhyay[*]

Division of Infectious Diseases and Immunology, CSIR-Indian Institute of Chemical Biology, 4, Raja S. C. Mullick Road, Jadavpur, Kolkata 700032, West Bengal, India

ARTICLE INFO

ABSTRACT

Background:
Intracellular protein trafficking is crucial for survival of cell and proper functioning of the organelles; however, these pathways are not well studied in the malaria parasite. Its unique cellular architecture and organellar composition raise an interesting question to investigate.
Methods:
The interaction of *Plasmodium falciparum* Rab7 (*Pf*Rab7) with vacuolar protein sorting-associated protein 26 (*Pf*VPS26) of retromer complex was shown by coimmunoprecipitation (co-IP). Confocal microscopy was used to show the localization of the complex in the parasite with respect to different organelles. Further chemical tools were employed to explore the role of digestive vacuole (DV) in retromer trafficking in parasite and GTPase activity of *Pf*Rab7 was examined.
Results:
*Pf*Rab7 was found to be interacting with retromer complex that assembled mostly near DV and the Golgi in trophozoites. Chemical disruption of DV by chloroquine (CQ) led to its disassembly that was further validated by using compound 5f, a heme polymerization inhibitor in the DV. *Pf*Rab7 exhibited Mg^{2+} dependent weak GTPase activity that was inhibited by a specific Rab7 GTPase inhibitor, CID 1067700, which prevented the assembly of retromer complex in *P. falciparum* and inhibited its growth suggesting the role of GTPase activity of *Pf*Rab7 in retromer assembly.
Conclusion:
Retromer complex was found to be interacting with *Pf*Rab7 and the functional integrity of the DV was found to be important for retromer assembly in *P. falciparum*.
General significance:
This study explores the retromer trafficking in *P. falciparum* and describes a mechanism to validate DV targeting antiplasmodial molecules.

1. Introduction

Plasmodium falciparum is an intracellular parasite that infects the erythrocytes of its host. The intraerythrocytic stages of the parasite are responsible for its pathogenesis when it digests host hemoglobin in its DV that is a temporary organelle formed only during intraerythrocytic stages of the parasite [1]. DV is often regarded as the metabolic headquarter of the parasite and a known target for several antiplasmodial compounds [2]. The parasite thrives in the host erythrocyte and depends on its hemoglobin for nutrition and growth. It has a specialized machinery of various proteases to digest host hemoglobin inside DV [3]. Hemoglobin digestion in DV results in the release of free heme that is highly toxic to the cell. The DV of the parasite utilizes a unique mechanism where it converts free heme into an insoluble and non-toxic crystalline pigment called hemozoin [4]. Because of these factors, DV is one of the most potential targets of antiplasmodial molecules. Organellar architecture of *Plasmodium* is highly dissimilar from other eukaryotes. It has a very unusual single mitochondrion per cell [5], its endoplasmic reticulum is not well defined [6], Golgi bodies in *Plasmodium* are primitive [7]. This peculiar organization of organelles

India International Science Festival 2020

Science for Self-Reliant India and Global Welfare

MINISTRY OF SCIENCE AND TECHNOLOGY
MINISTRY OF EARTH SCIENCES
MINISTRY OF HEALTH & FAMILY WELFARE
GOVERNMENT OF INDIA

Certificate of Participation and Oral Presentation

This is to certify that Prof./Dr./Mrs./Mr./Ms. **SUBHASHIS DEBSHARMA** of

CSIR INDIAN INSTITUTE OF CHEMICAL BIOLOGY has participated and delivered

an oral presentation entitled "**ABERRANT MITOCHONDRIAL DYNAMICS: A NEW THERAPEUTIC TARGET**

FOR THE MANAGEMENT OF PAIN KILLER-INDUCED GASTROPATHY"

under the theme " **FRONTIERS AREA OF RESEARCH - LIFE SCIENCES** " in the **Young**

Scientists' Conference organized during 22-12-2020 to 24-12-2020 as a part of **India**

International Science Festival- 2020 by the Ministry of Science and Technology, Ministry of

Earth Sciences, and Ministry of Health and Family Welfare, Govt. of India in collaboration

with Vijnana Bharati (VIBHA).

Dr. Shekhar C. Mande
DG, CSIR & Secretary, DSIR

Dr. Vijay P. Bhatkar
President, Vijnana Bharati

Congratulations! Frontiers in Cancer Science 2021 Poster Presentation ▸ Inbox ×

CSI Singapore <csi_singapore@nus.edu.sg>
to me ▾

Oct 6, 2021, 2:32 PM

Dear Mr. Subhashis Debsharma

Congratulations! On behalf of the Frontiers in Cancer Science organising committee, we are pleased to inform that you have been selected as a "Poster Presenter" for your abstract **NON-STEROIDAL ANTI-INFLAMMATORY DRUGS INDUCE MITOCHONDRIAL HYPERFISSION AND BIOENERGETIC CRISIS TO INDUCE GASTRIC CANCER CELL DEATH**

Your unique poster no is **PA32**

To facilitate the upload of your poster and presentation, please read the poster guidelines for the virtual Frontiers in Cancer Science 2021.

After you have completed and adjusted your slides, please upload them here with the respective file names to be named after. The deadline to submit the files is **22 October, 12pm**

<poster-number> <space> <presenter-name>.mp4
<poster-number> <space> <presenter-name>.pdf

More information on access to virtual posters and poster judging process will be conveyed to you closer to date.

In the meanwhile, please let us know if you require any further assistance, thank you.

Subhashis Debsharma <subhashis2060@gmail.com>
to CSI ▾

Nov 3, 2021, 11:06 PM

Dear Organizer,
My name is Subhashis Debsharma. I have presented a poster in your platform. My poster ID was PA32. Will I get any certificate for presenting the poster??

With Regards,
Subhashis Debsharma
DBT-SRF
c/o Dr. Uday Bandyopadhyay
Senior Principal Scientist
Infectious Diseases & Immunology
CSIR-Indian Institute of Chemical Biology
Contact no: 7699923244

***

CSI Singapore <csi_singapore@nus.edu.sg>
to me ▾

Nov 8, 2021, 11:51 AM

Dear Subhashis,

Thank you for reaching out. Unfortunately, we will not be issuing any certificates for poster presentation. Alternatively, letter of participation will be available upon request.

Please let me know if you would still require it, thank you.
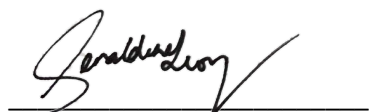
Regards,
FCS 2021 Conference Secretariat

Dear Sir/Madam,

Confirmation of Participation – Frontiers in Cancer Science 2021, 1-3 November 2021

On behalf of the Organizing Committee of the Frontiers in Cancer Science (FCS) 2021, we hereby confirm that Mr. Subhashis Debsharma has participated in the Frontiers in Cancer Science virtual conference, which took place on 1st - 3rd November 2021.

Yours sincerely,
Geraldine Leong
CONFERENCE SECRETARIAT
Frontiers in Cancer Science 2021

Organizing Committee Members:

Patrick TAN (GIS) (Chair)
TAM Wai Leong (GIS) (Vice-Chair)
Edward Kai-Hua CHOW (CSI Singapore)
Anand D JEYASEKHARAN (NCIS)
Sudhakar JHA (CSI Singapore)
Joanne NGEOW (LKCMedicine)
ONG Sin Tiong (Duke-NUS)
Shazib PERVAIZ (YLLSoM)
Kanaga SABAPATHY (NCCS)
Vinay TERGAONKAR (IMCB)
David VIRSHUP (Duke-NUS)

JADAVPUR UNIVERSITY

KOLKATA-700 032

MARK SHEET

NO.: CW/16052/ 000645

(For Ph.D/M. Phil. Course Work)

Results of the	PH.D. COURSE WORK EXAMINATION, 2019
In LIFE SCIENCE & BIO-TECHNOLOGY held in	DECEMBER,2018 - JANUARY, 2019
Name SUBHASHIS DEBSHARMA	Class Roll No. 201820502003
Examination Roll No. PHDLSBT19104	Registration No. of

Subject Code / Name	Credit Hr.(c_i)	Marks
COMPULSORY UNITS:: EX/LSBT/PHD/1.1 REVIEW OF LITERATURE & RESEARCH METHODOLOGY	4	88
ELECTIVE UNITS ::	4	55
EX/LSBT/PHD/1.2A :: TISSUE CULTURE TECHNIQUES EX/LSBT/PHD/1.2B :: MICROBIOLOGY EX/LSBT/PHD/1.2C :: PRINCIPLE OF MOLECULAR BIOLOGY TECHNIQUES EX/LSBT/PHD/1.2D :: INTRODUCTION TO MOLECULAR BIOLOGY TECHNIQUES		

Total Marks : 143 (out of 200)

Remarks: P

Prepared by : ₨s

Checked by : ℓγ

Date of issue : 20 - 03 - 2019

Controller of Examinations

No. Sc. 0272

Jadavpur University

Registration Certificate

Shri/~~Sm~~ _Subhashis Debsharma_

has been registered as a student of Ph.D. programme of this
university

His/~~her~~ Registration Number is ..... _SLSBT1111418_ .....

Kolkata ..... _8th March 2018_ .....

_4.4.19_

Registrar

Enrolment No. : PhD CW / **2016/68**

CSIR - Indian Institute of Chemical Biology

(An autonomous body, under the Ministry of Science & Technology, Government of India)

Certificate

(Courses offered as per UGC guidelines, July 2009)

This is to certify that Mr. / Ms. **Subhashis Debsharma** ....

has successfully completed the Ph.D Course Work conducted by CSIR-IICB for the session

2016
....

Uday Bandyopadhyay
Chairperson, Academic Affairs Committee

Samit Chattopadhyay
Director

Ref.No.: *L-7/Sc/121/2018*

Dated : 02. 02. 2018.

q

To
Sri Subhashis Debsharma
C/O. – Dr. Uday Bandyopadhyay
Scientist
Indian Institute of Chemical Biology
4, Raja S. C. Mullick Road
Jadavpur
Kolkata – 700 032.

INDEX NO : 114|18|Life Sc.|25

Dear Sir,

With reference to your application for the registration for Ph.D.(Science) degree of Jadavpur University, I am to inform you that you are permitted to register your name on payment of requisite fees for Ph.D. programme of Rs.22,000/- (Rupees Twenty-Two Thousand Only), payable in three installments (Rs.8000/- + Rs.8000/- + Rs.6000/-). It may be noted that this offer is provisional until all the documents mentioned below are submitted.

The registration will be valid from the date on which the fees are paid and shall remain valid for six years from that date. Subsequently the period of registration may be extended as per Regulation 2017 if the grounds for extension satisfy the Research Advisory Committee, Ph.D. Research Committee and the Doctorate Committee accordingly. An application requesting extension and citing the grounds for the same must be submitted in due time, duly forwarded and recommended by the supervisor(s), before the date on which the validity of the registration expires.

The scheme of the work and title of the thesis, if not submitted along with the application, shall have to be submitted within two years from the date of registration or within one year from the date of successful completion of the course work result of the candidate. Otherwise, the registration is liable to cancellation as per Regulations 2017 of the University.

If the registration fee is not paid within one month from the date of issue of this letter, your application stated above will be treated as cancelled. A report on the progress of the research work shall have to submit once in every six months from the date of registration as per Regulation 2017. The registration is liable to cancellation if the progress of work is not satisfactory. It may be noted that you will have to fulfill the condition as per Regulation 2017 and have to complete the course work within two years from the date of registration.

Mode of payment as follows:

1st instalment – within 30 days.
2nd instalment – within 180 days
3rd instalment – within 365 days.

List of required documents:
i)   Migration Certificate in Original. ⎤ – Submitted
ii)   Nil.   ⎦   on 8|3|18 .

Yours faithfully,

(Dr. Atiskumar Chattopadhyay)
Secretary
Faculty Council of Science.